The Quantum Backflow Phenomenon

Harkan J. Kirk-Karakaya

PhD

University of York
Department of Mathematics

September 2025

Abstract

It has been known since at least 1969, that there exist quantum states of a free particle on the line with purely positive momentum that exhibit probability transfer towards the negative half-line. This phenomenon, the quantum backflow effect, is the subject of this thesis. The largest amount of backflow any state can exhibit over a single time interval, the Bracken–Melloy constant, was initially calculated to be $c_{\mathrm{BM}} \approx 0.04$.

In the first half of this thesis, we consider the question of how much quantum backflow states can exhibit over disjoint time intervals. This is done by formulating the question in terms of the spectra of bounded operators. When considering more than one disjoint time interval, we discuss a new phenomenon where a state exhibits more probability transfer in the same direction as its momentum than any classical state. We call this effect quantum overflow. Given a number M of disjoint time intervals, we give bounds on the maximum amount of backflow and overflow a state can exhibit over any M many intervals. The limiting cases in which two disjoint intervals merge into one is particularly studied. Finally, we show plots of the time $t = 0$ momentum space wavefunction of states exhibiting multiple quantum backflow and quantum overflow.

The second half of the thesis contains a detailed numerical investigation into the backflow problem for a single time interval. Based on previous conjectures, we construct the maximum backflow state from a given set of normalised states closely resembling the sinc function. The Bracken—Melloy constant is then bounded from below by the largest solution to a generalised eigenvalue problem. Using a multi-step numerical procedure, we solve a high precision large dense generalised eigenvalue problem. From this we obtain new numerical approximation to the backflow state and the best known rigorous lower bound of the Bracken—Melloy constant.

Contents

List of Figures

Dedication

To my dear Nana Doreen
January 1940 – September 2025

Acknowledgements

Firstly I want to thank my supervisor Professor Christopher J. Fewster for his wisdom, patience and vast scientific expertise. The many discussions we have had will continue to inspire me for a lifetime. In particular I want to thank him for his belief in me even prior to starting this PhD, something that I will never forget. I could not have asked for a better teacher.

A thank you is required of Simon Eveson, Ed Corrigan, Bernard Kay and Atsushi Higuchi whose scientific discussions in the department I much appreciated. I would like to thank all of those at the Institute for Quantum Optics and Quantum Information (IQOQI) in Vienna. The ability to speak at the Quantum Advantages in Mechanical Systems workshop there in 2023 was a great privilege. Specifically, I'd like to recognise Reinhardt Werner's fascinating question at the workshop asking if there are quantum states that could exhibit backflow over disjoint time intervals.

Next I would like to thank all of those PhD students that brought me under their proverbial wing and made me feel welcome in the department when I first started. In particular I'd like to thank Diego Vidal Cruz for all the discussions we had, both scientific and social.

On the note of past PhD students, I must recognise the friendship with Vasilios Letsios that I cherish dearly. Thanks for the great moments we have had throughout my PhD and I look forward to many more. To Nikos Koutsonikos, the best of luck with the rest of your PhD in Patras. Further to that point, I want to wish all of the current PhD students at the department good luck for the remainder of their doctorates, in particular to Ben G, Ben M, Laurens, Nick, Ricky, Sam E, Filippo and Zane.

To my dear girlfriend Emma, meeting you during my PhD was the best thing

that ever happened to me. I adore you with all of my being, and you continue to make me so proud every day. It was only with your unending support that writing this thesis was even possible. Thank you. There are too many treasured memories with you to recount, and I cannot wait for our future together.

Now, a special thanks to all of my close friends, especially Sean and Dax. I'd also like to mention Leon and Dan who are my oldest friends. They have, over the 26 and 24 years respectively of knowing them, consistently listened to my fascinations with quantum mechanics. To Billy, Caitlin, Elliot, Emily, Evie, Grady, Isaac A, Isaac D, Joel, Kallum, Kita and Shannon - thanks for your friendship and the endless laughs.

It is important to thank my close extended family. I would like to thank my Auntie Vicky for her constant support, my cousin Amber for her humour and friendship and my great Auntie Diana for her wisdom. I would also like to thank my Uncles Spencer and Russell.

I would like to thank my father Yahya and his wife Nuresh for their love and affection throughout my PhD. In particular, I want to thank my father for his endless ability to listen to me talk about my research and for being a constant inspiration to me.

To my mother Samantha and stepfather Phil, thank you for your endless support and love. It is my mother who I have to specifically thank for instilling in me a love of science. The stories you told me as a child of Alexander Graham Bell inventing the telephone and Edward Jenner inventing the first vaccine still stay with me to this day.

Here I want to say how proud I am of my brother Nathan and sister Ella. I love both of you dearly.

I want to express my heartfelt thanks to my Grandad Jack. I will never forget all of the great stories he told me as he walked me to primary school.

Finally, I would like to mention my late Nana Doreen for playing no small part in raising me into the man I am today. I dedicate this thesis to her.

Author's declaration

I declare that the work presented in this thesis, except where otherwise stated, is original and based on joint research with Professor Christopher Fewster carried out at the University of York and has not been submitted previously for any degree at this or any other university. The content in chapters 2 and 3 are based on the joint work *Repeated quantum backflow and overflow* with Professor Christopher Fewster [33]. I declare that this thesis is a presentation of original work and I am the sole author. This work has not previously been presented for an award at this, or any other, University. All sources are acknowledged as References. Sources are acknowledged by explicit references.

— 1 —

Introduction

1.1 QUANTUM ADVANTAGE

In the game of rugby, a player may only legally pass the ball to their teammate backwards. That is, the player must be positioned further towards the opposing team's posts than the intended recipient of the ball. Fortunately, rugby league is a sport played by macroscopic players obeying the laws of classical mechanics, most rugby players do not find it so difficult to obey this rule and avoid losing their team possession of the ball. The same cannot be said for a rugby game played with a quantum rugby ball. Imagine a player Bob passing a quantum rugby ball backwards to their teammate Alice with Charlie positioned further up the pitch. It is possible, despite the fact that Bob aimed to legally pass the ball to Alice, for Charlie to find the ball in his hands. However, the upset was not Bob's fault. This was due to the phenomenon that goes by the name of *quantum backflow*.

Quantum backflow (QB) is the counterintuitive phenomenon whereby a free particle moving on the line with momentum in the positive spatial direction can exhibit probability flow in the negative spatial direction. This is in sharp contrast to the case of a classical ensemble of free particles which will always exhibit probability transfer in the same direction as its momentum. The first example of quantum states exhibiting QB was found by Allcock [2] in 1969 while studying the problem of time of arrival in quantum mechanics. In his study, he showed that the quantum mechanical current of a state with non-negative momentum could be negative, giving rise to the QB phenomenon. The work of Allcock was significantly expanded by Bracken and Melloy in 1994 [12], who conducted the first thorough study of QB.

The phenomenon of quantum backflow can be firmly placed among physical

effects exhibited by quantum systems that outdo some bound obeyed by the system's classical counterpart. Quantum effects that display this behaviour of exceeding some classical bound are often labelled under the umbrella term *quantum advantage*, for which the canonical example would be *quantum tunneling*. Tunneling is the well studied quantum effect [54] whereby a quantum particle, initially localised in some classically insurmountable energy well, may be measured to be outside of this well some time later.

Quantum advantages in general transport tasks have been studied by Trillo, Le and Navascués [64]. In their paper they study the *quantum projectile scenario* whereby a quantum particle is prepared such that it is localised in some bounded region B with momentum distribution ρ and left to freely propagate to some region R far away from B. The behaviour of these states are then compared to the behaviour of an analogous classical particle with momentum distribution $|\rho|^2$. In the paper, they find that there exist ultrafast and ultraslow quantum states in the sense that in expectation, these states will be measured in the distant region R quicker and slower than the associated classical particle respectively. As is shown in [64], this transport problem is closely related to the quantum backflow phenomenon. Intuitively, one may suppose that such an ultraslow state is one exhibiting backflow in some time intervals between B and R.

Another related quantum effect is Tsirelson precession. Consider a one dimensional classical harmonic oscillator of frequency ω with some initial position x, and three distinct equally spaced times $0, 2\pi/(3\omega), 4\pi/(3\omega)$. Now suppose one of these times is chosen at random, and the position coordinate of the oscillator is measured. This process is called the Tsirelson protocol, and the probability of measuring the chosen position coordinate as positive is called the Tsirelson score. It was shown by Tsirelson, in an unpublished preprint [65], that the Tsirelson score of this classical oscillator will never exceed $2/3$. Now turn to the analogous quantized oscillator. Again in [65], it was shown that there are initial states of the quantum harmonic oscillator for which the Tsirelson score can exceed $2/3$. This protocol has been studied extensively by Zaw and others in [18, 70, 72]. In particular, in [71], it was shown that the maximum Tsirelson score for the quantum harmonic oscillator associated with any three times (satsifying some technical condition) P_3 satisfies the bound $0.709364 \leq P_3 \leq 0.709511$. The original Tsirelson protocol has further been generalised to an arbitrary odd number of times in the unpublished thesis of Zaw. There is good reason to believe that this phenomenon has a firm link to the

quantum backflow of a free particle, based on work by both myself and Zaw, which it is hoped will be developed elsewhere.

In the different setting of quantum field theory, there are also well known examples of the observables of quantum fields exceeding the bounds obeyed by their classical counterparts. In classical relativistic field theories, the energy density of a field is described by its stress–energy tensor T_{ab}. This is a quantity typically made up of local quantities associated with the field. One of the assumptions of general relativity is the *weak energy condition*, which is the proposition that all observers measure the local energy density of matter to be non-negative. Mathematically, this can be expressed as $T_{ab}u^a u^b \geq 0$ for all timelike vectors u^a. This condition, as well as others like it, are assumptions added into the theory of general relativity alongside the Einstein equations. The story for the quantum fields is quite different, as has been known since at least 1965 [28]. For even the simplest quantum fields, there are states of the field for which the quantized stress-energy tensor's expectation value does not obey the weak energy condition. Furthermore, such states of a quantum field can possess pointwise negative energy densities that can be arbitrarily negative. However, it was first shown by Ford [37] that temporally averaged expectation values of the quantum stress–energy tensor, when appropriately smeared, admit bounds from below. These are known as quantum energy inequalities, for which there are examples in globally hyperbolic manifolds of arbitrary dimension [31, 22, 34]. Many other examples exist in globally hyperbolic manifolds of dimension two [21] and yet more examples for four dimensonal Minkowski space [35]. For a full pedagogical overview, the reader is guided to [32].

The overall theme of this thesis is to describe the extent of the quantum advantage of generalised backflow problems, as well as describe some of the states that possess this advantage. To do this, we first note the following. All of the examples given above possess a common feature. That is, quantum systems typically violate bounds obeyed by their classical counterparts. All of these examples admit a mathematical description in terms of the extremal spectral values of some operator. We now move on to describe an operator associated with the quantum backflow phenomenon.

1.2 BACKFLOW OPERATORS

Throughout the thesis, we work in units with $\hbar = 1$. A free quantum particle of mass $\mu > 0$ is described at time t by a quantum state $\psi_t \in L^2(\mathbb{R})$ obeying the free Schrödinger equation

$$i\partial_t \psi_t = H\psi_t \tag{1.1}$$

where $H = -1/(2\mu)\partial_x^2$ is the Hamiltonian of a free particle and with initial condition $\psi_0 = \psi$. Choosing $\mu = 1/2$, we find the formal solution is given by $\psi_t = \exp(it\partial_x^2)\psi$. Define the unitary $\mathcal{F}$ as the Fourier transform with explicit form

$$(\mathcal{F}\psi)(p) = \frac{1}{\sqrt{2\pi}} \int_{-\infty}^{\infty} dx\, \psi(x) e^{-ipx} \tag{1.2}$$

with the inverse Fourier transform denoted by $\mathcal{F}^*$. Commonly, we will make use of the abbreviation $\hat{\psi} := \mathcal{F}\psi$. By applying the Fourier transform to the Schrödinger equation, we find the general solution has momentum space representation

$$\hat{\psi}_t(p) = \exp\left(-itp^2\right)\hat{\psi}_0(p). \tag{1.3}$$

To discuss QB, we must first define the subspace $\mathcal{H}^+$ of position representation quantum states with non-negative momentum as

$$\mathcal{H}^+ = \left\{ \psi \in L^2(\mathbb{R}) \,\middle|\, \text{supp } \hat{\psi} \subseteq [0, \infty) \right\}. \tag{1.4}$$

Similarly, we define the momentum representation quantum states with non-negative momentum as $\mathcal{F}\mathcal{H}^+ = L^2(\mathbb{R}^+)$. Note that by (1.3), $\mathcal{H}^+$ is invariant under the free Schrödinger evolution. For fixed $t_1 < t_2$, the amount of QB a normalised quantum state $\psi \in \mathcal{H}^+$ can exhibit is given by

$$\Delta_{\langle t_1, t_2 \rangle}(\psi) = \text{Prob}_\psi\left(X \in (-\infty, 0] \mid t = t_2\right) - \text{Prob}_\psi\left(X \in (-\infty, 0] \mid t = t_1\right) \tag{1.5}$$

where for a spatial region $R \subseteq \mathbb{R}$, the probability of finding the particle in the state ψ at a time t in the region R is given by

$$\text{Prob}_\psi(X \in R \mid t) = \int_R dx\, |\psi_t(x)|^2. \tag{1.6}$$

According to classical intuition, the momentum of a particle expresses the direction that it is moving in. Since any state in $\mathcal{H}^+$ has non-negative momentum, one should expect the probability of finding the state in the left half-line $(-\infty, 0]$ to only ever

decrease in time. However there exist normalised states $\psi \in \mathcal{H}^+$ with $\Delta_{\langle t_1,t_2\rangle}(\psi) > 0$ and we call every such ψ a *backflow state*. The maximum amount of backflow any state can exhibit is the constant $c_{\mathrm{BM}} \approx 0.04$, first found by Bracken and Melloy in [12].

To understand the possible range of values $\Delta_{\langle t_1,t_2\rangle}$ can attain we first describe some important operators and note some symmetries. The position and momentum operators are denoted by X and P, each densely defined on the domains $\mathcal{D}_X$ and $\mathcal{D}_P$ which are given by

$$\mathcal{D}_X = \left\{\psi \in L^2(\mathbb{R}) : \int_{-\infty}^{\infty} dx|x\psi(x)|^2 < \infty\right\}, \tag{1.7}$$

$$\mathcal{D}_P = \left\{\psi \in L^2(\mathbb{R}) : \int_{-\infty}^{\infty} dx\,|\psi'(x)|^2 < \infty\right\}. \tag{1.8}$$

On these respective domains, the actions of X and P are given by

$$(X\psi)(x) = x\psi(x), \qquad (P\psi)(x) = -i\psi'(x) \tag{1.9}$$

and we note that together they generate a representation of the canonical commutation relation algebra (CCR). Let $S_t = \mathcal{F}^* \exp(-itP^2)\mathcal{F} : L^2(\mathbb{R}) \to L^2(\mathbb{R})$ be the Schrödinger evolution operator acting on wavefunctions in the position representation. Then firstly, as first shown by Bracken and Melloy in [12], we find that

$$\Delta_{\langle t_1+\tau,t_2+\tau\rangle}(\psi) = \Delta_{\langle t_1,t_2\rangle}(S_\tau\psi). \tag{1.10}$$

Secondly, for $a > 0$ let $D_a : L^2(\mathbb{R}) \to L^2(\mathbb{R})$ be the dilation operator with action

$$(D_a\psi)(x) = a^{1/4}\psi(a^{1/2}x). \tag{1.11}$$

A simple computation, again performed first in [12], shows that $S_{at} = D_a^* S_t D_a$ and consequently we find that

$$\Delta_{\langle at_1,at_2\rangle}(\psi) = \Delta_{\langle t_1,t_2\rangle}(D_a\psi). \tag{1.12}$$

For $a > 0$ and $t \in \mathbb{R}$, the unitaries D_a and S_t leave $\mathcal{H}^+$ invariant. Since for any $t_1 < t_2$ and $s_1 < s_2$, one can find a, b with $s_j = at_j + b$, $j = 1, 2$ it follows that $\Delta_{\langle t_1,t_2\rangle}(\mathcal{H}^+)$ remains fixed for any $t_1 < t_2$.

One easily sees that the amount of backflow over any continuous time interval must be bounded by

$$\Delta_{\langle t_1,t_2\rangle}(\mathcal{H}^+) \subseteq [-1, 1] \tag{1.13}$$

from the trivial bounds on probabilities. To improve the bound in (1.13), we follow a calculation first done by Bracken and Melloy. Let $\Pi^- : L^2(\mathbb{R}) \to L^2((-\infty, 0])$ be the projection onto the negative half-line. Then one can write the amount of backflow a normalised state $\psi \in \mathcal{H}^+$ exhibits over the interval (t_1, t_2) as

$$\Delta_{\langle t_1,t_2\rangle}(\psi) = \left\langle \psi_{t_2} \middle| \Pi^- \psi_{t_2} \right\rangle - \left\langle \psi_{t_1} \middle| \Pi^- \psi_{t_1} \right\rangle. \tag{1.14}$$

Writing $\phi = \hat{\psi}$ with supp $\phi \subseteq [0, \infty)$, for each $t \in \mathbb{R}$ one finds

$$\begin{aligned} \left\langle \psi_t \middle| \Pi^- \psi_t \right\rangle &= \left\langle S_t\psi \middle| \Pi^- S_t\psi \right\rangle \\ &= \left\langle \mathcal{F}^* e^{-iP^2t}\phi \middle| \Pi^- \mathcal{F}^* e^{-iP^2t}\phi \right\rangle \\ &= \left\langle \phi \middle| e^{iP^2t}\mathcal{F}\Pi^-\mathcal{F}^* e^{-iP^2t}\phi \right\rangle \end{aligned} \tag{1.15}$$

and hence

$$\Delta_{\langle t_1,t_2\rangle}(\psi) = \left\langle \phi \middle| B_{\langle t_1,t_2\rangle}\phi \right\rangle \tag{1.16}$$

where the manifestly self-adjoint Bracken–Melloy operator $B_{\langle t_1,t_2\rangle} : L^2(\mathbb{R}^+) \to L^2(\mathbb{R}^+)$ acting on quantum states with positive momentum in the momentum representation is given by

$$B_{\langle t_1,t_2\rangle} = S_{t_2}^*\mathcal{F}\Pi^-\mathcal{F}^*S_{t_2} - S_{t_1}^*\mathcal{F}\Pi^-\mathcal{F}^*S_{t_1}. \tag{1.17}$$

From equation (1.16), it is clear that $\Delta_{\langle t_1,t_2\rangle}(\psi)$ belongs to the numerical range[1] $\mathcal{N}(B_{\langle t_1,t_2\rangle})$ of the backflow operator $B_{\langle t_1,t_2\rangle}$ for any normalised $\psi \in L^2(\mathbb{R}^+)$. Consequently, the supremum value of $\Delta_{\langle t_1,t_2\rangle}(\mathcal{H}^+)$ is the top spectral point $\max \sigma(B_{\langle t_1,t_2\rangle})$.

Clearly, from (1.17), $B_{\langle t_1,t_2\rangle}$ is the difference of two non-negative self-adjoint bounded operators, each of which is bounded above by the identity. Hence, $B_{\langle t_1,t_2\rangle}$ is a self-adjoint bounded operator with spectrum $\sigma(B_{\langle t_1,t_2\rangle}) \subseteq [-1, 1]$.

To find an explicit form of $B_{\langle t_1,t_2\rangle}$, we first compute an explicit form of $\mathcal{F}\Pi^-\mathcal{F}^*$. Let ϕ be a compactly supported smooth function vanishing on the negative half-line,

[1] For a bounded operator A on a Hilbert Space $\mathcal{H}$, the numerical range is given by $\mathcal{N}(A) = \{\langle\phi|A\phi\rangle : \phi \in \mathcal{H}, \|\phi\| = 1\}$.

then

$$\begin{aligned}\left(\mathcal{F}\Pi^{-}\mathcal{F}^{*}\phi\right)(p) &= \frac{1}{2\pi}\int_{-\infty}^{0} dx\, e^{-ipx}\int_{0}^{\infty} dq\, e^{ixq}\phi(q)\\ &= \frac{1}{2\pi}\lim_{\epsilon\to 0^{+}}\int_{0}^{\infty} dq\,\phi(q)\int_{-\infty}^{0} dx\, e^{-i(p-q)x+\epsilon x}\\ &= \frac{1}{2\pi}\lim_{\epsilon\to 0^{+}}\int_{0}^{\infty} dq\,\frac{\phi(q)}{\epsilon - i(p-q)}\\ &= -\frac{1}{2\pi i}\lim_{\epsilon\to 0^{+}}\int_{0}^{\infty} dq\,\frac{\phi(q)}{p-q+i\epsilon}\\ &= -\frac{1}{2\pi i}\,\mathrm{PV}\int_{0}^{\infty} dq\frac{\phi(q)}{p-q}\end{aligned} \tag{1.18}$$

where on the second line of (1.18), we have made use of Fubini's theorem. On the final line PV denotes the principal value integral

$$\lim_{\epsilon\to 0^{+}}\left(\int_{0}^{p-\epsilon}+\int_{p+\epsilon}^{\infty}\right).$$

Both sides of (1.18) are continuous in ϕ, and since this holds on a dense subset of $L^2(\mathbb{R}^+)$, it follows that (1.18) holds for all $\phi\in L^2(\mathbb{R}^+)$. Furthermore, the calculation in (1.18) demonstrates the well known fact that $\mathcal{F}^{*}\Pi^{-}\mathcal{F}=-2i\mathfrak{H}$ [26] where $\mathfrak{H}$ is the restriction of the Hilbert transform to $L^2(\mathbb{R}^+)$. Returning to (1.17), we find that the Bracken–Melloy operator has the explicit form

$$\left(B_{\langle t_1,t_2\rangle}\phi\right)(p) = -\frac{1}{2\pi i}\int_{0}^{\infty} dq\,\frac{e^{it_2(p^2-q^2)}-e^{it_1(p^2-q^2)}}{p-q}\phi(q) \tag{1.19}$$

which holds pointwise almost everywhere for any $\phi\in L^2(\mathbb{R}^+)$. Note that the principal value is no longer required since the integral kernel is finite on the diagonal. A particular special case is

$$\left(B_{\langle-\tau,\tau\rangle}\phi\right)(p) = -\frac{1}{\pi}\int_{0}^{\infty} dq\frac{\sin\tau(p^2-q^2)}{p-q}\phi(q) \tag{1.20}$$

for any $\tau>0$. Both (1.19) and (1.20) were first given in [12] and will be generalised to new backflow operators in this thesis.

The backflow operators satisfy a covariance relation expressed as

$$S_{\tau}^{*}B_{\langle t_1,t_2\rangle}S_{\tau} = B_{\langle t_1+\tau,t_2+\tau\rangle}. \tag{1.21}$$

Furthermore, for $a>0$, the dilation operator alters a backflow operator as

$$D_{a}^{*}B_{\langle t_1,t_2\rangle}D_{a} = B_{\langle a^{-1}t_1,a^{-1}t_2\rangle}. \tag{1.22}$$

Combining (1.21) and (1.22), for any $\tau > 0$, we have

$$B_{\langle t_1,t_2\rangle} = S^*_{(t_1+t_2)/2} D^*_{\sqrt{2\tau/(t_2-t_1)}} B_{\langle -\tau,\tau\rangle} D_{\sqrt{2\tau/(t_2-t_1)}} S_{(t_1+t_2)/2} \tag{1.23}$$

which shows that all the operators $B_{\langle t_1,t_2\rangle}$ for $t_1 < t_2$ are unitarily equivalent and therefore have the same spectrum. Note also that $t \mapsto S_t^* \mathfrak{H} S_t$ is strongly continuous, because S_t and S_t^* are strongly continuous and uniformly bounded. It follows that $(t_1, t_2) \mapsto B_{\langle t_1,t_2\rangle}$ is strongly continuous on the set $\mathcal{T}_2 = \{(t_1, t_2) \in \mathbb{R}^2 : t_1 < t_2\}$.

One final unitary transform will play a central role in the thesis. For any $\tau > 0$ we may define a unitary $U_\tau : L^2(\mathbb{R}^+, dk) \to L^2(\mathbb{R}^+, dq)$ by

$$(U_\tau \phi)(q) = \frac{\phi(\sqrt{q/\tau})}{\sqrt{2}(q\tau)^{1/4}}, \tag{1.24}$$

where q is a dimensionless variable (representing action in units of $\hbar$). Making the change of variables $q \mapsto q^2$, one finds that

$$(U_\tau B_{\langle t_1,t_2\rangle} U_\tau^* \varphi)(p) = -\frac{1}{4\pi i} \int_0^\infty dq \frac{(e^{it_2(p-q)/\tau} - e^{it_1(p-q)/\tau})}{p-q} \left[\left(\frac{p}{q}\right)^{1/4} + \left(\frac{p}{q}\right)^{-1/4} \right] \varphi(q) \tag{1.25}$$

for $\varphi \in L^2(\mathbb{R}^+, dq)$ Accordingly, every single backflow operator $B_{\langle t_1,t_2\rangle}$ is unitarily equivalent to the bounded operator $C = U_\tau B_{\langle -\tau,\tau\rangle} U_\tau^* \in \mathcal{B}(L^2(\mathbb{R}^+, dq))$ given by

$$(C\varphi)(p) = -\frac{1}{2\pi} \int_0^\infty dq \frac{\sin(p-q)}{p-q} \left[\left(\frac{p}{q}\right)^{1/4} + \left(\frac{p}{q}\right)^{-1/4} \right] \varphi(q). \tag{1.26}$$

By definition, $c_{\mathrm{BM}} = \max \sigma(C)$, and as $\|C\| \leq 1$ it follows that $\sigma(C) \subset [-1, c_{\mathrm{BM}}]$.

Since the original calculation by Bracken and Melloy in 1994 that $c_{\mathrm{BM}} \approx 0.04$, there have been two further supposed improvements. In this thesis, we will present a new value for c_{BM}, accurate to 6 significant figures. The first was by Eveson, Fewster and Verch ($c_{\mathrm{BM}} \approx 0.03845(2)$) [29] and shortly thereafter by Penz *et al.* ($c_{\mathrm{BM}} \approx 0.0384517$) [53]. Recently, Trillo, Le and Navascués showed that $0.0315 c_{\mathrm{BM}} < 0.072$ [64]. The upper bound of 0.072 is of significance here since it is the first known upper bound of the c_{BM}. Due to the small value of c_{BM}, experimental verification of QB is an ongoing effort. Goussev has shown that when considering an angular analogue of QB for a particle on a ring, the associated maximum possible backflow is larger than in the linear case with $c_{\mathrm{ring}} \approx 2.6\, c_{\mathrm{BM}}$ [39]. Angular QB has also been studied in the case of a charged massless fermion [23]. Palmero *et al.* have shown how QB could be experimentally verified by measuring density fluctuations in a Bose-Einstein

condensate [52]. Bracken has explored a whole family of QB related problems where the quantum states considered have their momentum restricted to $p > p_0$ for some fixed $p_0 \in \mathbb{R}$ [11]. Other variations of QB that have been considered include but are not limited to: QB in two dimensions [4], QB in a relativistic setting [3], the relation between QB and the local wave number [7] and QB across a black hole horizon [9]. Finally, Bostelmann, Cadamuro and Lechner [10] studied the extent to which scattering states exhibit the backflow effect for general short-range potentials, while Yearsley and Halliwell showed that the dependency of the maximal QB on $\hbar$ reappears [68] once a realistic measurement apparatus is considered.

We note in particular here that all previous methods to numerically investigate quantum backflow have employed lattice methods, which have the following drawback. Any lattice method depends on the lattice spacing Δp, as well as the maximum lattice size $p_{\max}$. Therefore any attempt to calculate c_{BM} is found by taking the limit of some function $c(\Delta p, p_{\max})$ as $\Delta p \to 0$ and $p_{\max} \to \infty$. In practise one lets Δp and $p_{\max}$ depend on some independent parameter n so that $\Delta p(n) \to 0$ and $p_{\max}(n)$ as $n \to \infty$. Furthermore, previous attempts to estimate c_{BM}, such as in [53] and [29] have modelled the relation $c(\Delta p(n), p_{\max}(n))$ using a simple power law. This lays the basis for the numerical investigation that takes place in this thesis.

1.3 PLAN OF THE THESIS

Throughout the thesis, we generalise and expand on previous work on the quantum backflow problem. Previously, the question of how much backflow quantum states can exhibit has been restricted to the case of a single continuous time interval. In chapter 2, we introduce the notion of a state undergoing QB over multiple disjoint time intervals. This is done by first fixing an arbitrary integer number M and increasing list of times $t_1, t_2, \ldots, t_{2M-1}, t_{2M}$ which parametrise the M intervals as $[t_{2j-1}, t_{2j}]_{j=1}^{M}$. Given a collection of such intervals, we construct an associated M-fold backflow operator in the spirit of Bracken and Melloy. An explicit formula for such operators can be found in (2.25). From here, we introduce the phenomenon of *quantum overflow*. This is the existence of quantum states that exhibit more probability transfer in the same direction as their momentum than is classically allowed.

From there, by writing M-fold backflow operators as a sum of single backflow

operators, we establish general outer bounds on their spectra. This is given in theorem 2.3.1. After constructing a particular class of multiple backflow operators $C^{(M)}$ with closed form integral kernels, we show in theorem 2.4.1 that for each M one can find an M-fold backflow operator whose spectral suprema and infima grow as $\mathcal{O}(M^{1/4})$. This establishes that for any amount of backflow $b > 0$, one can find an $M \in \mathbb{N}$ and collection of times $t_1, t_2, \ldots, t_{2M-1}, t_{2M}$ parametrising disjoint time intervals and a state ψ_M exhibiting backflow larger than b. An analogous statement exists for quantum overflow. In theorem 2.5.1 and theorem 2.5.2, we establish various properties of the maximum amount of backflow and overflow that states can exhibit for a given parametrisation of time intervals. Particular care is taken in the limiting case where two disjoint time intervals coincide.

In chapter 3, we conduct a detailed numerical study of multiple backflow states for the specific multiple backflow operators $(C^{(M)})_{M=1}^{4}$. To do this we make use of a generalised Rayleigh-Ritz method. Given parameters $a > 0, |\delta| < 1$, we describe an arbitrary multiple backflow operator in terms of a dense sequence of exponentially damped monomial vectors $(\psi_{n,a,\delta})_{n=0}^{\infty} \subset L^2(\mathbb{R}^+)$ where

$$\psi_{n,a,\delta}(p) = p^{n+\delta} e^{-ap}.$$

The method, encapsulated in lemma 3.2.1, involves first fixing parameters a, δ and $N \in \mathbb{N}$ from which Hermitian matrices $C^{(M)}(a,\delta), P(a,\delta) \in \mathbb{C}^{(N+1)\times(N+1)}$ are generated. The matrix $C^{(M)}(a,\delta)$ is made up of the matrix elements of $C^{(M)}$ with respect to $(\psi_{n,a,\delta})_{n=0}^{N}$, and $P(a,\delta)$ is the Gram matrix for the same finite sequence of vectors. Formulae for these matrix elements can be found in appendix C and (3.18). With these matrices in place, the maximum backflow and overflow values exhibited by states in the span of $(\psi_{n,a,\delta})_{n=0}^{N}$ can be found by finding the largest and smallest λ that solve the generalised eigenvalue equation

$$C^{(M)}(a,\delta)v = \lambda P(a,\delta)v.$$

Furthermore, the associated such v can be used to construct time $t = 0$ quantum states $\psi_{\text{back/over}} \in L^2(\mathbb{R}^+)$ that exhibit backflow and overflow respectively over the time intervals that the operators $C^{(M)}$ correspond. Plots of these normalised quantum states, after multiplication by $p \mapsto p^{3/4}$, can be found in figures 3.4 to 3.10. A specific comment is made regarding the types of states exhibiting $C^{(1)}$ expectation value close to the lower bound -1. Plots of such states can be found in figure 3.11.

The final section of chapter 3 is devoted to a numerically accelerating the sequence of generalised eigenvalues found to better approximate c_{BM}. Using such techniques, we find a value of $c_{\mathrm{BM}} = 0.0384506$ to 6 significant figures. This is of note because of its contrast to the previous accepted value of 0.038452 found in [53] and [29].

The content of chapters 4 and 5 is made up of a more detailed numerical study of a single backflow operator, C, which is unitarily equivalent to the Bracken–Melloy operator. This is the same operator studied in [29]. As discussed in section 4.1.1, we are inspired by the conjecture of Halliwell and Yearsley that the maximizing vector of the Bracken–Melloy operator, should it exist, is asymptotic to $\sin(p^2)/p$. Expressed in the variables we use, this would suggest that a maximizing vector of C is asymptotic to $q^{-5/4}\sin(q)$. Using the same method as in chapter 3, namely lemma 3.2.1, we describe the operator C in terms of a doubly infinite sequence $(\varphi_{n=0}^{\infty}) \subset L^2(\mathbb{R}^+)$ where

$$\varphi_n^{\pm}(q) = \frac{1}{\pi} q^{\pm 1/4} \frac{\sin(q - n\pi)}{q - n\pi}, \qquad p > 0.$$

The density of this sequence is given in theorem 4.1.2 which is proven using methods from Paley-Wieiner and distribution theory. This method has the advantage that for each N chosen, the largest λ that solves an assoicated generalised eigenvalue problem provides a rigorous lower bound of c_{BM}. That is because this method solves for the largest backflow vector belonging to the span of $(\varphi_n^{\pm})_{n=0}^{N} \subset L^2(\mathbb{R}^+)$.

With this density result in place, for each N we construct matrices $C^{[N]}$ and $P^{[N]}$ whose generalised eigenvalue problem is solved to approximate c_{BM}. The remainder of chapter 3 is taken up by the computation of the matrix elements of $C^{[N]}$ and $P^{[N]}$. The reader is guided to (4.61) and (4.60), as well as (4.63) to (4.114) for the full formulae used. All of these formulae are proven in appendix D.

With these matrices constructed, in chapter 5 we describe a multi-stage numerical procedure for the computation of the generalised eigenpairs $(\lambda^{(N)}, V^{(N)})$ solving

$$C^{[N]} v^{(N)} = \lambda^{(N)} P^{[N]} v^{(N)}.$$

The strategy involves converting the generalised eigenvalue problem to a standard eigenvalue problem and is described in lemma 5.2.1. The transformation is done in such a way that the resulting matrix has an increased gap between the top two eigenvalues, thus allowing for faster computation of the top eigenvalue using the power method. A plot of the resulting sequence of eigenvalues is given in figure 5.1.

Of particular note is the largest rigorous lower bound λ_{1700} for c_{BM} which we find to be $\lambda_{1700} = 0.03837$ to 4 significant figures. Further, from this method we obtain a simple formulae, given in (5.19), for a backflow vector. The vector exhibits just under one third of the maximum backflow for a single interval and is a linear combination of just four of the basis vectors $(\varphi_n^{\pm})_{n=0}^{1}$. Using 602 basis vectors, we obtain a plot approximating the backflow maximizing vector in figure 5.6, which matches previous work done by Halliwell and Yearsley in [69] as well as that by Penz et. al. in [53]. A discussion on the numerical analysis of $(\lambda^{(N)})_{N=1}^{1700}$ is given in section 5.4.

— 2 —

Multiple Quantum Backflow

2.1 CLASSICAL STATISTICAL MECHANICS

Consider a classical ensemble of particles $\mathcal{C}$ of mass μ under free evolution on the line. The phase diagram is given in figure 2.1.

Figure 2.1: Phase diagram for free time evolution with initial position X_0

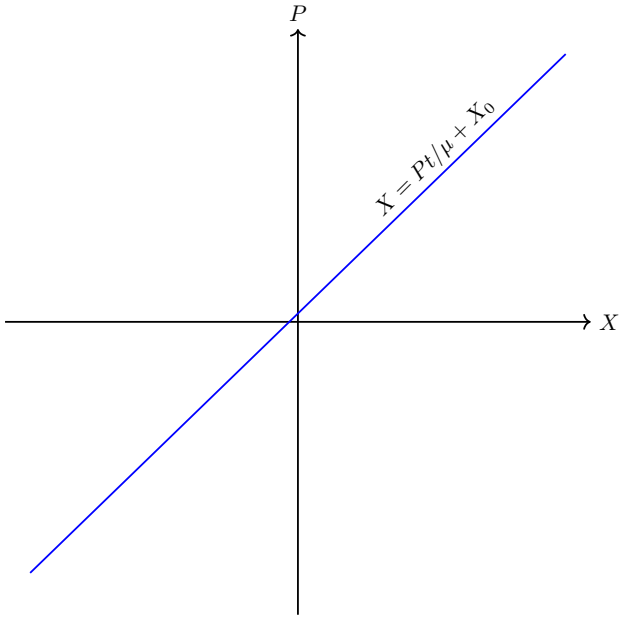

Let the distribution of particles on phase space $\mathcal{P} = \mathbb{R}^2$ at time t be given by a probability measure ρ_t so that a randomly chosen member of the ensemble has phase

space position (X, P) in a Borel subset $S \subseteq \mathcal{P}$ at time t with probability

$$\mathrm{Prob}_\rho((X,P) \in S \mid t) = \rho_t(S), \tag{2.1}$$

where we write $\rho = \rho_0$ for the state at time $t = 0$. Denote the continuous functions on phase space by $\mathcal{C}(\mathcal{P})$. The ensemble average of an observable $f \in \mathcal{C}(\mathcal{P})$ at time t is given by $\int f \, d\rho_t = \int f \circ \tau_t \, d\rho$ by Liouville's Theorem, where

$$\tau_t(x,p) = (x + pt/\mu, p) \tag{2.2}$$

is the forwards Hamiltonian time evolution through time t. Correspondingly, we find that $\rho_t(S) = \rho(\tau_t^{-1}(S))$. If the ensemble only contains particles with non-negative momentum then one has

$$\rho(S) = \rho(S \cap (\mathbb{R} \times [0,\infty))) \tag{2.3}$$

for any Borel subset $S \subseteq \mathcal{P}$, and consequently,

$$\begin{aligned}\mathrm{Prob}_\rho(X \in (-\infty,0) \mid t) &= \rho_t((-\infty,0) \times \mathbb{R}) \\ &= \rho(\tau_t^{-1}((-\infty,0) \times \mathbb{R})) \cap (\mathbb{R} \times [0,\infty)) \\ &= \mathrm{Prob}_\rho((X,P) \in \{(x,p) \in \mathcal{P} : x < -pt/\mu,\ p \geq 0\}).\end{aligned} \tag{2.4}$$

The difference between the probabilities of finding a randomly chosen particle on the left-hand half line at time t' and an earlier time t is therefore

$$\mathrm{Prob}_\rho(X \in (-\infty,0) \mid t') - \mathrm{Prob}_\rho(X \in (-\infty,0) \mid t) = -\mathrm{Prob}_\rho((X,P) \in S_{t,t'}), \tag{2.5}$$

where

$$S_{t,t'} = \{(x,p) \in \mathcal{P} : -pt'/\mu \leq x < -pt/\mu,\ p \geq 0\} \tag{2.6}$$

for any $t' > t$. Note that we may replace $p \geq 0$ by $p > 0$ in the formula $S_{t,t'}$ without loss because $S_{t,t'} \cap (\mathbb{R} \times \{0\}) = \emptyset$. Accordingly, $-\rho(S_{t,t'})$ measures the probability backflow between times t and t'; as it is clearly nonpositive, we see that there is no classical backflow.

Now consider adding together the backflow for a set of disjoint time intervals. Specifically, given $M \in \mathbb{N}$ and times $t_1 < t_2 < \cdots < t_{2M-1} < t_{2M}$, the total amount of probability backflow is given by

$$\begin{aligned}\Delta^{(M)}_{\text{classical}}(\rho) &:= \sum_{j=1}^{M} (\mathrm{Prob}_\rho(X \in (-\infty,0) \mid t_{2j}) - \mathrm{Prob}_\rho(X \in (-\infty,0) \mid t_{2j-1})) \\ &= -\sum_{j=1}^{M} \mathrm{Prob}_\rho(X \in S_{t_{2j-1},t_{2j}}) = -\mathrm{Prob}_\rho\left(X \in \bigcup_{j=1}^{M} S_{t_{2j-1},t_{2j}}\right)\end{aligned} \tag{2.7}$$

because the sets $S_{t_{2j-1},t_{2j}}$ are disjoint for distinct j.

It follows that, for a classical ensemble with non-negative momentum, the total amount of probability backflow over multiple disjoint time periods is bounded by

$$-1 \leq \Delta^{(M)}_{\text{classical}}(\rho) \leq 0 \tag{2.8}$$

for every M. In particular, a classical ensemble cannot exhibit positive probability backflow, and the probability transfer in the forward direction is bounded by unity. By contrast, it is well known that quantum particles can exhibit backflow over a single time interval, thus violating the upper bound in the analogue of (2.8). One of the main results of this paper is that the violation increases with M, and that the lower bound of (2.8) is also violated in quantum theory for $M \geq 2$.

2.2 QUANTUM MECHANICS

We turn to the quantum case, using units in which $\hbar = 1$. Consider the motion of a free quantum particle of mass μ with normalised state vector $\psi_t \in L^2(\mathbb{R}^+)$ at time t, whose dynamics is governed by the free Schrödinger equation

$$i\partial_t \psi_t = -\frac{1}{2\mu}\partial_x^2 \psi_t \tag{2.9}$$

and initial condition $\psi_0 = \psi$, so $\psi_t = e^{-ip^2 t}\psi$, where $p = -i\partial_x$ and we have chosen units so that $\mu = \frac{1}{2}$, as we shall do from now on for simplicity. The states with nonnegative momentum form the subspace

$$\mathscr{H}_+ = \{\psi \in L^2(\mathbb{R}, dx) : \operatorname{supp} \hat{\psi} \subseteq [0, \infty)\}, \tag{2.10}$$

where

$$\hat{\psi}(p) = \frac{1}{\sqrt{2\pi}} \int_{\mathbb{R}} dx\, e^{-ipx}\psi(x) \tag{2.11}$$

is the Fourier transform of ψ.

Let $t_1 < t_2$. The probability backflow exhibited by the normalised $t = 0$ state ψ between times t_1 and t_2 is quantified by

$$\Delta_{\langle t_1,t_2\rangle}(\psi) := \text{Prob}_\psi(X < 0 \mid t_2) - \text{Prob}_\psi(X < 0 \mid t_1). \tag{2.12}$$

where $\text{Prob}_\psi(X \in R \mid t) = \int_R dx\, |\psi_t(x)|^2$ is the probability of measuring the position of the particle to lie in the region $R \subseteq \mathbb{R}$ at time t. There are simple examples of

states $\psi \in \mathscr{H}_+$ for which $\Delta_{\langle t_1,t_2\rangle}(\psi) > 0$, showing that quantum mechanical particles can exhibit nontrivial backflow (see e.g., [41]) whereas the classical backflow quantity for particles always lies in $[-1, 0]$.

We are interested in the range of values assumed by $\Delta_{\langle t_1,t_2\rangle}(\psi)$ as ψ varies over normalised states of $\mathscr{H}_+$. As a difference of probabilities, its range is contained in $[-1, 1]$. Moreover, because $\mathscr{H}_+$ is invariant under both the free time evolution and dilations, the range is invariant under $\langle t_1, t_2\rangle \mapsto \langle t_1+\tau, t_2+\tau\rangle$ and $\langle t_1, t_2\rangle \mapsto \langle \lambda t_1, \lambda t_2\rangle$ for all $\tau \in \mathbb{R}$ and all $\lambda > 0$. This is given in more detail in equations (1.10) and (1.12). It follows that the range is independent of both t_1 and t_2, provided $t_1 < t_2$, as was observed by Bracken and Melloy [13]. As noted in [40], Dollard's lemma (Lemma 4 of [25]) shows that $\mathrm{Prob}_\psi(X < 0 \mid t_1) \to 1$ as $t_1 \to -\infty$ and $\mathrm{Prob}_\psi(X < 0 \mid t_2) \to 0$ as $t_2 \to +\infty$ for any fixed $\psi \in \mathscr{H}_+$, thus giving $\Delta_{\langle t_1,t_2\rangle}(\psi) \to -1$ when both limits are taken. Intuitively, Dollard's Lemma shows that the probability of finding a quantum particle with positive momentum in the negative (resp. positive) half-line vanishes in the far future (resp. past) limit. Thus -1 belongs to the closure of the range of $\Delta_{\langle t_1,t_2\rangle}$ for any $t_1 < t_2$.

More detailed information can be found by reformulating backflow in terms of operators. For normalised $\psi \in \mathscr{H}_+$, a calculation due to Bracken and Melloy [13] gives $\Delta_{\langle t_1,t_2\rangle}(\psi)$ as a quadratic form

$$\Delta_{\langle t_1,t_2\rangle}(\psi) = -\frac{1}{2\pi i}\int_0^\infty dp \int_0^\infty dq\, \frac{e^{i(p^2-q^2)t_2} - e^{i(p^2-q^2)t_1}}{p-q}\hat{\psi}^*(p)\hat{\psi}(q), \tag{2.13}$$

which can be written as

$$\Delta_{\langle t_1,t_2\rangle}(\psi) = \left\langle \hat{\psi}\middle| B_{\langle t_1,t_2\rangle}\hat{\psi}\right\rangle. \tag{2.14}$$

An algebraic form of (2.14) was given in (1.15). Here, the operator $B_{\langle t_1,t_2\rangle}$ on $L^2(\mathbb{R}^+)$ has the following properties, which are established in the introduction, drawing on arguments in [53].

Theorem 2.2.1. *For any $t_1 < t_2$, $B_{\langle t_1,t_2\rangle}$ is a bounded self-adjoint operator with $\|B_{\langle t_1,t_2\rangle}\| = 1$. There is a unitary equivalence between $B_{\langle t_1,t_2\rangle}$ and the operator $C \in \mathcal{B}(L^2(\mathbb{R}^+, dq))$ with action*

$$(C\varphi)(p) = -\frac{1}{2\pi}\int_0^\infty dq \frac{\sin(p-q)}{p-q}\left[\left(\frac{p}{q}\right)^{1/4} + \left(\frac{p}{q}\right)^{-1/4}\right]\varphi(q) \tag{2.15}$$

on $\varphi \in L^2(\mathbb{R}^+, dq)$, where (2.15) holds pointwise almost everywhere on $\mathbb{R}^+$. The map $(t_1, t_2) \mapsto B_{\langle t_1,t_2\rangle}$ is strongly continuous on $\{(t_1, t_2) \in \mathbb{R}^2 : t_1 < t_2\}$.

The unitary equivalence in Theorem 2.2.1 is a combination of translations, scale transformation and a change of variables. It follows from (2.14) that the range of $\Delta_{\langle t_1,t_2\rangle}(\psi)$, as ψ varies over the normalised elements of $\mathscr{H}_+$, is the *numerical range* of the operator $B_{\langle t_1,t_2\rangle}$. We recall the definition and main properties of numerical range of a bounded operator (see e.g., Section 9.3 of [20]). We denote the spectrum of a bounded operator A by $\sigma(A)$.

Definition 2.2.2. *Let A be a bounded self-adjoint operator on a Hilbert space $\mathscr{H}$. The* numerical range $\mathcal{N}(A) \subset \mathbb{R}$ *of A is given by*

$$\mathcal{N}(A) = \left\{ \frac{\langle\phi|A\phi\rangle}{\langle\phi|\phi\rangle} \Big| \phi \in \mathscr{H} \setminus \{0\} \right\}. \tag{2.16}$$

One has $\mathcal{N}(A) = \mathcal{N}(UAU^*)$ for any unitary $U \in \mathcal{B}(\mathscr{H})$, and

$$\sigma(A) \subseteq \overline{\mathcal{N}(A)} = \operatorname{Conv}\sigma(A), \tag{2.17}$$

where $\overline{\cdot}$ denotes topological closure and Conv *the convex hull. In particular $\sigma(A)$ and $\mathcal{N}(A)$ have the same supremum and infimum.*

It follows immediately that, for all $t_1 < t_2$,

$$\overline{\mathcal{N}(B_{\langle t_1,t_2\rangle})} = \operatorname{Conv}\sigma(C) \subseteq [-1,1], \tag{2.18}$$

using $\|C\| = 1$. We have already noted that $-1 \in \overline{\mathcal{N}(B_{\langle t_1,t_2\rangle})}$. Defining the *Bracken–Melloy constant* as the largest spectral point of C,

$$c_{\mathrm{BM}} = \sup\sigma(C) = \max\sigma(C), \tag{2.19}$$

the possible values of the backflow $\Delta_{\langle t_1,t_2\rangle}(\psi)$ obey

$$-1 \leq \Delta_{\langle t_1,t_2\rangle}(\psi) \leq c_{\mathrm{BM}} \tag{2.20}$$

for all normalised $\psi \in \mathscr{H}_+$. Note that the second equality in (2.19) holds due to the spectrum of a bounded operator being closed.

These ideas, first exhibited in [12], are readily generalised to consider the total backflow over $M \geq 1$ disjoint time intervals $[t_{2j-1}, t_{2j}]$ for $1 \leq j \leq M$, which can be represented by a list $\langle \boldsymbol{t}_M\rangle = \langle t_1, ..., t_{2M}\rangle$ in strictly increasing order.

Definition 2.2.3. *For positive integer M, let*

$$\mathcal{T}_M = \left\{ \langle \boldsymbol{t}_M\rangle = \langle t_1, ..., t_{2M}\rangle \Big| t_1 < t_2 < \cdots < t_{2M-1} < t_{2M} \right\}. \tag{2.21}$$

The total probability backflow exhibited by the initial state $\psi \in L^2(\mathbb{R}, dx)$ over the intervals parameterised by $\langle \boldsymbol{t}_M \rangle \in \mathcal{T}_M$ is defined as

$$\Delta^{(M)}_{\langle \boldsymbol{t}_M \rangle}(\psi) := \sum_{j=1}^{M} \left(\mathrm{Prob}_\psi(X < 0 | t = t_{2j}) - \mathrm{Prob}_\psi(X < 0 | t = t_{2j-1}) \right), \tag{2.22}$$

so that, for example, $\Delta^{(1)}_{\langle \boldsymbol{t}_1 \rangle}(\psi) = \Delta_{\langle t_1, t_2 \rangle}(\psi)$.

For normalised $\psi \in \mathscr{H}_+$, one has

$$\Delta^{(M)}_{\langle \boldsymbol{t}_M \rangle}(\psi) = \left\langle \hat{\psi} \middle| B^{(M)}_{\langle \boldsymbol{t}_M \rangle} \hat{\psi} \right\rangle, \tag{2.23}$$

where the *M-fold backflow operator*

$$B^{(M)}_{\langle \boldsymbol{t}_M \rangle} = \sum_{j=1}^{M} B_{\langle t_{2j}, t_{2j-1} \rangle} \tag{2.24}$$

is a bounded self-adjoint operator on $L^2(\mathbb{R}^+, dq)$ acting as

$$\left(B^{(M)}_{\langle \boldsymbol{t}_M \rangle} \phi \right)(p) = -\frac{1}{2\pi i} \int_0^\infty dq \, \sum_{k=1}^{M} \frac{e^{i(p^2 - q^2)t_{2k}} - e^{i(p^2 - q^2)t_{2k-1}}}{p - q} \phi(q). \tag{2.25}$$

In the same way as before, the set of possible values taken by $\Delta^{(M)}_{\langle \boldsymbol{t}_M \rangle}(\psi)$ for normalised $\psi \in \mathscr{H}_+$ is the numerical range of $B^{(M)}_{\langle \boldsymbol{t}_M \rangle}$ and can be studied via its spectrum. As before, if $\Delta^{(M)}_{\langle \boldsymbol{t}_M \rangle}(\psi) > 0$, we say that the state exhibits quantum backflow. We will also investigate states $\psi \in \mathscr{H}_+$ for which $\Delta^{(M)}_{\langle \boldsymbol{t}_M \rangle}(\psi) < -1$ for $M \geq 2$, a phenomenon we will call *quantum overflow*.

The following straightforward argument shows the existence of states exhibiting quantum overflow with $M = 2$. Fix $t_1 < t_2$ and suppose $\psi \in \mathscr{H}_+$ is such that $\Delta^{(1)}_{\langle t_1, t_2 \rangle}(\psi) = \lambda > 0$, i.e., there is nontrivial backflow between t_1 and t_2. Taking $T > \max(|t_1|, |t_2|)$, one can write the total backflow over $[-T, t_1] \cup [t_2, T]$ as

$$\Delta^{(2)}_{\langle -T, t_1, t_2, T \rangle}(\psi) = \Delta^{(1)}_{\langle -T, T \rangle}(\psi) - \Delta^{(1)}_{\langle t_1, t_2 \rangle}(\psi). \tag{2.26}$$

For any fixed $\epsilon \in (0, \lambda)$, one can find T sufficiently large such that $\Delta^{(1)}_{\langle -T, T \rangle}(\psi) < -1 + \epsilon$, because Dollard's lemma [25] implies that $\Delta^{(1)}_{\langle -T, T \rangle}(\psi) \to -1$ as $T \to \infty$. It follows that

$$\Delta^{(2)}_{\langle -T, t_1, t_2, T \rangle}(\psi) < -1 - \lambda + \epsilon < -1, \tag{2.27}$$

showing that the state ψ exhibits quantum overflow on $[-T, t_1] \cup [t_2, T]$. As ψ can be chosen to make λ arbitrarily close to c_{BM} and ϵ could be chosen arbitrarily

small, this already shows that 2-fold overflow can approach $-1 - c_{\mathrm{BM}}$ over suitable intervals. In this example, we chose the time interval after fixing the state, without any control on the size of T. However, in Section 2.4, we will consider M equally spaced intervals of equal width, and show that the total M-fold overflow can be made unboundedly negative as M increases, and similarly that the M-fold backflow can be made unboundedly positive as M increases.

The invariance of $\mathscr{H}_+$ under time evolution and dilations does not completely fix $\mathcal{N}(B^{(M)}_{\langle \boldsymbol{t}_M \rangle})$ if $M > 1$. However, time translation invariance shows that $\mathcal{N}(B^{(M)}_{\langle \boldsymbol{t}_M \rangle})$ is a function of the successive differences $(t_2 - t_1, t_3 - t_2, \ldots, t_{2M} - t_{2M-1})$, and the scaling invariance shows that it may be expressed in terms of successive ratios of these differences. For each $M > 1$, then, there are *backflow and overflow functions* $b^{(M)}_{\mathrm{back/over}} : \mathbb{R}^{2M-2}_{>0} \to \mathbb{R}$ (writing $\mathbb{R}^k_{>0} = (0,\infty)^{\times k}$) so that

$$\sup \mathcal{N}(B^{(M)}_{\langle \boldsymbol{t}_M \rangle}) = b^{(M)}_{\mathrm{back}}\left(\frac{t_3 - t_2}{t_2 - t_1}, \ldots, \frac{t_{2M} - t_{2M-1}}{t_{2M-1} - t_{2M-2}}\right) = b^{(M)}_{\mathrm{back}}(\mathrm{srsd}\langle \boldsymbol{t}_M \rangle) \tag{2.28}$$

$$\inf \mathcal{N}(B^{(M)}_{\langle \boldsymbol{t}_M \rangle}) = b^{(M)}_{\mathrm{over}}\left(\frac{t_3 - t_2}{t_2 - t_1}, \ldots, \frac{t_{2M} - t_{2M-1}}{t_{2M-1} - t_{2M-2}}\right) = b^{(M)}_{\mathrm{over}}(\mathrm{srsd}\langle \boldsymbol{t}_M \rangle), \tag{2.29}$$

where srsd is the operation of forming the sequence of successive ratios of successive differences. By convention, we write $b^{(1)}_{\mathrm{back}} = c_{\mathrm{BM}}$, $b^{(1)}_{\mathrm{over}} = -1$ and dictate that srsd maps any element of $\mathcal{T}_1$ to the empty list.

The dependence of the backflow and overflow functions on the successive ratios of successive differences of times, as in (2.28) and (2.29) can be seen by the following argument. Take some function $f : \mathbb{R}^{2M} \to \mathbb{R}$ obeying $f(t_1, \ldots, t_{2M}) = f(t_1 + t, \ldots, t_{2M} + t)$ for all $t, t_1, \ldots, t_{2M} \in \mathbb{R}$ (scalar translation invariance) and dilation invariance. For $j = 1, \ldots, 2M-1$ let $d_j = t_{j+1} - t_j$ be the sequence of successive differences. Immediately it is seen that

$$f(t_1, t_2, \ldots, t_{2M}) = f(0, t_2 - t_1, \ldots, t_{2M} - t_1) = f(0, d_1, d_1 + d_2, \ldots, d_1 + \cdots + d_{2M-1}) \tag{2.30}$$

by the scalar translation invariance property. Now by dilation invariance and (2.30) we find

$$f(t_1, \ldots, t_{2M}) = f\left(0, 1, \frac{d_1 + d_2}{d_2}, \ldots, \frac{d_1 + \cdots + d_{2M-1}}{d_2}\right) \tag{2.31}$$

$$= f\left(0, 1, \frac{t_3 - t_2}{t_2 - t_1}, \ldots, \frac{t_{2M} - t_{2M-1}}{t_2 - t_1}\right) \tag{2.32}$$

Let $r_j = (t_{j+2} - t_{j+1})/(t_{j+1} - t_j)$ for $j = 1, ..., 2M-2$, then by a simple calculation we find that

$$r_1 \cdots r_k = \frac{t_{k+2} - t_{k+1}}{t_2 - t_1} \qquad \text{for } k = 1, \ldots, 2M-2. \tag{2.33}$$

Hence

$$f(t_1, \ldots, t_{2M}) = f(0, 1, r_1, \ldots, r_1 \cdots r_{2M-2}) = f\left(0, 1, \frac{t_3 - t_2}{t_2 - t_1}, \ldots, \frac{t_{2M} - t_{2M-1}}{t_{2M-1} - t_{2M-2}}\right) \tag{2.34}$$

and so the backflow and overflow functions depend only on the successive ratios of the successive differences of the times.

As we now describe, the backflow and overflow functions are semicontinuous.

Lemma 2.2.4. *For each $M > 1$, the functions $b^{(M)}_{\text{back/over}}$ are lower/upper semicontinuous on $\mathbb{R}^{2M-2}_{>0}$. That is, for all $u_0 \in \mathbb{R}^{2M-2}_{>0}$, one has*

$$\liminf_{u \to u_0} b^{(M)}_{\text{back}}(u) \geq b^{(M)}_{\text{back}}(u_0), \qquad \limsup_{u \to u_0} b^{(M)}_{\text{over}}(u) \leq b^{(M)}_{\text{over}}(u_0), \tag{2.35}$$

as $u \to u_0$ in $\mathbb{R}^{2M-2}_{>0}$.

Proof. The function $\langle \boldsymbol{t}_M \rangle \mapsto B^{(M)}_{\langle \boldsymbol{t}_M \rangle}$ is strongly continuous on $\mathcal{T}_M$ due to (2.24) and Theorem 2.2.1, so for each normalised $\phi \in L^2(\mathbb{R}^+, dq)$, $\langle \boldsymbol{t}_M \rangle \mapsto \left\langle \phi \middle| B^{(M)}_{\langle \boldsymbol{t}_M \rangle} \phi \right\rangle$ is continuous on $\mathcal{T}_M$. As $\langle \boldsymbol{t}_M \rangle \mapsto \sup \mathcal{N}(B^{(M)}_{\langle \boldsymbol{t}_M \rangle}) = b^{(M)}_{\text{back}}(\text{srsd}\langle \boldsymbol{t}_M \rangle)$ is the pointwise supremum over ϕ of a family of continuous functions, it is lower semicontinuous (see, e.g., Chapter 2 of [58]). Fixing $\tau > 0$, it follows that $b^{(M)}_{\text{back}} \circ \text{srsd}$ is lower semicontinuous on the subset $\{\langle 0, \tau, t_3, \ldots, t_{2M} \rangle \in \mathcal{T}_M\}$ (in the relative topology). As this subset is mapped homeomorphically to $\mathbb{R}^{2M-2}_{>0}$ by srsd, we conclude that $b^{(M)}_{\text{back}}$ is lower semicontinuous on $\mathbb{R}^{2M-2}_{>0}$. The proof for the overflow functions is similar. □

We also introduce sequences of backflow and overflow constants, by

$$c^{(M)}_{\text{back}} = \sup_{\mathbb{R}^{2M-2}_{>0}} b^{(M)}_{\text{back}}, \qquad c^{(M)}_{\text{over}} = \inf_{\mathbb{R}^{2M-2}_{>0}} b^{(M)}_{\text{over}} \tag{2.36}$$

for $M \geq 1$, in which the Bracken–Melloy constant appears as the first backflow constant: $c_{\text{BM}} = c^{(1)}_{\text{back}}$, while the first overflow constant is $c^{(1)}_{\text{over}} = -1$. Just as with c_{BM}, the functions $b^{(M)}_{\text{back/over}}$ and constants $c^{(M)}_{\text{back/over}}$ are quantities that are fixed by the free quantum dynamics on the line. However, as the $b^{(M)}_{\text{back/over}}$ are dimensionless functions of dimensionless variables, they are manifestly independent of Planck's constant. In the remainder of this thesis, we will initiate the study of these functions and constants using both analytical and numerical methods, starting by considering the spectrum of the operators $B^{(M)}_{\langle \boldsymbol{t}_M \rangle}$ for $\langle \boldsymbol{t}_M \rangle \in \mathcal{T}_M$.

2.3 THE SPECTRUM OF M-FOLD BACKFLOW OPERATORS

2.3.1 BOUNDS ON THE SPECTRUM

Our aim in this section is to obtain estimates on $\sigma(B^{(M)}_{\langle \boldsymbol{t}_M\rangle})$ for a variety of $\langle \boldsymbol{t}_M\rangle \in \mathcal{T}_M$. The simplest estimate arises from the triangle inequality: since $\|B_{\langle t_1,t_2\rangle}\| = 1$ for all $t_1 < t_2$, we have from (2.24) that $\|B^{(M)}_{\langle \boldsymbol{t}_M\rangle}\| \leq M$ and consequently $\sigma(B^{(M)}_{\langle \boldsymbol{t}_M\rangle}) \subseteq [-M, M]$ for all $\langle \boldsymbol{t}_M\rangle \in \mathcal{T}_M$ and $M \geq 1$.

To get a better estimate of the upper bound on the spectrum, we note that any sum of self-adjoint bounded operators obeys

$$\sup \sigma \left(\sum_{j=1}^{M} A_j \right) \leq \sum_{j=1}^{M} \sup \sigma(A_j) \tag{2.37}$$

and therefore

$$\sup \sigma\Big(B^{(M)}_{\langle \boldsymbol{t}_M\rangle}\Big) \leq \sum_{j=1}^{M} \sup \sigma(B_{\langle t_{2j-1},t_{2j}\rangle}) = Mc_{\mathrm{BM}}. \tag{2.38}$$

To get a lower bound on the spectrum, it is convenient to rewrite $\Delta^{(M)}_{\langle \boldsymbol{t}_M\rangle}(\psi)$ as

$$\begin{aligned}\Delta^{(M)}_{\langle \boldsymbol{t}_M\rangle}(\psi) = {} & \mathrm{Prob}_\psi(X < 0 | t = t_{2M}) - \mathrm{Prob}_\psi(X < 0 | t = t_1) \\ & - \sum_{j=1}^{M-1} \left(\mathrm{Prob}_\psi(X < 0 | t = t_{2j+1}) - \mathrm{Prob}_\psi(X < 0 | t = t_{2j}) \right), \end{aligned} \tag{2.39}$$

from which it follows that

$$B^{(M)}_{\langle \boldsymbol{t}_M\rangle} = B_{\langle t_1,t_{2M}\rangle} - B^{(M-1)}_{\langle t_2,\ldots,t_{2M-1}\rangle}. \tag{2.40}$$

Iterating, one obtains the formula

$$B^{(M)}_{\langle \boldsymbol{t}_M\rangle} = \sum_{j=1}^{M} (-1)^{j-1} B_{\langle t_j,t_{2M-j+1}\rangle}, \tag{2.41}$$

which will be used later on.

Returning to (2.40), an analogue of (2.37) gives

$$\begin{aligned}\inf \sigma \left(B^{(M)}_{\langle \boldsymbol{t}_M\rangle} \right) &\geq \inf \sigma \left(B_{\langle t_1,t_{2M}\rangle} \right) + \inf \sigma \left(-B^{(M-1)}_{\langle t_2,\ldots,t_{2M-1}\rangle} \right) \\ &= -1 - \sup \sigma \left(B^{(M-1)}_{\langle t_2,\ldots,t_{2M-1}\rangle} \right) \\ &\geq -1 - (M-1)c_{\mathrm{BM}}, \end{aligned} \tag{2.42}$$

where we have used (2.38). Summarising, we have shown the following.

Theorem 2.3.1. *For any $M \in \mathbb{N}$ and $\langle \boldsymbol{t}_M \rangle \in \mathcal{T}_M$, the spectrum of $B^{(M)}_{\langle \boldsymbol{t}_M \rangle}$ satisfies*

$$\sigma(B^{(M)}_{\langle \boldsymbol{t}_M \rangle}) \subseteq [-1-(M-1)c_{\mathrm{BM}}, Mc_{\mathrm{BM}}]. \tag{2.43}$$

Thus one has bounds

$$b^{(M)}_{\mathrm{back}}(u_1,\ldots,u_{2M-2}) \leq c^{(M)}_{\mathrm{back}} \leq Mc_{\mathrm{BM}} \tag{2.44}$$

$$b^{(M)}_{\mathrm{over}}(u_1,\ldots,u_{2M-2}) \geq c^{(M)}_{\mathrm{over}} \geq -1-(M-1)c_{\mathrm{BM}} \tag{2.45}$$

for all $(u_1,\ldots,u_{2M-2}) \in \mathbb{R}^{2M-2}_{>0}$.

Theorem 2.3.1 shows that $c^{(M)}_{\mathrm{back/over}}$ do not grow faster than linearly in M, but does not answer the question of whether they grow at all. In the following subsections we will prove rigorously that for a particular class of backflow operators, both the infimum and supremum of $\sigma(B^{(M)}_{\langle \boldsymbol{t}_M \rangle})$ tend to $\pm\infty$ as $M \to \infty$ at least as fast as $\mathcal{O}(M^{1/4})$. This is in stark contrast to the classical case where, irrespective of the number of disjoint backflow intervals, the total backflow always lies in $[-1, 0]$. The rigorous results presented will be supplemented by a numerical investigation for values of $1 \leq M \leq 4$ which clearly indicate monotonicity of the infimum and supremum of $\sigma(B^{(M)}_{\langle \boldsymbol{t}_M \rangle})$.

2.4 UNBOUNDED M-FOLD BACKFLOW AND OVERFLOW AS $M \to \infty$

In this subsection we will show that $c^{(M)}_{\mathrm{back}}$ and $-c^{(M)}_{\mathrm{over}}$ grow unboundedly with M, by considering the M-fold backflow operator corresponding to M backflow periods of equal duration, separated by $M-1$ intervals of the same duration. Specifically, for $M \in \mathbb{N}$ and fixed $T > 0$ consider the M-fold backflow problem for the times

$$\langle \boldsymbol{t}_M \rangle = \left\langle -T\frac{2M-1}{2}, -T\frac{2M-3}{2}, ..., -\frac{T}{2}, \frac{T}{2}, ..., T\frac{2M-1}{2} \right\rangle, \tag{2.46}$$

displayed in figure **??**for which the total backflow is bounded between $b^{(M)}_{\mathrm{over}}(1,\ldots,1)$ and $b^{(M)}_{\mathrm{back}}(1,\ldots,1)$.

Figure 2.2: Equally spaced times, as in (2.46)

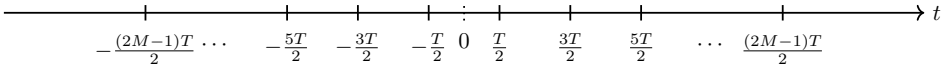

Note that $b^{(M)}_{\text{over}}(1,...,1)$ and $b^{(M)}_{\text{back}}(1,...,1)$ are invariant under the choice of $T > 0$. One can write the associated M-fold backflow operator $B^{(M)}_{\langle \boldsymbol{t}_M \rangle}$ as

$$B^{(M)}_{\langle \boldsymbol{t}_M \rangle} = \sum_{j=1}^{M} (-1)^{j-1} B^{(1)}_{\langle -T(j-1/2), T(j-1/2) \rangle} \tag{2.47}$$

using (2.41). Each of the $B^{(1)}_{\langle -T(j-1/2),T(j-1/2)\rangle}$ operators has the closed form

$$(B^{(1)}_{\langle -T(j-1/2),T(j-1/2)\rangle}\phi)(k) = -\frac{1}{\pi}\int_0^\infty dl\, \frac{\sin\left(T(j-1/2)(k^2-l^2)/2\right)}{k-l}\phi(l). \tag{2.48}$$

Let $U : L^2(\mathbb{R}^+, dk) \to L^2(\mathbb{R}^+, dp)$ be the unitary implementing the change of variables $p = k^2T/2$, $(U\phi)(p) = (2pT)^{-1/4}\phi(\sqrt{2p/T})$, so that $U^* B^{(1)}_{\langle -T/2,T/2\rangle} U = C$ is the operator defined in (2.15). The identity

$$\sum_{j=1}^{M} (-1)^{M-j} \sin(2(j-1/2)(p-q)) = \frac{\sin 2M(p-q)}{2\cos(p-q)}, \tag{2.49}$$

is easily proven by expressing sin in terms of complex exponentials and can be verified in Maple$^{\text{TM}}$ 2024 or higher. From (2.49), we find that the operator $C^{(M)} = U^* B^{(M)}_{\langle \boldsymbol{t}_M \rangle} U \in \mathcal{B}(L^2(\mathbb{R}^+, dq))$ is independent of T and has the action

$$\left(C^{(M)}\varphi\right)(p) = -\frac{1}{4\pi}\int_0^\infty dq\, \frac{\sin(2M[p-q])}{(p-q)\cos(p-q)} \left[\left(\frac{p}{q}\right)^{1/4} + \left(\frac{p}{q}\right)^{-1/4}\right]\varphi(q). \tag{2.50}$$

The following theorem shows that the suprema and infima of $\mathcal{N}(B^{(M)}_{\langle \boldsymbol{t}_M \rangle}) = \mathcal{N}(C^{(M)})$ grow arbitrarily large in magnitude with M at least as fast as $\mathcal{O}(M^{1/4})$.

Theorem 2.4.1. *For $M \in \mathbb{N}$, let $C^{(M)} \in \mathcal{B}(L^2(\mathbb{R}^+, dq))$ be the backflow operator defined in (2.50) describing M backflow periods of unit duration separated by $M-1$ periods of unit duration. Then there is a constant $k > 0$ so that*

$$\sup \sigma\left(C^{(M)}\right) \geq kM^{1/4} \tag{2.51}$$

for all positive even M, and furthermore,

$$\liminf_{M\to\infty} M^{-1/4} \sup \sigma\left(C^{(M)}\right) \geq k > 0, \qquad \limsup_{M\to\infty} M^{-1/4} \inf \sigma\left(C^{(M)}\right) \leq -k < 0, \tag{2.52}$$

where the limits are taken over all $M \in \mathbb{N}$.

Proof. We begin by proving (2.51). For even $M \in \mathbb{N}$ and $\epsilon \in (0, \frac{\pi}{6}]$, define the intervals $\mathcal{I}_0, \mathcal{I}_1 \subseteq \mathbb{R}$ by

$$\mathcal{I}_0 = \left[0, \frac{\epsilon}{M}\right], \qquad \mathcal{I}_1 = \left[\frac{\pi}{2} - \frac{\epsilon}{2M}, \frac{\pi}{2} + \frac{\epsilon}{2M}\right] \tag{2.53}$$

and associated normalised $\psi_M \in L^2(\mathbb{R}^+, dq)$ by

$$\psi_M(q) = \begin{cases} \sqrt{\frac{M}{2\epsilon}} & q \in \mathcal{I}_0 \cup \mathcal{I}_1 \\ 0 & \text{otherwise} \end{cases}. \tag{2.54}$$

We will estimate the supremum of the spectrum using the bound $\sup \sigma(C^{(M)}) \geq \left\langle \psi_M | C^{(M)} \psi_M \right\rangle$. The following Lemma is established in Appendix A.

Lemma 2.4.2. *For even $M \in \mathbb{N}$ and $\epsilon \in (0, \pi/6]$,*

$$\left\langle \psi_M | C^{(M)} \psi_M \right\rangle \geq \frac{2^{7/4} \epsilon^{3/4}}{3\pi^{11/4}} M^{1/4} S\left(\frac{2\epsilon}{\pi M}\right), \tag{2.55}$$

where

$$S(\eta) = 1 - \frac{31\pi^2}{80}\eta^{1/4} - \frac{5}{8}\eta - \frac{9\pi^2}{176}\eta^{5/4}. \tag{2.56}$$

Clearly $S(\eta) > 0$ for sufficiently small $\eta \geq 0$. Fixing $\epsilon \in (0, \pi/6]$ sufficiently small that $S > 0$ on $[0, \epsilon/\pi]$, and using continuity of S, let

$$k = \min_{\eta \in [0, \epsilon/\pi]} \frac{2^{7/4} \epsilon^{3/4}}{3\pi^{11/4}} S(\eta). \tag{2.57}$$

Then (2.51) follows because $2\epsilon/(\pi M) \in [0, \epsilon/\pi]$ for all even $M \geq 2$. (The value of k can be optimised by varying ϵ.)

To establish the first result in (2.52), we need some information on $\sup \sigma(C^{(M)})$ for odd $M \geq 1$. Writing

$$B^{(M+1)}_{\langle \boldsymbol{t}_{M+1} \rangle} = B^{(M)}_{\langle -T\frac{2M+1}{2}, \ldots, -\frac{T}{2}, \frac{T}{2}, \ldots, T\frac{2M-3}{2} \rangle} + B^{(1)}_{\langle T\frac{2M-1}{2}, T\frac{2M+1}{2} \rangle}, \tag{2.58}$$

the left-hand side is unitarily equivalent to $C^{(M+1)}$, while by making time translations and dilations, the first and second terms on the right-hand side are unitarily equivalent to $C^{(M)}$ and $C^{(1)}$ respectively. Consequently $C^{(M+1)}$ is a sum of operators unitarily equivalent to $C^{(M)}$ and $C^{(1)}$. As the supremum of the spectrum is a sub-additive function on bounded self-adjoint operators, and spectra are invariant under unitary equivalence, it follows that

$$\sup \sigma\left(C^{(M+1)}\right) \leq \sup \sigma\left(C^{(M)}\right) + \sup \sigma\left(C^{(1)}\right) = c_{\mathrm{BM}} + \sup \sigma\left(C^{(M)}\right), \tag{2.59}$$

and therefore $\sup\sigma\left(C^{(M)}\right) \geq k(M+1)^{1/4} - c_{\mathrm{BM}}$ for all odd $M \geq 1$, using (2.51). Combining with the bound (2.51) for even M, one has $\sup\sigma\left(C^{(M)}\right) \geq kM^{1/4} - c_{\mathrm{BM}}$ for all $M \in \mathbb{N}$ and the first part of (2.52) follows immediately.

Finally, for any $M \geq 1$, $B^{(M+1)}_{\langle \boldsymbol{t}_{M+1}\rangle}$ can be rewritten as

$$B^{(M+1)}_{\langle \boldsymbol{t}_{M+1}\rangle} = B^{(1)}_{\langle -T^{\frac{2M+1}{2}}, T^{\frac{2M+1}{2}}\rangle} - B^{(M)}_{\langle \boldsymbol{t}_M\rangle} \tag{2.60}$$

which, because all single-backflow operators are unitarily equivalent, gives

$$C^{(M+1)} = \widetilde{C}^{(1)} - C^{(M)} \tag{2.61}$$

where $\widetilde{C}^{(1)}$ is unitarily equivalent to $C^{(1)}$. Using invariance of the spectrum under unitary equivalence and the fact that $\sup\sigma(-A) = -\inf\sigma(A)$ for any bounded self-adjoint operator A, we find

$$\sup\sigma\left(C^{(M+1)}\right) \leq \sup\sigma\left(C^{(1)}\right) - \inf\sigma\left(C^{(M)}\right) \tag{2.62}$$

and consequently

$$\inf\sigma\left(C^{(M)}\right) \leq c_{\mathrm{BM}} - \sup\sigma\left(C^{(M+1)}\right). \tag{2.63}$$

Thus $\limsup_{M\to\infty} M^{-1/4}\inf\sigma\left(C^{(M)}\right) \leq -\liminf_{M\to\infty} M^{-1/4}\sup\sigma\left(C^{(M+1)}\right) \leq -k$. □

Numerically, the first positive zero of $S(\eta)$ occurs at $\eta_0 = 0.0046$ to two significant figures and S is decreasing on the interval $[0, \eta_0]$. Then the constant k in Theorem 2.4.1 may be taken as

$$k = \max_{\epsilon\in[0,\pi\eta_0]} \frac{2^{7/4}\epsilon^{3/4}}{3\pi^{11/4}} S(\epsilon/\pi) = 2.1 \times 10^{-4}, \tag{2.64}$$

computing the maximum numerically to 2 significant figures. By considering more complicated trial functions, it seems likely that we can increase the coefficient; at any rate, the main point is to establish the growth of at least $\mathcal{O}(M^{1/4})$. For comparison, the numerical results of Section 3.1 show that $\sup\sigma(C^{(4)}) \gtrsim 0.095$, which far exceeds the lower bound $4^{1/4}k = 0.0003$ for this case.

Theorem 2.4.1 has an immediate corollary relating to the asymptotics of the backflow and overflow constants.

Corollary 2.4.3. *Let $c^{(M)}_{\mathrm{back}}$ and $c^{(M)}_{\mathrm{over}}$ be the M-fold backflow and overflow constants defined in (2.36). Then*

$$\liminf_{M\to\infty} M^{-1/4} c^{(M)}_{\mathrm{back}} > 0, \qquad \limsup_{M\to\infty} M^{-1/4} c^{(M)}_{\mathrm{over}} < 0. \tag{2.65}$$

Proof. Since $C^{(M)}$ is unitarily equivalent to $B^{(M)}_{\langle \boldsymbol{t}_M(T)\rangle}$, we find that

$$\sup \sigma\left(C^{(M)}\right) = b^{(M)}_{\text{back}}(1,...,1) \leq c^{(M)}_{\text{back}}, \qquad \inf \sigma\left(C^{(M)}\right) = b^{(M)}_{\text{over}}(1,...,1) \geq c^{(M)}_{\text{over}}. \tag{2.66}$$

The result follows on multiplying each inequality by $M^{-1/4}$ and employing Theorem 2.4.1, together with elementary properties of lim sup and lim inf. □

Theorem 2.4.1 and Corollary 2.4.3 demonstrate the unboundedness of the quantum backflow and overflow effects as $M \to \infty$. In Section 3.1, we will find numerical estimates of the spectral extrema for M equally spaced intervals of equal width, with $2 \leq M \leq 4$, showing in particular that

$$\sup\left(C^{(M)}\right) > c_{\text{BM}}, \qquad \inf\left(C^{(M)}\right) < -1 \tag{2.67}$$

and further give numerical evidence for lower bounds on $c^{(M)}_{\text{back}}$ as well as plots of vectors in $L^2(\mathbb{R}^+, dp)$ exhibiting backflow and overflow.

2.5 LIMITING CASES AND MONOTONICITY OF THE BACKFLOW CONSTANTS

In Lemma 2.2.4 we have already seen that the M-fold backflow and overflow functions are semicontinuous for limits taken within $\mathbb{R}^{2M-2}_{>}$. We now consider certain limiting cases, which show how backflow and overflow functions with different numbers of parameters are related and establish monotonicity properties of the backflow constants.

Theorem 2.5.1. *Let $M \in \mathbb{N}$ and $j,k \in \mathbb{N}_0$ so that $j+k = 2L$ is even and positive. Consider any $u \in \mathbb{R}^{(2M-2)}_{>}$ and any sequences $(v_n)_{n\in\mathbb{N}}$ in $\mathbb{R}^j_>$ and $(w_n)_{n\in\mathbb{N}}$ in $\mathbb{R}^k_>$ whose last and first components obey $v_{n,j} \to 0$ and $w_{n,1} \to \infty$. (In the case $M = 1$ one omits u; similarly, in the cases $j = 0$ resp., $k = 0$ one omits v resp., w.)*

If j (and hence also k) is even, then

$$\liminf_n b^{(M+L)}_{\text{back}}(v_n,u,w_n) \geq b^{(M)}_{\text{back}}(u), \qquad \limsup_n b^{(M+L)}_{\text{over}}(v_n,u,w_n) \leq b^{(M)}_{\text{over}}(u) \tag{2.68}$$

where we use the shorthand notation

$$(v,u,w) = (v_1,\ldots,v_j,u_1,\ldots,u_{2M-2},w_1,\ldots,w_k)$$

.

On the other hand, if j (and hence also k) is odd, then

$$\begin{aligned}\liminf_n b^{(M+L)}_{\text{back}}(v_n,u,w_n) &\geq -1-b^{(M)}_{\text{over}}(u),\\ \limsup_n b^{(M+L)}_{\text{over}}(v_n,u,w_n) &\leq -1-b^{(M)}_{\text{back}}(u).\end{aligned} \tag{2.69}$$

Consequently, the sequence of backflow constants $c^{(M)}_{\text{back}}$ is nondecreasing in M, and the sequence of overflow constants $c^{(M)}_{\text{over}}$ is nonincreasing in M; moreover, $c^{(M+L)}_{\text{back}} \geq -1-c^{(M)}_{\text{over}}$ and $c^{(M+L)}_{\text{over}} \leq -1-c^{(M)}_{\text{back}}$ for all $L\in\mathbb{N}$.

We remark that the result holds also, with the same proof, if the discrete index n on v and w is replaced with a continuous $\alpha\in\mathbb{R}$.

Proof. Choose any $\langle \boldsymbol{t}_M\rangle \in \mathcal{T}_M$ so that $u=\text{srsd}\langle \boldsymbol{t}_M\rangle$ (if $M=1$, any element of $\mathcal{T}_1$ can be chosen). With this choice, for each $v\in(\mathbb{R}^+_>)^j$ and $w\in(\mathbb{R}^+_>)^k$ there are unique $r\in\mathbb{R}^j$ and $s\in\mathbb{R}^k$ so that $\langle \hat{\boldsymbol{t}}_{M+L}\rangle = \langle r_1,\dots,r_j,t_1,\dots,t_{2M},s_1,\dots,s_k\rangle \in \mathcal{T}_{M+L}$ satisfies $\text{srsd}\langle \hat{\boldsymbol{t}}_{M+L}\rangle = (v,u,w)$. Specifically, the components are defined recursively by

$$r_{a-1}=r_a+\frac{r_a-r_{a+1}}{v_{a-1}},\qquad s_{a+1}=s_a+(s_a-s_{a-1})w_{a+1} \tag{2.70}$$

with $s_0=t_{2M}$, $s_{-1}=t_{2M-1}$, $r_{j+1}=t_1$, $r_{j+2}=t_2$. It is easily seen from (2.70) that $v_j\to 0+$ implies $r_j\to-\infty$ (and therefore also $r_a\to-\infty$ for each $1\leq a\leq j$), while if $w_1\to+\infty$ then $s_1\to+\infty$ (and therefore also $s_a\to+\infty$ for each $1\leq a\leq k$).

For any $\epsilon>0$, we may choose $\psi\in\mathscr{H}_+$ so that

$$\Delta^{(M)}_{\langle \boldsymbol{t}_M\rangle}(\psi) > \sup_{\varphi\in\mathscr{H}_+}\Delta^{(M)}_{\langle \boldsymbol{t}_M\rangle}(\varphi)-\epsilon, \tag{2.71}$$

whereupon Dollard's lemma [25] gives

$$\begin{aligned}\Delta^{(M+L)}_{\langle \hat{\boldsymbol{t}}_{M+L}\rangle}(\psi) &= \sum_{a=1}^{j}(-1)^a\text{Prob}_\psi(X<0|t=r_a)+(-1)^j\Delta^{(M)}_{\langle \boldsymbol{t}_M\rangle}(\psi)\\ &\quad+\sum_{a=1}^{k}(-1)^{k-a}\text{Prob}_\psi(X<0|t=s_a)\end{aligned} \tag{2.72}$$

$$\longrightarrow \begin{cases}-1-\Delta^{(M)}_{\langle \boldsymbol{t}_M\rangle}(\psi) & j \text{ odd}\\ \Delta^{(M)}_{\langle \boldsymbol{t}_M\rangle}(\psi) & j \text{ even.}\end{cases} \tag{2.73}$$

as $v_j \to 0+$ and $w_1 \to +\infty$. As the limit is approached, in the case where j is even, it eventually holds that $\Delta^{(M+L)}_{\langle \hat{\boldsymbol{t}}_{M+L}\rangle}(\psi) > \Delta^{(M)}_{\langle \boldsymbol{t}_M\rangle}(\psi) - \epsilon$ and thus the inequalities

$$\Delta^{(M+L)}_{\langle \hat{\boldsymbol{t}}_{M+L}\rangle}(\psi) > \sup_{\varphi\in\mathscr{H}_+} \Delta^{(M)}_{\langle \boldsymbol{t}_M\rangle}(\varphi) - 2\epsilon \tag{2.74}$$

and

$$b^{(M+L)}_{\text{back}}(v,u,w) = \sup_{\psi\in\mathscr{H}_+} \Delta^{(M+L)}_{\langle \hat{\boldsymbol{t}}_{M+L}\rangle}(\psi) > \sup_{\varphi\in\mathscr{H}_+} \Delta^{(M)}_{\langle \boldsymbol{t}_M\rangle}(\varphi) - 2\epsilon = b^{(M)}_{\text{back}}(u) - 2\epsilon \tag{2.75}$$

are eventually true. Replacing v and w by sequences as in the statement and using the fact that $\epsilon > 0$ was arbitrary, we have proved the first statement in (2.68); the second part is proved analogously.

If j is odd, we argue in a similar way that for any $\epsilon > 0$,

$$b^{(M+L)}_{\text{back}}(v,u,w) = \sup_{\psi\in\mathscr{H}_+} \Delta^{(M+L)}_{\langle \hat{\boldsymbol{t}}_{M+L}\rangle}(\psi) > -1 - \inf_{\varphi\in\mathscr{H}_+} \Delta^{(M)}_{\langle \boldsymbol{t}_M\rangle}(\varphi) - 2\epsilon = -1 - b^{(M+L)}_{\text{over}}(u) - 2\epsilon. \tag{2.76}$$

is eventually true as the limit is taken, thus giving the first statement in (2.69); the second is again proved analogously.

To establish the monotonicity of the backflow constants, for any $M \in \mathbb{N}$, let $\epsilon > 0$ be arbitrary and choose $u \in \mathbb{R}^{(2M-2)}_>$ so that $b^{(M)}_{\text{back}}(u) > c^{(M)}_{\text{back}} - \epsilon$. Then (2.68) with $L = 1$ and $j = 2$, $k = 0$ (or $j = 0$, $k = 2$) implies that $c^{(M+1)}_{\text{back}} > c^{(M)}_{\text{back}} - \epsilon$ and taking $\epsilon \to 0+$, we deduce that $c^{(M+1)}_{\text{back}} \geq c^{(M)}_{\text{back}}$; an analogous argument proves that $c^{(M+1)}_{\text{over}} \leq c^{(M)}_{\text{over}}$. Finally, for any $L \in \mathbb{N}$, we may use (2.69) with e.g., $j = 1$ and $k = 2L - 1$ to prove $c^{(M+L)}_{\text{back}} \geq -1 - c^{(M)}_{\text{over}}$ and $c^{(M+L)}_{\text{over}} \geq -1 - c^{(M)}_{\text{back}}$ by similar means. □

Theorem 2.5.1 has a number of consequences. First, the bound $c^{(2)}_{\text{over}} \leq -1 - c^{(1)}_{\text{back}}$ can be combined with (2.45) to give the sharp value

$$c^{(2)}_{\text{over}} = -1 - c_{\text{BM}}. \tag{2.77}$$

Second, as the overflow constants are nonincreasing, we see that for every $M \geq 2$ and $\epsilon > 0$ there exists $\langle \boldsymbol{t}_M\rangle \in \mathcal{T}_M$ and $\psi \in \mathscr{H}_+$ so that

$$\Delta^{(M)}_{\langle \boldsymbol{t}_M\rangle}(\psi) \leq -1 - c_{\text{BM}} + \epsilon \tag{2.78}$$

which (taking $0 < \epsilon < c_{\text{BM}}$) provides another proof, independent to Theorem 2.4.1, of the existence of overflow states for any $M \geq 2$. Similarly, we may deduce that

there are backflow states for every $M \in \mathbb{N}$. This follows from combining (2.78) with the final statement in Theorem 2.5.1 to find

$$c_{\text{back}}^{(M)} \geq -1 - c_{\text{over}}^{(1)} = c_{\text{BM}} \tag{2.79}$$

for all $M \in \mathbb{N}$.

Third, the proof of Theorem 2.5.1 can be modified slightly to give the following result (many other variations are possible) which may be useful for further studies. The notation Li will be explained after the statement.

Theorem 2.5.2. *For $M \in \mathbb{N}$ and $\langle \boldsymbol{t}_M \rangle \in \mathcal{T}_M$, one has*

$$-1 - \mathcal{N}\left(B^{(M)}_{\langle \boldsymbol{t}_M \rangle}\right) \subseteq \operatorname*{Li}_{T_\pm \to \pm\infty} \mathcal{N}\left(B^{(M+1)}_{\langle T_-, \boldsymbol{t}_M, T_+ \rangle}\right) \tag{2.80}$$

and

$$\mathcal{N}\left(B^{(M)}_{\langle \boldsymbol{t}_M \rangle}\right) \subseteq \operatorname*{Li}_{\substack{T, T' \to -\infty \\ T < T'}} \mathcal{N}\left(B^{(M+1)}_{\langle T, T', \boldsymbol{t}_M \rangle}\right). \tag{2.81}$$

Here, Li denotes the *Painlevé-Kuratowski lower closed limit*, see e.g. Chapter 29 of [47] and Chapter 5 of [6], defined as follows.

Definition 2.5.3. *Given a net of sets $(A_\alpha)_{\alpha \in I}$ in a topological space X, where I is a directed set, $\operatorname{Li} A_\alpha \subseteq X$ is the set of points $p \in X$ with the property that, for every neighbourhood N of p, there exists $\alpha_0 \in I$ with $A_\alpha \cap N \neq \emptyset$ for all $\alpha > \alpha_0$, i.e., every neighbourhood of p is eventually intersected by A_α.*

Proof of Theorem 2.5.2. For the first inclusion, fix $\langle \boldsymbol{t}_M \rangle \in \mathcal{T}_M$ and let $T_- < 0 < T_+$ so that $\langle T_-, \boldsymbol{t}_M, T_+ \rangle \in \mathcal{T}_{M+1}$. As in the proof of Theorem 2.5.1, take $j = k = 1$ and let $r_1 = T_-, s_1 = T_+$. By (2.72),

$$\Delta^{(M+1)}_{\langle T_-, \boldsymbol{t}_M, T_+ \rangle}(\psi) \longrightarrow -1 - \Delta^{(M)}_{\langle \boldsymbol{t}_M \rangle}(\psi) \qquad \text{for any } \psi \in \mathcal{H}_+ \tag{2.82}$$

as $T_\pm \to \pm\infty$. So for each $\lambda \in \mathcal{N}(B^{(M)}_{\langle \boldsymbol{t}_M \rangle})$ and $\epsilon > 0$, one can find $T_- < 0 < T_+$ such that

$$[-1 - \lambda - \epsilon, -1 - \lambda + \epsilon] \cap \mathcal{N}\left(B^{(M+1)}_{\langle T_-, \boldsymbol{t}_M, T_+ \rangle}\right) \neq \emptyset, \tag{2.83}$$

whereupon the first result follows by Definition 2.5.3. The second follows in a similar way, taking $j = 2, k = 0$ and $r_1 =$ and $r_1 = T, r_2 = T'$. □

A fourth consequence of Theorem 2.5.1 is that it provides an understanding of how the spectrum of an two-fold backflow operator $B^{(2)}_{\langle t_1,t_2,t_3,t_4\rangle}$ behaves in a limit in which the two backflow intervals merge together, i.e., $t_2, t_3 \to \tau$ for some $\tau \in (t_1, t_4)$, with t_1, t_4 held fixed and maintaining $t_2 < t_3$. An obvious question is whether the spectrum converges in some sense to that of $B^{(1)}_{\langle t_1,t_4\rangle}$. As we now show, this is not the case. Writing $\mathrm{srsd}\langle t_1, t_2, t_3, t_4\rangle = (v, w)$, we have $v \to 0+$ and $w \to +\infty$ in the limit. Using the $M = j = k = 1$ case of Theorem 2.5.1, we find

$$\limsup b^{(2)}_{\mathrm{over}}(v, w) \leq -1 - b^{(1)}_{\mathrm{back}} = -1 - c_{\mathrm{BM}} \tag{2.84}$$

from (2.69) in the limit of interest. Hence $b^{(2)}_{\mathrm{over}}(v, w) \to -1 - c_{\mathrm{BM}}$ because we also have $b^{(2)}_{\mathrm{over}} \geq c^{(2)}_{\mathrm{over}} = -1 - c_{\mathrm{BM}}$. Thus, $\sigma(B^{(2)}_{\langle t_1,t_2,t_3,t_4\rangle})$ contains points approaching $-1 - c_{\mathrm{BM}}$ arbitrarily closely in the limit, while $\sigma(B^{(1)}_{\langle t_1,t_2\rangle}) \subseteq [-1, c_{\mathrm{BM}}]$. Therefore the spectra do not coincide in the limit; in fact, we have

$$\liminf_{\substack{t_2,t_3\to\tau \\ t_2<t_3}} d_{\mathrm{Haus}}\left(\sigma(B^{(2)}_{\langle t_1,t_2,t_3,t_4\rangle}), \sigma(B^{(1)}_{\langle t_1,t_4\rangle})\right) \geq c_{\mathrm{BM}}, \tag{2.85}$$

where the Hausdorff distance between compact $A, B \subset \mathbb{R}$ is

$$d_{\mathrm{Haus}}(A, B) = \max\{\sup_{a\in A}\inf_{b\in B}|a - b|, \sup_{b\in B}\inf_{a\in A}|a - b|\}, \tag{2.86}$$

and gives the collection of non-empty compact subsets of $\mathbb{R}$ the structure of a complete metric space (see, e.g., Theorem 3.2.4 of [6]). As one has the inequality $d_{\mathrm{Haus}}(\sigma(A), \sigma(B)) \leq \|A - B\|$ for self-adjoint bounded operators on Hilbert spaces (see e.g., Theorem V.4.10 in [46]), we may infer that the backflow operators $B^{(2)}_{\langle t_1,t_2,t_3,t_4\rangle}$ do not converge in norm to $B^{(1)}_{\langle t_1,t_4\rangle}$ in the limit considered. This can also be seen directly as follows, noting that

$$B^{(2)}_{\langle t_1,t_2,t_3,t_4\rangle} - B^{(1)}_{\langle t_1,t_4\rangle} = -B^{(1)}_{\langle t_2,t_3\rangle} \tag{2.87}$$

and therefore

$$\|B^{(2)}_{\langle t_1,t_2,t_3,t_4\rangle} - B^{(1)}_{\langle t_1,t_4\rangle}\| = 1 \tag{2.88}$$

by recalling that all single backflow operators have unit norm. It would be interesting to study other mergers of multiple backflow intervals in a similar way.

We end this discussion with a cautionary note. For $\Lambda > 0$, let $L^2([0, \Lambda], dk)$ be the space of positive momentum states with momentum cutoff Λ, in momentum representation. Let $\iota_\Lambda : L^2([0, \Lambda], dk) \to L^2(\mathbb{R}^+, dk)$ be the subspace inclusion

map, whereupon ι_Λ^* is the subspace projection. The following Lemma describes the continuity of single backflow operators restricted to the space of finite momentum states.

Lemma 2.5.4. *Let $\iota_\Lambda : L^2([0,\Lambda], dk) \to L^2(\mathbb{R}^+, dk)$ be the subspace inclusion. Then $(s,t) \mapsto \iota_\Lambda^* B_{\langle s,t\rangle} \iota_\Lambda \in \mathcal{B}(L^2([0,\Lambda], dk))$ is norm continuous on $\mathcal{T}_2$.*

Proof. For $\phi \in L^2([0,\Lambda])$ we have (almost everywhere)

$$|(S_s\phi - S_t\phi)(p)|^2 = \sin^2\left(\frac{(t-s)p^2}{2}\right)|\phi(p)|^2 \leq \frac{\Lambda^4}{4}|s-t|^2|\phi(p)|^2 \tag{2.89}$$

and consequently, in the operator norm on $\mathcal{B}(L^2([0,\Lambda], dk), L^2(\mathbb{R}^+, dk))$

$$\|(S_s - S_t)\iota_\Lambda\| \leq \frac{\Lambda^2|s-t|}{2}. \tag{2.90}$$

Thus the restricted Schrödinger time evolution operators $S_t\iota_\Lambda : L^2([0,\Lambda], dk) \to L^2(\mathbb{R}^+, dk)$ are norm continuous in t. Using the general inequality

$$\|A^*CA - B^*CB\| = \|A^*C(A-B) + (A-B)^*CB\| \leq \|C\|(\|A\| + \|B\|)\|A-B\|,$$

for bounded Hilbert space operators $A, B \in \mathcal{B}(\mathscr{H}, \mathscr{K})$ and $C \in \mathcal{B}(\mathscr{K})$ it follows that $\iota_\Lambda^* S_t^* \mathcal{R}^* \Pi^- \mathcal{R} S_t \iota_\Lambda$ is also norm continuous in t and the result follows. □

Considering (2.87) again, it follows that

$$\|\iota_\Lambda^*(B^{(2)}_{\langle t_1,t_2,t_3,t_4\rangle} - B^{(1)}_{\langle t_1,t_4\rangle})\iota_\Lambda\|_\Lambda \longrightarrow 0 \tag{2.91}$$

as the backflow intervals merge, so

$$\lim_{t_3-t_2\to 0^+} d_{\mathrm{Haus}}\left(\sigma\left(\iota_\Lambda^* B^{(2)}_{\langle t_1,t_2,t_3,t_4\rangle}\iota_\Lambda\right), \sigma\left(\iota_\Lambda^* B^{(1)}_{\langle t_1,t_4\rangle}\iota_\Lambda\right)\right) \longrightarrow 0 \tag{2.92}$$

in this limit. Accordingly, any numerical scheme implementing a fixed momentum cutoff will give the erroneous impression of a convergence of spectra as backflow intervals merge. To see the true behaviour of the backflow operators as in (2.85), it would therefore be necessary to increase the momentum cutoff as $t_3 - t_2$ decreases.

— 3 —

Numerical Investigation of Multiple Quantum Backflow

3.1 NUMERICAL CALCULATION

The goal of this section is to numerically investigate the multiple quantum backflow and quantum overflow effect over M disjoint intervals of equal duration separated by gaps of the same length, corresponding to the bounded operator $C^{(M)}$ given in (2.50). Although our method would in principle apply to arbitrary M, the computational effort rises quickly with M and we have chosen to restrict to $M \leq 4$. The numerical results give lower bounds on the magnitudes of $b^{(M)}_{\text{back/over}}(1,\ldots,1)$ for $1 \leq M \leq 4$. In particular, we will find for $2 \leq M \leq 4$ that $\max \sigma\left(C^{(M)}\right) > c_{\text{BM}}$ and $\min \sigma\left(C^{(M)}\right) < -1$. This complements the analytic results in Theorem 2.4.1 and Corollary 2.4.3 on the large M asymptotics of $\sigma(C^{(M)})$ and the mononotonicity results in Theorem 2.5.1. By numerical acceleration methods, we will give improved estimates for $b^{(M)}_{\text{back/over}}(1,\ldots,1)$ for $1 \leq M \leq 4$. In addition, we will investigate the properties of states that come close to maximising the backflow or overflow for these operators.

3.2 BACKGROUND THEORY

Our numerical calculations are based on the following basic observation. (See Section XIII.1 of [56] for a discussion of other min-max results and Theorem VII.12 of [55] for Weyl's criterion.) Here, $\sigma(B,Q) = \{\lambda \in \mathbb{R} : \det(B - \lambda Q) = 0\}$ is the set of

generalised eigenvalues for Hermitian matrix B with respect to a positive definite matrix Q of the same dimension.

Lemma 3.2.1. *Let A be a bounded self-adjoint operator on Hilbert space $\mathscr{H}$ and let $(\chi_n)_{n\in\mathbb{N}} \subset \mathscr{H}$ be a sequence of linearly independent vectors with dense span. Define sequences of self-adjoint $N \times N$ matrices $(A^{[N]})_{N\in\mathbb{N}}$ and $(P^{[N]})_{N\in\mathbb{N}}$ with matrix elements*

$$A^{[N]}_{mn} = \langle \chi_m | A\chi_n \rangle \,, \qquad P^{[N]}_{mn} = \langle \chi_m | \chi_n \rangle \tag{3.1}$$

for $1 \leq m, n \leq N$. Then $\sigma(A^{[N]}, P^{[N]}) \subseteq \mathcal{N}(A)$, and $\max \sigma(A^{[N]}, P^{[N]})$ (resp., $\min \sigma(A^{[N]}, P^{[N]})$) is a bounded nondecreasing (resp., nonincreasing) sequence with

$$\begin{aligned} \max \sigma(A) &= \lim_{N\to\infty} \max \sigma(A^{[N]}, P^{[N]}) \\ \min \sigma(A) &= \lim_{N\to\infty} \min \sigma(A^{[N]}, P^{[N]}). \end{aligned} \tag{3.2}$$

For each $N \in \mathbb{N}$, suppose $v^{(N)} \in \mathbb{C}^N$ is a generalised eigenvector obeying

$$A^{[N]} v^{(N)} = \lambda_N P^{[N]} v^{(N)}, \qquad v^{(N)\dagger} P^{[N]} v^{(N)} = 1 \tag{3.3}$$

and define $\psi^{(N)} \in \mathcal{H}$ by

$$\psi^{(N)} = \sum_{n=1}^{N} v^{(N)}_n \chi_n. \tag{3.4}$$

If $\psi^{(N)} \to \psi \in \mathcal{H}$ in norm then

1. *the sequence of generalised eigenvalues $(\lambda_N)_{N\in\mathbb{N}}$ converges;*
2. *the sequence of vectors $(\psi^{(N)})_{N\in\mathbb{N}}$ is a Weyl sequence for $\lambda = \lim_{N\to\infty} \lambda_N$, i.e., $\|\psi^{(N)}\| = 1$ and $\|(A - \lambda I)\psi^{(N)}\| \to 0$;*
3. *the limiting vector ψ is an eigenvector for A with eigenvalue λ.*

Proof. If $\lambda \in \sigma(A^{[N]}, P^{[N]})$ with $A^{[N]} v = \lambda P^{[N]} v$ for nonzero v, then

$$\lambda = \frac{v^\dagger A^{[N]} v}{v^\dagger P^{[N]} v} = \frac{\langle \phi | A\phi \rangle}{\langle \phi | \phi \rangle}, \tag{3.5}$$

where $\phi = \sum_{r=1}^{N} v_r \chi_r$, so $\lambda \in \mathcal{N}(A)$, which is a bounded set. Let

$$S_N = \operatorname{span}(\chi_1, \ldots, \chi_N),$$

then monotonicity of the sequences of maximum and minimum generalised eigenvalues is guaranteed because $S_N \subset S_{N+1}$. Finally, as $\bigcup_N S_N$ is dense in $\mathscr{H}$ and A is bounded, we easily compute

$$\begin{aligned}\max\sigma(A) = \sup\mathcal{N}(A) &= \lim_{N\to\infty}\sup_{\phi\in S_N\setminus\{0\}}\frac{\langle\phi|A\phi\rangle}{\langle\phi|\phi\rangle} = \lim_{N\to\infty}\sup_{v\in\mathbb{C}^N\setminus\{0\}}\frac{v^\dagger A^{[N]}v}{v^\dagger P^{[N]}v}\\ &= \lim_{N\to\infty}\max\sigma(A^{[N]},P^{[N]}),\end{aligned} \tag{3.6}$$

where in the final equality we have made use of the (generalised) Courant–Fischer min-max principle – see, e.g., Theorem 2.1 of [48]. The proof for the minimum of $\sigma(A)$ is analogous.

For each $N\in\mathbb{N}$, let Q_N be the projection onto S_N. First we show that $\psi^{(N)}$ is an eigenvector of Q_NA. Since $Q_NA\psi^{(N)}\in S_N$, we must have

$$Q_NA\psi^{(N)} = \sum_{k=1}^N w_k^{(N)}\chi_k \tag{3.7}$$

for some $w^{(N)}\in\mathbb{C}^N$. For $1\le j\le N$, the inner product of (3.7) with χ_j can be written as both

$$\left\langle\chi_j\middle|Q_NA\psi^{(N)}\right\rangle = \sum_{k=1}^N\langle\chi_j|\chi_k\rangle\,w_k^{(N)} = \left(P^{[N]}w^{(N)}\right)_j \tag{3.8}$$

and

$$\left\langle\chi_j\middle|Q_NA\psi^{(N)}\right\rangle = \sum_{k=1}^N v_k^{(N)}\langle\chi_j|A\chi_k\rangle = \left(A^{[N]}v^{(N)}\right)_j = \lambda_N\left(P^{[N]}v^{(N)}\right)_j. \tag{3.9}$$

By the linear independence of the χ_j, $P^{[N]}$ has trivial kernel and we find $w^{(N)} = \lambda_Nv^{(N)}$, from which it follows that

$$Q_NA\psi^{(N)} = \lambda_N\psi^{(N)}. \tag{3.10}$$

Note that $\|\psi^{(N)}\| = 1$ because of the normalisation condition on $v^{(N)}$. Property (1) follows from the fact that

$$\lambda_N = \left\langle Q_N\psi^{(N)}\middle|A\psi^{(N)}\right\rangle \tag{3.11}$$

converges to some $\lambda\in\mathbb{R}$ by the norm convergence of the $\psi^{(N)}$ to ψ and boundedness of A. To prove property (2), note that

$$\|(A-\lambda I)\psi^{(N)}\| \le \|(A-\lambda_NI)\psi^{(N)}\| + |\lambda_N-\lambda| \tag{3.12}$$

so since $\lambda_N \to \lambda$, it suffices to note that

$$\begin{aligned} \|(A-\lambda_N I)\psi^{(N)}\| &= \|(A-Q_N A)\psi^{(N)}\| \\ &\leq \|(I-Q_N)A\psi\| + \|(I-Q_N)A\|\|\psi^{(N)}-\psi\| \to 0 \end{aligned} \tag{3.13}$$

by the density of $\bigcup_N S_N$ in $\mathcal{H}$ and convergence of $(\psi^{(N)})_{N\in\mathbb{N}}$ proving property (2). The final property follows from

$$\|(A-\lambda I)\psi\| \leq \|(A-\lambda I)\psi^{(N)}\| + (\|A\|+|\lambda|)\|\psi^{(N)}-\psi\| \to 0 \tag{3.14}$$

and hence ψ is an eigenvector of A with eigenvalue λ. □

The generalised eigenvalue problems in Lemma 3.2.1 reduce to standard eigenvalue problems if the trial vectors χ_n are orthonormal. In principle one could always orthogonalise to express the matrix elements in a Gram-Schmidt basis, but this introduces a nontrivial computational overhead and the generalised eigenproblem may be preferred.

3.3 NUMERICAL METHODOLOGY AND RESULTS

We will apply Lemma 3.2.1 to the operators $C^{(M)}$, but our methodology also applies to general backflow operators. Given $\delta > -1/2$ and $a > 0$, define the sequence of normalized $L^2(\mathbb{R}^+, dq)$ vectors $(\psi_{n,a,\delta})_{n=0}^{\infty}$ by

$$\psi_{n,a,\delta}(q) = E_n(a,\delta)q^{n+\delta}e^{-aq}, \tag{3.15}$$

with the normalization constant $E_n(a,\delta)$ given by

$$E_n(a,\delta) = \frac{(2a)^{n+\delta+1/2}}{\sqrt{\Gamma(2n+2\delta+1)}}. \tag{3.16}$$

The reason that the vectors $(\psi_{n,a,\delta})_{n=0}^{\infty}$ were chosen is two fold. The first is that for small q, the vectors replicate the behaviour of monomials, with the exponential factor playing the role of L^2 normalisation. The second is that the matrix elements of arbitrary backflow operators with respect to the sequence can be computed in closed form, a feat that has previously not been done before. The following density result is found in Theorem 5.7.1 of [63] in the case $a = 1/2$, and follows for general $a > 0$ by a unitary scale change.

Lemma 3.3.1. *For $a > 0$ and $-\frac{1}{2} < \delta < \frac{1}{2}$, the sequence $(\psi_{n,a,\delta})_{n=0}^{\infty}$ has a dense span in $L^2(\mathbb{R}^+, dq)$.*

To apply Lemma 3.2.1 to $C^{(M)}$, we require the matrix elements

$$C^{(M)}(a,\delta)_{mn} = \left\langle \psi_{m,a,\delta} \middle| C^{(M)} \psi_{n,a,\delta} \right\rangle, \qquad P(a,\delta)_{mn} = \langle \psi_{m,a,\delta} | \psi_{n,a,\delta} \rangle \tag{3.17}$$

for $m, n \in \mathbb{N}_0$. The components $P(a,\delta)_{mn}$ admit the closed form

$$P(a,\delta)_{mn} = \frac{\sqrt{B_{\text{diag}}(m+\delta+1/2) B_{\text{diag}}(n+\delta+1/2)}}{B(m+\delta+1/2, n+\delta+1/2)}, \tag{3.18}$$

where $B(x,y) = \Gamma(x)\Gamma(y)/\Gamma(x+y)$ is the beta function and $B_{\text{diag}}(x) = B(x,x) = \Gamma(x)^2/\Gamma(2x)$. The components $C^{(M)}(a,\delta)_{mn}$ (or indeed, those of general multiple backflow operators) also have a closed form expression in terms of incomplete Beta functions, for which the reader is referred to Appendix C.

For each M, and for fixed $a > 0$, $\delta \in (-1/2, 1/2)$, the matrix elements $P(a,\delta)_{mn}$ and $C^{(M)}(a,\delta)_{mn}$ can be computed for $0 \leq m, n \leq N$, giving $(N+1)$-dimensional square matrices. The minimum eigenvalue of $P^{[N]}$ tends to zero as N increases, so the generalised eigenvalue problem is increasingly ill-conditioned and requires high-precision calculation to obtain accurate results. The following theorem, stated as Corollary VI.3.3 in [62], shows how the numerical precision of a pair of Hermitian matrices affects the accuracy of the associated generalised eigenvalues.

Theorem 3.3.2. *Let A, B be n-dimensional Hermitian matrices with B positive definite, and consider n-dimensional Hermitian perturbations $\Delta A, \Delta B$. If*

$$\sqrt{\|\Delta A\|_{\text{op}}^2 + \|\Delta B\|_{\text{op}}^2} < \gamma(A,B) := \min_{\|x\|_2 = 1} \sqrt{(x^\dagger A x)^2 + (x^\dagger B x)^2}, \tag{3.19}$$

where $\|\cdot\|_{\text{op}}$ is the operator norm induced by the Euclidean vector norm $\|\cdot\|_2$ on $\mathbb{R}^n$, then the matrix pair $(A + \Delta A, B + \Delta B)$ is definite and, for all $1 \leq i \leq n$,

$$\frac{|\lambda_i - \tilde{\lambda}_i|}{\sqrt{(1+\lambda_i^2)(1+\tilde{\lambda}_i^2)}} \leq \frac{\sqrt{\|\Delta A\|_{\text{op}}^2 + \|\Delta B\|_{\text{op}}^2}}{\gamma(A,B)}, \tag{3.20}$$

where $\lambda_1 \leq \cdots \leq \lambda_n$ and $\tilde{\lambda}_1 \leq \cdots \leq \tilde{\lambda}_n$ are the generalised eigenvalues of (A,B) and $(A + \Delta A, B + \Delta B)$ respectively.

We adapt this theorem to our numerical calculation in the following corollary.

Corollary 3.3.3. *Let A, B be n-dimensional Hermitian matrices with B positive definite, and let $\lambda_1 \leq \cdots \leq \lambda_n$ be the generalised eigenvalues of the matrix pair (A, B). If n-dimensional Hermitian perturbations $\Delta A, \Delta B$ obey*

$$C_{\max} := n(1 + \max(|\lambda_1|, |\lambda_n|)^2)\frac{\|\Delta A\|_\infty^2 + \|\Delta B\|_\infty^2}{\min \sigma(B)^2} < \frac{1}{2}, \tag{3.21}$$

where $\lambda_{\max} = \max(|\lambda_1|, |\lambda_n|)$ and $\|\cdot\|_\infty$ is the elementwise maximum modulus matrix norm, then the matrix pair $(A+\Delta A, B+\Delta B)$ is definite, with generalised eigenvalues $\tilde{\lambda}_1 \leq \cdots \leq \tilde{\lambda}_n$ satisfying

$$|\lambda_i - \tilde{\lambda}_i|^2 \leq \frac{C_{\max}}{1 - 2C_{\max}}(1 + 2\lambda_i^2) \tag{3.22}$$

for all $1 \leq i \leq n$.

Proof. First note that $C_{\max} < 1/2$ implies that $\|\Delta A\|_\infty^2 + \|\Delta B\|_\infty^2 < \min \sigma(B)^2 \leq \gamma(A, B)^2$, using the trivial bound

$$\gamma(A, B) \geq \min_{\|x\|_2 = 1} x^\dagger B x = \min \sigma(B). \tag{3.23}$$

Then $(A+\Delta A, B+\Delta B)$ is definite by Theorem 3.3.2, and we proceed to obtain (3.22) by estimating and rearranging (3.20). Applying the inequality

$$n^{-1/2}\|M\|_{\text{op}} \leq \|M\|_\infty := \max_{1 \leq i,j \leq n} |M_{ij}|, \tag{3.24}$$

for n-dimensional square matrices (see [43], pp. 313-314) and Theorem 3.3.2 we obtain

$$|\lambda_i - \tilde{\lambda}_i|^2 \leq (1 + \tilde{\lambda}_i^2)C_i, \tag{3.25}$$

where

$$C_i = n(1 + \lambda_i^2)\frac{\|\Delta A\|_\infty^2 + \|\Delta B\|_\infty^2}{\min \sigma(B)^2}. \tag{3.26}$$

Now note that $\tilde{\lambda}_i^2 \leq (|\lambda_i| + |\lambda_i - \tilde{\lambda}_i|)^2 \leq 2(\lambda_i^2 + |\lambda_i - \tilde{\lambda}_i|^2)$ (using $(a+b)^2 \leq 2(a^2+b^2)$). Combining with (3.25), we find

$$|\lambda_i - \tilde{\lambda}_i|^2 \leq C_i(1 + 2\lambda_i^2 + 2|\lambda_i - \tilde{\lambda}_i|^2). \tag{3.27}$$

Rearranging the above, we obtain

$$|\lambda_i - \tilde{\lambda}_i|^2 \leq \frac{C_i(1 + 2\lambda_i^2)}{1 - 2C_i} \leq \frac{C_{\max}(1 + 2\lambda_i^2)}{1 - 2C_{\max}}, \tag{3.28}$$

by making use of the fact that $x \mapsto 2x/(1 - 2x)$ is monotonically increasing on $[0, 1/2]$ and where $C_{\max} = \max_i C_i$ has the closed form (3.21) with $1 - 2C_{\max} > 0$. □

In our application, using (3.18), numerical experiments showed that

$$\min \sigma(P^{[N]}(a,\delta)) \approx 10^{2-0.94N}$$

independently of δ. Further, any generalised eigenvalue $\lambda \in \sigma(C^{(M)[N]}, P^{[N]}) \subseteq \mathcal{N}(C^{(M)})$ obeys $|\lambda| \leq 1 + (M-1)c_{\mathrm{BM}} \leq M$ by Theorem 2.3.1. Letting $A = C^{(M)[N]}(a,\delta)$ and $B = P(a,\delta)^{[N]}$ in Corollary 3.3.3, we find that condition (3.21) is satisfied if the maximum error ϵ in the matrix elements obeys

$$\epsilon \lessapprox \frac{10^{2-0.94N}}{2\sqrt{(N+1)(1+M^2)}}. \tag{3.29}$$

As we study $1 \leq M \leq 4$, this constraint is satisfied, with some room to spare, by computing the matrix elements to $N+30$ digits of precision, whereupon the maximum error $\Delta\lambda_N$ on the elements of $\sigma(C^{(M)[N]}, P^{[N]})$ is bounded by

$$|\Delta\lambda_N| \lessapprox 10^{-0.06N-32}\sqrt{2(N+1)}\sqrt{(1+M^2)(1+2M^2)} \tag{3.30}$$

For the $N = 500$, $1 \leq M \leq 4$ calculations we find it is possible – in theory – to calculate the generalised eigenvalues to $|\Delta\lambda| \leq 7.5 \times 10^{-60}$ or around 59 digits.

To calculate the matrix elements of $C^{(M)}(a,\delta)$ and $P(a,\delta)$ to high precision, we make use of the Python 3.11 library python-flint (a wrapper for the FLINT package [36]) whose method `good` automatically increases working precision to produce results accurate to the required precision. In particular, python-flint was used to calculate the incomplete beta function in terms of hypergeometric functions, implemented as described in [45]. The generalised eigenvalue spectrum

$$\sigma(C^{(M)[N]}(a,\delta), P^{[N]}(a,\delta))$$

was computed numerically using Maple$^{\mathrm{TM}}$ 2023, using $N+20$ digits of precision. Although Corollary 3.3.3 gives a bound on the theoretical error for the generalised eigenvalues, it does not take account of numerical error accumulated in the generalised eigenvalue solver. In practice, we found that, when calculating the first $N_{\max}$ generalised eigenvalues, the Nth generalised eigenvalue is accurate to around $N_{\max} + 3 - 0.91N$ digits. This means for $N_{\max} = 500$, the final eigenvalue is accurate to 48 digits, rather than the 59 digits estimated above, but for $N < N_{\max}$, the Nth generalised eigenvalue is accurate to higher precision, with over 90 digits expected for $N \leq 450$.

Further experimentation was used to find the values of a_M, δ_M that appear to produce the best, i.e., approximately largest magnitude, values of $\lambda^{(M)}_{\text{back/over}}(a, \delta; N)$ for given M across the range of N studied, resulting in choices $a_M = 2M/\pi$ and $\delta_M = -1/4$. (We do not claim that these values are precisely optimal.) Our choice relies on the following observations. Each $\psi_{n,a,\delta}(q)$ has a unique global maximum at $q = a^{-1}(n + \delta)$ and hence for each number of backflow periods M, we expect that a good choice of a_M^{-1} would be comparable with the gap between consecutive peaks of the top approximate eigenvector $\psi^{(M)}_{\text{back}}(a, \delta; N)$. Early numerical results suggested that for $M = 1$, this gap tends to π as N increases and the best numerical results were found when using $a_1 = 2/\pi$. For larger values of M, the top approximate eigenvector has M times as many stationary points (see Figures 3.5, 3.7 and 3.9 below) and so we selected $a_M = Ma_1 = 2M/\pi$. To motivate the choice $\delta_M = -1/4$, consider the action of a vector of the form $\psi(q) = q^{-1/4} f(q)$ under $C^{(M)}$, we find

$$\begin{aligned}(C^{(M)}\psi)(p) = &-\frac{p^{-1/4}}{4\pi}\int_0^\infty dq\, \frac{\sin(2M(p-q))}{(p-q)\cos(p-q)} f(q) \\ &- \frac{p^{1/4}}{4\pi}\int_0^\infty dq\, \frac{\sin(2M(p-q))}{(p-q)\cos(p-q)} q^{-1/2} f(q),\end{aligned} \tag{3.31}$$

suggesting that any eigenfunction of $C^{(M)}$ is likely to diverge as $\mathcal{O}(p^{-1/4})$ as $p \to 0^+$. We define $\lambda^{(M)}_{\text{back/over}}(N) = \lambda^{(M)}_{\text{back/over}}(a_M, -\frac{1}{4}; N)$.

We present numerical results for $M \in \{1, 2, 3, 4\}$ in graphical form in Figures 3.1 and 3.2 for $100 \le N \le 500$ and tabulate the values of $\lambda^{(M)}_{\text{back/over}}(500)$ in Table 3.1. The values obtained for all N stored at 150 digits may be found in the Supplementary Material.[1] Note that the Nth eigenvalue should only be trusted to around $503 - 0.91N$ decimal places. The plots display the values for $N \ge 100$, over which range they increasingly resemble smooth curves. Each separate eigenvalue sequence is monotone and would tend to the maximum or minimum of the appropriate spectrum $\sigma(C^{(M)})$ as $N \to \infty$. We will discuss the convergence rates and estimated limits with more detail in the next subsection, but it is already clear that the $M = 1$ values stay below the previously estimated value of the Bracken–Melloy constant $c_{\text{BM}} \approx 0.03845$ [29, 40], that one has $c^{(M)}_{\text{back}} \ge b^{(M)}_{\text{back}}(1, ..., 1) > c_{\text{BM}}$ and $c^{(M)}_{\text{over}} \le b^{(M)}_{\text{over}}(1, ..., 1) < -1$ for $2 \le M \le 4$, and that the value of $b^{(2)}_{\text{over}}(1, 1)$ appears to be much closer to -1 than to the 2-fold overflow constant $c^{(2)}_{\text{over}} = -1 - c_{\text{BM}}$.

The final values for each of our sequences $\lambda^{(M)}_{\text{back}}$ and $\lambda^{(M)}_{\text{over}}$ are shown in Table 3.1.

[1] See https://github.com/hkk506/Repeated-quantum-backflow-and-quantum-overflow/.

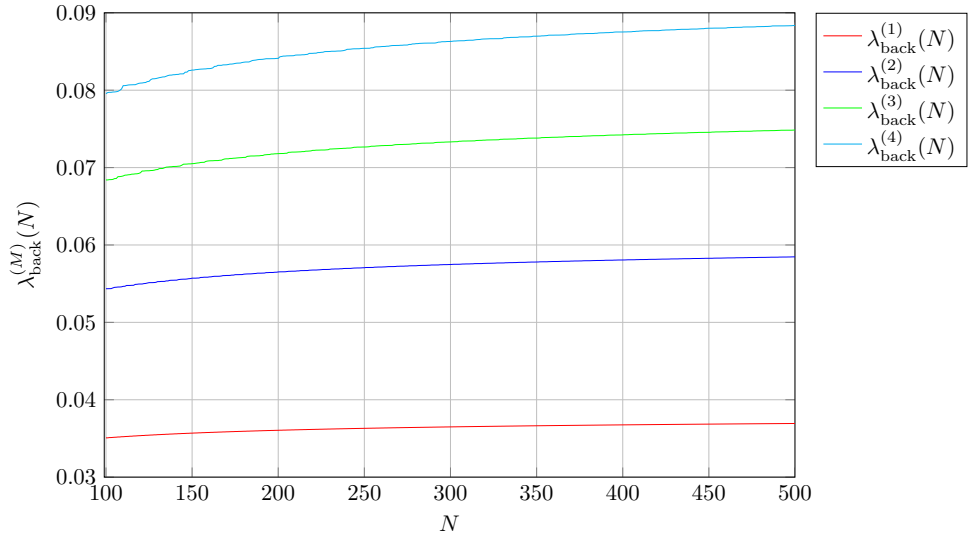

Figure 3.1: Plot of $\lambda^{(M)}_{\text{back}}(N)$ for $100 \leq N \leq 500$.

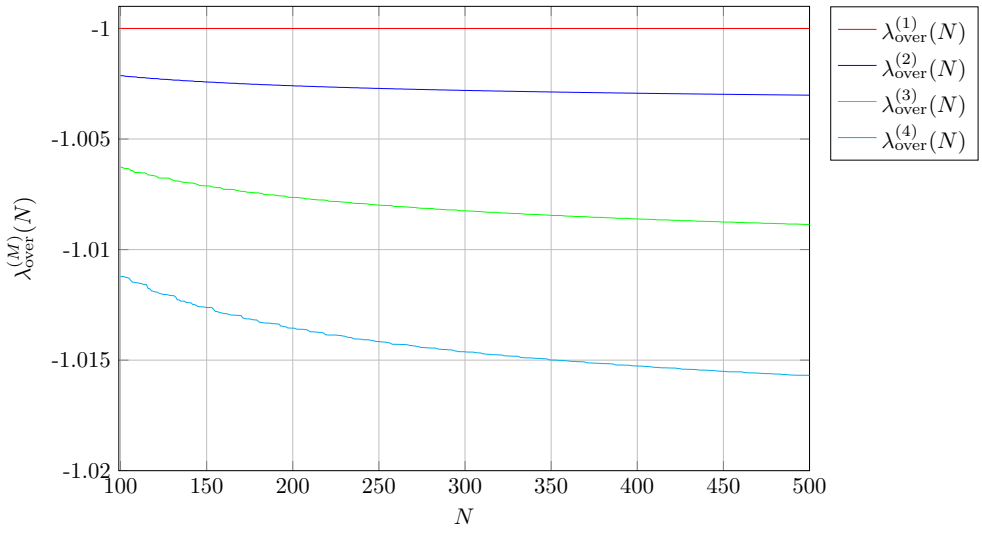

Figure 3.2: Plot of $\lambda^{(M)}_{\text{over}}$ for $100 \leq N \leq 500$.

M	$\lambda^{(M)}_{\text{back}}(500)$	$\lambda^{(M)}_{\text{over}}(500)$
1	0.036933	-1
2	0.058464	-1.0030
3	0.074860	-1.0089
4	0.088378	-1.0157

Table 3.1: Values of $\lambda^{(M)}_{\text{back/over}}(500)$ for $1 \leq M \leq 4$.

As well as estimates for the backflow and overflow values of $C^{(M)}$, we also computed the associated approximate eigenvectors as follows. As in Lemma 3.2.1, each vector $v \in \mathbb{R}^{N+1}$ with $v^\dagger P^{[N]}(a,\delta)v = 1$ defines an approximate eigenvector $\psi \in L^2(\mathbb{R}^+)$ for $C^{(M)}$,

$$\psi = \sum_{n=0}^{N} v_n \psi_{n,a,\delta}. \tag{3.32}$$

Define $\psi^{(M)}_{\text{back/over}}(a,\delta;N;)$ as the $L^2(\mathbb{R}^+)$ vector given by applying (3.32) to the generalised eigenvectors associated with the largest/smallest generalised eigenvalues of $(C^{(M)[N]}(a,\delta), P^{[N]}(a,\delta))$. Figure 3.3 shows the vectors $\psi^{(M)}_{\text{back}}(a_M, -1/4; 500; p)$ for $p \in [0,10]$. As can be seen, all the M-fold backflow maximizing vectors appear to diverge as $p \to 0$. In line with $\delta = -1/4$ giving the best approximate eigenvalue results, we conjecture that all of the M-fold backflow maximizing vectors behave like $p^{-1/4}$ for $p \sim 0$.

Figures 3.4–3.11 show the approximate backflow and overflow eigenvectors for $1 \le M \le 4$. A common feature is that the envelope of the wavefunction decays as $p^{-3/4}$ for large p; in all cases except for $\psi^{(1)}_{\text{over}}(a_1, -1/4; 500); p)$, we plot the eigenfunction multiplied by a factor of $p^{3/4}$ to better illustrate the oscillatory structure. From Figures 3.5, 3.7 and 3.9, one sees that all $M \ge 2$ backflow vectors have higher frequency contributions when compared with the $M = 1$ backflow vector. This is not a surprise when considering the integral kernel of the $C^{(M)}$ for $M \ge 2$ in (2.50).

As shown in Lemma 3.2.1, if the sequences $(\psi^{(M)}_{\text{back/over}}(a_M, -1/4; N; \cdot))_{N\in\mathbb{N}}$ converge in norm, then they are Weyl sequences and the associated limiting vector and spectral point constitute an eigenpair. For integers n, m, let $d^{(M)}_{\text{back/over}}(n,m)$ be defined as

$$d^{(M)}_{\text{back/over}}(n,m) = \|\psi^{(M)}_{\text{back/over}}(a_M, -1/4; n; \cdot) - \psi^{(M)}_{\text{back/over}}(a_M, -1/4; m; \cdot)\|_{L^2(\mathbb{R}^+)}. \tag{3.33}$$

As a crude test, we have computed $d^{(M)}_{\text{back}}(N, 500)$ for $1 \le N \le 499$. For each $M = 1, 2, 3, 4$ the values form a decaying nonincreasing sequence with final values tabulated in Table 3.2. Similar results are obtained for the norm differences of overflow vectors $d^{(M)}_{\text{over}}(N, 500)$ for $1 \le N \le 499$ and $M = 2, 3, 4$. Though far from a rigorous proof, our numerical results suggest that $b^{(M)}_{\text{back}}(1, \ldots, 1) = \max \sigma(C^{(M)})$ is an eigenvalue of $C^{(M)}$ for $1 \le M \le 4$, while $b^{(M)}_{\text{over}}(1, \ldots, 1) = \min \sigma(C^{(M)})$ is an eigenvalue of $C^{(M)}$ for $2 \le M \le 4$.

M	$d^{(M)}_{\text{back}}(499, 500)$
1	0.0058
2	0.0017
3	0.0041
4	0.0084

Table 3.2: Values of norm differences of the approximate backflow eigenvectors for $1 \leq M \leq 4$ given to 2 significant figures.

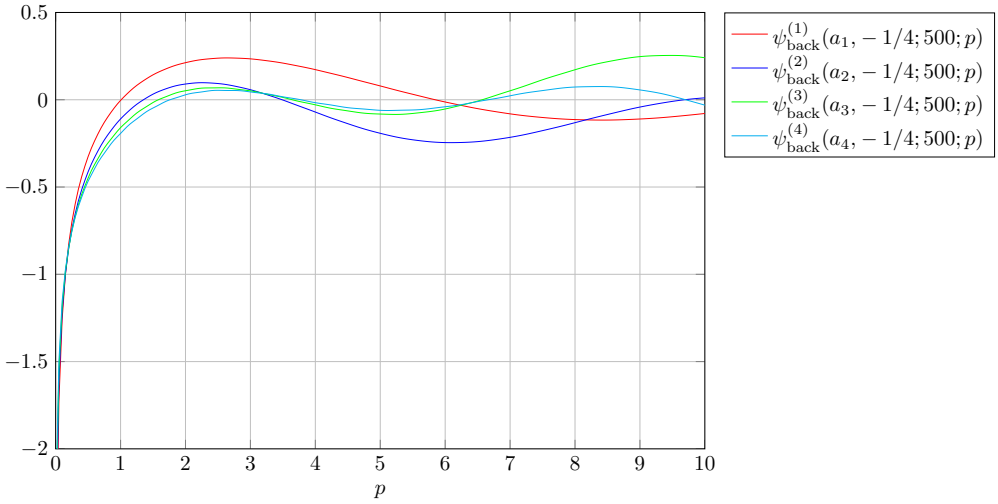

Figure 3.3: Plot of $\psi^{(M)}_{\text{back}}(a_M, -1/4; 500; p)$ for $p \in [0, 10]$

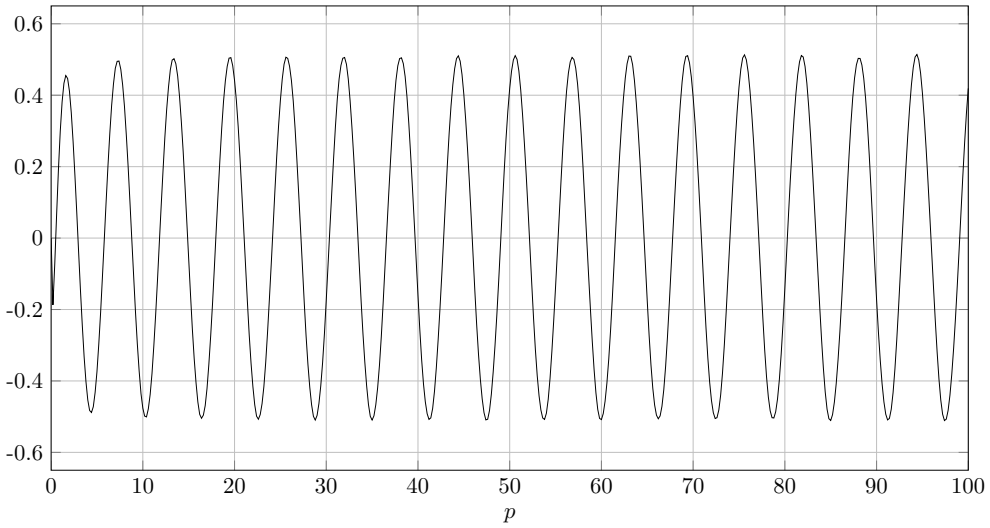

Figure 3.4: Plot of $p^{3/4}\psi^{(1)}_{\text{back}}(a_1, -1/4; 500; p)$ for $p \in [0, 100]$

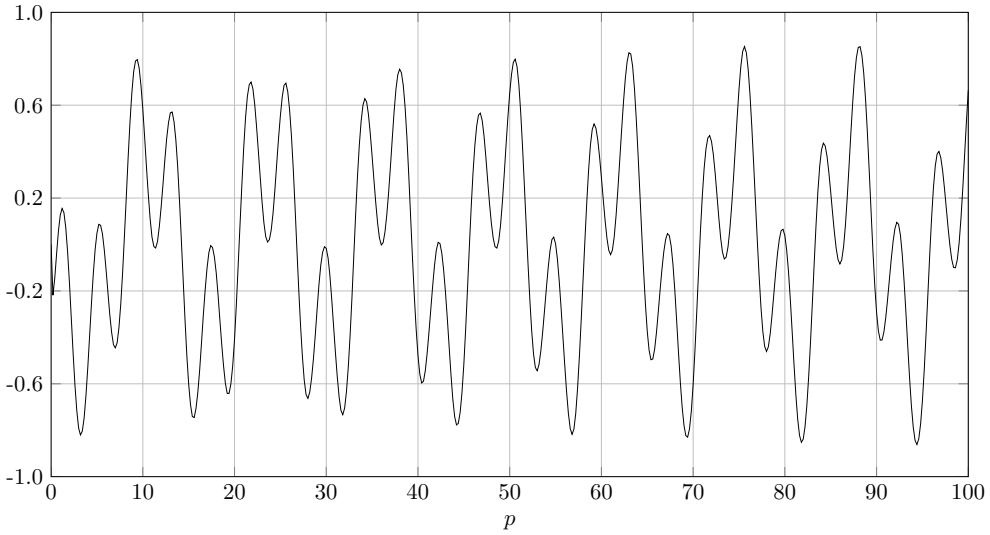

Figure 3.5: Plot of $p^{3/4}\psi^{(2)}_{\text{back}}(a_2, -1/4; 500; p)$ for $p \in [0, 100]$

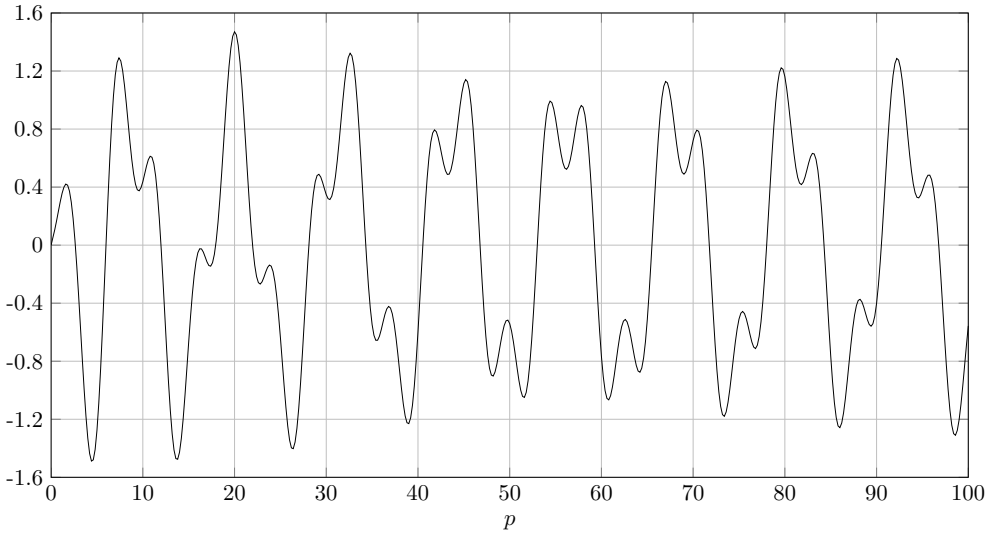

Figure 3.6: Plot of $p^{3/4}\psi^{(2)}_{\text{over}}(a_2, -1/4; 500; p)$ for $p \in [0, 100]$

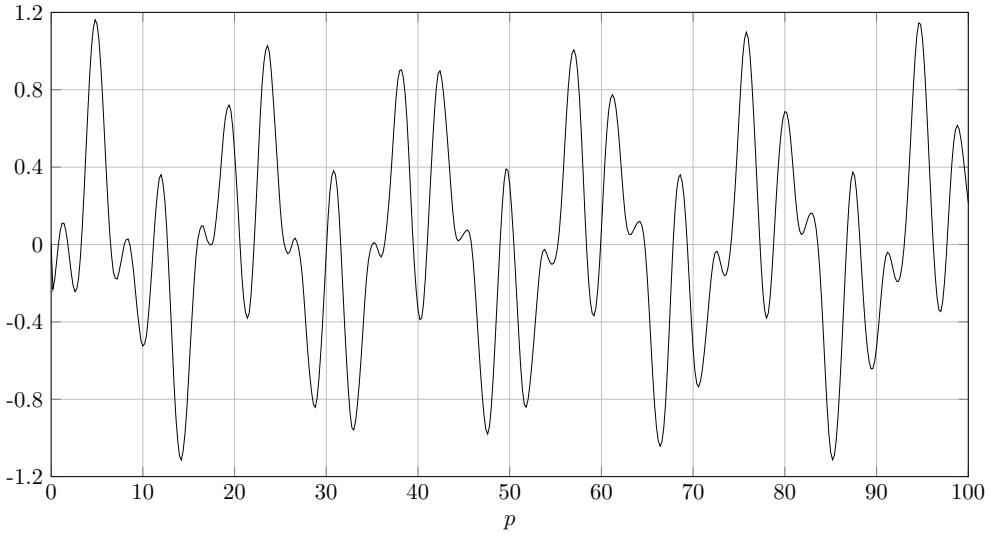

Figure 3.7: Plot of $p^{3/4}\psi^{(3)}_{\text{back}}(a_3, -1/4; 500; p)$ for $p \in [0, 100]$

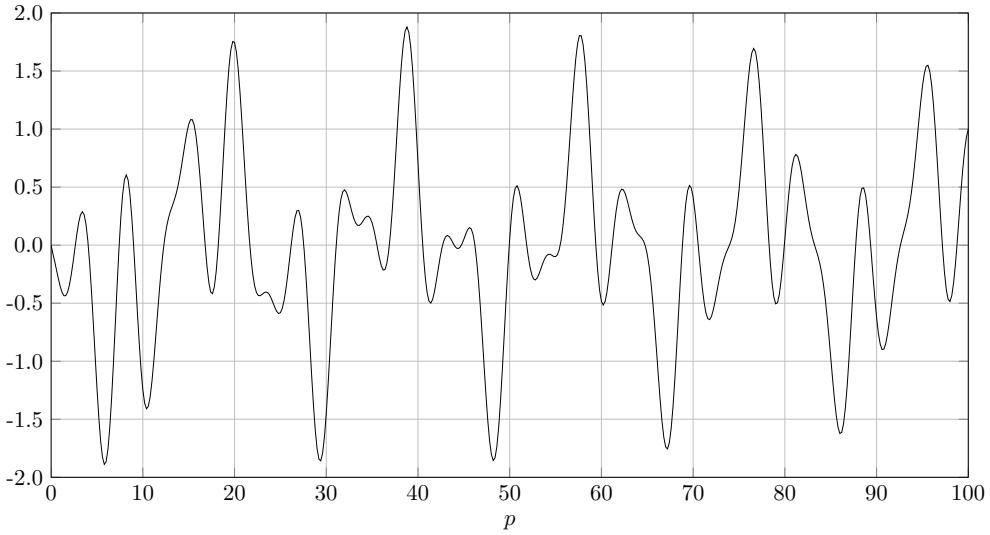

Figure 3.8: Plot of $p^{3/4}\psi^{(3)}_{\text{over}}(a_3, -1/4; 500; p)$ for $p \in [0, 100]$

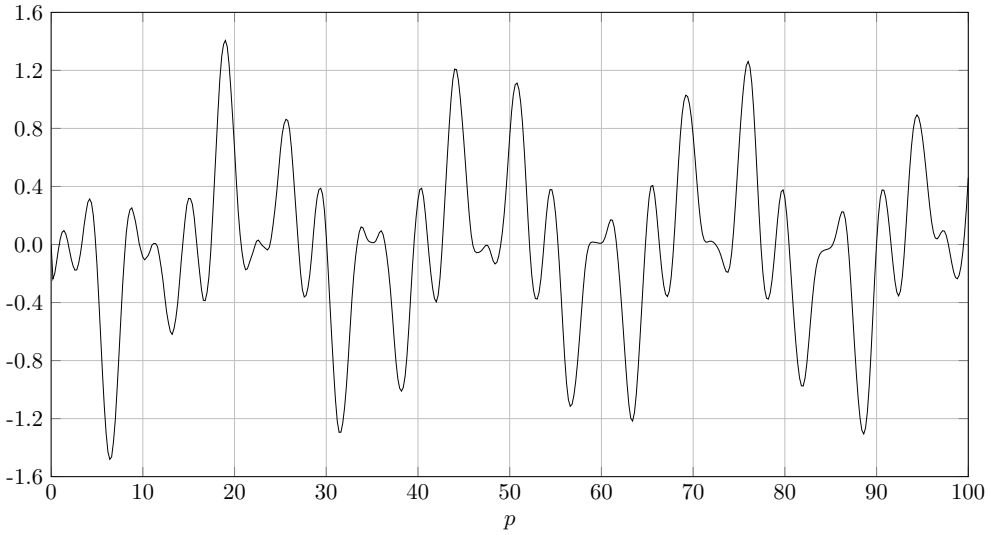

Figure 3.9: Plot of $p^{3/4}\psi^{(4)}_{\text{back}}(a_4, -1/4; 500; p)$ for $p \in [0, 100]$

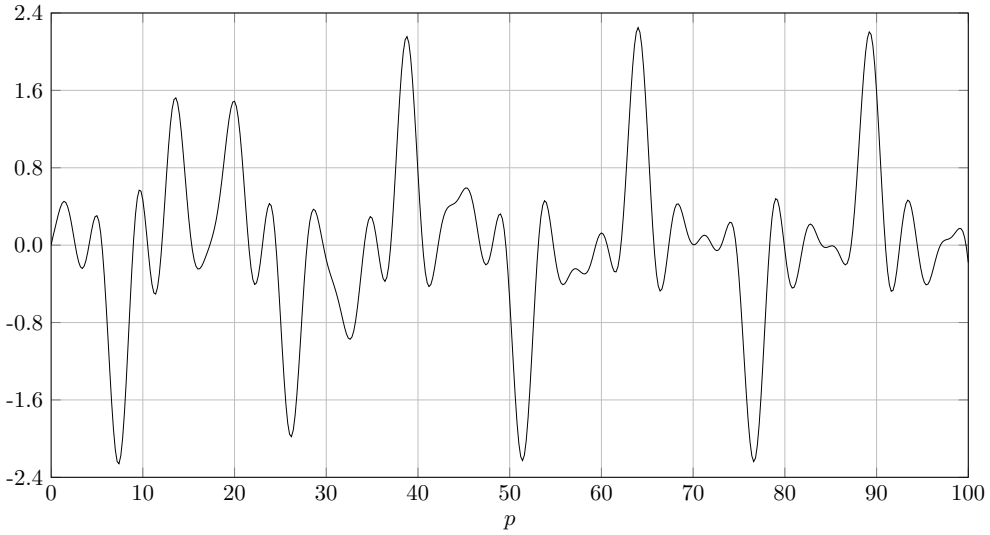

Figure 3.10: Plot of $p^{3/4}\psi^{(4)}_{\text{over}}(a_4, -1/4; 500; p)$ for $p \in [0, 100]$

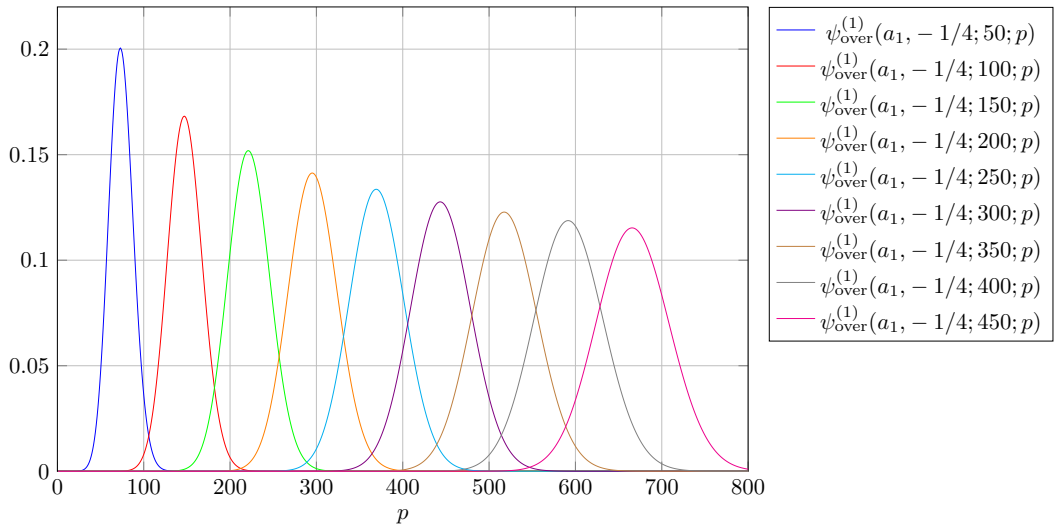

Figure 3.11: Plots of $\psi^{(1)}_{\text{over}}(a_1, -1/4; N; p)$ for N in multiples of 50 and $p \in [0, 800]$.

The plots illustrating the structure of the backflow and overflow maximizing vectors in Figures 3.4 to 3.10 show a particular feature. That is, the higher M backflow/overflow maximizing vectors resemble the $M = 1$ backflow/overflow maximizing vector with higher frequency contributions increasing with M. Physically, one expects that the quantum states maximizing higher M backflow and overflow are more spatially extended[2].

The infimum of the spectrum of the $M = 1$ operator $C^{(1)}$ requires particular discussion. Fig. 3.11 shows the vectors $\psi^{(1)}_{\text{over}}(a_1, -1/4; N)$ for N running from 50 to 450 inclusive in multiples of 50, generated from $N_{\max} = 500$ data. Each plot consists of a single peak centred roughly at $1.5N$, which broadens as N increases. This suggests a sequence of vectors weakly converging to the zero vector in $L^2(\mathbb{R}^+, dp)$ as N increases, whose $C^{(1)}$-expectation values tend to -1. Such a sequence would constitute a singular Weyl sequence for $C^{(1)}$ at -1, from which one could deduce that $-1 \in \sigma_{\text{ess}}(C^{(1)})$ (see e.g., Theorem 2 in of [8]) – a fact that was proved rigorously in [53]. Our numerical results are therefore in line with this result.

3.4 NUMERICAL ACCELERATION

The sequences $\lambda^{(M)}_{\text{back/over}}$ are guaranteed to converge to the backflow/overflow values $b^{(M)}(1, \ldots, 1)$, but the rate of convergence is slow. For example, $\lambda^{(1)}_{\text{back}}(500) = 0.03693$

[2]This is shown in Section J of http://dx.doi.org/10.6084/m9.figshare.c.8174360.

can be compared with the expected value $b^{(1)}_{\text{back}} = 0.03845$ to 4 significant figures. In this section we consider numerical acceleration techniques that modify a convergent sequence, while preserving its limit, but increasing the speed of convergence, at least for sequences of interest. The aim is to provide a better estimate of the eventual limit from the available data.

Let l^{conv} be the vector space of convergent real-valued sequences in $\ell^\infty(\mathbb{N})$.

Definition 3.4.1. *A map $A : l^{\text{conv}} \to l^{\text{conv}}$ is called a* sequence accelerator *for $x \in l^{\text{conv}}$ if Ax and x have the same limit and*

$$\frac{(Ax)_n - x_\infty}{x_n - x_\infty} \longrightarrow 0. \tag{3.34}$$

as $n \to \infty$, where $x_\infty = \lim_{n\to\infty} x_n$.

Richardson accelerators provide a particularly useful class of sequence accelerators; see Chapter 1 of [15] for a modern overview and [60] for detailed theory and generalisations.

Definition 3.4.2. *The* Richardson accelerator *of order γ is the linear map R_γ on l^{conv} with action*

$$(R_\gamma x)_n = \frac{2^\gamma x_{2n} - x_n}{2^\gamma - 1}. \tag{3.35}$$

It is clear that $R_\gamma x$ is convergent with the same limit as x. Moreover, every sequence $(n^{-\alpha})_{n\in\mathbb{N}}$ is an eigenvector of R_γ, with eigenvalue $(2^{\gamma-\alpha} - 1)/(2^\gamma - 1)$, while for any sequence x with $|x_n| \le n^{-\alpha}$ we have a bound

$$|(R_\gamma x)_n| \le \frac{2^{\gamma-\alpha} + 1}{2^\gamma - 1} n^{-\alpha}. \tag{3.36}$$

As R_γ is linear, if

$$x_n = a + \frac{b}{n^\gamma} + \epsilon_n, \qquad |\epsilon_n| \le \frac{C}{n^\alpha} \tag{3.37}$$

for constants a, b, C, and $\alpha > \gamma$, then

$$R_\gamma x_n = a + (R_\gamma \epsilon)_n, \qquad |(R_\gamma \epsilon)_n| \le \frac{2^{\gamma-\alpha} + 1}{2^\gamma - 1} \frac{C}{n^\alpha}. \tag{3.38}$$

and it is clear that the rate of convergence has been improved from $O(n^{-\gamma})$ to $O(n^{-\alpha})$; moreover, the error terms are suppressed if

$$\gamma > 1 - \log_2(1 - 2^{-\alpha}). \tag{3.39}$$

The Richardson acceleration can be iterated, but a significant disadvantage is that the number of the available terms in the resulting sequence is approximately halved on each iteration. Alternatively, one can generalise the Richardson method as follows – see [60] for yet further generalisations and discussion. Suppose, for some integer $k \geq 2$, that

$$x_n = \sum_{j=1}^{k} \frac{a_j}{n^{\gamma_j}} + \epsilon_n, \qquad |\epsilon_n| \leq \frac{C}{n^{\gamma_{k+1}}} \tag{3.40}$$

where $0 = \gamma_1 < \gamma_2 < \cdots < \gamma_k < \gamma_{k+1}$, $a_1, \ldots, a_k$ and C are constant real numbers, so $x_n \to a_1$ as $n \to \infty$. Let $1 = r_1 < r_2 < \ldots < r_k$ be integers and write $\boldsymbol{\gamma} = (\gamma_1, \ldots, \gamma_k)$, $\boldsymbol{r} = (r_1, \ldots, r_k)$. Let $v \in \mathbb{R}^k$ be the unique solution (the relevant generalised Vandermonde determinant is nonvanishing by the remark at the end of [57]) to

$$\sum_{j=1}^{k} \frac{v_j}{(r_j)^{\gamma_i}} = \begin{cases} 1 & i = 1 \\ 0 & i \neq 0 \end{cases}. \tag{3.41}$$

Then

$$(R_{\boldsymbol{\gamma},\boldsymbol{r}} x)_n := \sum_{j=1}^{k} v_j x_{nr_j} = a_1 + (R_{\boldsymbol{\gamma},\boldsymbol{r}} \epsilon)_n, \qquad |(R_{\boldsymbol{\gamma},\boldsymbol{r}} \epsilon)_n| \leq \frac{C}{n^{\gamma_{k+1}}} \sum_{j=1}^{k} \frac{|v_j|}{r_j^{\gamma_{k+1}}}. \tag{3.42}$$

The accelerator $R_{\boldsymbol{\gamma},\boldsymbol{r}}$ removes $k-1$ power-law terms, while reducing the number of available terms by a factor of approximately r_k. Provided that $r_k < 2^{k-1}$ this represents an advantage over the iterated Richardson accelerator $R_{\gamma_k} \circ \cdots \circ R_{\gamma_2}$. The simplest usage is to set $r_j = j$ for $1 \leq j \leq k$ and we will do that from now on, dropping the vector $\boldsymbol{r}$ from the notation.

Our aim is to apply (generalised) Richardson accelerators to the sequences $\lambda^{(M)}_{\text{back/over}}$ for $1 \leq M \leq 4$. As the asymptotics of these sequences are unknown we also have to determine that the sequences are well-described by expansions of the form in (3.40), and to determine the relevant exponents. Another issue is that the sequences $\lambda^{(M)}_{\text{back}}$ contain oscillatory components with amplitude and period increasing with M. These oscillations become apparent in the accelerated sequences, once the dominant power law terms are removed, obstructing attempts to estimate the limit.

To dampen the oscillations in the sequences Kolmogorov–Zurbenko (KZ) low-pass filters [74, 67] are applied before Richardson acceleration. The KZ filter $\text{KZ}_{m,k}$ can be regarded as $k \in \mathbb{N}$ iterations of a moving average over an odd number of points $m \in \mathbb{N}$, and preserves limits of convergent sequences. We chose $k = 5$ for each filter application and then for each M chose the parameters m_M such that the 3rd

M	1	2	3	4
Filter	$\mathrm{KZ}_{7,5}$	$\mathrm{KZ}_{13,5} \circ \mathrm{KZ}_{7,5}$	$\mathrm{KZ}_{24,5} \circ \mathrm{KZ}_{7,5}$	$\mathrm{KZ}_{38,5} \circ \mathrm{KZ}_{7,5}$

Table 3.3: KZ filters applied for $1 \leq M \leq 4$.

successive differences have significantly diminished oscillations. Table 3.3 shows the choice of filtering for each sequence of approximate eigenvalues. With the oscillations significantly dampened, we begin analyzing the non-decreasing backflow sequences by assuming that each sequence $\lambda_{\mathrm{back}}^{(M)}$ has successive differences of the form

$$\lambda(N+1) - \lambda(N) = \frac{\beta\gamma}{N^{\gamma+1}} + \mathcal{O}\left(\frac{1}{N^{\gamma+1+\delta}}\right) \tag{3.43}$$

for some $\beta, \gamma, \delta > 0$. Resumming, this implies that each $\lambda_{\mathrm{back}}^{(M)}$ has the form

$$\lambda(N) = \alpha - \frac{\beta}{N^{\gamma}} + \mathcal{O}\left(\frac{1}{N^{\gamma+\delta}}\right) \tag{3.44}$$

for some constant $\alpha \in \mathbb{R}$, which is the limit of $\lambda(N)$ as $N \to \infty$ and estimates the supremum of the spectrum of the relevant backflow operator. We will write $\beta_{\mathrm{back}}^{(M)}, \gamma_{\mathrm{back}}^{(M)}$ to indicate the leading order parameters of the sequences $\lambda_{\mathrm{back}}^{(M)}$.

To find the leading order parameters of $\lambda_{\mathrm{back}}^{(M)}$, we make use of two tools: a log - log plot and the Pearson correlation coefficient.

Taking the logarithm of (3.43), we find that

$$\log(\lambda_{N+1} - \lambda_N) = \log(\beta\gamma) - (\gamma+1)\log(N) + \mathcal{O}\left(\frac{1}{N^{\delta}}\right) \tag{3.45}$$

and so one can estimate the parameters β, γ by the estimating the intercept and gradient of the plot of $\log(\lambda_{N+1} - \lambda_N)$ against $\log N$.

The second tool in our arsenal is the Pearson correlation coefficient. Given two sequences X, Y, their Pearson correlation coefficient $\rho(X,Y) \in [-1,1]$ is given by

$$\rho(X,Y) = \frac{\mathrm{Cov}(X,Y)}{\sqrt{\mathrm{Var}(X)\,\mathrm{Var}(Y)}}, \tag{3.46}$$

which measures the extent to which Y is linearly dependent on X, with values of $\rho(X,Y) = \pm 1$ for the case of perfect linear correlation with positive/negative coefficient, and values closer to 0 indicating poor linear correlation. For a given $\gamma > 0$ and sequence λ, consider the sequence

$$\mu(\gamma;\lambda)_N = N^{\gamma+2}(\lambda_{N+1} - \lambda_N). \tag{3.47}$$

Comparing with (3.43), we will choose the value of γ so as to maximise the Pearson coefficient.

Using the log-log plots, we obtained Table 3.4 of approximate values of $\beta_{\text{back}}^{(M)}, \gamma_{\text{back}}^{(M)}$ to 3 significant figures. Meanwhile, computation of the Pearson coefficients all give peaks within 0.02 of $\gamma = 0.5$. On natural grounds, we argue that $\gamma_{\text{back}}^{(M)} = 0.5$ for each M, which justifies applying the accelerator $R_{0.5}$ to each sequence. We can then repeat the process of trying to estimate the next term in a putative asymptotic expansion for $\lambda_{\text{back}}^{(M)}$. In the case $M = 1$, we obtained good evidence for a power $\gamma = 1$, and after applying the combined accelerator $R_{(0.5,1)}$ to the original sequence, we found evidence that the next power is below 2. This suggests a conjecture that $\lambda_{\text{back}}^{(1)}$ admits an asymptotic series of the form

$$\lambda_{\text{back}}^{(1)}(N) \sim c_{\text{BM}} - \sum_{k\geq 1} \frac{\beta_k}{N^{k/2}} \tag{3.48}$$

for some coefficients β_k with $\beta_1 > 0$.

Using generalised Richardson accelerators, we obtain conjectural bounds on c_{BM}. Application of $R_{(0.1,1,1.5,2,2.5,3)}$ and $R_{(0.5,1,1.5,2,2.5,3,3.5)}$ to $\lambda_{\text{back}}^{(1)}$ result in descending and ascending sequences respectively as shown in Figure 3.12. By selecting the final values of each sequence, we obtain conjectured upper and lower bounds to the Bracken-Melloy constant. To eight significant figures, we find

$$0.038450556 \leq c_{\text{BM}} \leq 0.038450568 \tag{3.49}$$

and thus $c_{\text{BM}} = 0.0384506$ correct to the first 6 significant figures. Of particular note is that the upper bound we obtain is strictly below the previously accepted figure of 0.038452. Possible reasons for this are discussed below. Note that while the accelerators we use result in sequences whose eventual limit is guaranteed to be equal to c_{BM}, it is conceivable that the limited number of terms available may give a misleading impression. For example, we cannot be sure that the two sequences arising from $R_{(0.5,1,1.5,2,2.5,3)}$ and $R_{(0.5,1,1.5,2,2.5,3,3.5)}$ remain monotonic and provide upper and lower bounds to c_{BM}. It is conceivable that if more terms were computed, these sequences might cross, perhaps many times, before approaching their common limit. However, problems of this sort are common to all numerical computation that is unsupported by rigorous bounds. We are currently conducting an independent calculation of c_{BM} which it is hoped will serve as a cross-check on these values.

Our estimate for c_{BM} agrees with those of [29, 53] to 4 significant figures but differs beyond that. In fact the 5th significant figure in [29] was stated tentatively,

M	$\beta_{\text{back}}^{(M)}$	$\gamma_{\text{back}}^{(M)}$
1	0.0329	0.494
2	0.0739	0.495
3	0.118	0.502
4	0.0168	0.514

Table 3.4: Values of $\beta_{\text{back}}^{(M)}, \gamma_{\text{back}}^{(M)}$ for $1 \leq M \leq 4$.

though it was then apparently confirmed and refined in [53]. We briefly compare the methods used to argue that our new estimate is likely to be the more accurate of the three, based on the following two observations. First, in [29, 53] the backflow operator (or an operator unitarily equivalent to it) on $L^2(\mathbb{R}^+)$ was numerically diagonalised by truncating to a subspace $L^2([0,\Lambda])$ and then discretising the resulting operator by setting a mesh size $\delta \ll \Lambda$ resulting in a matrix problem of dimension $\mathcal{O}(\Lambda/\delta)$. Although the techniques in [29, 53] were different in detail, they share the feature that c_{BM} is obtained in a double limit $\delta \to 0$ and $\Lambda \to \infty$. In practice, a mesh size $\delta(\Lambda) > 0$ is selected that appears to give reasonable estimate of the $\delta \to 0$ limit at fixed Λ, and a sequence of results is obtained by increasing Λ through some sequence of cutoff sizes Λ_N. Consequently, the sequence of results can depend on the sequence Λ_N as well as the dependence of δ on Λ. By contrast, our method is based on closed form expressions for the matrix elements in terms of special functions, avoiding cutoffs and discretisation. Once we have chosen our sequence of basis functions, the sequence of eigenvalue estimates is labelled by the single parameter N that indicates how many basis vectors have been used; we are also able to compute these estimates to high precision based on the error analysis in Section 3.2. Second, [29, 53] used relatively straightforward fitting or extrapolation methods to estimate the limiting value c_{BM}, whereas we have used sequence acceleration to systematically remove terms in the asymptotic series resulting in sequences that converge significantly faster to c_{BM} than the raw sequence $\lambda_{\text{back}}^{(1)}$.

The numerical evidence for an asymptotic expansion of $\lambda_{\text{back}}^{(M)}$ for $M = 2, 3, 4$ beyond the initial $N^{-1/2}$ term is rather weaker, but we conjecture that they have a similar asymptotic expansion to the case $M = 1$. However, the results of successive acceleration are limited by the extra smoothing required to limit the impact of the more complicated oscillations in the sequences. Plots of the accelerated sequences

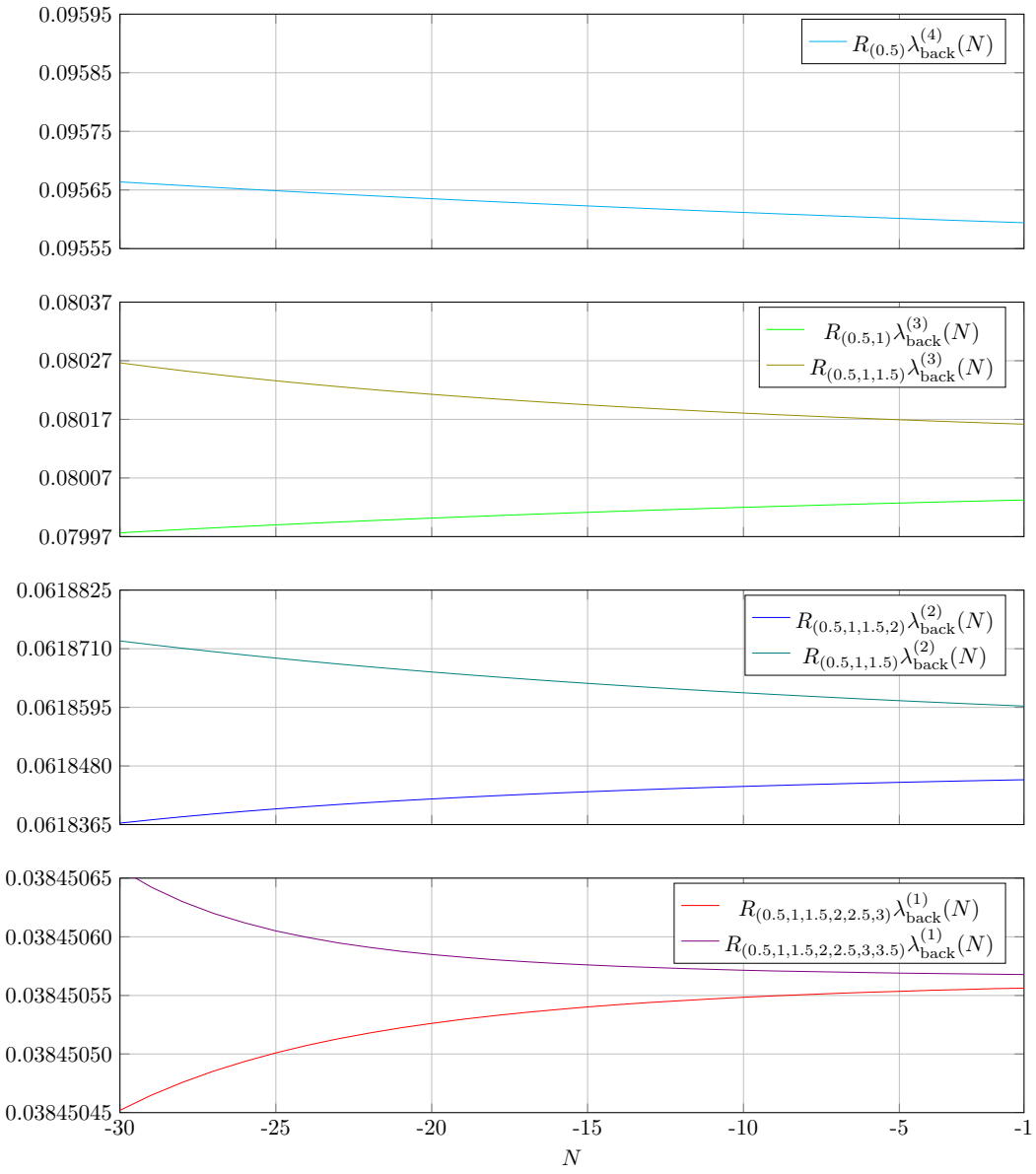

Figure 3.12: Plots of $R_{\boldsymbol{\gamma}_M}\lambda^{(M)}_{\text{back}}$ for selected powers $\boldsymbol{\gamma}_M$ and $1 \leq M \leq 4$

are presented in Figure 3.12, with the resulting bounds tabulated in Table 3.5. As with the $M = 1$ case, these 'bounds' are not rigorous, but indicate that accelerated sequences appear to sandwich the limiting value.

M	Acceleration parameters	Lower bound (LB)	Upper bound (UB)
1	LB: $(0.5, 1, 1.5, 2, 2.5, 3)$, UB: $(0.5, 1, 1.5, 2, 2.5, 3, 3.5)$	0.0384505563	0.0384505678
2	LB: $(0.5, 1, 1.5, 2)$, UB: $(0.5, 1, 1.5)$	0.0618453024	0.0618597497
3	LB: $(0.5, 1)$, UB: $(0.5, 1, 1.5)$	0.0800324618	0.0801617473
4	UB: (0.5)	–	0.0955940854

Table 3.5: Conjectured upper and lower bounds for c_{BM} and $b^{(M)}_{\mathrm{back}}(1, \ldots, 1)$ for $1 \leq M \leq 4$.

As a check on our attempts to numerically accelerate $\lambda^{(1)}_{\mathrm{back}}$, we also made use of Theorem 5 from [49], which gives an acceleration method based on the Raabe-Duhamel (RD) convergence test.

Theorem 3.4.3. *If a sequence x obeys*

$$\lim_{n\to\infty}\left[(n+1)\frac{x_{n+2}-x_{n+1}}{x_{n+1}-x_n}-n\right]<0 \tag{3.50}$$

then x converges and the nonlinear sequence transformation

$$\mathrm{RD}[x]_n = x_n - \frac{n(x_{n+1}-x_n)^2}{(n+1)(x_{n+2}-x_{n+1})-n(x_{n+1}-x_n)} \tag{3.51}$$

accelerates the convergence of x.

The sequence $\lambda^{(1)}_{\mathrm{back}}$ appears to satisfy equation (3.50) for large N, as does $\mathrm{RD}^k[\lambda^{(1)}_{\mathrm{back}}]$ for $k = 1, 2, 3$. After four applications of Theorem 3.4.3 (with some intermediate KZ-smoothing) to $\lambda^{(1)}_{\mathrm{back}}$, we find $c_{\mathrm{BM}} \approx 0.0384506$, backing up the values we find in Table 3.5 from the generalised Richardson accelerator. We were only able to apply the accelerator once to each of the sequences $\lambda^{(M)}_{\mathrm{back}}$ for $M = 2, 3, 4$ and the Richardson results of Table 3.5 appear to be more stable estimates on the basis of the data for $N = 500$, though they rely on our assumption that the asymptotic behaviour mirrors that in the $M = 1$ case.

We now turn to the analysis of the minimum spectral estimates $\lambda^{(M)}_{\mathrm{over}}$ for $2 \leq M \leq 4$. Note that we do not include any analysis of $M = 1$ since it is known that $\lambda^{(1)}_{\mathrm{over}}(N) \to \min \sigma(C^{(1)}) = -1$ as $N \to \infty$. Our analysis follows that of the maximum spectral estimates and we assume that each $\lambda^{(M)}_{\mathrm{over}}$ has asymptotics satisfying (3.43), however now we will have $\beta < 0$ in line with $\lambda^{(M)}_{\mathrm{over}}$ being monotonically decreasing

M	$\beta_{\text{over}}^{(M)}$	$\gamma_{\text{over}}^{(M)}$
2	-0.0141	0.46
3	-0.0439	0.479
4	-0.0826	0.497

Table 3.6: Values of $\beta_{\text{over}}^{(M)}$ and $\gamma_{\text{over}}^{(M)}$ for $2 \leq M \leq 4$.

M	Acceleration parameters	Lower bound (LB)	Upper bound (UB)
2	LB: $(0.5, 1, 1.5)$, UB: $(0.5, 1, 1.5, 2)$	-1.0037916	-1.0037899
3	LB: $(0.5, 1, 1.5)$, UB: $(0.5, 1)$	-1.011078	-1.011029
4	UB: (0.5), $(0.5, 1)$	-1.01947	-1.01934

Table 3.7: Conjectured upper and lower bounds of $b_{\text{over}}^{(M)}(1, \ldots, 1)$ for $M = 2, 3, 4$ intervals of equal length and spacing.

sequences for $M = 2, 3, 4$. Before going ahead with our analysis, we applied KZ filters to $\lambda_{\text{over}}^{(M)}$ with the same parameters as in Table 3.3.

Using the log-log plots, for each $M = 2, 3, 4$ let $\beta_{\text{over}}^{(M)}$ and $\gamma_{\text{over}}^{(M)}$ be the leading order parameters as in (3.43). The values we find are tabulated in Table 3.6. Similarly to the parameters of maximum spectral estimates, we find peaks of the Pearson correlation coefficient within 0.03 of $\gamma = 0.5$ and we infer $\gamma_{\text{over}}^{(M)} = 1/2$ for each $M = 2, 3, 4$. Following as we did for the maximum spectral estimates, we conjecture that the $\lambda_{\text{over}}^{(M)}$ admit an asymptotic expansion of the form (3.48). Again by making use of the generalised Richardson accelerators, we accelerate the convergence of the minimum spectral estimates. The plots of these accelerated sequences are shown in Figure 3.13.

The final values of the generalised Richardson accelerated overflow estimates are tabulated in Table 3.7. The values are written as upper and lower bounds on the overflow values $b_{\text{over}}^{(M)}(1, \ldots, 1)$ for M intervals of equal length and spacing, in line with the assumption that the monotonicity of the sequences remain fixed. We note in particular that the overflow value $b_{\text{over}}^{(2)}(1, 1)$ for two intervals of equal length and spacing is far from the $M = 2$ overflow constant $c_{\text{over}}^{(2)} = -1 - c_{\text{BM}}$ arising from all possible pairs of intervals.

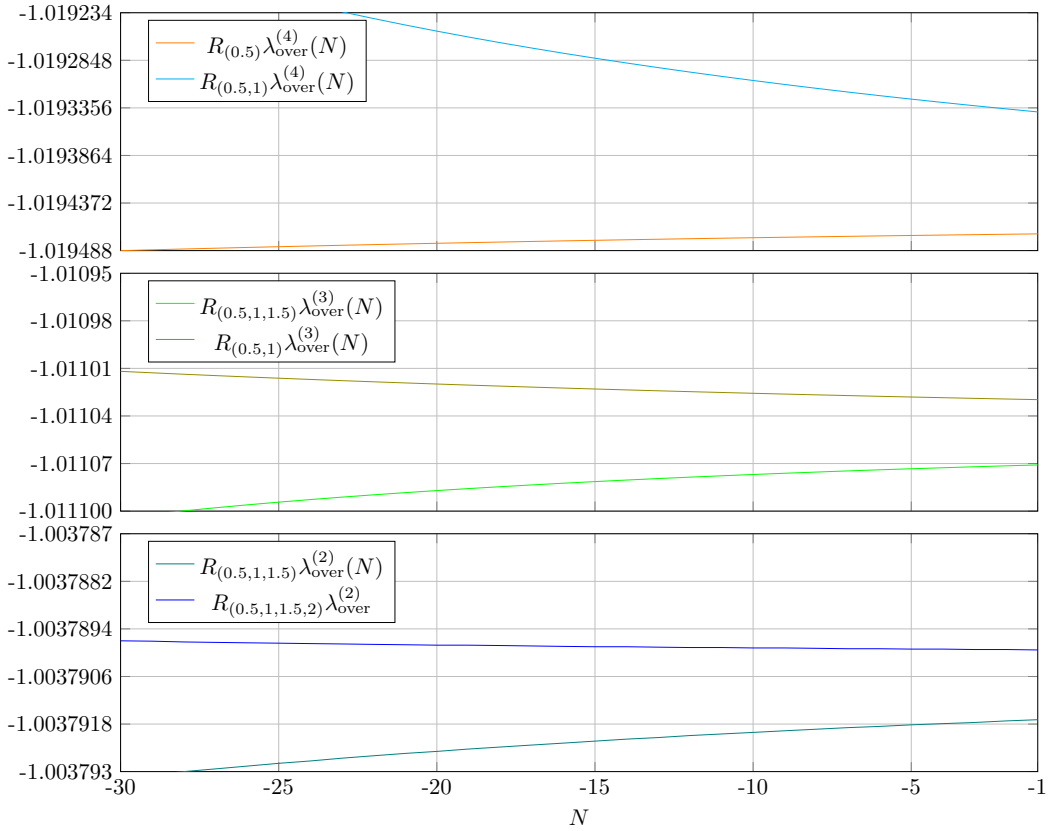

Figure 3.13: Plots of $R_{\boldsymbol{\gamma}_M}\lambda^{(M)}_{\text{over}}$ for selected powers $\boldsymbol{\gamma}_M$ and $2 \leq M \leq 4$.

— 4 —

Numerical Investigation of the Bracken–Melloy Operator

4.1 MATRIX APPROXIMATION AND A DENSITY PROOF

As defined in (1.17) and (1.19), the backflow operator for a pair of times $t_1 < t_2$ is given by

$$\left(B_{\langle t_1,t_2\rangle}\phi\right)(p) = -\frac{1}{2\pi i}\int_0^\infty dq\, \frac{e^{it_2(p^2-q^2)} - e^{it_1(p^2-q^2)}}{p-q}\phi(q) \tag{4.1}$$

for $\phi \in L^2(\mathbb{R}^+)$. As has been discussed in 1 and 2, the largest possible amount of quantum backflow for a single continuous time interval, named the Bracken–Melloy constant c_{BM}, was first approximated in [12] to be $c_{\mathrm{BM}} \approx 0.04$. In particular we have

$$c_{\mathrm{BM}} = \max \sigma(B_{\langle t_1,t_2\rangle}) \tag{4.2}$$

for any $t_1 < t_2$. We restrict our attention to the particular Bracken–Melloy operator $B := B_{\langle -1,1\rangle}$ which has the simplified form

$$(B\phi)(p) = -\frac{1}{\pi}\int_0^\infty dq\, \frac{\sin(p^2-q^2)}{p-q}\phi(q) \tag{4.3}$$

for $\phi \in L^2(\mathbb{R}^+)$. Rather than work with the Bracken–Melloy operator, we instead work with a unitarily equivalent operator $C = U^*BU$ where $U \in L^2(\mathbb{R}^+)$ has the action

$$(U\phi)(q) = \frac{\phi(\sqrt{q})}{\sqrt{2}q^{1/4}}. \tag{4.4}$$

It is a straight-forward calculation to verify that the bounded operator C then has the action

$$(C\varphi)(q) = -\frac{1}{2\pi}\int_0^\infty dq\, \frac{\sin(p-q)}{p-q}\left[\left(\frac{p}{q}\right)^{1/4} + \left(\frac{p}{q}\right)^{-1/4}\right]\varphi(q) \tag{4.5}$$

for $\varphi \in L^2(\mathbb{R}^+)$.

4.1.1 The Strategy

The strategy to find the largest spectral point of C is encapsulated in the following lemma, first given in Chapter 3 but reiterated without proof for readability.

Proposition 4.1.1. *Let A be a bounded self-adjoint operator on Hilbert space $\mathscr{H}$ and let $(\chi_n)_{n\in\mathbb{N}} \subset \mathscr{H}$ be a sequence of linearly independent vectors with dense span. Define sequences of self-adjoint $N\times N$ matrices $(A^{[N]})_{N\in\mathbb{N}}$ and $(P^{[N]})_{N\in\mathbb{N}}$ with matrix elements*

$$A^{[N]}_{mn} = \langle\chi_m|A\chi_n\rangle\,, \qquad P^{[N]}_{mn} = \langle\chi_m|\chi_n\rangle \tag{4.6}$$

for $1 \le m,n \le N$. Then $\sigma(A^{[N]},P^{[N]}) \subseteq \mathcal{N}(A)$, and $\max\sigma(A^{[N]},P^{[N]})$ (resp., $\min\sigma(A^{[N]},P^{[N]})$) is a bounded nondecreasing (resp., nonincreasing) sequence with

$$\begin{aligned}\max\sigma(A) &= \lim_{N\to\infty}\max\sigma(A^{[N]},P^{[N]})\\ \min\sigma(A) &= \lim_{N\to\infty}\min\sigma(A^{[N]},P^{[N]}).\end{aligned} \tag{4.7}$$

For each $N\in\mathbb{N}$, suppose $v^{(N)}\in\mathbb{C}^N$ is a generalised eigenvector obeying

$$A^{[N]}v^{(N)} = \lambda_N P^{[N]}v^{(N)}, \qquad v^{(N)\dagger}P^{[N]}v^{(N)} = 1 \tag{4.8}$$

and define $\psi^{(N)}\in\mathcal{H}$ by

$$\psi^{(N)} = \sum_{n=1}^{N} v_n^{(N)}\chi_n. \tag{4.9}$$

If $\psi^{(N)}\to\psi\in\mathcal{H}$ in norm then

1. *the sequence of generalised eigenvalues $(\lambda_N)_{N\in\mathbb{N}}$ converges;*
2. *the sequence of vectors $(\psi^{(N)})_{N\in\mathbb{N}}$ is a Weyl sequence for $\lambda = \lim_{N\to\infty}\lambda_N$, i.e., $\|\psi^{(N)}\| = 1$ and $\|(A-\lambda I)\psi^{(N)}\|\to 0$;*
3. *the limiting vector ψ is an eigenvector for A with eigenvalue λ.*

Hence, by finding the closed form of the matrix elements of C with respect to some dense sequence in $L^2(\mathbb{R}^+)$, it will be possible to obtain rigorous lower bounds on c_{BM}. This method is akin to a finite element method, often used in the numerical analysis of partial differential equations. All previous attempts to numerically study the Bracken–Melloy operator have used lattice methods. Typically, the Bracken–Melloy operator is studied by first fixing a finite lattice $\Lambda(p_{\max}, \delta) \subset \mathbb{R}^2$ with maximum size $p_{\max} > 0$ and minimum distance $\delta > 0$. Let K_{BM} be the integral kernel of the Bracken–Melloy operator. Then the matrices $B(p_{\max}, \delta)$ with

$$B(p_{\max}, \delta)_{nm} = K_{\mathrm{BM}}(\delta n, \delta m), \qquad 0 \leq n, m \leq \lfloor p_{\max} \rfloor, \tag{4.10}$$

approximate the Bracken–Melloy operator. The largest eigenvalue $\lambda(p_{\max}, \delta)$ of $B(p_{\max}, \delta)$ then satisfies

$$\lim_{\delta \to 0,\, p_{\max} \to \infty} \lambda(\delta, p_{\max}) = c_{\mathrm{BM}}. \tag{4.11}$$

In particular, two limits are required to find c_{BM}. The finite element method used in this chapter has the advantage that c_{BM} arises from the limit of a single discrete variable and the resulting spectral estimates constitute rigorous lower bounds on c_{BM}.

The choice of dense sequence is inspired by the conjecture by Yearsley and Halliwell [69] that the Backflow maximizing vector for B has the asymptotic form $\phi(q) \sim \sin(q^2)/q$. This would imply that the vector maximizing the expectation value of C has the asymptotic form $\varphi(q) \sim \sin(q)/q^{3/4}$. Additionally, by inspecting the integral kernel of C, one might expect the asymptotic form of a vector in the image of C to be

$$A\frac{\sin(p-\alpha)}{p^{3/4}} + B\frac{\sin(p-\alpha)}{p^{5/4}} \tag{4.12}$$

for fixed α. It is this heuristic that led to choosing the sequence

$$(\varphi_{n,\pm 1/4})_{n\geq 0} = (\varphi_{n,1/4}, \varphi_{n,-1/4})_{n\geq 0} \subseteq L^2(\mathbb{R}^+) \tag{4.13}$$

to be the sequence of trial vectors used to estimate c_{BM} where for integer n and $|\alpha| < 1/2$, $\varphi_{n,\alpha}$ is given by

$$\varphi_{n,\alpha}(q) = \frac{1}{\sqrt{\pi}} q^{\alpha} \frac{\sin(q - n\pi)}{q - n\pi}. \tag{4.14}$$

Before applying Lemma 3.2.1 to the backflow operator C and the sequence $(\varphi_{n,\pm 1/4})_{n\geq 0}$, we require density of the sequence. We make an important comment

here. It was only possible to prove that $(\varphi_n^{\pm})_{n\in\mathbb{Z}}$ is dense in $L^2(\mathbb{R}^+)$. We do, however, conject that $(\varphi_n^{\pm})_{n\geq 0}$ is dense in $L^2(\mathbb{R}^+)$. The proof of the density of $(\varphi_{n,\pm 1/4})_{n\in\mathbb{Z}}$ is given by the following theorem.

Theorem 4.1.2. *For $|\alpha| < 1/2$ and integer $n \in \mathbb{Z}$, let $\varphi_{n,\alpha} \in L^2(\mathbb{R}^+)$ be defined by*

$$\varphi_{n,\alpha}(q) = \frac{1}{\sqrt{\pi}} q^{\alpha} \frac{\sin(q - n\pi)}{q - n\pi}. \tag{4.15}$$

Then $(\varphi_{n,\alpha})_{n\in\mathbb{Z}}$ is dense in $L^2(\mathbb{R}^+)$.

Before stating the proof we make a short digression to discuss and prove some facts about band-limited functions. A band-limited function is one whose Fourier transform is compactly supported.

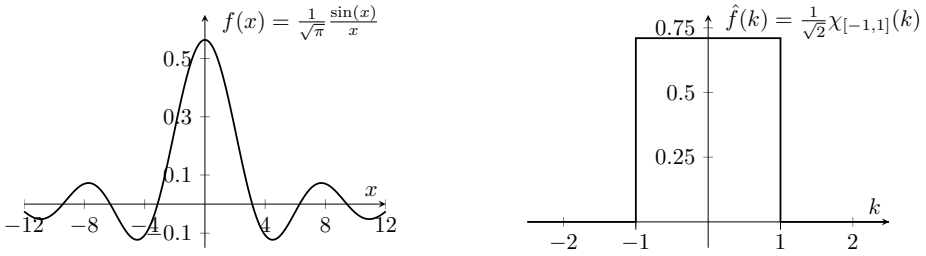

Figure 4.1: Example of typical band-limited function

A typical example of a band-limited function is shown in Figure 4.1. The compactly supported nature of $\hat{f}$ means that f is intuitively a very smooth function, since it imposes limits on how fast f can oscillate.

Definition 4.1.3. *For $p, \sigma > 0$, let $PW^{p,\sigma}$ be the class of Paley-Wiener functions defined by*

$$PW^{p,\sigma} = \left\{ f \in L^p(\mathbb{R}) : \text{supp } \hat{f} \subseteq [-\sigma, \sigma] \right\}. \tag{4.16}$$

Elements of Paley-Wieiner spaces are also called band-limited functions. An important property of band-limited functions is that they can be extended to holomorphic functions on $\mathbb{C}$. This can be seen in the following argument. For $f \in PW^{2,1}$, we have

$$f(x) = \frac{1}{\sqrt{2\pi}} \int_{-1}^{1} dk\, \hat{f}(k) e^{ikx}. \tag{4.17}$$

As can be seen, by substituting x with $x + iy$ for some $y \in \mathbb{R}$, we obtain

$$f(x + iy) = \frac{1}{\sqrt{2\pi}} \int_{-1}^{1} dk\, \hat{f}(k) e^{-ky} e^{ikx} \tag{4.18}$$

which clearly converges for any $x, y \in \mathbb{R}$. Differentiating (4.18), it follows that f is holomorphic on $\mathbb{C}$. An immediate corollary of this is that for any $p > 1$, $PW^{p,1} \subseteq \mathcal{C}^\infty(\mathbb{R})$. The Paley-Wieiner spaces $PW^{p,1}$ for $p > 1$ will play an important role in the proof of theorem 4.1.2 for the following reason. For $n \in \mathbb{Z}$, let $s_n \in L^2(\mathbb{R})$ be the shifted sinc vector

$$s_n(q) = \frac{\sin(q - n\pi)}{q - n\pi}. \tag{4.19}$$

Note that for $n \in \mathbb{Z}$ and $q \in \mathbb{R}$, we have

$$\frac{1}{\sqrt{2\pi}} \int_{-\infty}^{\infty} dk \, \frac{1}{\sqrt{2}} e^{-ikn\pi} \chi_{[-1,1]}(k) e^{ikq} = \frac{1}{\sqrt{\pi}} \frac{1}{2(q - n\pi)} \left(e^{i(q-n\pi)} - e^{-i(q-n\pi)} \right) \tag{4.20}$$

$$= \frac{1}{\sqrt{\pi}} \frac{\sin(q - n\pi)}{q - n\pi} \tag{4.21}$$

and hence by the Fourier inversion theorem on $L^2(\mathbb{R})$, we find that $\hat{s}_n \in PW^{2,1}$ for all $n \in \mathbb{Z}$. As was first shown by Shannon in 1948 [59], one can reconstruct a function $f \in PW^{2,1}$ by its samples on the grid $(n\pi)_{n\in\mathbb{Z}}$ using the shifted sinc functions s_n. For a modern overview of sampling theorems, the reader is guided to [16, 17]. The classical Shannon sampling theorem says that if $f \in PW^{p,\sigma}$ for some $p > 1$ and $\sigma > 0$, then f admits a representation as an infinite sum of sinc functions. The following theorem is a precise version of this, taken from Theorem 1 of [30].

Theorem 4.1.4. (Shannon sampling theorem) *Let $\sigma > 0$ and $1 < p < \infty$. If $f \in PW^{p,\sigma}$ then*

$$\lim_{N\to\infty} \left\| f - \sum_{|k|\leq N} f\left(\frac{k\pi}{\sigma}\right) s_k(\sigma \cdot) \right\|_p = 0. \tag{4.22}$$

Furthermore,

$$f(x) = \sum_{k=-\infty}^{\infty} f\left(\frac{k\pi}{\sigma}\right) s_k(\sigma x) \tag{4.23}$$

for all $x \in \mathbb{R}$.

Theorem 4.1.4 tells us that if $f \in PW^{p,\sigma}$, then f may be reconstructed from its samples. The following Lemma will be used in the proof of theorem 4.1.2.

Lemma 4.1.5. *Let $1 < p < \infty$, $f \in PW^{p,1}$ and $|\alpha| < 1/2$. Then*

$$\left\| X^\alpha \left(f - \sum_{|n|\leq N} f(n\pi) s_n \right) \right\|_2 \to 0 \text{ as } N \to \infty, \tag{4.24}$$

where X is the densely defined position operator with action $(Xf)(x) = xf(x)$.

For the proof, we require the notion of Schwartz functions[1], defined by

$$\mathcal{S}(\mathbb{R}) = \left\{ f : \mathbb{R} \to \mathbb{C} \middle| f \text{ smooth and } \|f\|_{p,q} < \infty \text{ for all } p, q \in \mathbb{N}_0 \right\} \tag{4.25}$$

where $\|f\|_{p,q}$ are The Schwartz seminorms given by

$$\|f\|_{p,q} = \sup_{x \in \mathbb{R}} \left| x^q \left(\frac{d}{dx} \right)^p f(x) \right|. \tag{4.26}$$

Proof of lemma 4.1.5. Note that for any $N \in \mathbb{N}$ we can write

$$\begin{aligned} &\left\| X^\alpha \left(f - \sum_{|n| \le N} f(n\pi) s_n \right) \right\|_2^2 \\ &\quad = \left(\int_0^1 + \int_1^\infty \right) dx\, x^{2\alpha} \left| f(x) - \sum_{|n| \le N} f(n\pi) \frac{\sin(x - n\pi)}{x - n\pi} \right|^2 . \end{aligned} \tag{4.27}$$

Let $I_1(N)$ and $I_2(N)$ denote the first and second integrals in (4.27). Then we find that

$$\begin{aligned} I_1(N) &\le \sup_{0 \le x \le 1} \left| f(x) - \sum_{|n| \le N} f(n\pi) \frac{\sin(x - n\pi)}{x - n\pi} \right|^2 \int_0^1 dx\, x^{2\alpha} \\ &= \frac{1}{2\alpha + 1} \sup_{0 \le x \le 1} \left| f(x) - \sum_{|n| \le N} f(n\pi) \frac{\sin(x - n\pi)}{x - n\pi} \right|^2 . \end{aligned} \tag{4.28}$$

Since supp $\hat{f} \subseteq [-1, 1]$, f extends to an entire function on $\mathbb{C}$. Applying equation 4.23 of theorem 4.1.4, we have

$$I_1(N) \to 0 \text{ as } N \to \infty \tag{4.29}$$

Now consider the integral $I_2(N)$ given by and obeying

$$I_2(N) = \int_{x_0}^\infty dx\, x^{2\alpha} \left| f(x) - \sum_{|n| \le N} f(n\pi) \frac{\sin(x - n\pi)}{x - n\pi} \right|^2 \tag{4.30}$$

$$\le \sup_{x \ge 1} \left(x^{2\alpha} \left| f(x) - \sum_{|n| \le N} f(n\pi) \frac{\sin(x - n\pi)}{x - n\pi} \right|^{1-\epsilon} \right) \left\| f - \sum_{|n| \le N} f(n\pi) s_n \right\|_{1+\epsilon}^{1+\epsilon} \tag{4.31}$$

[1] An exposition of Schwartz functions and the associated Schwartz distributions can be found in [42].

for $0 < \epsilon < 1 - |2\alpha|$. We will now show that the supremum is bounded from which convergence will follow from the convergence of the Whittaker series in the $L^{1+\epsilon}$ norm. First let

$$S(N) = \sup_{x \geq 1} \left(x^{2\alpha} \left| f(x) - \sum_{|n| \leq N} f(n\pi) \frac{\sin(x - n\pi)}{x - n\pi} \right|^{1-\epsilon} \right). \tag{4.32}$$

By the triangle inequality

$$S(N) \leq \left(\sup_{x \geq 1} x^{2\alpha/(1-\epsilon)} |f(x)| + \sum_{|n| \leq N} |f(n\pi)| \sup_{x \geq 1} x^{2\alpha/(1-\epsilon)} \left| \frac{\sin(x - n\pi)}{x - n\pi} \right| \right)^{1-\epsilon}. \tag{4.33}$$

The first term in (4.33) is finite from the fact that $f \in \mathcal{S}(\mathbb{R})$. For the second term, note that for any $x \geq 1$ we have

$$x^{2\alpha/(1-\epsilon)} \left| \frac{\sin(x - n\pi)}{x - n\pi} \right| \leq x \left| \frac{\sin(x - n\pi)}{x - n\pi} \right| \leq |\sin(x - n\pi)| + |n\pi| \left| \frac{\sin(x - n\pi)}{x - n\pi} \right| \tag{4.34}$$

where we have added and subtracted $n\pi s_n(x)$ under the absolute value and applied the triangle inequality. Taking the supremum over $x \geq 1$, we find

$$\sup_{x \geq 1} \left| x^{1/(2(1+\epsilon))} \frac{\sin(x - n\pi)}{x - n\pi} \right| \leq 1 + |n\pi|. \tag{4.35}$$

Substituting this into the sum in (4.33), we find that

$$\begin{aligned} S(N) &\leq \left(\sup_{x \geq 1} x^{2\alpha(1+\epsilon)} |f(x)| + \sum_{|n| \leq N} |f(n\pi)|(1 + |n\pi|) \right)^{1-\epsilon} \\ &\leq \left(\sup_{x \geq 1} x^{2\alpha/(1-\epsilon)} |f(x)| + \sum_{n=-\infty}^{\infty} |f(n\pi)|(1 + |n\pi|) \right)^{1-\epsilon} \\ &< \infty \end{aligned} \tag{4.36}$$

since $f \in \mathcal{S}(\mathbb{R})$. Now note that there is a continuous embedding $S(\mathbb{R}) \hookrightarrow L^{1+\epsilon}(\mathbb{R})$ since

$$\|f\|_{1+\epsilon}^{1+\epsilon} \leq \int_{-\infty}^{\infty} dx \, \frac{\|f\|_{0,2}^{1+\epsilon}}{(1 + x^2)^{1+\epsilon}} = C_\epsilon \|f\|_{0,2}^{1+\epsilon}. \tag{4.37}$$

where for $p, q \in \mathbb{N} \cup \{0\}$, $\| \cdot \|_{p,q}$ is the Schwartz seminorm defined by

$$\|f\|_{p,q} = \sup_{x \in \mathbb{R}} \left| x^q \left(\frac{d}{dx} \right)^p f(x) \right|. \tag{4.38}$$

and $C_\epsilon > 0$ is a constant independent of f. Hence $f \in L^{1+\epsilon}(\mathbb{R})$ and by assumption supp $\hat{f} \subseteq [-1, 1]$. By equation 4.22 of theorem 4.1.4, the right hand side of (**??**) vanishes in the limit as $N \to \infty$. This completes the proof. □

Proof of theorem 4.1.2. First note the natural embedding, $M_\vartheta : L^2(\mathbb{R}^+) \hookrightarrow L^2(\mathbb{R})$, given by multiplication by the Heaviside function ϑ. From here onwards we will drop the ι with the understanding that $L^2(\mathbb{R}^+) \subset L^2(\mathbb{R})$. A well known property of Hilbert spaces is that a sequence is dense if and only if there is no non-trivial vector orthogonal to every element. Assume that there exists some $g \in L^2(\mathbb{R})$ with

$$\text{supp } g \subseteq \mathbb{R}^+, \qquad \langle g|\varphi_{n,\alpha}\rangle = 0 \tag{4.39}$$

for all $n \in \mathbb{Z}$. Recall the definitions of the unbounded position operator X and that the shifted sinc functions $s_n \in L^2(\mathbb{R})$. We can write the orthogonality condition on g as

$$0 = \langle g||X|^\alpha s_n\rangle \text{ for all } n \in \mathbb{Z}. \tag{4.40}$$

For g obeying (4.39), let $T_g : \mathcal{S}(\mathbb{R}) \to \mathbb{R}$ be the map defined by

$$T_g(f) = \langle g|X^\alpha f\rangle\,. \tag{4.41}$$

Immediately, we find that

$$\begin{aligned} T_g(f) &= \int_0^\infty dx\, \overline{g(x)} x^\alpha f(x) = \int_0^\infty dx\, \frac{x^\alpha \overline{g(x)}}{1+x^2}(1+x^2)f(x) \\ &= \left\langle \frac{X^\alpha}{1+X^2} g \middle| (1+X^2)f \right\rangle. \end{aligned} \tag{4.42}$$

Since $X^\alpha(1+X^2)^{-1}g, (1+X^2)f \in L^1(\mathbb{R}^+)$, by Hölder's inequality, $T_g(f)$ exists for all $f \in \mathcal{S}(\mathbb{R})$ and

$$|T_g(f)| \leq \left\| \frac{X^\alpha}{1+X^2} g \right\|_1 \|f\|_{0,2} \tag{4.43}$$

where the Schwartz seminorms $\|\cdot\|_{p,q}$ are described in (4.26). Consequently we find $T_g \in \mathcal{S}'(\mathbb{R})$. We will now show that supp $\hat{T}_g \cap [-1,1] = \emptyset$ in the distributional sense. Recall that for $n \in \mathbb{Z}$, $s_n \in L^2(\mathbb{R})$ is the shifted sinc vector $s_n(x) = \sin(x-n\pi)/(x-n\pi)$. Then for $f \in \mathcal{S}(\mathbb{R})$ and any $N \in \mathbb{N}$ one can write

$$T_g(f) = \left\langle g \middle| X^\alpha \sum_{n=-N}^{N} f(n\pi) s_n \right\rangle + \left\langle g \middle| X^\alpha \left(f - \sum_{n=-N}^{N} f(n\pi) s_n \right) \right\rangle. \tag{4.44}$$

By hypothesis, the first term of (4.44) vanishes. By the Cauchy-Schwarz inequality we have

$$|T_g(f)| \leq \|g\|_2 \left\| X^\alpha \left(f - \sum_{n=-N}^{N} f(n\pi) s_n \right) \right\|_2, \tag{4.45}$$

for any $N \in \mathbb{N}$.

For a distribution $u \in \mathcal{S}'(\mathbb{R})$, let $\hat{u} \in \mathcal{S}'(\mathbb{R})$ be its Fourier transform defined by $\hat{u}(f) = u(\hat{f})$. Now suppose that f satisfies supp $\hat{f} \subseteq [-1, 1]$. Then by taking the limit of (4.45) as $N \to \infty$ and applying lemma 4.1.5, we find

$$T_g(f) = 0 \tag{4.46}$$

for any $f \in \mathcal{S}(\mathbb{R}) \cap PW^{2,1}$ or equivalently

$$\operatorname{supp} \hat{T}_g \cap [-1, 1] = \emptyset. \tag{4.47}$$

Now we turn to the bulk of the theorem. For $\psi \in \mathcal{C}_0^\infty(\mathbb{R})$ with supp $\psi \subseteq [-1+\delta, 1-\delta]$ for some small $0 < \delta < 1$, let $\hat{t}_g = \hat{T}_g * \psi \in \mathcal{C}^\infty(\mathbb{R})$. The support of $\hat{t}_g$ obeys supp $\hat{t}_g \subseteq \operatorname{supp} \hat{T}_g + \operatorname{supp} \psi$ and so $\operatorname{supp} \tilde{t}_g \cap [-\delta, \delta] = \emptyset$. One can express $\hat{t}_g$ as a distribution,

$$\begin{aligned}
\hat{t}_g(f) &= \int_{-\infty}^{\infty} dx\, f(x) \int_{-\infty}^{\infty} dy\, \overline{g(y)} |y|^\alpha \int_{-\infty}^{\infty} dk\, \psi(k-x) e^{-iky} && (4.48)\\
&= \int_{-\infty}^{\infty} dx\, f(x) \int_{-\infty}^{\infty} dy\, \overline{g(y)} |y|^\alpha \int_{-\infty}^{\infty} dk\, \psi(k) e^{-i(k+x)y} && (4.49)\\
&= \int_{-\infty}^{\infty} dx\, f(x) \int_{-\infty}^{\infty} dy\, \overline{g(y)} |y|^\alpha \hat{\psi}(y) e^{-ixy} && (4.50)\\
&= \int_{-\infty}^{\infty} dy\, \overline{g(y)} |y|^\alpha \hat{\psi}(y) \hat{f}(y) && (4.51)\\
&= \hat{T}_{g\hat{\psi}}(f). && (4.52)
\end{aligned}$$

Note that since $\psi \in \mathcal{C}_0^\infty(\mathbb{R})$, we have $\hat{\psi} \in \mathcal{S}(\mathbb{R})$. If there exists a non-trivial $g \in L^2(\mathbb{R}^+)$ satisfying $\langle g | \varphi_{n,\alpha} \rangle = 0$ for all $n \in \mathbb{Z}$, then setting $h = g\hat{\psi}$ one finds a distribution $\hat{T}_h \in \mathcal{C}^\infty(\mathbb{R}) \cap \mathcal{S}'(\mathbb{R})$ satisfying supp $\hat{T}_h \cap [-\delta, \delta] = \emptyset$ for some $\delta > 0$. We can then assume there exists a $h \in L^2(\mathbb{R})$ satisfying

$$\operatorname{supp}\, h \subseteq \mathbb{R}^+, \qquad \operatorname{supp}\, \hat{T}_h \cap [-\delta, \delta] = \emptyset, \qquad P(X)h \in L^2(\mathbb{R}^+) \tag{4.53}$$

for all polynomials P where the condition involving polynomials follows from the fact that $\hat{\psi} \in \mathcal{S}(\mathbb{R})$. Let us further assume that ψ satisfies $\int \psi = 0$. This implies that $\hat{\psi}(0) = 0$. Since $\psi \in \mathcal{C}_0^\infty(\mathbb{R})$, it follows that $\hat{\psi}$ is entire. For z in an open set containing 0, we have $\hat{\psi}(z) = \psi'(0)z + \mathcal{O}(z^2)$. Consequently $|X|^\alpha \hat{\psi}$ is bounded and it follows that $|X|^\alpha h = |X|^\alpha \hat{\psi} g \in L^2(\mathbb{R})$. The distribution T_h is then simply the image of $|X|^\alpha h$ in the natural embedding $L^2(\mathbb{R}) \hookrightarrow \mathcal{S}'(\mathbb{R})$ given by $f \mapsto (\phi \in \mathcal{S}(\mathbb{R}) \mapsto \langle f | \phi \rangle)$. For convenience we write $T_h \in L^2(\mathbb{R})$ now obeying (4.53) and

$$\operatorname{supp}\, \tilde{T}_h \cap [-\delta, \delta] = \emptyset. \tag{4.54}$$

Define $\mathbb{C}^{\pm}$ as the upper $(+)$ and lower $(-)$ complex half planes. From the support property of T_h in (4.54), we find that $\hat{T}_h$ given by

$$\hat{T}_h(z) = \frac{1}{2\pi}\int_0^\infty dx\, T_h(x)e^{-izx} \tag{4.55}$$

is analytic on the lower half plane $\mathbb{C}^-$. We now make use of the Schwarz reflection principle, for which the reader is guided to Chapter 6 of [1] for an overview. The Schwartz reflection principle says that from an analytic function $s^- : \mathbb{C}^- \to \mathbb{C}$, one can define an analytic function $s^+ : \mathbb{C}^+ \to \mathbb{C}$ by $s^+(z) = \overline{s^-(\overline{z})}$ for $z \in \mathbb{C}^+$. From the reflection principle, we find that G_h given by $S_h(z) = \overline{\hat{T}_h(\overline{z})}$ is analytic on the upper half plane $\mathbb{C}^+$ and furthermore both $\hat{T}_h$ and S_h agree on the real line.

Here, we make use of a edge of the wedge-like theorem for complex functions of a single complex variable. Letting the region $[0,\delta]\times\mathbb{R}$ be our wedge with edge $[0,\delta]$, we find that the function F defined on $[0,\delta]\times(\mathbb{R}\setminus\{0\})$ by

$$F(z) = \begin{cases} \hat{T}_h(z) & z \in \mathbb{C}^- \cap ([0,\delta]\times\mathbb{R}) \\ S_h(z) & z \in \mathbb{C}^+ \cap ([0,\delta]\times\mathbb{R}) \end{cases} \tag{4.56}$$

is analytic on its domain. Furthermore, one can distributionally define F on smooth test functions $\phi \in \mathcal{C}^\infty(0,\delta)$ by

$$\langle F|\phi\rangle = \lim_{y\to 0}\int_0^\delta dx\, F(x+iy)\phi(x). \tag{4.57}$$

By [66, page 53], we find F is in fact holomorphic on all of $[0,\delta]\times\mathbb{R}$. However, by (4.54), F vanishes on an open interval and so $F = 0$ identically. The only way this can be the case is if $T_h = 0$ identically from which it follows that $|X|^\alpha\hat{\psi}g = h = 0$. Since ψ is compactly supported, $\hat{\psi}$ must be analytic and consequently has isolated zeroes. We conclude that $g = 0$ up to L^2 equivalence. Hence there is no non-trivial vector g obeying

$$\langle g|\varphi_{n,\alpha}\rangle = 0 \tag{4.58}$$

for all integer $n \geq 0$.

□

Applying theorem 4.1.2 with $\alpha = 1/4$ and $\alpha = -1/4$, we find that $(\varphi_{n,\pm 1/4})_{n\geq 0}$ is dense in $L^2(\mathbb{R}^+)$. As such, we can now safely apply lemma 3.2.1 to find lower bounds on the Bracken–Melloy constant c_{BM}.

4.2 MATRIX ELEMENTS

As in lemma 3.2.1, we now construct the matrices of Gram elements and operator matrix elements for the sequence $(\varphi_{n,\pm 1/4})_{n\geq 0}$ and Bracken–Melloy operator C. For integer $N \in \mathbb{N}$, let

$$\left(P^{[N]}_{\sigma\tau}\right)_{nm} = \left\langle \varphi_{n-1,\sigma 1/4} \middle| \varphi_{m-1,\tau 1/4} \right\rangle, \qquad \left(C^{[N]}_{\sigma\tau}\right)_{nm} = \left\langle \varphi_{n-1,\sigma 1/4} \middle| C\varphi_{m-1,\tau 1/4} \right\rangle \tag{4.59}$$

for $\sigma, \tau \in \{+,-\}$. Further for $i,j \in \{1,2\}$, let $e_{ij} \in \mathbb{R}^{2\times 2}$ be the basis matrices with entries $(e_{ij})_{mn} = \delta_{im}\delta_{jn}$. Then we define

$$P^{[N]} = P^{[N]}_{++} \otimes e_{11} + P^{[N]}_{+-} \otimes e_{12} + P^{[N]}_{-+} \otimes e_{21} + P^{[N]}_{--} \otimes e_{22}, \tag{4.60}$$

$$C^{[N]} = C^{[N]}_{++} \otimes e_{11} + C^{[N]}_{+-} \otimes e_{12} + C^{[N]}_{-+} \otimes e_{21} + C^{[N]}_{--} \otimes e_{22} \tag{4.61}$$

as the complex valued $2N+1$ square matrices. From these two sequences of square matrices, we will find an approximation to the Bracken–Melloy constant c_{BM} and associated approximate eignvector according to proposition 3.2.1.

4.2.1 P AND C MATRIX ELEMENTS

This subsection is concerned with calculating the matrix elements of the bounded integral operator C, which as in (4.5), has the action

$$(C\varphi)(p) = -\frac{1}{2\pi}\int_0^\infty dq\, \frac{\sin(p-q)}{p-q}\left[\left(\frac{p}{q}\right)^{1/4} + \left(\frac{p}{q}\right)^{-1/4}\right]\varphi(q), \tag{4.62}$$

for $\varphi \in L^2(\mathbb{R}^+)$.

Much of the following work was done prior to the start of my PhD by Chris Fewster. However, every calculation done prior has been repeated and furthermore generalised by myself, as can be found in appendix D.

For $\sigma, \tau \in \{+,-\}$ let $P_{\sigma,\tau}$ and $C_{\sigma,\tau}$ be the infinite matrices with elements

$$(P_{\sigma,\tau})_{m+1,n+1} = \left\langle \varphi_{n,\sigma/4} \middle| \varphi_{m,\tau/4} \right\rangle, \qquad (C_{\sigma,\tau})_{m+1,n+1} = \left\langle \varphi_{m,\sigma/4} \middle| C\varphi_{n,\tau/4} \right\rangle \tag{4.63}$$

for $m,n \in \mathbb{Z}$. The elements of P are given by

$$(P_{\sigma,\tau})_{m+1,n+1} = \frac{1}{\pi}\int_0^\infty dq\, q^{(\sigma+\tau)/4}\frac{\sin(q-n\pi)\sin(q-m\pi)}{(q-n\pi)(q-m\pi)} \tag{4.64}$$

$$= \frac{(-1)^{m+n}}{\pi}\int_0^\infty dq\, q^{(\sigma+\tau)/4}\frac{\sin^2 q}{(q-n\pi)(q-m\pi)}. \tag{4.65}$$

Letting $f_{\sigma,\tau}$ be given by

$$f_{\sigma,\tau}(x,y) = \left[\frac{x^{(1+\sigma)/4}}{y^{(1-\tau)/4}} + \frac{y^{(1+\tau)/4}}{x^{(1-\sigma)/4}}\right], \tag{4.66}$$

then

$$(C_{\sigma,\tau})_{m,n} \tag{4.67}$$

$$= -\frac{1}{2\pi^2}\int_0^\infty dx \int_0^\infty dy\, \frac{\sin(x-m\pi)\sin(x-y)\sin(y-n\pi)}{(x-m\pi)(x-y)(y-n\pi)} f_{\sigma,\tau}(x,y) \tag{4.68}$$

$$= \frac{(-1)^{m+n+1}}{2\pi^2}\int_0^\infty dx \int_0^\infty dy\, \frac{\sin x(\sin x\cos y - \cos x\sin y)\sin y}{(x-m\pi)(x-y)(y-n\pi)} f_{\sigma,\tau}(x,y) \tag{4.69}$$

$$= \frac{(-1)^{m+n+1}}{4\pi^2}\int_0^\infty dx \int_0^\infty dy\, \frac{\sin^2 x\sin 2y - \sin 2x\sin^2 y}{(x-m\pi)(x-y)(y-n\pi)} f_{\sigma,\tau}(x,y). \tag{4.70}$$

Define

$$D^{\pm}_{mn} = \int_0^\infty dx\, x^{\pm 1/2}\int_0^\infty dy\, \frac{\sin^2 x\sin 2y - \sin 2x\sin^2 y}{(x-m\pi)(x-y)(y-n\pi)}, \tag{4.71}$$

$$E_{mn} = \int_0^\infty dx\, \int_0^\infty dy\, \frac{\sin^2 x\sin 2y - \sin 2x\sin^2 y}{(x-m\pi)(x-y)(y-n\pi)}, \tag{4.72}$$

$$F_{mn} = \int_0^\infty dx\, x^{1/2}\sin(x-\alpha)\int_0^\infty \frac{dy}{y^{1/2}}\, \frac{\sin^2 x\sin 2y - \sin 2x\sin^2 y}{(x-m\pi)(x-y)(y-n\pi)}. \tag{4.73}$$

Then

$$(C_{\sigma\sigma})_{mn} = \frac{(-1)^{m+n+1}}{4\pi^2}(D^{\sigma}_{mn} + D^{\sigma}_{nm}), \tag{4.74}$$

$$(C_{+-})_{mn} = \frac{(-1)^{m+n+1}}{4\pi^2}(E_{mn}+F_{mn}), \qquad (C_{-+})_{mn} = \frac{(-1)^{m+n+1}}{4\pi^2}(E_{mn}+F_{mn}). \tag{4.75}$$

For $|c|<1, \alpha,\beta\in\mathbb{R}$ let

$$F(c,\alpha;x) = \mathrm{PV}\int_0^\infty \frac{dy}{y^c}\frac{\sin 2y}{(x-y)(y-\alpha)}, \tag{4.76}$$

$$G(c,\alpha;x) = \mathrm{PV}\int_0^\infty \frac{dy}{y^c}\frac{\sin^2 y}{(x-y)(y-\alpha)}, \tag{4.77}$$

$$H(c,\alpha;x) = F(c,\alpha;x)\sin^2 x - G(c,\alpha;x)\sin 2x, \tag{4.78}$$

then we have

$$C^{\pm}_{mn} = \int_0^\infty dx \frac{x^{\pm 1/2} H(0, n\pi; x)}{x - m\pi}, \tag{4.79}$$

$$D_{mn} = \int_0^\infty dx \frac{H(0, n\pi; x)}{x - m\pi}, \tag{4.80}$$

$$E_{mn} = \int_0^\infty dx \frac{x^{1/2} H(1/2, n\pi; x)}{x - m\pi}, \tag{4.81}$$

$$(P_{\sigma,\tau})_{m+1,n+1} = (-1)^{m+n+1} G\left(-\frac{\sigma+\tau}{4}, n\pi, m\pi\right). \tag{4.82}$$

The closed forms of $C^{\pm}_{mn}, D_{mn}$ and E_{mn} are given by

$$C^{\pm}_{mn} = \begin{cases} -(f(0,n\pi)+\pi)G(\mp 1/2, n\pi; m\pi) + \dfrac{1}{2} g(0,n\pi) F(\mp 1/2, n\pi; m\pi) \\ \qquad + K(\mp 1/2, 0; n\pi, m\pi) & , n \neq 0 \\ J(\mp 1/2, m\pi) & , n = 0. \end{cases}$$

$$D_{mn} = \begin{cases} -(f(0,n\pi)+\pi)G(0, n\pi; m\pi) + \dfrac{1}{2} g(0,n\pi) F(0, n\pi; m\pi) \\ \qquad + K(0, 0; n\pi, m\pi) & , n \neq 0 \\ J(0, m\pi) & , n = 0 \end{cases}$$

$$\begin{aligned} E_{mn} = {} & -f(1/2, n\pi) G(-1/2, n\pi; m\pi) - \pi G(0, n\pi; m\pi) \\ & + \frac{1}{2} g(1/2, n\pi) F(-1/2, n\pi; m\pi) + K(-1/2, 1/2; n\pi, m\pi) \end{aligned} \tag{4.83}$$

where for $m \neq n$

$$\begin{aligned}
K(\mp 1/2, 0; n\pi, m\pi) = \mp & \frac{1-\delta_{mn}}{2} \operatorname{Im} \frac{q(\mp 1/2, m\pi) - q(\mp 1/2, n\pi)}{m-n} \\
& - \delta_{mn} \frac{\pi^{\pm 1/2} e^{i\pi(\vartheta(n)(1\mp 1/2)-1/2)}}{2|n|^{1\mp 1/2}} \left(\frac{1}{2} \log|n\pi| - \frac{i\pi\varepsilon(n)}{4} \pm 1 \right) \\
& - \frac{(1-\delta_{mn})\pi^{\pm 1/2}\Gamma(1\pm 1/2)}{m-n} \\
& \times \operatorname{Re}\Big[e^{\mp i\pi\vartheta(n)/2} |n|^{\pm 1/2} \tilde{\Gamma}(\mp 1/2, -2n\pi i) \\
& - e^{\mp i\pi\vartheta(m)/2} |m|^{\pm 1/2} \tilde{\Gamma}(\mp 1/2, -2m\pi i) \Big] \\
& + \frac{\delta_{mn}\pi^{\pm 1/2}\Gamma(1\mp 1/2)}{4|n|^{1\mp 1/2}} \\
& \times \operatorname{Im} e^{i\pi((1\mp 1/2)\vartheta(n)-1/2)} \Big[e^{\mp i\pi\varepsilon(n)/2} |2n\pi|^{\mp 1/2} \\
& - \Gamma(1\mp 1/2) + (2n\pi i \mp 1/2)\Gamma(\mp 1/2, -2n\pi i) \Big] \\
& + (1-\delta_{mn}) \operatorname{Im} e^{\mp i\pi/4} \frac{P(\mp 1/2, m\pi) - P(\mp 1/2, n\pi)}{2\pi(m-n)} \\
& + \delta_{mn} \operatorname{Im} e^{\mp i\pi/4} P'(\mp 1/2, n\pi),
\end{aligned} \tag{4.84}$$

$$\begin{aligned}
K(0, 0; n\pi, m\pi) = & \frac{1-\delta_{nm}}{4\pi^2} \frac{q(0, n\pi) - q(0, m\pi)}{m-n} - \frac{\delta_{nm}\varepsilon(n)}{4n} \\
& + \frac{1-\delta_{nm}}{4(m-n)} \operatorname{Re}\big[\log|n\pi| + \Gamma(0, -2n\pi i) \\
& - \log|m\pi| - \Gamma(0, -2m\pi i) - i\pi(\varepsilon(n) - \varepsilon(m))/2 \big] \\
& - \frac{\pi\delta_{nm}}{2} \operatorname{Im}\Gamma(0, -2n\pi i)
\end{aligned} \tag{4.85}$$

$$\begin{aligned}
K(-1/2, 1/2; n\pi, m\pi) = & (1-\delta_{mn}) \frac{L(m\pi) - L(n\pi)}{2\sqrt{\pi}(m-n)} - \delta_{mn} n\pi^{3/2} L_2(n\pi) + \frac{\delta_{mn}}{2n} \\
& + \frac{\delta_{mn}\varepsilon(n)}{2} \sqrt{\frac{\pi}{|n|}} \operatorname{Im}(1-i)\Gamma(1/2, 2|n|\pi i) \\
& + \delta_{mn}\vartheta(n)\pi^{3/2} \operatorname{Re}\Gamma(1/2, 2n\pi i)
\end{aligned} \tag{4.86}$$

for $m, n \in \mathbb{Z} \setminus \{0\}$. The derivation of the closed form expressions for F, G, H, J, P, L and L_2 can be found in Appendix D.1. We give the general formulae for the functions, as well as the more specific values for arguments on $\pi\mathbb{Z}$. The function F is given by

$$F(c, \alpha; x) = \frac{f(c, \alpha) - f(c, x)}{x - \alpha}, \tag{4.87}$$

where

$$f(c,x) = \Gamma(1-c)\,\mathrm{Im}\, e^{-i\pi c/2}(ix)^{-c}e^{2xi}\Gamma(c,2xi) + \frac{\pi\vartheta(x)\cos 2x}{x^c}, \tag{4.88}$$

$$= \frac{\Gamma(1-c)}{|x|^c}\,\mathrm{Im}\, e^{-i\vartheta(x)\pi c}e^{2xi}\Gamma(c,2xi) + \frac{\pi\vartheta(x)\cos 2x}{x^c}. \tag{4.89}$$

In particular, we have

$$f(1/2,x) = -\sqrt{\frac{\pi}{x}}\,\mathrm{Re}\, e^{2xi}\Gamma(1/2,2xi) + \frac{\pi\cos(2x)}{\sqrt{x}}, \tag{4.90}$$

$$f(1/2,n\pi) = -\frac{1}{\sqrt{|n|}}\,\mathrm{Re}\, e^{i\pi\vartheta(-n)/2}\Gamma(1/2,2\pi ni) + \vartheta(n)\sqrt{\frac{\pi}{n}}, \tag{4.91}$$

$$f(1/2,0) = 2\sqrt{\pi}, \tag{4.92}$$

$$f(0,x) = \mathrm{Im}\, e^{2xi}\Gamma(0,2xi) + \pi\cos 2x, \tag{4.93}$$

$$f(0,n\pi) = \mathrm{Im}\,\Gamma(0,2\pi ni) + \vartheta(n)\pi, \tag{4.94}$$

$$f(0,0) = \frac{\pi}{2}, \tag{4.95}$$

$$f(-1/2,x) = \frac{\sqrt{\pi x}}{2}\,\mathrm{Re}\, e^{2xi}\Gamma(-1/2,2xi) + \pi\sqrt{x}\cos 2x, \tag{4.96}$$

$$f(-1/2,n\pi) = \frac{\pi\sqrt{n}}{2}\,\mathrm{Im}\, e^{i\vartheta(n)\pi/2}\Gamma(-1/2,2\pi ni) + \vartheta(n)\pi^{3/2}\sqrt{n}, \tag{4.97}$$

$$f(-1/2,0) = \frac{\sqrt{\pi}}{2}. \tag{4.98}$$

Making use of (4.87), the specific values of $F(c,n\pi;x)$ at $x = n\pi$ for $n \in \mathbb{Z}\setminus\{0\}$ are given by

$$F(1/2,n\pi;n\pi) = \mathrm{Im}\,\frac{e^{-i\vartheta(n)\pi/2}}{2\pi|n|^{3/2}}(1-4n\pi i)\Gamma(1/2,2n\pi i) - \frac{1}{n\sqrt{\pi}} + \frac{\vartheta(n)}{2n^{3/2}\sqrt{\pi}}, \tag{4.99}$$

$$F(0,n\pi;n\pi) = 2\mathrm{Ci}(2n\pi), \tag{4.100}$$

$$F(-1/2,n\pi;n\pi) = \mathrm{Im}\,\frac{e^{-i\vartheta(n)\pi/2}}{4\sqrt{|n|}}(1+4n\pi i)\Gamma(-1/2,2n\pi i) + \frac{1}{2n\sqrt{\pi}} - \frac{\sqrt{\pi}\vartheta(n)}{2\sqrt{n}}. \tag{4.101}$$

Similarly for G, its closed form is given by

$$G(c,\alpha;x) = \frac{g(c,\alpha)-g(c,x)}{2(x-\alpha)} \tag{4.102}$$

where

$$g(c,x) = \frac{\pi}{|x|^c}\left(\vartheta(x)\cot\pi c + \vartheta(-x)\csc\pi c\right) - \frac{\Gamma(1-c)}{|x|^c}\operatorname{Re} e^{-i\pi c\vartheta(x)}e^{2xi}\Gamma(c,2xi) + \frac{\pi\vartheta(x)\sin 2x}{x^c}. \tag{4.103}$$

Furthermore, we have

$$L(n\pi) = \sqrt{\pi}\operatorname{Re}\Gamma(0,2|n|\pi i) - 2\pi^{3/2}\operatorname{Im}\operatorname{erfc}(\sqrt{|n|\pi}(1+i)) + \sqrt{\pi}(\log(8|n|\pi)+\gamma) + 4\pi\sqrt{|n|}\operatorname{Im}{}_2F_2(1,1;3/2,2;-2|n|\pi i), \tag{4.104}$$

$$L_2(n\pi) = -\frac{1}{\sqrt{\pi}|n|}\operatorname{Im}\Gamma(0,-2|n|\pi i) + \frac{\sqrt{\pi}}{|n|}\operatorname{Re}\operatorname{erfc}(\sqrt{|n|\pi}(1-i)) - \frac{1}{2\pi^{3/2}n^2} - \frac{1}{2\sqrt{\pi}|n|^{3/2}}. \tag{4.105}$$

for $n \in \mathbb{Z}\setminus\{0\}$ and

$$L(0) = 2\sqrt{\pi}\log 2. \tag{4.106}$$

The values for the function q are given by

$$q(\mp 1/2, n\pi) = e^{\mp i\pi\vartheta(n)/2}|n\pi|^{\mp 1/2}\left(\log|n\pi| - \frac{i\pi\varepsilon(n)}{2}\right), \tag{4.107}$$

$$q(0,n\pi) = \left(\log|n\pi| - \frac{i\pi\varepsilon(n)}{2}\right)^2. \tag{4.108}$$

The values for the function $\tilde{J}$ are given by

$$\begin{aligned}\tilde{J}(\mp 1/2, n\pi) = \mp &\frac{\Gamma(1\pm 1/2)}{|n\pi|^{1\mp 1/2}}\operatorname{Im} e^{i\pi\vartheta(n)(1\mp 1/2)}\Gamma(0,2n\pi i)\tilde{\Gamma}(1\mp 1/2,-2n\pi i)\\ &\pm\frac{\pi^{\pm 1/2}\Gamma(1\pm 1/2)}{|n|^{1\mp 1/2}}\operatorname{Re} e^{-i\pi\vartheta(n)(1\mp 1/2)}\Big(\Gamma(1\mp 1/2)+\frac{\pi}{2}\\ &-2\Gamma(1\mp 1/2,-2n\pi i))\\ &-\frac{2^{1\mp 1/2}\gamma\Gamma(1\pm 1/2)}{1\mp 1/2}\operatorname{Im}{}_2F_2(1,1\mp 1/2;2,2\mp 1/2;2n\pi i)\\ &\pm\frac{2\Gamma(1\pm 1/2)}{|n\pi|^{1\mp 1/2}}\operatorname{Im} e^{-i\pi\vartheta(n)(1\mp 1/2)}\left[\Gamma(1\mp 1/2)\psi(1\mp 1/2)\right.\\ &-\Gamma(1\mp 1/2,-2n\pi i)\left(\log|2n\pi| - \frac{i\pi\varepsilon(n)}{2}\right)\\ &\left.+\frac{\pi(\log|2n\pi| - i\pi\varepsilon(n)/2 - \psi(\pm 1/2)}{\Gamma(1\pm 1/2)}\right],\end{aligned} \tag{4.109}$$

$$\begin{aligned}\tilde{J}(0,n\pi) = \frac{\gamma}{2n\pi} - \frac{\varepsilon(n)}{4n} + \frac{1}{2n\pi}\operatorname{Im}\Gamma(0,-2n\pi i) + \operatorname{Re}{}_2F_2(1,1;2,2;-2n\pi i)\\ - (1+\gamma)\operatorname{Re}{}_2F_2(1,1;2,2;2n\pi i)\\ - \operatorname{Re}\frac{d}{dc}\bigg|_{c=1}{}_3F_3(1,1,1;c,2,2;2n\pi i) + \frac{\gamma}{2n\pi}\operatorname{Im}\Gamma'(0,-2n\pi i)\\ - \frac{\gamma\varepsilon(n)}{2n} - \frac{1}{2n\pi}\operatorname{Im}\left(\gamma - \log|2n\pi| + \frac{i\pi\varepsilon(n)}{2}\right)\Gamma'(1,-2n\pi i)\\ - \frac{1}{4n\pi}\operatorname{Im}\Gamma''(1,-2n\pi i). \qquad (4.110)\end{aligned}$$

Finally, the P values are given by

$$\begin{aligned}P(\mp 1/2,n\pi) = e^{\pm i\pi\varepsilon(n)/2}|n\pi|^{\pm 1/2}\Gamma(1\pm 1/2)\Gamma(0,2n\pi i)\tilde{\Gamma}(\mp 1/2,-2n\pi i)\\ \pm e^{\pm i\pi\varepsilon(n)/4}\pi^{1\pm 1/2}|n|^{\pm 1/2}\Gamma(1\pm 1/2)\Gamma(\mp 1/2,2n\pi i)\\ + e^{\pm i\pi\varepsilon(n)/4}|n\pi|^{\pm 1/2}\Gamma(1\pm 1/2)\left[\Gamma'(1\mp 1/2,-2n\pi i)\right.\\ \left.-\Gamma(\mp 1/2,-2n\pi i)\left(\log|n\pi| - \frac{i\pi\varepsilon(n)}{2} + \psi(1\pm 1/2)\right)\right], \qquad (4.111)\end{aligned}$$

$$\begin{aligned}P(0,n\pi) = (-\gamma + i\pi\varepsilon(n))\Gamma(0,2n\pi i) - 2\operatorname{Im}\Gamma'(0,2n\pi i)\\ - |\Gamma(0,2n\pi i)|^2 + G^{3,1}_{2,3}\left(\begin{smallmatrix}0,1\\0,0,0\end{smallmatrix}\middle|\,2n\pi i\right)\\ - \Gamma(0,-2n\pi i)\left(\log|n\pi| - \frac{i\pi\varepsilon(n)}{2} + \gamma\right), \qquad (4.112)\end{aligned}$$

$$
\begin{aligned}
P'(\mp 1/2, n\pi) = {} & (im\pi \pm 1/2) e^{i\pi\varepsilon(n)(1\mp 1/2)/2} |n\pi|^{\pm 1/2-1} \\
& \times \Gamma(1 \pm 1/2)\tilde{\Gamma}(\mp 1/2, -2n\pi i)\Gamma(0, 2n\pi i) \\
& + \frac{i 2^{\mp 1/2}\Gamma(1 \pm 1/2)\Gamma(0, 2n\pi i)}{n\pi} \\
& - 2e^{\mp i\pi\varepsilon(n)/2}\Gamma(1 \pm 1/2)|n\pi|^{\pm 1/2}\Gamma(\mp 1/2, -2n\pi i)\Gamma(0, 2n\pi i) \\
& - e^{i\pi\varepsilon(n)(1\mp 1/2)/2}|n\pi|^{\pm 1/2-1}\Gamma(1 \pm 1/2)\tilde{\Gamma}(\mp 1/2, -2n\pi i) \\
& \mp \pi\Gamma(1 \pm 1/2) \\
& \times \Big[(\mp 1/2 - 2n\pi i) e^{i\pi\varepsilon(n)(1\mp 1/2)/2}|n\pi|^{\pm 1/2-1}\Gamma(\mp 1/2, 2n\pi i) \\
& \pm \frac{2^{\mp 1/2}}{n\pi}\Big] \\
& + e^{-i\pi\varepsilon(n)(1\mp 1/2)/2}|n\pi|^{\pm 1/2-1}\Gamma(1 \pm 1/2) G^{3,1}_{2,3}\left(\begin{smallmatrix} \mp 1/2, 1 \\ 1\mp 1/2, \mp 1/2, 0 \end{smallmatrix} \middle| \, 2n\pi i\right) \\
& + (b \pm 2n\pi i)\Gamma(1 \pm 1/2) e^{i\pi\varepsilon(n)(1\mp 1/2)/2}|n\pi|^{\pm 1/2-1} \\
& \times \left[\Gamma(\mp 1/2, -2n\pi i)\left(\log|n\pi| - \frac{i\pi\varepsilon(n)}{2} + \psi(1 \pm 1/2)\right)\right. \\
& \left. -\Gamma'(\mp 1/2, -2n\pi i)\right] \\
& + e^{i\pi(1\mp 1/2)\varepsilon(n)/2}|n\pi|^{\pm 1/2-1}\Gamma(1 \pm 1/2)\left[\frac{\Gamma(\mp 1/2, -2n\pi i)}{n\pi i}\right. \\
& \left. + 2^{\mp 1/2} e^{i\pi(1\pm 1/2)\varepsilon(n)/2}|n\pi|^{\mp 1/2-1}(\psi(1 \pm 1/2) - \log 2)\right], \qquad (4.113)
\end{aligned}
$$

$$
\begin{aligned}
P'(0, n\pi) = {} & 2\left[(-\gamma + i\pi\varepsilon(n))\Gamma(0, 2n\pi i) - \Gamma'(0, 2n\pi i)\right] \\
& - \left[\frac{\pi\varepsilon(n) + i\gamma}{n\pi} + \frac{i\log|2n\pi| - \pi\varepsilon(n)/2}{n\pi}\right] \\
& - 2i\,\mathrm{Re}\,\Gamma(0, 2n\pi i) + 2\partial G^{3,1}_{2,3}\left(\begin{smallmatrix} 0, 1 \\ 1, 0, 0 \end{smallmatrix} \middle| \, 2n\pi i\right) \\
& - 2\left[\Gamma'(0, -2n\pi i) + (\gamma - (\log|n\pi| - i\pi\varepsilon(n)/2)\Gamma(0, -2n\pi i)\right. \\
& \left. - i\frac{\log 2 + \gamma + \Gamma(0, -2n\pi i)}{n\pi}\right] \qquad (4.114)
\end{aligned}
$$

for $n \in \mathbb{Z} \setminus \{0\}$.

With these matrix elements calculated, it remains to compute the generalised eigenpairs of (C, P) which is done in the following chapter.

— 5 —

Numerical Analysis of the Bracken–Melloy Operator

5.1 NUMERICAL EVALUATION OF THE MATRIX ELEMENTS

This chapter is dedicated to the solution of the generalised eigenproblem

$$C^{[N]}v = \lambda P^{[N]} \tag{5.1}$$

for $N \in \mathbb{N}$. From Section 4.2 of chapter 3, we have closed form expressions for the elements of $C^{[N]}$ and $P^{[N]}$. To numerically compute these elements, we make use of the arbitrary precision C libraries Arb [44] and FLINT (Fast LIbrary for Number Theory). Arb makes use of a computational tool known as ball arithmetic. Each value in Arb is represented as a ball, a subset of the real line in the form $[m-r, m+r]$ where m (the midpoint) and r (the radius) are both given as binary floating point numbers, i.e. values of the form $u2^v$ for $u, v \in \mathbb{Z}$ or one of the special values $\pm\infty$, NaN(Not a Number). In practice the radius r is the error on the value m. The real benefit of using Arb is that with every step of a numerical computation, the radius r accommodates any additional numerical error that may arise through rounding or other approximation.

With this data structure in place, Arb implements functions as follows. Suppose we have some function $f : A \to B$, then a *ball implementation* of f is some F such that

$$F([m-r, m+r]) = [f(m) - r', f(m) + r'] \tag{5.2}$$

for some known $r' > 0$ depending on m, r and f. The Arb ball data structure is very useful for computing special functions which are typically calculated using some

infinite series or integral. To demonstrate this, suppose some function f is defined as

$$f(x) = \sum_{n=0}^{\infty} a_n(x) \tag{5.3}$$

where the $(a_n)_{n=0}^{\infty}$ are functions that are 'easy' to compute. Then, as is typical in any numerical computation, a ball implementation of f only needs to compute $\sum_{n=0}^{N} a_n(x)$ where N is the smallest N such that $|f(x) - \sum_{n=0}^{N-1} a_n(x)| \leq 10^{-\text{dps}}$ where dps is the decimal precision as set by the user. The ball implementation of $f(x)$ for some x will then be

$$F(x) \subseteq \left[\sum_{n=0}^{N} a_n(x) - \epsilon, \sum_{n=0}^{\infty} a_n(x) + \epsilon\right] \tag{5.4}$$

with the guarantee by Arb that $f(x) \in F(x)$. This guarantee, coupled with the well benchmarked speedup [44] that ball arithmetic demonstrates compared to standard floating point arithmetic, is why Arb was necessary for the computation of the matrix elements of P and C.

Now using corollary 3.3.3 from chapter 3, we find that the error $\Delta\lambda$ on the generalised eigenvalues λ satisfying

$$C^{[N]}v = \lambda P^{[N]}v \tag{5.5}$$

is bounded by

$$|\Delta\lambda| \leq N(1 + c_{\text{BM}}) \frac{\|\Delta P^{[N]}\|_{\infty}^2 + \|\Delta C^{[N]}\|_{\infty}}{\min \sigma(P^{[N]})^2} \tag{5.6}$$

where $\Delta P^{[N]}$ and $\Delta C^{[N]}$ are error matrices associated with $P^{[N]}$ and $C^{[N]}$ respectively. Early numerical experiments showed that $\min \sigma(P^{[N]}) \approx 10^{-2.7N}$ and so using Arb, we ensure the matrix elements are computed to $10^{2.7N} + 50$ decimal places. It is worthy of note that without computing these matrix elements to this level of precision, the resulting generalised eigenvalues are wildly incorrect. In this sense, the calculation automatically reveals when it is wrong.

5.2 THE GENERALISED EIGENVALUE PROBLEM

To estimate c_{BM}, we will generate a sequence of 1700 values $(\lambda^{(N)})_{N=1}^{1700}$ with

$$C^{[N]}v^{(N)} = \lambda^{(N)} P^{[N]}v^{(N)} \tag{5.7}$$

such that for each N, $\lambda^{(N)}$ is the largest generalised eigenvalue. By construction, $(\lambda^{(N)})_{N=1}^{1700}$ is a monotonically increasing sequence all elements of which are bounded above by c_{BM}, as shown in Proposition 3.2.1. As discussed in section 5.1, to obtain the maximal eigenvalue $\lambda^{(N)}$ generated from the $2N+1$ dimensional matrices $(C^{[N]}, P^{[N]})$ to 50dps, the matrices must be generated to $2.7 \times 1700 + 50 = 4640$dps. As such this section is dedicated to the solution of the generalised eigenvalue problem of dense matrices of dimension $2 \leq N \leq 3402$, stored to 4640dps. This required the writing of bespoke algorithms and access to the University of York's high performance computing Viking cluster[1].

To find the approximate eigenpairs $(\lambda^{(N)}, v^{(N)})$, we use a shift and invert strategy to convert the generalised eigenvalue problem into an equivalent standard eigenvalue problem with improved convergence properties. From there, we make use of the standard power method, detailed in algorithm 1, to find the largest eigenvalue. The transformation of the generalised eigenvalue problem into a standard eigenvalue problem is given by following lemma. A point on notation, for an invertible $M \in \mathbb{C}^{N\times N}$ we let $M^{-\dagger} = (M^{-1})^{\dagger} = (M^{\dagger})^{-1}$.

Lemma 5.2.1. *Let $A, B \in \mathbb{C}^{N\times N}$ with A, B Hermitian and B positive definite and $\mu > \max \sigma(A, B)$. Further, let $L, E \in \mathbb{C}^{N}$ with L lower triangular be defined by*

$$LL^{\dagger} = \mu B - A, \qquad E = L^{-1}BL^{-\dagger}. \tag{5.8}$$

Then

$$\sigma(A, B) = \left\{ \mu - \frac{1}{\lambda'} \middle| \lambda' \in \sigma(E) \right\}. \tag{5.9}$$

Proof. If $\lambda \in \sigma(A, B)$, then $Av = \lambda Bv$ for some $v \in \mathbb{C}^{N}$. By assumption $\mu > \lambda$. By subtracting μBv from both sides and rearranging, we find

$$(\mu B - A)v = (\mu - \lambda)Bv \tag{5.10}$$

Since B is positive definite and Hermitian, we can write $B = KK^{\dagger}$ for some lower triangular matrix K, a unique representation known as the Cholesky decomposition. Using this representation, we can write

$$K^{-1}(\mu B - A)K^{-\dagger}v = (\mu - \lambda)v \tag{5.11}$$

and since $\mu - \lambda > 0$ by construction, it follows that $K^{-1}(\mu B - A)K^{-\dagger} > 0$. Here we make use of the fact that positivity is preserved under conjugation to conclude that

[1] More information regarding Viking can be found at https://vikingdocs.york.ac.uk

$\mu B - A > 0$. Hence, we can write $\mu B - A$ in its Cholesky representation, $LL^\dagger$ with L lower triangular. Substituting this representation into (5.10) and rearranging, we obtain

$$Bv = \frac{1}{\mu - \lambda} LL^\dagger v \tag{5.12}$$

Since $A - \mu B$ is strictly positive, L is invertible and so by writing $w = L^\dagger v$ for some $w \in \mathbb{C}^N$ we find

$$L^{-1}BL^{-\dagger}w = \frac{1}{\mu - \lambda} w \tag{5.13}$$

This is precisely what it means for $0 \neq 1/(\mu - \lambda) \in \sigma(L^{-1}BL^{-\dagger})$. Each step in the proof is reversible, so the lemma holds. □

A note on Lemma 5.2.1, the map $\lambda \mapsto \mu - 1/\lambda$ is order preserving and so finding the largest value of $\sigma(A, B)$ comes from finding the maximum eigenvalue of E.

As shown in theorem 5.2.2, the power method applied to a self-adjoint matrix $A \in \mathbb{C}^{d\times d}$ converges as $\mathcal{O}(|\lambda_2/\lambda_1|^n)$ where λ_1 and λ_2 are the two largest eigenvalues by absolute value. By choosing a shift parameter μ such that $\mu > \max \sigma(A, B)$, after a shift and invert, the power method applied to the matrix E as defined in 5.2.1, will converge as $\mathcal{O}(|(\mu - \lambda_1)/(\mu - \lambda_2)|^n)$. Selecting a μ close to λ_1, the improved convergence is evident.

The matrix L may be calculated using [38, chapter 4, algorithm 4.2.1]. We will denote the Cholesky decomposition of a positive self-adjoint matrix $A \in \mathbb{C}^{d\times d}$, $\mathrm{Chol}(A)$ as the unique lower triangular $L \in \mathbb{C}^{d\times d}$ satisfying $A = LL^\dagger$. The matrix E may be calculated using a combination of forward and backward substitution as in [38, chapter 4, algorithms 4.3.2 and 4.3.3]. With the generalised eigenvalue problem transformed into a standard eigenvalue problem, it remains to solve for the largest eigenvalue of the resulting matrix. We choose to do this using the power method. The algorithm for the power method is described in [38, chapter 7, section 7.3.1] and given below in algorithm 1.

With this algorithm written out, the following theorem, again found in [38, chapter 7, section 7.3.1] shows the convergence properties of the power method.

Theorem 5.2.2. *For $N \in \mathbb{N}$, let $A \in \mathbb{C}^{N\times N}$ be self-adjoint such that $X^{-1}AX = \mathrm{diag}(\lambda_1, \ldots, \lambda_n)$ with $X = [x_1, ..., x_N]$ and $|\lambda_1| > |\lambda_2| \geq \cdots \geq |\lambda_N|$. For $q^{(0)} \in \mathbb{C}^N$ with $\|q^{(0)}\|_2 = 1$ and for $k \in \mathbb{N}$ let $(\lambda^{(k)}, q^{(k)})$ be a sequence of scalar-vector pairs*

Algorithm 1 Power Method

Input: Self-adjoint matrix $A \in \mathbb{C}^{d\times d}$, vector $q^{(0)} \in \mathbb{C}^d$, tolerance ϵ, max steps K.
Output: Scalar λ, vector q.
for k in $1 : K$ **do**
  $r^{(k)} \leftarrow Aq^{(k-1)}$
  $q^{(k)} \leftarrow r^{(k)}/\|r^{(k)}\|_2$
  $\lambda^{(k)} \leftarrow q^{(k)\dagger} A q^{(k)}$
  if $\|Aq^{(k)} - \lambda^{(k)} q^{(k)}\| < \epsilon$ **then**
    return $(\lambda^{(k)}, q^{(k)})$
  end if
end for
return $(\lambda^{(K)}, q^{(K)})$

obtained by algorithm 1. If $x_1^\dagger w^{(0)} \neq 0$*, then*

$$|\lambda^{(k)} - \lambda_1| = \mathcal{O}\left(\left|\frac{\lambda_2}{\lambda_1}\right|^k\right), \qquad \operatorname{dist}(\operatorname{span} q^{(k)}, \operatorname{span} v_1) = \mathcal{O}\left(\left|\frac{\lambda_2}{\lambda_1}\right|^k\right). \tag{5.14}$$

With the theory laid out, we discuss the details of implementing Lemma 5.2.1 and algorithm 1 for $(C^{[N]}, P^{[N]})$. From Lemma 5.2.1, we will choose $\mu = 0.039$ for which the reason will become clear. For each $N \in \mathbb{N}$, let

$$L^{[N]} = \operatorname{Chol}\left(C^{[N]} - 0.039P^{[N]}\right), \qquad E^{[N]} = \left(L^{[N]}\right)^{-1} C^{[N]} \left(L^{[N]}\right)^{-\dagger}, \tag{5.15}$$

and let $\sigma^{(N)} = \sigma_1^{(N)} > \sigma_2^{(N)} \geq \cdots \geq \sigma_{2N+2}^{(N)}$ be the eigenvalues of $E^{[N]}$ with associated eigenvectors $w_{\max}^{(N)}, w_2^{(N)}, \ldots, w_{\min}^{(N)}$. Selecting $\mu = 0.039$ significantly amplifies the ratio $|\sigma^{(N)}/\sigma_2^{(N)}|$ compared to $|\lambda^{(N)}/\lambda_2^{(N)}|$ and consequently when applying the power method to $E^{[N]}$ we obtain drastically better convergence. First we discuss the efficient computation of $L^{[N]}$ and $E^{[N]}$. To speed up the computation of $L^{[N]}$ and $E^{[n]}$, we make use of parallelised Cholesky and linear systems solver algorithms. These parallelised algorithms split the task into chunks of equal complexity according to algorithms 2 and 4. As is common, we denote the integers (inclusive) between $a \in \mathbb{Z}$ and $b \in \mathbb{Z}$ with $a : b$. Further, we use $\lfloor\cdot\rceil$ to denote the nearest integer.

The following algorithms were originally written by Fewster, though they were improved to their current form by both Fewster and myself.

Given a matrix $L \in \mathbb{C}^{d\times d}$ for which we wish to compute the Cholesky decomposition, the standard Cholesky algorithm [38, chapter 4, algorithms 4.3.2] takes a row $1 \leq i \leq d$ and performs computations on the matrix elements $(L_{ij})_{i\leq j\leq d}$ in

series. Computing the i, j element of the Cholesky decomposition has complexity proportional to $j - i$. In the parallelised Cholesky algorithm, we account for this and for each row index i, the corresponding column indices $[i : d]$ are split into p chunks for which the computations necessary are of roughly equal complexity. A longer discussion of a parallel Cholesky algorithm can be found in [38, Section 6.3].

Algorithm 2 Complexity Splitting 1, (split_1)

Input: Parameter n, number of parallel processes p,
Output: Array of ranges S.
$S \leftarrow \left[0, \left\lfloor \sqrt{\frac{n(n+1)}{p}} \right\rfloor, ..., \left\lfloor \sqrt{\frac{n(n+1)(p-1)}{p}} \right\rfloor, n\right]$
$S \leftarrow [S_1 + 1 : S_2, \ldots, S_p + 1 : S_{p+1}]$
Return: S

With this complexity splitting algorithm written out, we write out the algorithm for the parallelised Cholesky decomposition. This algorithm is parallelised and more efficient version of [38, chapter 4, algorithm 4.2.1]. The notation **parfor** in the algorithm denotes the parallelised for loop.

Algorithm 3 Parallelised Cholesky, (ParChol)

Input: Matrix $L \in \mathbb{C}^{d\times d}$, number of parallel processes p.
Output: Lower triangular matrix L.
$d \leftarrow \dim L$
for i from 1 to $d-1$ **do**
  $L_{ii} \leftarrow \sqrt{L_{ii}}$
  for j from $i+1$ to d **do**
    $L_{ji} \leftarrow L_{ji}/L_{ii}$
  end for
  if $d-i > p$ **then**
    $Q \leftarrow \text{split}_1(d-i, \min(d-i, 6))$
    $\underline{R} \leftarrow [[q_1 + i : q_2 + i] \text{ for } q \text{ in } Q]$
  else
    $\underline{R} \leftarrow [i : d]$
  end if
  parfor r in R
    for j in r **do**
      for k from $i+1$ to j **do**
        $L_{jk} \leftarrow L_{jk} - L_{ji}L_{ki}$
      end for
    end for
  end parfor
end for
$L_{dd} \leftarrow \sqrt{L_{dd}}$
Return: L as lower triangular.

The following two algorithms present a method for the parallelised computation of $L^{-1}CL^{-\dagger}$ where L is lower triangular. The first algorithm allows for the splitting of the computation according to tasks of equal complexity. The second presents the computation of $L^{-1}CL^{-\dagger}$ itself using a combination of the forward and backward substitution algorithms.

Algorithm 4 Complexity Splitting 2, (split_2)

Input: Parameter n, number of parallel processes p.
Output: Array of ranges S.
if $d < p - 1$ **then**
  $l \leftarrow [1 : n]$
else
  $l \leftarrow [\text{iquo}(r(n+1), p), r = 0 : p]$
end if
if $|l| = 1$ **then**
  return $[0]$
else
  return $[[l_r, l_{r+1} - 1] \text{ for } 1 \leq r < |l|]$
end if

In algorithm 4, for $n, m \in \mathbb{N}$, $\text{iquo}(m, n)$ refers to the integer quotient of m divided by n and for an array l, $|l|$ refers to its size.

Algorithm 5 In place $L^{-1}CL^{-\dagger}$, (LeftInvRightInvDagger)

Input: Matrices $L, C \in \mathbb{C}^{d\times d}$ with L lower triangular, number of parallel processes p.
Output: Matrix $C \in \mathbb{R}^{d\times d}$
for j from d to 1 by $-p$ **do**
  parfor k from 1 to $\min(j, p)$
    $m \leftarrow \max(1, j-p+1)+k-1$
    for i from 1 to d **do**
      $x \leftarrow C_{i,m}/L_{i,i}$
      for l from $i+1$ to d **do**
        $C_{l,m} \leftarrow C_{l,m} - L_{r,i}x$
      end for
      if i<k **then**
        $C_{i,m} \leftarrow 0$
      else
        $C_{i,m} \leftarrow x$
      end if
      $x \leftarrow 0$
    end for
  end parfor
  for n from 0 to $\min(j, p)$ **do**
    $C_{j-n:d,j-n} \leftarrow C_{j-n:d,m+\min(j,p)-n}$
  end for
end for
note: At this stage lower triangular part of C holds the lower triangular part of the solution X to $LX = C$.
for i from 1 to d **do**
  $R \leftarrow [\text{split}_2(d-1, p)_1 + i : \text{split}_2(d-1, p)_{2+i}$
  parfor r in R
    for j in r **do**
      $C_{ij} \leftarrow \frac{1}{L_{ii}}(C_{ij} - \sum_{k=1}^{i-1} L_{ik}C_{kj})$
    end for
  end parfor
end for
return C
note: The lower triangular part of C now agrees with the lower triangular part of $L^{-1}CL^{-\dagger}$.

One important benefit to algorithms 3 and 5 is that they compute L and $L^{-1}CL^{-\dagger}$ respectively in place. That is to say, no auxiliary matrices are required that take up additional memory. With these algorithms written out, we now perform the

following set of instructions.

1. $L^{[N]} \leftarrow C^{[N]} - 0.039P^{[N]}$
2. ParChol($L^{[N]}$)
3. LeftInvRightInvDagger($L^{[N]}, C^{[N]}$)

This procedure works as it does because the algorithms perform the numerical linear algebra in place without the need for additional auxillary matrices. After performing these steps, the matrix $L^{[N]}$ now holds the matrix $E^{[N]}$. To find the generalised eigenvalues, we now perform the power method as described in algorithm 1 on the matrix $E^{[N]}$ to find its largest eigenvalue $\sigma_{\max}^{(N)}$ and associated eigenvector $w_{\max}^{(N)}$. To obtain the generalised eigenvalues $\lambda_{\max}^{(N)}$ that converges to c_{BM}, we perform the simple computation $\lambda_{\max}^{(N)} = 0.039 - 1/\sigma_{\max}^{(N)}$.

5.3 NUMERICAL ANALYSIS OF THE BRACKEN–MELLOY OPERATOR'S SPECTRAL ESTIMATES

From here on, we will refer to the sequence $(\lambda_{\max}^{(N)})_{N=1}^{1700}$ as the approximate spectral estimates. Figure 5.1 shows the approximate spectral estimates in full followed by Figure 5.2 showing the final 500 values.

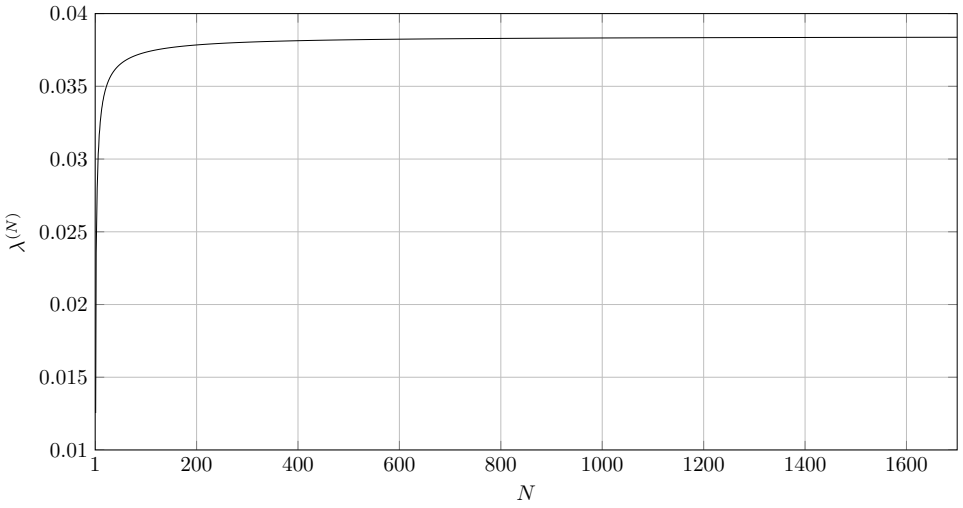

Figure 5.1: Plot of $\lambda_{\max}^{(N)}$ for $1 \leq N \leq 1700$

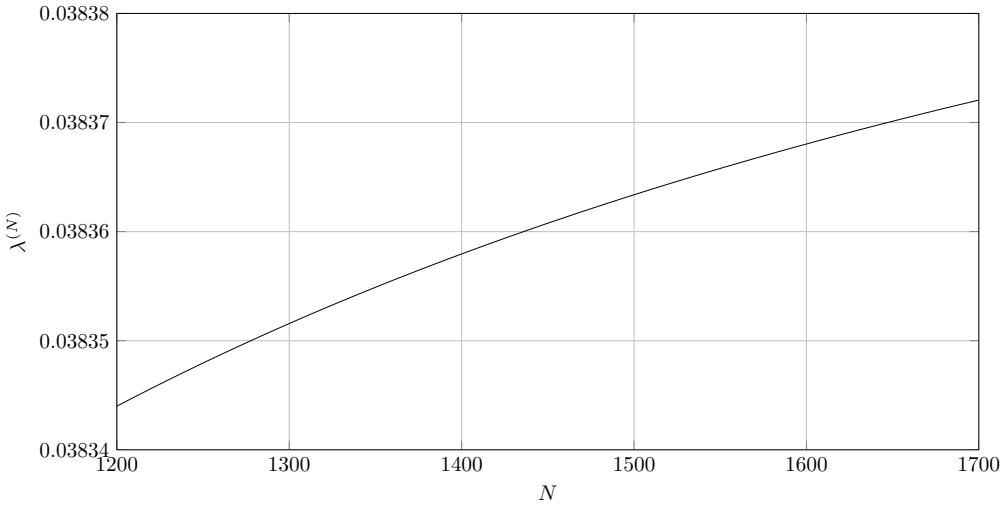

Figure 5.2: Plot of $\lambda_{\max}^{(N)}$ for $1200 \leq N \leq 1700$

The histogram in Figure 5.3 shows the spread of generalised eigenvalues $\sigma(C^{[400]}, P^{[400]})$.

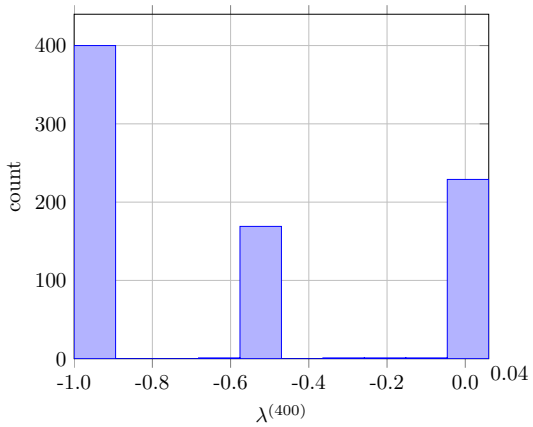

Figure 5.3: Generalised spectrum $\sigma(C^{[400]}, P^{[400]})$

We note several features of Figure 5.3. First, note the significant concentration of eigenvalues around $\min \sigma(B) = -1$. As shown by Penz et al in [40], -1 is not an eigenvalue of the backflow operator B and so one may conjecture that this feature of Figure 5.3 indeed indicates a feature of the Bracken–Melloy operator which certainly has a continuous part of the spectrum containing -1. Another important feature that one can point to is the largest spectral point close to 0.04 that approximates c_{BM}, as has been previously discussed.

One must be very careful to extract any more information about $\sigma(B)$ from Figure 5.3 due to the phenomenon of spectral pollution. For a detailed discussion on spectral pollution see [19]. Spectral pollution is the following phenomemon. Let A be some bounded self-adjoint operator on a Hlbert space $\mathcal{H}$, some nested sequence of subspaces $(L_n)_{n\in\mathbb{N}} \subseteq \mathcal{H}$ with $\cup_n L_n$ dense in $\mathcal{H}$ and let P_n denote the projection onto L_n. If there is some sequence $\lambda_n \in \sigma(P_n A P_n)$ with $\lambda_n \to \lambda \in \mathbb{R}$ such that $\lambda \notin \sigma(A)$, then λ is a point of spectral pollution. Fortunately Proposition 3.2.1 ensures that the sequences $\lambda^{(N)}_{\text{max/min}}$ will not be points of spectral pollution however any sequence of spectral points that do not reside on the boundary of $\sigma(C^{(N)}, P^{[N]})$ are not afforded this same guarantee. There are simple examples of spectral pollution described in [19]. The fact that there do appear to be converging sequences of discrete points in the spectra of $\sigma(C^{[N]}, P^{[N]})$ suggests that this numerical scheme is indeed prone to spectral pollution.

Similarly to the approximate spectral estimates, we find the sequence of generalised eigenvectors $v^{(N)}_{\text{max}}$ that, together with $\lambda^{(N)}_{\text{max}}$, solve equation 5.7 by

$$v^{(N)}_{\text{max}} = \frac{L^{-\dagger} w^{(N)}_{\text{max}}}{\sqrt{\left\langle L^{-\dagger} w^{(N)}_{\text{max}} \middle| P^{(N)} L^{-\dagger} w^{(N)}_{\text{max}} \right\rangle}}. \tag{5.16}$$

To find approximate eigenvectors close to the bottom of $\sigma(B)$, we use a different strategy. Our method of approximating the spectrum of the Bracken–Melloy operator is optimized for calculating approximate spectral values close to c_{BM}, through the shift and invert strategy as discussed earlier. One may expect it is possible to adjust this shift and invert strategy to efficiently calculate approximate eigenvalues and associated eigenvectors close to the bottom of the spectrum $-1 = \min \sigma(B_{\langle -1,1\rangle})$. This is incorrect. For a given, sufficiently large N, numerical experiments showed that the generalised eigenvalue spectrum $\sigma(C^{[N]}, P^{[N]})$ contains a bulk of eigenvalues very close to -1. This can be clearly seen in Figure 5.3. This means it is not possible to use the power method efficiently and we rely on the `eigenvectors` procedure built into Maple 2024. For $N \in \mathbb{N}$, we find the approximate eigenvector $\phi^{(N)}_{\text{min}}$ as follows. Let $v^{(N)}_{\text{min}}$ be the vector obeying

$$C^{[N]} v^{(N)}_{\text{min}} = \lambda^{(N)}_{\text{min}} P^{[N]} v^{(N)}_{\text{min}}, \qquad \left\langle v^{(N)} \middle| P^{[N]} v^{(N)} \right\rangle = 1 \tag{5.17}$$

with $\lambda^{(N)}_{\text{min}} = \min \sigma(C^{[N]}, P^{[N]})$. The normalisation in equations 5.16 and (5.17) are done so that the associated $L^2(\mathbb{R}^+)$ vectors $\phi^{(N)}_{\text{max/min}}$, constructed according to

Proposition 3.2.1 and given explicitly as

$$\phi^{(N)}_{\max/\min} = \sum_{k=1}^{N+1} \left[\left(v^{(N)}_{\max/\min} \right)_{2k-1} \varphi^{+}_{k-1} + \left(v^{(N)}_{\max/\min} \right)_{2k} \varphi^{-}_{k-1} \right] \tag{5.18}$$

have unit $L^2(\mathbb{R}^+)$ norm. The ordering of the vectors in (5.18) is inherited from the construction of the matrices $C^{[N]}, P^{[N]}$ given in (4.61) and (4.60). The plot of $\phi^{(300)}_{\max}$ is given below.

Figure 5.4: Plot of $\phi^{(300)}_{\max}(p)$ for $0 \leq p \leq 100$.

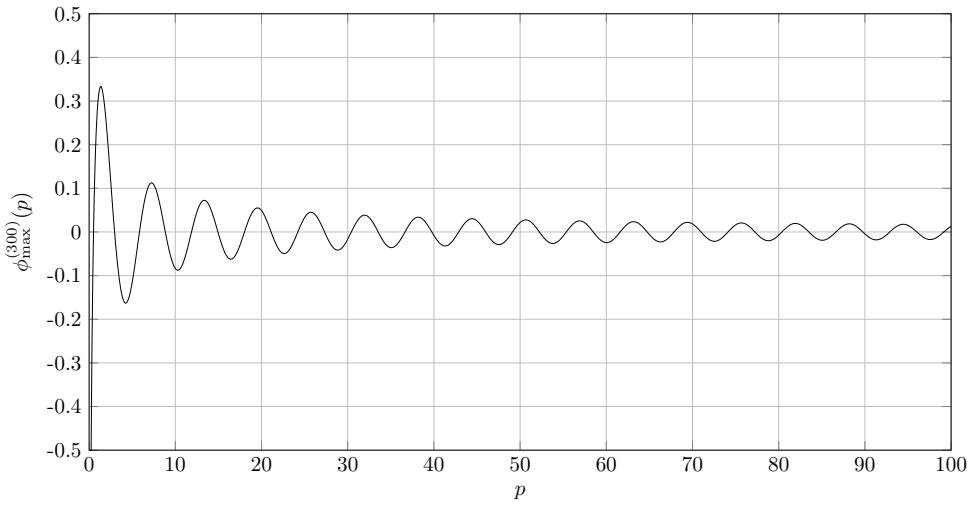

Note that the $v^{(300)}_{\max}$ vector has elements of order 10^{393} and so the vector $\phi^{(300)}_{\min}$ is the result of a lot of cancellation. The plot in Figure 5.4 of the backflow maximizing vector for the time interval $[-1, 1]$ matches precisely what was found by Penz et. al. in Figure 3 of [40] and matches the shape of the vector found by Halliwell and Yearsley in Figure 4 of [68]. Immediately, one notices that the $p \sim 0$ behaviour of $\phi^{(100)}_{\max}$ follows that of the function $p \mapsto p^{-1/4}$. Just as was found in Figure 3.4, we again notice that the envelope of $\phi^{(100)}_{\max}$ for large p follows $p^{-3/4}$. Figure 5.5 of $p \mapsto p^{3/4}\phi^{(300)}_{\max}(p)$, that closely replicates an oscillating wave of constant amplitude illustrates this.

Figure 5.5: Plot of $p^{3/4}\phi_{\max}^{300)}(p)$ for $0 \leq p \leq 100$.

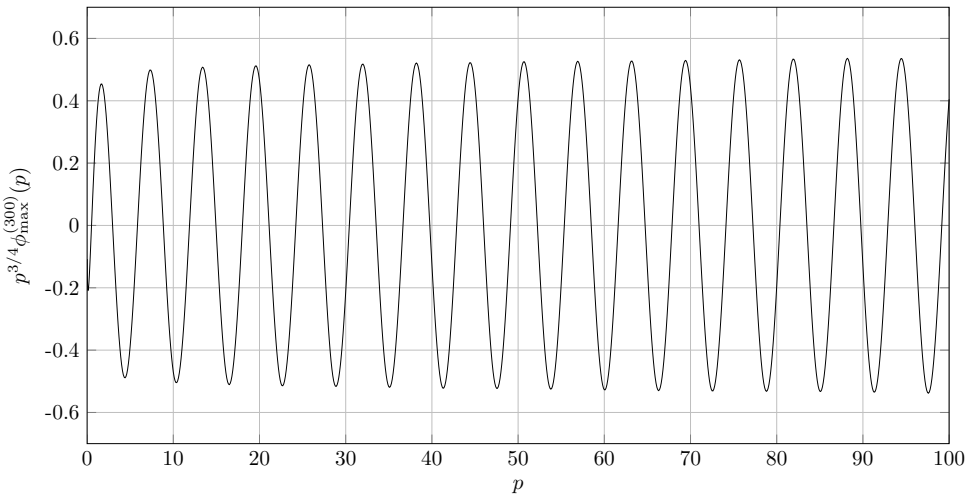

Here, we note that the approximate backflow vector $\psi^{(1)}(a_1, -1/4; 500; \cdot)$, with $a_1 = 2/\pi$, computed in chapter 3 and plotted with a multiplication by $p^{3/4}$ in Figure 3.4 was the maximium backflow vector for the time interval $[-1/2, 1/2]$. One can find a normalised approximation backflow vector for the time interval $[-1, 1]$ by applying the unitary D_4, defined in 1.11 with explit form $(D_4 f)(p) = \sqrt{2} f(2p)$. Figure 5.6 shows $\phi_{\max}^{(300)}$ plotted on the same axes as $D_4\psi^{(1)}(a_1, -1/4; 500; \cdot)$. As can be seen, both approximations agree to a high degree. We note that the vector $\phi^{(300)}$ exhibits the most backflow of the two.

Figure 5.6: Comparison of the approximations of the maximum backflow eigenvector.

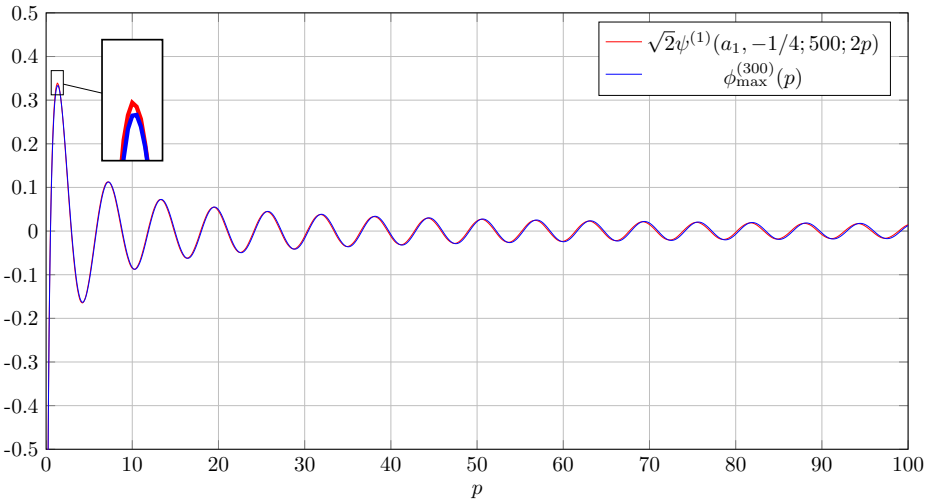

At the other end of the spectrum, just as in section 3.1, we find approximately Gaussian states whose expectation value with respect to the backflow operator approximate -1.

Figure 5.7: Plot of $\phi^{(N)}_{\min}(p)$ for $100 \leq N \leq 400$ in steps of 50 and $0 \leq p \leq 1000$.

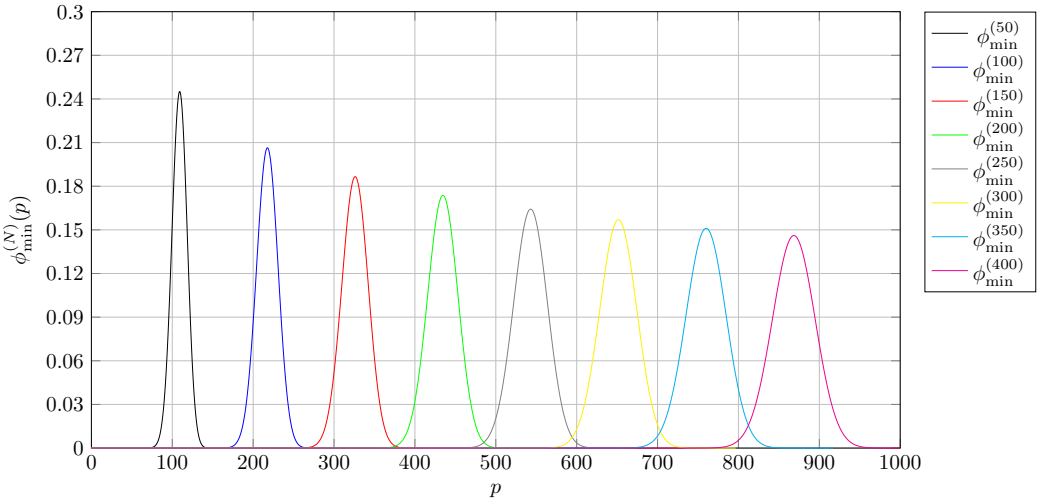

These approximate eigenvectors for the bottom of the spectrum $-1 \in \sigma(C)$ appear to be Gaussian vectors with reducing maximum and larger spread as N increases. This pattern is very similar to what was found in Figure 3.11 using the exponentially damped monomial vectors as trial vectors.

Returning to the sequence of approximate spectral estimates, one feature of the sequence $\lambda_{\max}$ that we highlight is that, to 3 significant figures, $\lambda^{(2)}_{\max} = 0.0125 > 0$. From this we conclude that the vector $\phi^{(2)}_{\max}$ given by

$$\phi^{(2)}_{\max}(p) = \mathcal{N}\left[\frac{\sin p}{p}\left(\alpha_+ p^{1/4} + \alpha_- p^{-1/4}\right) - \frac{\sin(p)}{p-\pi}\left(\beta_+ p^{1/4} + \beta_- p^{-1/4}\right)\right] \tag{5.19}$$

where $\mathcal{N}$ is a normalisation constant and

$$\alpha_+ = 4.38, \qquad \alpha_- = -2.42, \qquad \beta_+ = 4.33, \qquad \beta_- = -7.62 \tag{5.20}$$

to 3 significant figures, is a backflow vector exhibiting slightly below one third of maximum backflow for a single time interval. Each $\lambda_{\max}(N)$ gives the total amount of backflow exhibited by vectors belonging to $\operatorname{span}(\varphi^{\pm}_0, \ldots, \varphi^{\pm}_N) \subset L^2(\mathbb{R}^+)$

and hence are each rigorous lower bounds on c_{BM}. Notice that $\lambda_{\max}^{(1700)} = 0.03837$ (to 4 significant figures) gives the best rigorous lower bound on c_{BM} to date. This value is an improvement compared to the lower bound 0.036933 found in chapter 3 using the exponentially damped monomial vectors $\psi_{n,a,\delta}$ as given in (3.15).

5.4 NUMERICAL ANALYSIS

The goal of this section is to accelerate the sequence of estimates $\lambda_{\max}$ using convergence acceleration methods discussed in section 3.4, chapter 3. One common feature of convergence accelerators is that they amplify oscillations in the sequences they are attempting to improve the convergence of. One important feature of the approximate spectral estimates λ is the presence of structured oscillations. To discuss this, first let e and o denote the even and odd subsequences of $\lambda_{\max}$. Further, for $k \in \mathbb{N}$ and a sequence s, let $\mathrm{sd}_k(s)$ denote the k^{th} successive difference of s. Figure 5.8 below shows the second successive differences of the even and odd subsequences of the approximate spectral estimates.

Figure 5.8: Second successive differences of $e^{(N)}$ and $o^{(N)}$ for $700 \leq N \leq 720$.

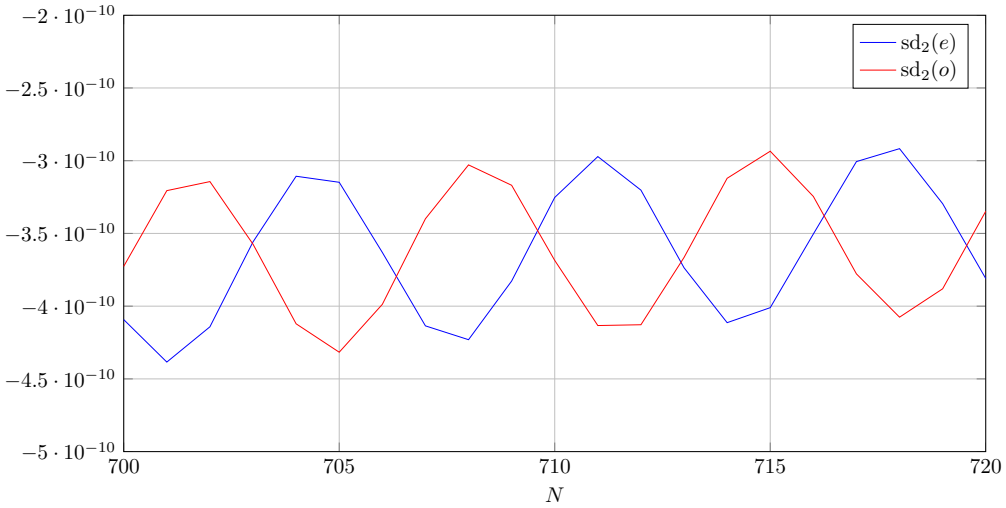

As can be seen in Figure 5.8, the even and odd subsequences of λ possess oscillations with a of period of 7 that are almost exactly out of phase with one

another. To dampen the oscillations, we perform the following. Compute

$$\lambda_{\text{smooth}} = \text{KZ}_{7,10}\left(\frac{1}{2}\left[e + o\right]\right) \tag{5.21}$$

where the addition of sequences is done element-wise and KZ is the Kolmogorov–Zurbenko filter discussed in Chapter 3, section 3.4. A longer exposition of this filter can be found in [74, 67]. After the application of the KZ filter, the oscillations in λ_{smooth} are only visible after 8 successive differences where the oscillations in the final 100 elements have an amplitude of order 10^{-24}.

There are significant problems with trying to accelerate the sequence λ_{smooth}. First one can attempt to fit the sequence $(\lambda_{\text{smooth}}(N))_N$ to an ansatz of the form

$$c_{\text{bm}} - \frac{a_1}{N^{\alpha_1}} + \frac{a_2}{N^{\alpha_2}} + \cdots \tag{5.22}$$

however it is clear that the sequence does not follow this simple pattern. The most reliable method for determining the leading order power α_1 is using a log–log plot. Simply, if

$$x(N) = c - \frac{a_1}{N^{\alpha_1}} + \frac{a_2}{N^{\alpha_2}} + \cdots \tag{5.23}$$

with $\alpha_1 < \alpha_2 < \cdots$ then the sequence

$$\frac{\log(x_{N+2} - x_{N+1}) - \log(x_{N+1} - x_N)}{\log(N+1) - \log N} \to -(\alpha_1 + 1) \tag{5.24}$$

as $N \to \infty$. Performing this log–log analysis on λ_{smooth} leads to a value of $\alpha_1 \approx -0.2$. Clearly, λ_{smooth} is converging, and so cannot possess a leading asymptotic of the form $N^{0.2}$. We can conclude that the ansatz given in (5.23) is incorrect.

Since the asymptotics of λ_{smooth} do not follow a simple sum of powers rule, this effectively rules out linear accelerators to improve the convergence and we are left at the mercy of nonlinear accelerators. Many nonlinear accelerators were used to attempt to improve the convergence of λ_{smooth}, all of which suffered from the same problem which can be summed up in the following way.

A good acceleration regime, even with nonlinear accelerators, involves gathering evidence of the asymptotic ansatz of the sequence. Selecting the correct nonlinear accelerator to use requires knowledge of the ansatz as without this, many nonlinear accelerators do not come with guaranteed limit preservation. Discussion of nonlinear sequence accelerators can be found in [14] and [61]. One can try to test for more complicated asymptotics such as $N^{-\alpha}e^{-aN}$. However, attempts to test for asymptotics

of the form $N^{-\alpha}e^{-aN}$ were inconclusive. Clearly the asymptotics of λ_{smooth} are complicated and so far it has not possible to accelerate the convergence of λ_{smooth}.

Many other attempts to calculate c_{BM} have involved plotting the approximating sequence against $1/N^{\alpha}$ for some appropriately chosen α such that the resulting curve looks approximately straight. Once α is chosen, a straight line is drawn from the end of this approximately straight line to the y axis to predict the value of c_{BM}. Despite the fact that the approximate spectral estimate $\lambda_{\text{max}}^{(N)}$ does not follow a power law, previous attempts to calculate c_{BM}, such as in [53], have plotted their estimates against $1/N$. Hence, Figure 5.9 shows the curve resulting from plotting $\lambda_{\text{max}}^{(N)}$ against $1/N$.

Figure 5.9: Plot of $\lambda_{\text{max}}^{(N)}$ against $1/N$ for $500 \leq N \leq 1700$

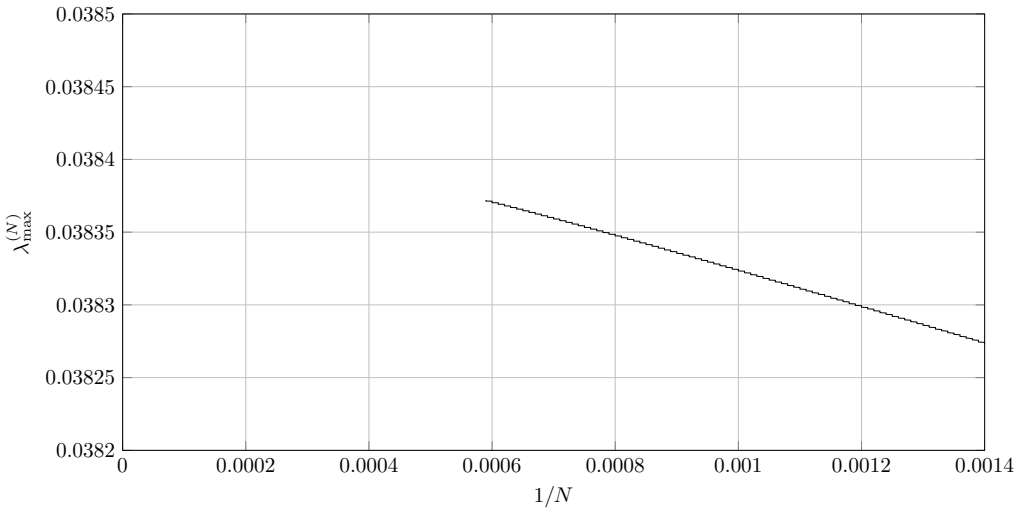

It is clear that, after extrapolation, the curve in Figure 5.9 will meet the y axis somewhere around 0.03845. Taking a linear fit of the final 10 data points meets the y axis of Figure 5.9 at 0.038436 to 5 significant figures. One should not take this as the value of c_{BM} as clearly $\lambda_{\text{max}}^{(N)}$ does not follow a simple $1/N$ relation, however it does show the estimates are heading for a similar value to that found before by Fewster [29] and Penz et. al. [53]. This value is also very close to the value given in chapter 3 of $c_{\text{BM}} \approx 0.0384505$.

— 6 —

Conclusion

In the first half of this thesis, we describe two new quantum mechanical phenomena and analyse them in detail. The first of these is the existence of quantum states that repeatedly exhibit the quantum backflow phenomena over multiple disjoint time intervals. The second new phenomenon we have demonstrated is *quantum overflow*. This is the existence of quantum states undergoing free Schrödinger evolution that exhibit more probability transfer in the direction of their momentum than is possible for any freely evolving classical ensemble. The quantum overflow effect is a phenomenon only visible when multiple disjoint time intervals are considered, thus explaining why it has not yet been seen in the literature.

In addition to demonstrating these new phenomena, a numerical study into the single backflow maximizing vector led to a new conjectured value for $c_{\mathrm{BM}} \approx 0.0384506$. This marks a contrast from previous calculations in [53] and [29] in that the new value is lower than the previously expected value of 0.038452.

A particular point of interest, as shown in Theorem 2.4.1, is that the largest amount of quantum backflow that some state can exhibit is unbounded as a function of the number of disjoint time intervals. The same is true of quantum overflow. States that exhibit such maximal multiple backflow and overflow for $1 \leq M \leq 4$ have also been described in chapter 3 using a numerical scheme. It is particularly interesting that states exhibiting backflow over multiple disjoint time intervals appear to mimic the backflow vector for a single time interval but with higher frequency contributions. This suggests that such states are more physically extended in position space, a prediction that requires further study.

Prior to this year, the only examples of experimental verification of backflow have come from classical optical systems [27]. We particularly note the work of Zhang

et. al. [73], who earlier this in 2025 showed the existence of azimuthal backflow. Specifically they showed that a photon prepared in a state with only negative azimuthal angular momentum can exhibit positive azimuthal angular momentum some time later. This was done using a weak measurement, a type of measurement that minimally modifies the state under investigation. We note that given the amount of quantum backflow a state exhibits can grow arbitrarily large when the state's probability density is measured at more than 2 times, it may allow for the experimental verification of quantum backflow of a system undergoing evolution on a line. Such an experimental scheme would have to make use of some kind of weak measurement to avoid disturbing the state under investigation. We note that there is increasing interest in controlling the quantum backflow phenomenon, in particular for its use in imaging and metrology [73] as well as transportation tasks [64].

In the second half of the thesis, we conducted a thorough numerical study of the backflow effect over a single time interval. This numerical study led to the best raw estimate and rigorous lower bound on c_{BM}, namely that $c_{\mathrm{BM}} \geq \lambda^{(1700)} = 0.03837$. In principle, this sequence of estimates obtained can be accelerated to find more digits of c_{BM}. There are a number of challenges which make it difficult to be confident in any numerical scheme. This is a challenge for more advanced numerical methods in the future. A next step to obtain more more digits of c_{BM} would be to use a larger number of exponentially damped monomial vectors. This is due to the clear asymptotic pattern that the estimates follow. An ideal future project would involve finding basis vectors that produce eigenvalue estimates converging exponentially fast. In addition to the estimate of c_{BM}, we were also able to provide the second independent verification of the shape of the backflow maximizing vector, as seen in Figure 5.6.

There are a number of future directions that can be worked on in the study of quantum backflow. One project that is close to completion, that I will report elsewhere, is quantum referenced quantum backflow. That is, the study of states exhibiting quantum backflow when the device measuring the position itself obeys the laws of quantum mechanics. In practice this is very similar to the study of quantum backflow in the presence of non-sharp measurements as discussed in [69] when deriving the classical limit of quantum backflow. Another interesting avenue, particularly in the context of experimental verification, is the study of quantum backflow in the presence of electromagnetic fields. We note here that this has been studied in the context of angular quantum backflow by Goussev [39].

Finally, we make a comment regarding conjectural features of the backflow effect. In Bracken and Melloy's first paper on the backflow effect [12], it was conjectured that the Bracken–Melloy operator has a positive eigenvalue at the top of the spectrum (corresponding to c_{BM}) and a sequence of positive eigenvalues with accumulation point 0. There is clear evidence, described in Section 5.3, that the single backflow operator has an eigenvalue at the top of the spectrum. The plot of the full approximate spectrum, given in Figure 5.3, would easily lead to the spurious conclusion that the Bracken–Melloy operator also has eigenvalues at $-1, -0.5$ and 0. However, as is discussed in the material surrounding Figure 5.3, this conclusion is likely false and a consequence of the spectral pollution phenomenon. Numerical experiments of the same type also suggested that the Bracken–Melloy operator may have a tower of positive eigenvalues roughly of the form $(c_{\mathrm{BM}} \times 10^{-3n})_{n\geq 0}$. Once again, one must be careful to infer genuine properties of the Bracken–Melloy spectrum outside of the spectral maxima and minima.

Furthermore, there are analogous conjectures for $M \geq 2$ multiple backflow operators. One conjectures that the top and bottom of the spectrum of multiple backflow operators, corresponding to backflow and overflow maximizing states, are indeed eigenvalues. Similar to the $M = 1$ backflow operator, it is possible that the $M \geq 2$ multiple backflow operators also have sequences of eigenvalues above 0 and below -1. It is clear that the backflow problem requires new analytical techniques in order to find answers to these conjectures.

— A —

Proof of Lemma 2.4.2

The expectation value of $C^{(M)}$ in the state ψ_M (see (2.54)) can be written in the form

$$\left\langle \psi_M \middle| C^{(M)} \psi_M \right\rangle = -\frac{M^2}{4\pi\epsilon}\Big[I_{00} + 2I_{01} + I_{11}\Big] \tag{A.1}$$

where, for $i, j \in \{0, 1\}$,

$$I_{ij} = \int_{\mathcal{I}_i \times \mathcal{I}_j} dp\, dq\, g_M(p-q)\Big[\Big(\frac{p}{q}\Big)^{1/4} + \Big(\frac{p}{q}\Big)^{-1/4}\Big] \tag{A.2}$$

with

$$\mathcal{I}_0 = \Big[0, \frac{\epsilon}{M}\Big], \qquad \mathcal{I}_1 = \Big[\frac{\pi}{2} - \frac{\epsilon}{2M}, \frac{\pi}{2} + \frac{\epsilon}{2M}\Big] \tag{A.3}$$

and $g_M \in \mathcal{C}^\infty(\mathbb{R})$ is given by

$$g_M(x) = \frac{\sin(2Mx)}{2Mx\cos(x)} \tag{A.4}$$

except at the isolated zeros of the denominator, where one extends by continuity.

We first show that $|g_M(x)| \leq 1$ for all $x \in \mathbb{R}$. Recall that $\mathrm{sinc}(x) = \sin(x)/x$ for $x \neq 0$ and $\mathrm{sinc}(0) = 1$. By insertion of the factor $\sin(x)/\sin(x)$ in the definition of g_M and using the double angle formula for the sin function, one finds

$$g_M(x) = \frac{\sin(2Mx)}{2M\sin(x)\cos(x)} \cdot \frac{\sin(x)}{x} = \frac{\sin(2Mx)}{M\sin(2x)}\,\mathrm{sinc}(x) \tag{A.5}$$

$$= \frac{1}{M} U_{M-1}(\cos(2x))\,\mathrm{sinc}(x), \tag{A.6}$$

where U_n are the Chebyshev polynomials of the second kind defined by

$$U_n(\cos(x)) = \frac{\sin((n+1)x)}{\sin(x)} \tag{A.7}$$

and, as shown in Lemma B.0.1 of Appendix B, obey $|U_n(\cos(\theta))| \leq n+1$ for all $\theta \in \mathbb{R}$. Thus $|g_M(x)| \leq |\operatorname{sinc}(x)| \leq 1$ as claimed.

Using $|g_M(x)| \leq 1$ on $\mathcal{I}_0$, one can bound I_{00} by

$$I_{00} \leq \int_{\mathcal{I}_0 \times \mathcal{I}_0} dp\, dq \left[\left(\frac{p}{q}\right)^{1/4} + \left(\frac{p}{q}\right)^{-1/4} \right] = \frac{32\epsilon^2}{15M^2}. \tag{A.8}$$

Similarly,

$$I_{11} \leq \int_{\mathcal{I}_1 \times \mathcal{I}_1} dp\, dq \left[\left(\frac{p}{q}\right)^{1/4} + \left(\frac{p}{q}\right)^{-1/4} \right] \leq \frac{2\epsilon^2}{M^2} \left(\frac{1+\epsilon/(\pi M)}{1-\epsilon/(\pi M)} \right)^{1/4}, \tag{A.9}$$

where we use the fact that

$$\frac{p}{q} \leq \frac{1+\epsilon/(\pi M)}{1-\epsilon/(\pi M)} \tag{A.10}$$

for $p, q \in \mathcal{I}_1$. One can write

$$\left(\frac{1+\epsilon/(\pi M)}{1-\epsilon/(\pi M)} \right)^{1/4} = \left(1 + \frac{2\epsilon/(\pi M)}{1-\epsilon/(\pi M)} \right)^{1/4} \leq 1 + \frac{\epsilon/(\pi M)}{2(1-\epsilon/(\pi M))} \tag{A.11}$$

by Bernoulli's inequality. Clearly, for $M \geq 2$ and $\epsilon \leq \frac{\pi}{6}$ we have $\frac{\epsilon}{\pi M} \leq \frac{1}{12}$ and hence

$$\left(\frac{1+\epsilon/(\pi M)}{1-\epsilon/(\pi M)} \right)^{1/4} \leq 1 + \frac{\epsilon/(\pi M)}{2(1-\epsilon/(\pi M))} \leq 1 + \frac{6\epsilon}{11\pi M}. \tag{A.12}$$

Combining this inequality with (A.9) we find

$$I_{11} \leq \frac{2\epsilon^2}{M^2} \left(1 + \frac{6\epsilon}{11\pi M} \right). \tag{A.13}$$

Finally, consider I_{01}, the integral over $\mathcal{I}_0 \times \mathcal{I}_1$. We claim that

$$g_M(p-q) \leq -\frac{2\operatorname{sinc}(3\epsilon)}{\pi} \left(1 - \frac{\epsilon}{\pi M} \right) \tag{A.14}$$

holds for $(p, q) \in \mathcal{I}_0 \times \mathcal{I}_1$, for which one also has

$$\frac{\pi}{2} - \frac{3\epsilon}{2M} \leq q - p \leq \frac{\pi}{2} + \frac{\epsilon}{2M}. \tag{A.15}$$

To establish the claim, we first rewrite the even function $g_M(x)$ for $x \neq 0$ as

$$g_M(x) = \frac{\sin(2Mx)}{2Mx\cos(x)} = -\frac{\sin(2M(x-\pi/2))}{2Mx\sin(x-\pi/2)} = -\frac{\operatorname{sinc}(2M(x-\pi/2))}{x\ \operatorname{sinc}(x-\pi/2)} \tag{A.16}$$

after recalling that M is even, so

$$g_M\left(\frac{\pi}{2}+y\right) = -\frac{\operatorname{sinc}(2My)}{(\pi/2+y)\,\operatorname{sinc}(y)} = -\frac{U_{2M-1}(\cos(y))}{2M\,(\pi/2+y)}. \tag{A.17}$$

By Lemma B.0.2 in Appendix B, the even expression $U_{2M-1}(\cos(y))$ is nonnegative and nonincreasing on $[0,\frac{\pi}{2M}]$. It therefore follows that for $0<\epsilon\le\frac{\pi}{6}$ and $y\in[-\frac{3\epsilon}{2M}\frac{\epsilon}{2M}]$, we have

$$g_M\left(\frac{\pi}{2}+y\right) \le -\frac{\operatorname{sinc}(3\epsilon)}{(\pi/2+y)\operatorname{sinc}(3\epsilon/(2M))} \le -\frac{2\operatorname{sinc}(3\epsilon)}{\pi}\left(1-\frac{2y}{\pi}\right), \tag{A.18}$$

where the last step uses the elementary inequalities $\operatorname{sinc}(x)\le 1$ and $-1/(1+x)\le -(1-x)$ for all $x\in\mathbb{R}$. Since $y\in[-\frac{3\epsilon}{2M},\frac{\epsilon}{2M}]$, we deduce

$$g_M\left(\frac{\pi}{2}+y\right) \le -\frac{2\operatorname{sinc}(3\epsilon)}{\pi}\left(1-\frac{\epsilon}{\pi M}\right), \tag{A.19}$$

which establishes the claim (A.14). Now we can use (A.14) to obtain an upper bound for I_{01} by

$$I_{01} \le -\frac{2\operatorname{sinc}(3\epsilon)}{\pi}\left(1-\frac{\epsilon}{\pi M}\right)\int_{\mathcal{I}_0\times\mathcal{I}_1} dp\,dq\left[\left(\frac{p}{q}\right)^{1/4}+\left(\frac{p}{q}\right)^{-1/4}\right] \tag{A.20}$$

$$< -\frac{32\operatorname{sinc}(3\epsilon)\epsilon^{3/4}}{15\pi M^{3/4}}\left(1-\frac{\epsilon}{\pi M}\right)\left[\left(\frac{\pi}{2}+\frac{\epsilon}{2M}\right)^{5/4}-\left(\frac{\pi}{2}-\frac{\epsilon}{2M}\right)^{5/4}\right], \tag{A.21}$$

where we have dropped the contribution from the first term in the integrand in the second line. By the mean value theorem, we have

$$0<\begin{cases}\alpha y^{\alpha-1} & 0<\alpha<1\\ \alpha x^{\alpha-1} & \alpha>1\end{cases} < \frac{y^\alpha-x^\alpha}{y-x} < \begin{cases}\alpha x^{\alpha-1} & 0<\alpha<1\\ \alpha y^{\alpha-1} & \alpha>1\end{cases}. \tag{A.22}$$

Applying (A.22) with $\alpha=5/4$, we find

$$\left(\frac{\pi}{2}+\frac{\epsilon}{2M}\right)^{5/4}-\left(\frac{\pi}{2}-\frac{\epsilon}{2M}\right)^{5/4} \ge \frac{5\epsilon}{4M}\left(\frac{\pi}{2}\right)^{1/4}\left(1-\frac{\epsilon}{\pi M}\right)^{1/4}, \tag{A.23}$$

and substituting back into (A.21) gives

$$I_{01} \le -\frac{8\operatorname{sinc}(3\epsilon)\epsilon^{7/4}}{3\cdot 2^{1/4}\pi^{3/4}M^{7/4}}\left(1-\frac{\epsilon}{\pi M}\right)^{5/4}. \tag{A.24}$$

An application of Taylor's theorem yields $(1-x)^{5/4}\ge 1-\frac{5x}{4}$ for all $x\in(0,1)$. Recalling that $0<\epsilon\le\frac{\pi}{6}$ so that $\operatorname{sinc}(3\epsilon)\ge\operatorname{sinc}(\pi/2)=\frac{2}{\pi}$ we obtain the final bound

$$I_{01} \le -\frac{4}{3}\left(\frac{2\epsilon}{M\pi}\right)^{7/4}\left(1-\frac{5\epsilon}{4\pi M}\right). \tag{A.25}$$

Recombining the bounds for I_{00}, I_{01} and I_{11}, we find

$$\sup \sigma \left(J^{(M)} \right) \geq \frac{2^{11/4} \epsilon^{3/4}}{3\pi^{11/4}} M^{1/4} S\left(\frac{2\epsilon}{\pi M} \right) \tag{A.26}$$

where

$$S(\eta) = 1 - \frac{31\pi^2}{80}\eta^{1/4} - \frac{5}{8}\eta - \frac{9\pi^2}{176}\eta^{5/4}. \tag{A.27}$$

thus completing the proof of Lemma 2.4.2.

— B —

Chebyshev Polynomials

This appendix concerns the value and distribution of the extrema of Chebyshev polynomials of the second kind as defined in (A.7). The results are presumably known, though we did not find a reference. The following Lemma bounds the absolute value of the extrema of $U_n(x)$.

Lemma B.0.1. *For $n \in \mathbb{N}$, the Chebyshev polynomials of the second kind are bounded as*

$$|U_{n-1}(x)| \leq n \tag{B.1}$$

for all $x \in [-1, 1]$ and furthermore achieve this extremum for $x = \pm 1$.

Proof. As $U_0 \equiv 1$, we may restrict to $n \geq 2$ and $x \in (-1, 1)$, noting that

$$U_{n-1}(\pm 1) = (\pm 1)^{n-1} n.$$

The derivative of $U_{n-1}(x)$ is given for $x \in (-1, 1)$ by

$$U'_{n-1}(\cos(\theta)) = -\frac{n \sin(\theta)\cos(n\theta) - \cos(\theta)\sin(n\theta)}{\sin^3(\theta)}, \tag{B.2}$$

so the stationary points of $U_{n-1}(x)$ with $x \in (-1, 1) \setminus \{0\}$ occur when we have $x = \cos(\theta)$ with

$$\tan(n\theta) = n \tan(\theta). \tag{B.3}$$

We can rewrite $U_{n-1}(x)^2$ as

$$U_{n-1}(x)^2 = \frac{\tan^2(n\theta)}{\tan^2(\theta)} \cdot \frac{1 + \tan^2(\theta)}{1 + \tan^2(n\theta)} \tag{B.4}$$

Suppose $x_0 = \cos(\theta_0)$ satisfies (B.3), then

$$U_{n-1}(x_0)^2 = n^2 \frac{1+\tan^2(\theta_0)}{1+n^2\tan^2(\theta_0)} = \frac{n^2}{n^2+(1-n^2)x_0^2} \in (1, n^2), \tag{B.5}$$

using trigonometric identities and recallling that $x_0^2 \in (0,1)$. Therefore $|U_{n-1}(x_0)| < n$ at any extremum $x_0 \in (-1,1) \setminus \{0\}$. □

As well as an understanding of the best upper bound for $U_n(x)$, we would further like to bound the position of the nearest extremum of $U_n(\cos(\theta))$ to $\theta = 0$.

Lemma B.0.2. *For fixed $n \in \mathbb{N}$ with $n \geq 2$ the function $U_{n-1}(\cos(\theta))$ has no extrema for $\theta \in \left(0, \frac{\pi}{n}\right)$ and $U_{n-1}(\cos(\theta))$ is nonnegative and nonincreasing on $\left[0, \frac{\pi}{n}\right]$.*

Proof. Note that $U_{n-1}(\cos(\theta)) \to n > 0$ as $\theta \to 0$. There are no zeros of sin on $(0, \pi/n)$ so the extrema of $U_{n-1}(\cos(\theta))$ in this interval satisfy

$$t_n(\theta) := \tan(n\theta) - n\tan(\theta) = 0. \tag{B.6}$$

We will show that $t_n > 0$ on $(0, \pi/(2n))$ and $t_n < 0$ on $(\pi/(2n), \pi/n)$, and it is clear that $t_n(\theta) \to \pm\infty$ as $\theta \to \pi/(2n)\mp$. Hence there are no zeros of t_n in $(0, \pi/n)$ and therefore no extrema of $U_{n-1}(\cos(\theta))$. Since $U_{n-1}(\cos(\theta))$ is smooth, achieves its global maximum of n at $\theta = 0$, and satisfies $U_{n-1}(\cos(\pi/n)) = 0$, with no extrema in $(0, \pi/n)$, it follows that $U_{n-1}(\cos(\theta))$ is nonnegative and nonincreasing on $[0, \pi/n]$.

It remains to prove the statements made about t_n. First, for $\theta \in (0, \pi/n) \setminus \{\pi/(2n)\}$, the derivative of t_n is given by

$$t_n'(\theta) = n\Big(\sec^2(n\theta) - \sec^2(\theta)\Big), \tag{B.7}$$

which is positive on $(0, \pi/(2n))$ because $\sec^2(\theta)$ is a strictly increasing function on the range $\left(0, \frac{\pi}{2}\right)$. As $t_n(0) = 0$, this implies $t_n > 0$ on $(0, \pi/(2n))$. Second, by trigonometric identities, we may write t_n' equivalently as

$$t_n'(\theta) = n\frac{\sin([n+1]\theta)\sin([n-1]\theta)}{\cos^2(\theta)\cos^2(n\theta)}, \tag{B.8}$$

from which it is clear that the only zero t_n' has on $(0, \pi/n)$ is at $\theta = \frac{\pi}{n+1}$. At this point, one has

$$t_n\left(\frac{\pi}{n+1}\right) = \tan\left(\frac{n\pi}{n+1}\right) - n\tan\left(\frac{\pi}{n+1}\right) = -(n+1)\tan\left(\frac{\pi}{n+1}\right) < 0 \tag{B.9}$$

using $\tan(\pi - \theta) = -\tan(\theta)$. Now $t_n(\theta) \to -\infty$ as $\theta \to \pi/(2n)+$ and also

$$t_n(\theta) = \tan(n\theta) - n\tan(\theta) \leq \tan(\pi) - n\tan\left(\frac{\pi}{n+1}\right) = -n\tan\left(\frac{\pi}{n+1}\right) < 0 \quad \text{(B.10)}$$

for $\theta \in \left(\frac{\pi}{n+1}, \frac{\pi}{n}\right)$ by considering an upper bound for each term individually, using the fact that the tangent function is increasing on $\left[0, \frac{\pi}{2}\right)$ and $\left(\frac{\pi}{2}, \pi\right]$. As t_n is negative at its unique extremum in $(\pi/(2n), \pi/n)$ it follows that $t_n < 0$ on this interval, completing the proof. □

— C —

Exact Multiple Backflow Matrix Element Integrals

In this appendix we compute closed forms for the matrix elements of an arbitrary backflow operator with respect to the dense sequence $(\psi_{n,a,\delta})_{n\in\mathbb{N}}$, given in (3.15). Let $C^{(M)}_{\langle \boldsymbol{t}_M\rangle} = W^* B^{(M)}_{\langle \boldsymbol{t}_M\rangle} W$, where W is the unitary implementing the change of variables $q \mapsto q^{1/2}$, with action

$$\left(C^{(M)}_{\langle \boldsymbol{t}_M\rangle}\varphi\right)(p) = -\frac{1}{4\pi i}\int_0^\infty dq \sum_{k=1}^{M} \frac{e^{it_{2k}(p-q)} - e^{it_{2k-1}(p-q)}}{p-q} P(p,q)\varphi(q), \tag{C.1}$$

where $P(p,q) = (p/q)^{1/4} + (p/q)^{-1/4}$. As shown in (2.24), one can write an arbitrary multiple backflow operator as a sum of single backflow operators. Hence it suffices to compute the matrix elements of $C^{(1)}_{\langle s_1,s_2\rangle}$ with respect to $(\psi_{n,a,\delta})_{n=0}^\infty$ for general $s_1 < s_2$. For $n, m \in \mathbb{N}$ we have

$$\begin{aligned}
\langle \psi_{n,a,\delta} | C^{(1)}_{\langle s_1,s_2\rangle} \psi_{m,a,\delta}\rangle &= -\frac{E_n(a,\delta)E_m(a,\delta)}{4\pi i}\int_0^\infty dp \int_0^\infty dq\, p^{n+\delta}q^{m+\delta}P(p,q) \\
&\quad \times \frac{e^{is_2(p-q)} - e^{is_1(p-q)}}{p-q} e^{-a(p+q)} \\
&= -\frac{E_n(a,\delta)E_m(a,\delta)}{4\pi}\int_0^\infty dp \int_0^\infty dq\, p^{n+\delta}q^{m+\delta}P(p,q) \\
&\quad \times \int_{s_1}^{s_2} dt\, e^{it(p-q)} e^{-a(p+q)} \\
&= -\frac{E_n(a,\delta)E_m(a,\delta)}{4\pi}\int_{s_1}^{s_2} dt\, (I_+(n,m,\delta;t) + I_-(n,m,\delta;t)),
\end{aligned} \tag{C.2}$$

where we have interchanged the order of integration noting that the integral converges absolutely. Here, $E_n(a,\delta)$ is the normalization constant given in (3.16) and

$$\begin{aligned} I_\pm(n,m,\delta;t) &= \int_0^\infty dp \int_0^\infty dq\, p^{n+\delta\pm 1/4} q^{m+\delta\mp 1/4} e^{-(a-it)p} e^{-(a+it)q} \\ &= \Gamma(n+\delta\pm 1/4+1)\Gamma(m+\delta\mp 1/4+1)\times \qquad \text{(C.3)} \\ &\quad \times (a-it)^{-n-\delta\mp 1/4-1}(a+it)^{-m-\delta\pm 1/4-1}. \qquad \text{(C.4)} \end{aligned}$$

In the definition of $I_\pm$, the branches for noninteger powers are fixed so that z^α is real and positive for $z>0$ and the cut is taken along the negative real axis. Combining (C.2) with (C.4), we find that

$$\begin{aligned} \langle \psi_{n,a,\delta} | C^{(1)}_{\langle s_1,s_2\rangle} \psi_{m,a,\delta}\rangle = -\frac{1}{4\pi}\Big[& D_{nm}(a,\delta) J(s_1,s_2;\alpha_n^+,\alpha_m^-;a) \\ & + D_{mn}(a,\delta) J(s_1,s_2;\alpha_n^-,\alpha_m^+;a)\Big], \end{aligned} \qquad \text{(C.5)}$$

where $\alpha_n^\pm = n+\delta\pm\frac{1}{4}$ with

$$D_{nm}(a,\delta) = \pi\sqrt{2}\frac{(2a)^{n+m+2\delta+1}\sqrt{B_{\mathrm{diag}}(n+\delta+1/2)B_{\mathrm{diag}}(m+\delta+1/2)}}{B(n+\delta+1/2,3/4)B(m+\delta+1/2,1/4)}, \qquad \text{(C.6)}$$

in which B is the beta function, $B_{\mathrm{diag}}(x)=B(x,x)$, and

$$J(s_1,s_2;\alpha,\beta;a) = \int_{s_1}^{s_2} dt\,(a-it)^{-\alpha-1}(a+it)^{-\beta-1}. \qquad \text{(C.7)}$$

As shown below, the closed form expression for J is given for $s_1,s_2\in\mathbb{R}\setminus\{0\}$ by

$$J(s_1,s_2;\alpha,\beta;a) = \begin{cases} J_+(s_1,s_2;\alpha,\beta;a) & s_1 s_2 > 0 \\ J_-(s_1,s_2;\alpha,\beta;a) & s_1<0<s_2, \end{cases} \qquad \text{(C.8)}$$

where

$$J_+(s_1,s_2;\alpha,\beta;a) = -\frac{i}{(2a)^{\alpha+\beta+1}}\left[e^{-i\pi\,\mathrm{sgn}(s)(\beta+1)} B\left(\alpha+\beta+1,-\beta;\frac{2a}{a-si}\right)\right]_{s=s_1}^{s=s_2}, \qquad \text{(C.9)}$$

and

$$J_-(s_1,s_2;\alpha,\beta;a) = J_+(s_1,s_2;\alpha,\beta;a) + \frac{2\pi}{(2a)^{\alpha+\beta+1}}\frac{\Gamma(\alpha+\beta+1)}{\Gamma(\alpha+1)\Gamma(\beta+1)}. \qquad \text{(C.10)}$$

To obtain these closed form expressions, first make the transformation of variable $t\mapsto 2at$ in (C.7) so that

$$J(s_1,s_2;\alpha,\beta;a) = (2a)^{-\alpha-\beta-1}\int_{s_1/(2a)}^{s_2/(2a)} dt\left(\frac{1}{2}-it\right)^{-\alpha-1}\left(\frac{1}{2}+it\right)^{-\beta-1}. \qquad \text{(C.11)}$$

Next, recall that the incomplete beta function $B(\mu,\nu;z)$ is given for $\mu>0$, $\nu\in\mathbb{R}$ as a holomorphic function in $z\in\mathbb{C}\setminus((-\infty,0]\cup[1,\infty))$ by

$$B(\mu,\nu;z)=\int_0^z dv\, v^{\mu-1}(1-v)^{\nu-1}, \tag{C.12}$$

where the integral is taken over any contour avoiding $(-\infty,0]\cup[1,\infty)$. Thus, for $t\in\mathbb{R}\setminus\{0\}$,

$$\begin{aligned}\frac{d}{dt}B\left(\mu,\nu;(1/2-it)^{-1}\right)&=i\left(-\frac{1}{2}-it\right)^{\nu-1}\left(\frac{1}{2}-it\right)^{-\mu-\nu}\\&=ie^{-i\pi(\nu-1)\,\mathrm{sgn}(t)}\left(\frac{1}{2}+it\right)^{\nu-1}\left(\frac{1}{2}-it\right)^{-\mu-\nu}.\end{aligned} \tag{C.13}$$

Setting $\mu=\alpha+\beta+1$ and $\nu=-\beta$, we may evaluate (C.11) in cases where $\alpha+\beta>-1$ and $s_1,s_2\in\mathbb{R}\setminus\{0\}$ using the fundamental theorem of calculus to obtain $J(s_1,s_2;\alpha,\beta;a)=J_+(s_1,s_2;\alpha,\beta;a)$, where J_+ is given by (C.9).

In the case where $s_1<0$ and $s_2>0$, we can decompose the integral $\int_{s_1/(2a)}^{s_2/(2a)}$ in (2.15) as $\int_{s_1/(2a)}^{s_2/(2a)}=\int_{-\infty}^{\infty}-\int_{s_2/(2a)}^{\infty}-\int_{-\infty}^{s_1/(2a)}$. The first integral can be evaluated in closed form (see (5.12.8) in [24]) giving (C.15) below, while the others are limiting cases of the result just proved. Noting that

$$\lim_{s\to\pm\infty}B\left(\alpha+\beta+1,-\beta;\frac{2a}{a-si}\right)=0, \tag{C.14}$$

the overall effect is to add

$$\int_{-\infty}^{\infty}dt\,(a-it)^{-\alpha-1}(a+it)^{-\beta-1}=\frac{2\pi}{(2a)^{\alpha+\beta+1}}\frac{\Gamma(\alpha+\beta+1)}{\Gamma(\alpha+1)\Gamma(\beta+1)} \tag{C.15}$$

to $J_+(s_1,s_2;\alpha,\beta;a)$, thus obtaining $J_-(s_1,s_2;\alpha,\beta;a)$ as given in (C.10).

The incomplete beta function is computed using the hypergeometric representation

$$B(\mu,\nu;z)=\frac{z^\mu}{\mu}{}_2F_1(\mu,1-\nu;\mu+1;z). \tag{C.16}$$

given in Section 8.17 of [24]. We also make use of the identity $J(s_1,s_2;\alpha,\beta;a)=\overline{J(s_1,s_2;\beta,\alpha;a)}$, readily seen from (C.11).

— D —

Closed form of the auxillary functions for the matrix elements

Before beginning the calculation of the matrix elements found in chapter 4, we write down a few important integrals that will be made use of. First note the following integral, taken from the Digital Library of Mathematical Functions (DLMF) [24, Chapter 8, equation 8.6.4]. For $Re\,\lambda > 0, a \in \mathbb{C} \setminus (-\infty, 0]$ and $c < 1$ we find

$$\int_0^\infty \frac{dx}{x^c}\,\frac{e^{-\lambda x}}{x+a} = a^{-c}e^{\lambda a}\Gamma(1-c)\Gamma(c,\lambda a). \tag{D.1}$$

where $\Gamma(\cdot)$ is the gamma function and $\Gamma(\cdot,\cdot)$ denotes the incomplete gamma function whose definition is

$$\Gamma(\mu, z) = \int_z^\infty dt\, t^{\mu-1}e^{-t}, \qquad \mu, z \in \mathbb{C} \tag{D.2}$$

where the integral is taken over any contour connecting the end points. When the contour avoids the negative real axis, we say the incomplete gamma function takes its principal value, as described in [24, Chapter 8]. It is readily seen from the defining equation D.2, that for $\mu \in \mathbb{C}$, $\Gamma(a,\cdot)$ is analytic on $\mathbb{C} \setminus (-\infty, 0]$.

Continuing on from the integral in (D.1), for $a, b \in \mathbb{C} \setminus (-\infty, 0], c < 1, \lambda > 0$, we obtain

$$\int_0^\infty \frac{dx}{x^c}\frac{e^{-\lambda x}}{(x+a)(x+b)} = \frac{\Gamma(1-c)}{b-a}\left[a^{-c}e^{\lambda a}\Gamma(c,\lambda a) - b^{-c}e^{\lambda b}\Gamma(c,\lambda b)\right], \tag{D.3}$$

by means of partial fraction decomposition. For $|c| < 1$ and writing $\lambda = s - i\omega$, one can take the limit of (D.3) as $s \to 0^+$ giving

$$\int_0^\infty \frac{dx}{x^c}\frac{e^{i\omega x}}{(x+a)(x+b)} = \frac{\Gamma(1-c)}{b-a}\left[a^{-c}e^{-i\omega a}\Gamma(c,-i\omega a) - b^{-c}e^{-i\omega b}\Gamma(c,-i\omega b)\right], \tag{D.4}$$

where the left-hand side converges by the dominated convergence theorem. A final integral of use for the P elements is obtained by taking the limit of (D.3) as $\lambda \to 0$ which gives

$$\int_0^\infty \frac{dx}{x^c} \frac{1}{(x+a)(x+b)} = \frac{\Gamma(c)\Gamma(1-c)}{b-a}\left(a^{-c} - b^{-c}\right) = \frac{\pi(a^{-c} - b^{-c})}{(b-a)\sin(\pi c)} \tag{D.5}$$

by making use of the reflection identity of the gamma function as shown in [24, Chapter 5, equation 5.5.3]. The above integral holds for all $|c| < 1$ and $a, b \in \mathbb{C} \setminus (-\infty, 0]$.

D.1 CLOSED FORMS OF F, G AND H

To find closed forms of F, G and H, we will first make use of the following Lemma.

Lemma D.1.1. *Let A, B, C be holomorphic in $|\arg z| < \pi/2 + \delta$ for some $\delta > 0$, with A, B bounded on the first quadrant of the complex plane and C bounded on the fourth quadrant of the complex plane. Let*

$$F(z) = A(z) + B(z)e^{2iz} + C(z)e^{-2iz}, \tag{D.6}$$

and $c \in (-1, 1)$. For $\alpha \in \mathbb{R}$ and $x \in \mathbb{R} \setminus \{\alpha\}$, let $I_\alpha(x)$ be the integral

$$I_\alpha(x) = \mathrm{PV} \int_0^\infty \frac{dy}{y^c} \frac{F(y)}{(x-y)(y-\alpha)}. \tag{D.7}$$

Then for $\alpha \neq 0$,

$$\begin{aligned} I_\alpha(x) = {} & e^{i\pi(1-c)/2} \int_0^\infty \frac{dy}{y^c} \frac{A(iy) + B(iy)e^{-2y}}{(y+ix)(y+i\alpha)} + e^{-i\pi(1-c)/2} \int_0^\infty \frac{dy}{y^c} \frac{C(-iy)e^{-2y}}{(y-ix)(y-i\alpha)} \\ & - i\pi\vartheta(x) \frac{A(x) + B(x)e^{2xi} - C(x)e^{-2xi}}{x^c(x-\alpha)} + i\pi\vartheta(\alpha) \frac{A(\alpha) + B(\alpha)e^{2\alpha i} - C(\alpha)e^{-2\alpha i}}{\alpha^c(x-\alpha)} \end{aligned} \tag{D.8}$$

Furthermore, if $F(z)$ has a zero at $z = \alpha$ then

$$\begin{aligned} I_\alpha(x) = {} & e^{i\pi(1-c)/2} \int_0^\infty \frac{dy}{y^c} \frac{A(iy) + B(iy)e^{-2y}}{(y+ix)(y+i\alpha)} + e^{-i\pi(1-c)/2} \int_0^\infty \frac{dy}{y^c} \frac{C(-iy)e^{-2y}}{(y-ix)(y-i\alpha)} \\ & - i\pi\vartheta(x) \frac{A(x) + B(x)e^{2xi} - C(x)e^{-2xi}}{x^c(x-\alpha)} - 2i\pi\vartheta(\alpha) \frac{C(\alpha)e^{-2\alpha i}}{\alpha^c(x-\alpha)}. \end{aligned} \tag{D.9}$$

In the particular case $\alpha = 0$, we have

$$\begin{aligned} I_0(x) = e^{i\pi(1-c)/2} \int_0^\infty \frac{dy}{y^{c+1}} \frac{A(iy) + B(iy)e^{-2y} + C(0)}{y + ix} \\ + e^{-i\pi(1-c)/2} \int_0^\infty \frac{dy}{y^{c+1}} \frac{C(-iy)e^{-2y} - C(0)}{y - ix} \\ - i\pi\vartheta(x) \frac{A(x) + B(x)e^{2xi} - C(x)e^{-2xi} + 2C(0)}{x^{c+1}}. \end{aligned} \tag{D.10}$$

Finally, in the case where $F(z)$ has a zero of order 2 at $z = \alpha$ with $x, \alpha > 0$ then $I_\alpha(\alpha)$ has a finite value with

$$\begin{aligned} I_\alpha(\alpha) = e^{i\pi(1-c)/2} \int_0^\infty \frac{dy}{y^c} \frac{A(iy) + B(iy)e^{-2y}}{(y + i\alpha)^2} + e^{-i\pi(1-c)/2} \int_0^\infty \frac{dy}{y^c} \frac{C(-iy)e^{-2y}}{(y - i\alpha)^2} \\ + 2\pi i\vartheta(\alpha)e^{-2\alpha i} \left(\frac{C'(\alpha) - 2iC(\alpha)}{\alpha^c} - \frac{cC(\alpha)}{\alpha^{c+1}} \right) \end{aligned} \tag{D.11}$$

Proof. First, we deform the principal value integral to the contour Γ, illustrated in figure D.1, avoiding the poles x and α of the integrand if they are present to find

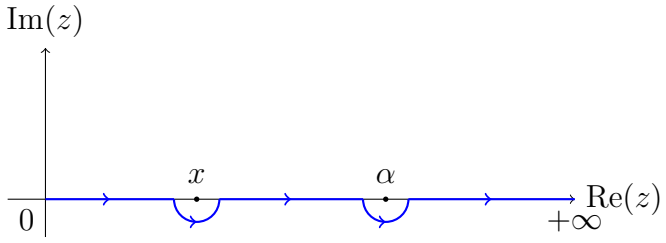

Figure D.1: The contour Γ

$$I(x) = \int_\Gamma \frac{dz}{z^c} \frac{F(z)}{(x - z)(z - \alpha)} + i\pi\vartheta(x)x^{-c} \frac{F(x)}{x - \alpha} - i\pi\vartheta(\alpha)\alpha^{-c} \frac{F(\alpha)}{x - \alpha}. \tag{D.12}$$

We now split the integrand up and deform the integrals to the positive and negative imaginary axes in such a way that the new integrals converge exponentially.

$$\begin{aligned} I_\alpha(x) = \int_0^\infty \frac{idy}{(iy)^c} \frac{A(iy) + B(iy)e^{-2y}}{(x - iy)(iy - \alpha)} + \int_0^\infty \frac{-idy}{(-iy)^c} \frac{C(-iy)e^{-2y}}{(x + iy)(-iy - \alpha)} \\ - 2i\pi\vartheta(x) \frac{A(x) + B(x)e^{2xi}}{x^c(x - \alpha)} + 2i\pi\vartheta(\alpha) \frac{A(\alpha) + B(\alpha)e^{2\alpha i}}{\alpha^c(x - \alpha)} \\ + i\pi\vartheta(x) \frac{F(x)}{x - \alpha} - i\pi\vartheta(\alpha) \frac{F(\alpha)}{x - \alpha} \end{aligned} \tag{D.13}$$

where we have picked up residue contributions for the integral rotated to the positive imaginary axis. Simplifying, we find

$$\begin{aligned} I_\alpha(x) = e^{i\pi(1-c)/2}\int_0^\infty \frac{dy}{y^c}\frac{A(iy)+B(iy)e^{-2y}}{(y+ix)(y+i\alpha)} + e^{-i\pi(1-c)/2}\int_0^\infty \frac{dy}{y^c}\frac{C(-iy)e^{-2y}}{(y-ix)(y-i\alpha)} \\ + i\pi\vartheta(x)\frac{C(x)e^{-2xi}}{x^c(x-\alpha)} - i\pi\vartheta(x)\frac{A(x)+B(x)e^{2xi}}{x^c(x-\alpha)} - i\pi\vartheta(\alpha)\frac{C(\alpha)e^{-2\alpha i}}{\alpha^c(x-\alpha)} \\ + i\pi\vartheta(\alpha)\frac{A(\alpha)+B(\alpha)e^{2\alpha i}}{\alpha^c(x-\alpha)}. \end{aligned} \tag{D.14}$$

Now with the additional assumption that $F(\alpha) = 0$, we find

$$\begin{aligned} I_\alpha(x) = e^{i\pi(1-c)/2}\int_0^\infty \frac{dy}{y^c}\frac{A(iy)+B(iy)e^{-2y}}{(y+ix)(y+i\alpha)} + e^{-i\pi(1-c)/2}\int_0^\infty \frac{dy}{y^c}\frac{C(-iy)e^{-2y}}{(y-ix)(y-i\alpha)} \\ + i\pi\vartheta(x)\frac{C(x)e^{-2xi}}{x^c(x-\alpha)} - i\pi\vartheta(x)\frac{A(x)+B(x)e^{2xi}}{x^c(x-\alpha)} - 2i\pi\vartheta(\alpha)\frac{C(\alpha)e^{-2\alpha i}}{\alpha^c(x-\alpha)}. \end{aligned} \tag{D.15}$$

from which equation (D.9) follows. For the case $\alpha = 0$, letting Γ' be a contour following the positive half-line and avoiding the pole at $z = x$ from below, we split up the integral as

$$I_0(x) = \int_{\Gamma'}\frac{dz}{z^{c+1}}\frac{A(z)+B(z)e^{2zi}+C(0)}{x-z} + \int_{\Gamma'}\frac{dz}{z^{c+1}}\frac{C(z)e^{-2zi}-C(0)}{x-z} + i\pi\vartheta(x)\frac{F(x)}{x-\alpha} \tag{D.16}$$

$$\begin{aligned} = e^{i\pi(1-c)/2}\int_0^\infty \frac{dy}{y^{c+1}}\frac{A(iy)+B(iy)e^{-2y}+C(0)}{y+ix} + i\pi\vartheta(x)\frac{F(x)}{x-\alpha} \\ + e^{-i\pi(1-c)/2}\int_0^\infty \frac{dy}{y^{c+1}}\frac{C(-iy)e^{-2y}-C(0)}{y-ix} \\ - 2\pi i\vartheta(x)\frac{A(x)+B(x)e^{2xi}+C(x)}{x^{c+1}} \end{aligned} \tag{D.17}$$

$$\begin{aligned} = e^{i\pi(1-c)/2}\int_0^\infty \frac{dy}{y^{c+1}}\frac{A(iy)+B(iy)e^{-2y}+C(0)}{y+ix} \\ + e^{-i\pi(1-c)/2}\int_0^\infty \frac{dy}{y^{c+1}}\frac{C(-iy)e^{-2y}-C(0)}{y-ix} \\ - \frac{i\pi\vartheta(x)}{x^{c+1}}\left(A(x)+B(x)e^{2xi}-C(x)e^{-2xi}+2C(0)\right). \end{aligned} \tag{D.18}$$

Finally for the case where $F(z)$ has a zero of order 2 at $z = \alpha$, we can calculate

$I_\alpha(\alpha)$ as

$$I_\alpha(\alpha) = e^{i\pi(1-c)/2}\int_0^\infty \frac{dy}{y^c}\frac{A(iy)+B(iy)e^{-2y}}{(y+i\alpha)^2} + e^{-i\pi(1-c)/2}\int_0^\infty \frac{dy}{y^c}\frac{C(-iy)e^{-2y}}{(y-i\alpha)^2} - i\pi\vartheta(\alpha)\lim_{x\to\alpha}\frac{1}{x-\alpha}\left[\frac{A(x)+B(x)e^{2xi}-C(x)e^{-2xi}}{x^c}+\frac{2C(\alpha)e^{-2\alpha i}}{\alpha^c}\right]. \tag{D.19}$$

By L'Hôpital's rule, we can write the limit as

$$\lim_{x\to\alpha}\frac{1}{x-\alpha}\left[\frac{A(x)+B(x)e^{2xi}-C(x)e^{-2xi}}{x^c}+\frac{2C(\alpha)e^{-2\alpha i}}{\alpha^c}\right]$$

$$= \frac{d}{dx}\bigg|_{x=\alpha}\left[\frac{A(x)+B(x)e^{2xi}-C(x)e^{-2xi}}{x^c}+\frac{2C(\alpha)e^{-2\alpha i}}{\alpha^c}\right] \tag{D.20}$$

$$= \frac{d}{dx}\bigg|_{x=\alpha}\left[\frac{F(x)}{x^c}-2\left(\frac{C(x)e^{-2xi}}{x^c}-\frac{C(\alpha)e^{-2\alpha i}}{\alpha^c}\right)\right] \tag{D.21}$$

$$= -2e^{-2\alpha i}\left[\frac{C'(\alpha)-2iC(\alpha)}{\alpha^c}-\frac{cC(\alpha)}{\alpha^{c+1}}\right] \tag{D.22}$$

since $F(\alpha)=0$ and $F'(\alpha)=0$ by assumption. Returning to (D.19), we find

$$I_\alpha(\alpha) = e^{i\pi(1-c)/2}\int_0^\infty \frac{dy}{y^c}\frac{A(iy)+B(iy)e^{-2y}}{(y+i\alpha)^2} + e^{-i\pi(1-c)/2}\int_0^\infty \frac{dy}{y^c}\frac{C(-iy)e^{-2y}}{(y-i\alpha)^2} + 2i\pi\vartheta(\alpha)e^{-2\alpha i}\left[\frac{C'(\alpha)-2iC(\alpha)}{\alpha^c}-\frac{cC(\alpha)}{\alpha^{c+1}}\right], \tag{D.23}$$

completing the proof of the lemma. □

As a brief comment, we note that if B and C are as in lemma D.1.1 with $B(iy)=\overline{C(-iy)}$ for all $y\in(0,\infty)$ then by a simple computation we have

$$e^{i\pi(1-c)/2}\int_0^\infty \frac{dy}{y^c}\frac{B(iy)e^{-2y}}{(y+ix)(y+i\alpha)} + e^{-i\pi(1-c)/2}\int_0^\infty \frac{dy}{y^c}\frac{C(-iy)}{(y-ix)(y-i\alpha)} = 2\,\mathrm{Re}\,e^{i\pi(1-c)/2}\int_0^\infty \frac{dy}{y^c}\frac{B(iy)e^{-2y}}{(y+ix)(y+i\alpha)} \tag{D.24}$$

provided that both integrals on the left hand side exist.

D.1.1 CALCULATION OF THE F AND G INTEGRALS

Recall that $F(c,\alpha;x)$ and $G(c,\alpha;x)$ are defined by

$$F(c,\alpha;x) = \mathrm{PV}\int_0^\infty \frac{dy}{y^c}\frac{\sin 2y}{(x-y)(y-\alpha)} \tag{D.25}$$

$$G(c,\alpha;x) = \mathrm{PV}\int_0^\infty \frac{dy}{y^c}\frac{\sin^2 y}{(x-y)(y-\alpha)}. \tag{D.26}$$

We begin with the F integral.

Using lemma D.1.1 we find

$$F(c,\alpha;x) = \mathrm{Re}\, e^{-i\pi c/2}\int_0^\infty \frac{dy}{y^c}\frac{e^{-2y}}{(y+ix)(y+i\alpha)} - \pi\vartheta(x)\frac{\cos(2x)}{x^c(x-\alpha)} + \pi\vartheta(\alpha)\frac{\cos(2\alpha)}{\alpha^c(x-\alpha)} \tag{D.27}$$

for general $|c|<1$ and $\alpha\in\mathbb{R}\setminus\{0\}$. By (D.3), this can be simplified to

$$F(c,\alpha;x) = \frac{f(c,\alpha)-f(c,x)}{x-\alpha}, \tag{D.28}$$

where

$$f(c,x) = \Gamma(1-c)\,\mathrm{Im}\, e^{-i\pi c/2}(ix)^{-c}e^{2xi}\Gamma(c,2xi) + \frac{\pi\vartheta(x)\cos 2x}{x^c} \tag{D.29}$$

$$= \frac{\Gamma(1-c)}{|x|^c}\,\mathrm{Im}\, e^{-i\vartheta(x)\pi c}e^{2xi}\Gamma(c,2xi) + \frac{\pi\vartheta(x)\cos 2x}{x^c} \tag{D.30}$$

where on the second line we have made use of the fact that for $c,x\in\mathbb{R}$, we have

$$(ix)^{-c} = \exp(-i\pi c\vartheta(x) + i\pi c/2)|x|^{-c}. \tag{D.31}$$

The case $x=\alpha$ for $\alpha\neq 0$ can be obtained by taking limits. Firstly we find

$$F(c,\alpha;\alpha) = -\partial_x\Big|_{x=\alpha} f(c,x) \tag{D.32}$$

and

$$-\partial_x f(c,x) = \Gamma(1-c)\,\mathrm{Im}\, e^{-i\pi c/2}\left[e^{2xi}\Gamma(c,2xi)\left(\frac{c}{x(ix)^c} - \frac{2i}{(ix)^c}\right) + \frac{2^c}{x}\right]$$
$$+ \frac{\pi\vartheta(x)}{x^{c+1}}\left[2x\sin(2x) + c\cos(2x)\right]. \tag{D.33}$$

Now we can rewrite

$$\frac{c}{x(ix)^c} - \frac{2i}{(ix)^c} = \frac{i}{(ix)^{c+1}}(c-2ix) \tag{D.34}$$

$$= -e^{-i\pi(c+1)\vartheta(x)+i\pi c/2}|x|^{-c-1}(c-2ix) \tag{D.35}$$

Combing (D.35) with (D.33) we find

$$F(c,\alpha;\alpha) = -\Gamma(1-c)\,\mathrm{Im}\,e^{-i\pi(c+1)\vartheta(\alpha)}\frac{e^{2\alpha i}\Gamma(c,2i\alpha)}{|\alpha|^{c+1}}(c-2i\alpha) - \frac{\Gamma(1-c)\sin(\pi c/2)}{\alpha} + \frac{\pi\vartheta(\alpha)}{\alpha^{c+1}}\left[2\alpha\sin(2\alpha)+c\cos(2\alpha)\right]. \tag{D.36}$$

At this stage, we calculate individual values of $f(c,x)$ for $c \in \{0, 1/2\}$ and $x = n\pi$ for $n \in \mathbb{Z}$, which is precisely what is required for the computation of the matrix elements as in equations (4.79) to (4.81). As we will make use of, for $x > 0$ and $n \in \mathbb{Z} \setminus \{0\}$, we have

$$f(1/2,x) = -\sqrt{\frac{\pi}{x}}\,\mathrm{Re}\,e^{2xi}\Gamma(1/2,2xi) + \frac{\pi\cos(2x)}{\sqrt{x}}, \tag{D.37}$$

$$f(1/2,n\pi) = -\frac{1}{\sqrt{|n|}}\,\mathrm{Re}\,e^{i\pi\vartheta(-n)/2}\Gamma(1/2,2\pi ni) + \vartheta(n)\sqrt{\frac{\pi}{n}}, \tag{D.38}$$

$$f(1/2,0) = 2\sqrt{\pi}. \tag{D.39}$$

For the case $c = 0$, we have

$$f(0,x) = \mathrm{Im}\,e^{2xi}\Gamma(0,2xi) + \pi\cos 2x, \tag{D.40}$$

$$f(0,n\pi) = \mathrm{Im}\,\Gamma(0,2\pi ni) + \vartheta(n)\pi, \tag{D.41}$$

$$f(0,0) = \frac{\pi}{2}. \tag{D.42}$$

Finally in the case $c = -1/2$, we have

$$f(-1/2,x) = \frac{\sqrt{\pi x}}{2}\,\mathrm{Re}\,e^{2xi}\Gamma(-1/2,2xi) + \pi\sqrt{x}\cos 2x, \tag{D.43}$$

$$f(-1/2,n\pi) = \frac{\pi\sqrt{n}}{2}\,\mathrm{Im}\,e^{i\vartheta(n)\pi/2}\Gamma(-1/2,2\pi ni) + \vartheta(n)\pi^{3/2}\sqrt{n}, \tag{D.44}$$

$$f(-1/2,0) = \frac{\sqrt{\pi}}{2}, \tag{D.45}$$

with the values for $F(c,n\pi;x)$ built from the corresponding f values as

$$F(c,n\pi;x) = \frac{f(c,n\pi) - f(c,x)}{x - n\pi}. \tag{D.46}$$

The specific values of $F(c, n\pi; x)$ at $x = n\pi$ for $n \in \mathbb{Z} \setminus \{0\}$ are given below

$$F(1/2, n\pi; n\pi) = \operatorname{Im} \frac{e^{-i\vartheta(n)\pi/2}}{2\pi|n|^{3/2}}(1 - 4n\pi i)\Gamma(1/2, 2n\pi i) - \frac{1}{n\sqrt{\pi}} + \frac{\vartheta(n)}{2n^{3/2}\sqrt{\pi}}, \quad \text{(D.47)}$$

$$F(0, n\pi; n\pi) = 2\mathrm{Ci}(2n\pi), \quad \text{(D.48)}$$

$$F(-1/2, n\pi; n\pi) = \operatorname{Im} \frac{e^{-i\vartheta(n)\pi/2}}{4\sqrt{|n|}}(1 + 4n\pi i)\Gamma(-1/2, 2n\pi i) + \frac{1}{2n\sqrt{\pi}} - \frac{\sqrt{\pi}\vartheta(n)}{2\sqrt{n}}. \quad \text{(D.49)}$$

Now with the values of f and F in place, we recall that the matrix elements are built out of linear combinations of $T_{s^2 s_2}(a, b; m\pi; n\pi)$ as

$$T_{s^2 s_2}(a, b; n\pi, m\pi) = \mathrm{PV} \int_0^\infty \frac{dx}{x^a} \frac{\sin^2(x)}{x - n\pi} F(b, m\pi; x) \quad \text{(D.50)}$$

$$= -f(b, \beta)G(a; \alpha, \beta) - \mathrm{PV} \int_0^\infty \frac{dx}{x^a} \frac{f(b, x)\sin^2 x}{(x - \alpha)(x - \beta)} \quad \text{(D.51)}$$

where

$$G(c, \alpha; x) = \mathrm{PV} \int_0^\infty \frac{dy}{y^c} \frac{\sin^2 y}{(x - y)(y - \alpha)}. \quad \text{(D.52)}$$

We begin by calculating $G(c, \alpha; x)$. Note that the integral in (D.52) corresponds to calculating $I_\alpha(x)$ in Lemma D.1.1 with $A = 1/2, B = C = -1/4$ and hence for arbitrary $|c| < 1$ and $\alpha, \beta \in \mathbb{R} \setminus \{0\}$ we have

$$\begin{aligned} G(c, \alpha; x) = {} & \frac{e^{i\pi(1-c)/2}}{4} \int_0^\infty \frac{dy}{y^c} \frac{2 - e^{-2y}}{(y + i\alpha)(y + ix)} \\ & - \frac{e^{-i\pi(1-c)/2}}{4} \int_0^\infty \frac{dy}{y^c} \frac{e^{-2y}}{(y - i\alpha)(y - ix)} \\ & - \frac{i\pi}{2(\beta - \alpha)} \left(\frac{\vartheta(x)}{x^c} - \frac{\vartheta(\alpha)}{\alpha^c} \right) \\ & - \frac{\pi}{2(x - \alpha)} \left(\frac{\vartheta(x)\sin 2x}{x^c} - \frac{\vartheta(\alpha)\sin 2\alpha}{\alpha^c} \right) \\ = {} & \frac{e^{i\pi(1-c)/2}}{2} \int_0^\infty \frac{dy}{y^c} \frac{1}{(y + i\alpha)(y + ix)} \quad \text{(D.53)} \\ & + \frac{1}{2} \operatorname{Re} e^{i\pi(1-c)/2} \int_0^\infty \frac{dy}{y^c} \frac{e^{-2y}}{(y + i\alpha)(y + ix)} \\ & - \frac{i\pi}{2(x - \alpha)} \left(\frac{\vartheta(x)}{x^c} - \frac{\vartheta(\alpha)}{\alpha^c} \right) \\ & - \frac{\pi}{2(x - \alpha)} \left(\frac{\vartheta(x)\sin 2x}{x^c} - \frac{\vartheta(\alpha)\sin 2\alpha}{\alpha^c} \right). \quad \text{(D.54)} \end{aligned}$$

Restricting to the case $0 < |c| < 1$, the integrals above can be calculated once again using (D.3) and we find

$$\begin{aligned} G(c,\alpha;x) = &-\frac{\pi e^{i\pi(1-c)/2}}{2}\frac{(ix)^{-c}-(i\alpha)^{-c}}{(x-\alpha)\sin(\pi c)} \\ &- \frac{\Gamma(1-c)}{2(x-\alpha)}\operatorname{Re} e^{-i\pi c/2}\left[(ix)^{-c}e^{2xi}\Gamma(c,2xi)-(i\alpha)^{-c}e^{2\alpha i}\Gamma(c,2\alpha i)\right] \\ &- \frac{i\pi}{2(x-\alpha)}\left(\frac{\vartheta(x)}{x^c}-\frac{\vartheta(\alpha)}{\alpha^c}\right) \\ &- \frac{\pi}{2(x-\alpha)}\left(\frac{\vartheta(x)\sin 2x}{x^c}-\frac{\vartheta(\alpha)\sin 2\alpha}{\alpha^c}\right) \end{aligned} \tag{D.55}$$

Note that we can write this as

$$G(c,\alpha;x) = \frac{g(c,\alpha)-g(c,x)}{2(x-\alpha)} \tag{D.56}$$

where

$$\begin{aligned} g(c;x) = &\frac{\pi e^{i\pi(1-c)/2}(ix)^{-c}}{\sin \pi c} - \Gamma(1-c)\operatorname{Re} e^{-i\pi c/2}(ix)^{-c}e^{2xi}\Gamma(c,2xi) + i\pi\vartheta(x)x^{-c} \\ &+ \pi\vartheta(x)x^{-c}\sin 2x \end{aligned} \tag{D.57}$$

can be simplified to

$$\begin{aligned} g(c,x) = &\pi\left(\vartheta(x)\cot\pi c + \vartheta(-x)\csc\pi c\right)|x|^{-c} - \Gamma(1-c)\operatorname{Re} e^{-i\pi c/2}(ix)^{-c}e^{2xi}\Gamma(c,2xi) \\ &+ \pi\vartheta(x)x^{-c}\sin 2x. \end{aligned} \tag{D.58}$$

For the case $\beta = 0$, using lemma D.1.1 we have

$$G(c,0;x) = \operatorname{PV}\int_0^\infty \frac{dy}{y^{c+1}}\frac{\sin^2 y}{x-y} \tag{D.59}$$

$$= \frac{1}{2}\operatorname{Re} e^{i\pi(1-c)/2}\int_0^\infty \frac{dy}{y^{c+1}}\frac{1-e^{-2y}}{y+ix} + \frac{\pi\vartheta(x)\sin 2x}{2x^{c+1}} \tag{D.60}$$

$$\begin{aligned} = &\frac{1}{2}\operatorname{Re} e^{-i\pi c/2}\frac{\Gamma(1-c)}{x}\left[\frac{2^c}{c}-(ix)^{-c}(\Gamma(c)-e^{2\alpha i}\Gamma(c,2\alpha i))\right] \\ &- \frac{\pi\vartheta(x)\sin 2x}{2x^{c+1}} \end{aligned} \tag{D.61}$$

$$\begin{aligned} = &\frac{\Gamma(1-c)2^{c-1}\cos(\pi c/2)}{xc} - \frac{\pi}{2|x|^{c+1}}(\vartheta(x)\cot\pi c + \vartheta(-x)\csc\pi c) \\ &- \frac{\Gamma(1-c)}{2|x|^{c+1}}\operatorname{Re} e^{-i\pi(c+1)\theta(x)}e^{2xi}\Gamma(c,2xi) \end{aligned} \tag{D.62}$$

for $|c| < 1, \beta \neq 0$ and

$$G(c,0;0) = \int_0^\infty \frac{dy}{y^c}\left(\frac{\sin y}{y}\right)^2 = \frac{\sqrt{\pi}\Gamma\left(\frac{1-c}{2}\right)}{2(1+c)\Gamma\left(\frac{c}{2}+1\right)}, \tag{D.63}$$

$$G(0,0;0) = \frac{\pi}{2}. \tag{D.64}$$

Both integrals directly above were computed using Maple 2024. For the case $c = 0$, we must take extra care. Firstly, using lemma D.1.1 we find

$$G(0,\alpha;x) = \frac{e^{i\pi/2}}{2}\int_0^\infty \frac{dy}{(y+i\alpha)(y+ix)} - \frac{1}{2}\operatorname{Re} e^{i\pi/2}\int_0^\infty dy \frac{e^{-2y}}{(y+i\alpha)(y+ix)} - \frac{i\pi[\vartheta(x)-\vartheta(\alpha)]}{2(x-\alpha)} - \frac{\pi\vartheta(x)}{2(x-\alpha)}\sin 2x + \frac{\pi\theta(\alpha)}{2(x-\alpha)}\sin 2\alpha \tag{D.65}$$

. By taking the limit of (D.5) as $c \to 0$, we find

$$-e^{i\pi/2}\int_0^\infty \frac{dy}{(y+i\alpha)(y+ix)} + i\pi[\vartheta(x)-\vartheta(\alpha)] = \frac{\log|\alpha| - \log|x|}{x-\alpha} \tag{D.66}$$

for all $\alpha, x \in \mathbb{R}$. Further making use of (D.3), $G(0,\alpha,\beta)$ admits the closed form

$$G(0,\alpha;x) = \frac{g(0,\alpha) - g(0,x)}{x-\alpha} \tag{D.67}$$

where

$$g(0,x) = \operatorname{Re} e^{2xi}\Gamma(0,2xi) + \log|x| + \pi\vartheta(x)\sin 2x. \tag{D.68}$$

We can calculate G in the limit as α and x coincide as

$$G(0,\alpha;\alpha) = \lim_{x\to\alpha} G(0,\alpha;x) \tag{D.69}$$

$$= \frac{1}{2}\frac{d}{dx}\bigg|_{x=\alpha} G(0,\alpha;x) \tag{D.70}$$

$$= \operatorname{Im} e^{2\alpha i}\Gamma(0,2\alpha i) + \frac{1}{2\alpha} - \vartheta(\alpha)\pi\cos 2\alpha. \tag{D.71}$$

To summarise, we present specific values of g that will be made us of in the calculation of the matrix elements. For $n \in \mathbb{Z}\setminus\{0\}$ and $x > 0$ we have

$$g(1/2,x) = -\sqrt{\frac{\pi}{x}}\operatorname{Im} e^{2xi}\Gamma(1/2,2xi) + \frac{\pi\sin 2x}{\sqrt{x}}, \tag{D.72}$$

$$g(1/2,n\pi) = -\frac{1}{\sqrt{|n|}}\operatorname{Im} e^{i\pi\vartheta(-n)/2}\Gamma(1/2,2\pi ni) + \vartheta(-n)\sqrt{\frac{\pi}{|n|}}, \tag{D.73}$$

$$g(1/2,0) = 2\sqrt{\pi}. \tag{D.74}$$

For the case $c = 0$ we have

$$g(0,x) = -\log x - \operatorname{Re} e^{2xi}\Gamma(0,2xi) + \pi \sin 2x, \tag{D.75}$$

$$g(0,n\pi) = -\log|n\pi| - \operatorname{Re}\Gamma(0,\pi n i), \tag{D.76}$$

$$g(0,0) = \gamma + \log 2. \tag{D.77}$$

Finally for $c = -1/2$, we have

$$g(-1/2,x) = \frac{\sqrt{\pi x}}{2} \operatorname{Im} e^{2xi}\Gamma(-1/2,2xi) + \pi\sqrt{x}\sin 2x, \tag{D.78}$$

$$g(-1/2,n\pi) = -\frac{\pi\sqrt{|n|}}{2} \operatorname{Re} e^{i\pi\vartheta(n)^2}\Gamma(-1/2,2n\pi i) - \vartheta(-n)\pi^{3/2}\sqrt{|n|}, \tag{D.79}$$

$$g(-1/2,0) = -\frac{\sqrt{\pi}}{2}. \tag{D.80}$$

At this stage we can construct the closed form of H as

$$H(c,\alpha;x) = \frac{2\sin^2 x(f(c,\alpha) - f(c,x)) - \sin 2x(g(c,n\pi) - g(c,x))}{2(x-\alpha)} \tag{D.81}$$

$$= H_0(c,\alpha;x) + \frac{g(c,x)\sin 2x - 2f(c,x)\sin^2 x}{2(x-\alpha)} \tag{D.82}$$

where

$$H_0(c,\alpha;x) = \frac{2f(c,\alpha)\sin^2 x - g(c,\alpha)\sin 2x}{2(x-\alpha)}. \tag{D.83}$$

At this stage we split up f and g into

$$f(c,x) = f_\Gamma(c,x) + \frac{\pi\cos 2x}{x^c}, \qquad g(c,x) = g_\Gamma(c,x) + \frac{\pi\sin 2x}{x^c}, \tag{D.84}$$

$$f_\Gamma(c,x) = \operatorname{Re} W(c,x), \qquad g_\Gamma(c,x) = \operatorname{Im} W(c,x), \tag{D.85}$$

$$W(c,x) = \begin{cases} -i\frac{\Gamma(1-c)}{|x|^c} e^{-i\theta(x)\pi c} e^{2xi}\Gamma(c,2xi), & c \neq 0 \\ -i(e^{2xi}\Gamma(0,2xi) + \log x), & c = 0 \end{cases}. \tag{D.86}$$

Combining all of this, we have

$$\int_0^\infty \frac{dx}{x^b}\frac{H(c,\alpha;x)}{x-\beta} = -f(c,\alpha)G(b,\alpha;\beta) + \frac{1}{2}g(c,\alpha)F(b,\alpha;\beta) - \pi G(b+c,\alpha;\beta)$$
$$+ \frac{1}{2}\operatorname{PV}\int_0^\infty \frac{dx}{x^b}\frac{g_\Gamma(c,x)\sin 2x - 2f_\Gamma(c,x)\sin^2 x}{(x-\alpha)(x-\beta)}. \tag{D.87}$$

Recalling the earlier discussion, we require (D.87) with

$$(b,c) \in \{(\pm 1/2, 0), (0,0), (-1/2, 1/2)\}. \tag{D.88}$$

By direct calculation,

$$g_\Gamma(c,x)\sin 2x - 2f_\Gamma(c,x)\sin^2 x = \mathrm{Re}(e^{-2xi}-1)W(c,x) \tag{D.89}$$

and consequently all remaining integrals are of the form

$$K(b,c;\alpha,\beta) = \frac{1}{2}\,\mathrm{Re}\,\mathrm{PV}\int_0^\infty \frac{dx}{x^b}\frac{(e^{-2xi}-1)W(c,x)}{(x-\alpha)(x-\beta)} \tag{D.90}$$

with $\alpha = m\pi, \beta = n\pi$, $b, c \in \{\pm 1/2, 0\}$.

D.2 CALCULATION OF THE K INTEGRALS

To begin calculating the K integrals, we first make a rotation in the complex plane to the negative imaginary axis, giving

$$\begin{aligned} K(b,c;\alpha,\beta) &= \frac{1}{2}\,\mathrm{PV}\int_0^\infty \frac{dx}{x^b}\frac{(e^{-2xi}-1)W(c,x)}{(x-\alpha)(x-\beta)} \qquad \text{(D.91)}\\ &= \frac{1}{2}\,\mathrm{Im}\,e^{i\pi b/2}\int_0^\infty \frac{dx}{x^b}\frac{(1-e^{-2x})W(c,-ix)}{(x-i\alpha)(x-i\beta)} \\ &\quad + \chi_{\pi\mathbb{Z}^+}(\alpha)\chi_{\pi\mathbb{Z}^+}(\beta)\delta_{\alpha\beta}\frac{\pi}{2}\,\mathrm{Im}\,\mathrm{Res}_{z=\alpha}\frac{(e^{-2zi}-1)W(c,z)}{z^b(z-\alpha)^2} \\ &\quad + \frac{\pi}{2}\chi_{\mathbb{R}^+\setminus\pi\mathbb{Z}^+}(\alpha)\,\mathrm{Im}\,\mathrm{Res}_{z=\alpha}\frac{(e^{-2zi}-1)W(c,z)}{z^b(z-\alpha)(z-\beta)} \\ &\quad + \frac{\pi}{2}\chi_{\mathbb{R}^+\setminus\pi\mathbb{Z}^+}(\beta)\,\mathrm{Im}\,\mathrm{Res}_{z=\beta}\frac{(e^{-2zi}-1)W(c,z)}{z^b(z-\alpha)(z-\beta)} \\ &\quad + \frac{\pi}{2}\chi_{\mathbb{R}^+\setminus\pi\mathbb{Z}^+}(\alpha)\chi_{\mathbb{R}^+\setminus\pi\mathbb{Z}^+}(\beta)\delta_{\alpha\beta}\,\mathrm{Im}\,\mathrm{Res}_{z=\alpha}\,\frac{(e^{-2zi}-1)W(c,z)}{z^b(z-\alpha)^2}, \qquad \text{(D.92)} \end{aligned}$$

where χ_S is the indicator function for the set $S \subseteq \mathbb{R}$ and the residue terms are the result of closing the principal value integral. Evaluating the residues, we find

$$\begin{aligned} K(b,c;\alpha,\beta) = \frac{1}{2}\operatorname{Im} e^{i\pi b/2}\int_0^\infty \frac{dx}{x^b}\frac{(1-e^{-2x})W(c,-ix)}{(x-im\pi)(x-in\pi)} \\ - \delta_{\alpha\beta}\chi_{\pi\mathbb{Z}^+}(\alpha)\chi_{\pi\mathbb{Z}^+}(\beta)\frac{\pi}{\alpha^b}\operatorname{Re} W(c,\alpha) \qquad \text{(D.93)} \\ + \frac{\pi}{2}\chi_{\mathbb{R}^+\setminus\pi\mathbb{Z}^+}(\alpha)\operatorname{Im}\frac{(e^{-2\alpha i}-1)W(c,\alpha)}{\alpha^b(\alpha-\beta)} \\ - \frac{\pi}{2}\chi_{\mathbb{R}^+\setminus\pi\mathbb{Z}^+}(\beta)\operatorname{Im}\frac{(e^{-2\beta i}-1)W(c,\beta)}{\beta^b(\alpha-\beta)} \\ + \frac{\pi}{2}\chi_{\mathbb{R}^+\setminus\pi\mathbb{Z}^+}(\alpha)\chi_{\mathbb{R}^+\setminus\pi\mathbb{Z}^+}(\beta)\delta_{\alpha\beta}\operatorname{Im}\left[\frac{(b-(b+2\alpha i)e^{-2\alpha i})W(c,\alpha)}{\alpha^{b+1}}\right. \\ \left. + \frac{e^{-2xi}-1}{x^b}\frac{\partial}{\partial x}\right|_{x=\alpha} W(c,x)\Bigg] \qquad \text{(D.94)} \\ = \tilde{K}(b,c;\alpha,\beta) + R(b,c;\alpha,\beta) \qquad \text{(D.95)} \end{aligned}$$

where

$$\begin{aligned} \tilde{K}(b,c;\alpha,\beta) = \frac{1}{2}\operatorname{Im} e^{i\pi b/2}\int_0^\infty \frac{dx}{x^b}\frac{(1-e^{-2x})W(c,-ix)}{(x-i\alpha)(x-i\beta)} \\ - \delta_{\alpha\beta}\chi_{\pi\mathbb{Z}^+}(\alpha)\chi_{\pi\mathbb{Z}^+}(\beta)\frac{\pi}{\alpha^b}\operatorname{Re} W(c,\alpha) \qquad \text{(D.96)} \end{aligned}$$

and $R(b,c;\alpha,\beta)$ contains the remaining residue terms that arise when α,β are not integer multiples of π. Specifically, for the specific case $\alpha = m\pi, \beta = n\pi$ with $n,m \in \mathbb{Z}$ we find the drastically simplified

$$\begin{aligned} K(b,c;m\pi,n\pi) = \tilde{K}(b,c;m\pi,n\pi) \qquad \text{(D.97)} \\ = \frac{1}{2}\operatorname{Im} e^{i\pi b/2}\int_0^\infty \frac{dx}{x^b}\frac{(1-e^{-2x})W(c,-ix)}{(x-im\pi)(x-in\pi)} \\ - \delta_{mn}\vartheta(n)\frac{\pi}{(n\pi)^b}\operatorname{Re} W(c,n\pi). \qquad \text{(D.98)} \end{aligned}$$

For the remainder, we will calculate the integral $\tilde{K}$ with the understanding that if ever a non-integer multiple of π may be required, then K is obtained by adding on the relevant residue contributions R.

For the case $c = 1/2$, this gives

$$K(b,1/2;m\pi,n\pi) = -\frac{\sqrt{\pi}}{2}\operatorname{Im} e^{i\pi(2b+1)/4}\int_0^\infty \frac{dx}{x^{b+1/2}}\frac{(1-e^{-2x})e^{2x}\Gamma(1/2,2x)}{(x-im\pi)(x-in\pi)} + \delta_{mn}\vartheta(n)\frac{\pi^{3/2}\operatorname{Re}\Gamma(1/2,2\pi ni)}{(n\pi)^{b+1/2}} \tag{D.99}$$

$$= -\frac{\sqrt{\pi}}{2}\operatorname{Im} e^{i\pi(2b+1)/4}\int_0^\infty \frac{dx}{x^{b+1/2}}\frac{(1-e^{-2x})U(1,3/2,2x)}{(x-im\pi)(x-in\pi)} + \delta_{mn}\vartheta(n)\frac{\pi^{3/2}\operatorname{Re}\Gamma(1/2,2\pi ni)}{(n\pi)^{b+1/2}} \tag{D.100}$$

where $U(a,b,z)$ is the confluent hypergeometric function related to the incomplete Γ-function by DLMF 8.5.3 as

$$\Gamma(c,z) = z^c e^{-z} U(1,1+c,z). \tag{D.101}$$

In particular for $b = -1/2$ we have

$$K(-1/2,1/2,m\pi,n\pi) = -\frac{\sqrt{\pi}}{2}\operatorname{Im}\int_0^\infty dx\,\frac{(1-e^{-2x})e^{2x}\Gamma(1/2,2x)}{(x-im\pi)(x-in\pi)} + \delta_{mn}\vartheta(n)\pi^{3/2}\operatorname{Re}\Gamma(1/2,2n\pi i). \tag{D.102}$$

For $m = n$, the integral may be split into partial fractions, to give

$$K(-1/2,1/2;m\pi,n\pi) = \frac{L(m\pi)-L(n\pi)}{2\sqrt{\pi}(m-n)}, \qquad (m\neq n) \tag{D.103}$$

where

$$L(\alpha) = \operatorname{Re}\int_0^\infty dx\,\frac{(1-e^{-2x})e^{2x}\Gamma(1/2,2x)}{x-\alpha i} = \int_0^\infty dx\,\frac{(1-e^{-2y})xe^{2x}\Gamma(1/2,2x)}{x^2+\alpha^2}. \tag{D.104}$$

For $m \in \mathbb{Z}$, we have

$$K(-1/2,1/2;m\pi,m\pi) = -m\pi^{3/2}\int_0^\infty dx\,\frac{(1-e^{-2x})xe^{2x}\Gamma(1/2,2x)}{(x^2+m^2\pi^2)^2} + \vartheta(m)\pi^{3/2}\operatorname{Re}\Gamma(1/2,2m\pi i). \tag{D.105}$$

For $\alpha \in \mathbb{R}\setminus\{0\}$, using integration by parts, we find

$$\int_0^\infty dx\,\frac{x\Gamma(1/2,2x)}{(x^2+\alpha^2)^2} = \frac{\sqrt{\pi}}{2\alpha^2} - \frac{1}{\sqrt{2}}\int_0^\infty \frac{dx}{x^{1/2}}\frac{e^{-2x}}{x^2+\alpha^2} \tag{D.106}$$

$$= \frac{\sqrt{\pi}}{2\alpha^2} + \frac{\sqrt{\pi}}{\sqrt{2}|\alpha|}\operatorname{Im}(i\alpha)^{-1/2}e^{2\alpha i}\Gamma(1/2,2|\alpha|i) \tag{D.107}$$

$$= \sqrt{\frac{\pi}{2}}\left(\frac{1}{\alpha^2} + \frac{1}{|\alpha|^{3/2}}\operatorname{Im} e^{-i\pi/4}e^{2|\alpha|i}\Gamma(1/2,2|\alpha|i)\right). \tag{D.108}$$

Combining (D.105) with equations (D.106) to (D.108), we find

$$K(-1/2,1/2;n\pi,n\pi) = -n\pi^{3/2}L_2(n\pi) + \frac{1}{2n} + \frac{\varepsilon(n)}{2}\sqrt{\frac{\pi}{|n|}}\,\mathrm{Im}(1-i)\Gamma(1/2,2|n|\pi i) + \vartheta(n)\pi^{3/2}\,\mathrm{Re}\,\Gamma(1/2,2n\pi i) \tag{D.109}$$

where

$$L_2(\alpha) = \int_0^\infty dx\,\frac{xe^{2x}\Gamma(1/2,2x)}{(x^2+\alpha^2)^2} = \sqrt{\pi}\int_0^\infty dx\,\frac{x\mathrm{erfc}(\sqrt{2x})}{(x^2+\alpha^2)^2} \tag{D.110}$$

for $\alpha \in \mathbb{R}^+\setminus\{0\}$. To calculate the $c=0$ case of K we find

$$K(b,0;m\pi,n\pi) = -\frac{1}{2}\,\mathrm{Re}\,e^{i\pi b/2}\int_0^\infty \frac{dx}{x^b}\frac{(1-e^{-2x})(e^{2x}\Gamma(0,2x)+\log x - i\pi/2)}{(x-im\pi)(x-in\pi)} - \delta_{mn}\vartheta(n)\frac{\pi}{(n\pi)^b}\,\mathrm{Im}\,\Gamma(0,2n\pi i) \tag{D.111}$$

for $(m,n)\neq(0,0)$. To calculate this, for $m,n\neq 0$, let

$$K(b,0;n\pi,m\pi) = K_0^{(1)}(b;n\pi,m\pi) + K_0^{(2)}(b;n\pi,m\pi) - \delta_{nm}\vartheta(m)\frac{\pi}{(m\pi)^b}\,\mathrm{Im}\,\Gamma(0,2m\pi i) \tag{D.112}$$

where for $\alpha,\beta\neq 0$

$$K_0^{(1)}(b;\alpha,\beta) = -\frac{1}{2}\,\mathrm{Re}\,e^{i\pi b/2}\int_0^\infty \frac{dx}{x^b}\frac{\log x - i\pi/2(1-e^{-2x})}{(x-i\alpha)(x-i\beta)}, \tag{D.113}$$

$$K_0^{(2)}(b;\alpha,\beta) = \mathrm{Im}\,e^{i\pi b/2}\frac{P(b,\beta)-P(b,\alpha)}{2(\alpha-\beta)}, \tag{D.114}$$

$$\tag{D.115}$$

and for $\alpha\in\mathbb{R}$ we have

$$K_0^{(2)}(b;\alpha,\alpha) = \mathrm{Im}\,e^{i\pi b/2}P'(b;\alpha) \tag{D.116}$$

where

$$P(b,\alpha) = \int_0^\infty \frac{dx}{x^b}\frac{(1-e^{-2x})e^{2x}\Gamma(0,2x) - e^{-2x}\log x}{x-i\alpha}, \tag{D.117}$$

$$P'(b,\alpha) = \int_0^\infty \frac{dx}{x^b}\frac{(1-e^{-2x})e^{2x}\Gamma(0,2x) - e^{-2x}\log x}{(x-i\alpha)^2}. \tag{D.118}$$

The integral $K_0^{(1)}$ can be calculated as

$$K_0^{(1)}(b;\alpha,\beta) = -\frac{1}{2}\operatorname{Re} e^{i\pi b/2}\int_0^\infty \frac{dx}{x^b}\frac{\log x - i\pi/2(1-e^{-2x})}{(x-i\alpha)(x-i\beta)} \tag{D.119}$$

$$= -\frac{1}{2}\operatorname{Re} e^{i\pi b/2}\int_0^\infty \frac{dx}{x^b}\frac{\log x}{(x-i\alpha)(x-i\beta)} - \frac{\pi}{4}\operatorname{Im} e^{i\pi b/2}\int_0^\infty \frac{dx}{x^b}\frac{1-e^{-2x}}{(x-i\alpha)(x-i\beta)} \tag{D.120}$$

$$\begin{aligned} = &-\frac{1}{2}\operatorname{Re} e^{i\pi b/2}\int_0^\infty \frac{dx}{x^b}\frac{\log x}{(x-i\alpha)(x-i\beta)} \\ &- (1-\delta_{\alpha\beta})\operatorname{Re}\frac{\pi\Gamma(1-b)}{4(\beta-\alpha)}\Big[e^{i\pi b\vartheta(\alpha)}|\alpha|^{-b}\tilde{\Gamma}(b,-2\alpha i) \\ &-e^{i\pi b\vartheta(\beta)}|\beta|^{-b}\tilde{\Gamma}(b,-2\beta i)\Big] \\ &+ \delta_{\alpha\beta}\frac{\pi\Gamma(1-b)}{4|\alpha|^{b+1}}\operatorname{Im} e^{i\pi(b+\varepsilon(\alpha)(b+1))/2}\Big[e^{-i\pi b\varepsilon(\alpha)/2}|2\alpha|^b \\ &-\Gamma(b+1)+(b+2\alpha i)e^{-2\alpha i}\Gamma(b,-2\alpha i)\Big] \end{aligned} \tag{D.121}$$

for $b \neq 0$ using the integral identities (D.3) and (D.5). Similarly, for $b = 0$ we find

$$\begin{aligned} K_0^{(1)}(0;\alpha,\beta) = &-\frac{1}{2}\operatorname{Re}\int_0^\infty dx\frac{\log x}{(x-i\alpha)(x-i\beta)} \\ &+ \delta_{\alpha\beta}\frac{\pi}{4(\beta-\alpha)}\operatorname{Re}\Big[\log|\alpha| + e^{-2\alpha i}\Gamma(0,-2\alpha i) \\ &-\log|\beta| - e^{-2\beta i}\Gamma(0,-2\beta i) - i\pi(\varepsilon(\alpha)-\varepsilon(\beta))/2\Big] \\ &-\delta_{\alpha\beta}\frac{\pi}{2}\operatorname{Im} e^{-2\alpha i}\Gamma(0,-2\alpha i) \end{aligned} \tag{D.122}$$

As for the logarithmic integral, this can by

$$\int_0^\infty \frac{dx}{x^b}\frac{\log x}{(x-i\alpha)(x-i\beta)} = -\frac{d}{db}\int_0^\infty \frac{dx}{x^b}\frac{1}{(x-i\alpha)(x-i\beta)} \tag{D.123}$$

$$= \frac{i\pi e^{-i\pi b/2}}{\sin(\pi b)(\beta-\alpha)}\left[q(b;\beta)-q(b;\alpha)\right] \tag{D.124}$$

where for $b \neq 0$,

$$q(b;x) = e^{i\pi b\vartheta(x)}|x|^{-b}\left(\pi\cot(\pi b) + \log|x| - \frac{i\pi\varepsilon(x)}{2}\right) b \neq 0. \tag{D.125}$$

To calculate the case $b = 0$, we take the limit of (D.123) as $b \to 0$ and first notice that

$$\lim_{b\to 0}[q(b,\alpha)-q(b,\beta)] = 0. \tag{D.126}$$

By LĤopital's rule, and with the assistance of Maple, we find

$$\int_0^\infty dx\,\frac{\log x}{(x-i\alpha)(x-i\beta)} = \frac{i}{2\pi(\beta-\alpha)}\left[q(0,\alpha)-q(0,\beta)\right] \tag{D.127}$$

where

$$q(0;x) = \left(\log|x| - \frac{i\pi\varepsilon(x)}{2}\right)^2. \tag{D.128}$$

For the case where $\alpha=\beta$, we can take the limit of (D.5) as $\beta\to\alpha$ to find that for $a\in\mathbb{C}\setminus\mathbb{R}^-$ and then subsequently differentiate in b to find

$$\int_0^\infty \frac{dx}{x^b}\frac{1}{(x+a)^2} = \frac{\pi c}{\sin\pi c}a^{-c-1}, \tag{D.129}$$

$$\int_0^\infty \frac{dx}{x^b}\frac{\log x}{(x+a)^2} = \pi a^{-b-1}\frac{-1+\pi b\cot(\pi b)+b\log a}{\sin\pi b}, \tag{D.130}$$

$$\int_0^\infty dx\frac{\log x}{(x+a)^2} = \frac{\log a}{a} \tag{D.131}$$

where on the final line we have taken the limit as $b\to 0$. For the specific case that $a=-i\alpha$ with $\alpha\in\mathbb{R}$, we obtain

$$\int_0^\infty \frac{dx}{x^b}\frac{1}{(x-i\alpha)^2} = \frac{e^{i\pi\varepsilon(\alpha)(1+b)/2}b}{|\alpha|^{b+1}\sin\pi b}, \tag{D.132}$$

$$\int_0^\infty \frac{dx}{x^b}\frac{\log x}{(x-i\alpha)^2} = \pi e^{i\pi\varepsilon(\alpha)(b+1)/2}\frac{-1+\pi b\cot(\pi b)+b\log|\alpha|-i\pi b\varepsilon(\alpha)/2}{|\alpha|^{b+1}\sin\pi b} \tag{D.133}$$

and specifically

$$\int_0^\infty dx\,x^{\pm1/2}\frac{\log x}{(x-n\pi i)^2} = \frac{\pi^{\pm1/2}e^{i\pi\varepsilon(n)(1\mp1/2)/2}}{|n|^{1\mp1/2}}\left(\pm1+\frac{1}{2}\log|n\pi|-\frac{i\pi\varepsilon(n)}{4}\right). \tag{D.134}$$

Combining (D.119)-(D.121) with (D.133), we find

$$\begin{aligned}
K_0^{(1)}(b;\alpha,\beta) = {}& (1-\delta_{\alpha\beta})\frac{\pi}{2\sin\pi b}\,\mathrm{Im}\,\frac{q(b,\beta)-q(b,\alpha)}{\beta-\alpha}\\
&-\delta_{\alpha\beta}\pi e^{i\pi(\vartheta(\alpha)(b+1)-1/2)}\frac{-1+\pi b\cot(\pi b)+b\log|\alpha|-i\pi b\varepsilon(\alpha)/2}{2|\alpha|^{b+1}\sin\pi b}\\
&-(1-\delta_{\alpha\beta})\frac{\pi\Gamma(1-b)}{4(\beta-\alpha)}\,\mathrm{Re}\left[e^{i\pi b\vartheta(\alpha)}|\alpha|^{-b}\tilde\Gamma(b,-2\alpha i)\right.\\
&\left.-e^{i\pi b\vartheta(\beta)}|\beta|^{-b}\tilde\Gamma(b,-2\beta i)\right]\\
&+\delta_{\alpha\beta}\frac{\pi\Gamma(1-b)}{4|\alpha|^{b+1}}\,\mathrm{Im}\,e^{i\pi(b+\varepsilon(\alpha)(b+1))/2}\left[e^{-i\pi b\varepsilon(\alpha)/2}|2\alpha|^b\right.\\
&\left.-\Gamma(b+1)+(b+2\alpha i)e^{-2\alpha i}\Gamma(b,-2\alpha i)\right],
\end{aligned} \tag{D.135}$$

for $b \neq 0$ and

$$\begin{aligned} K_0^{(1)}(0;\alpha,\beta) = \frac{1-\delta_{\alpha\beta}}{4\pi}\frac{q(0,\alpha)-q(0,\beta)}{\beta-\alpha} - \delta_{\alpha\beta}\frac{\pi\varepsilon(\alpha)}{4\alpha} \\ + (1-\delta_{\alpha\beta})\frac{\pi}{4(\beta-\alpha)}\operatorname{Re}\Big[\log|\alpha| + e^{-2\alpha i}\Gamma(0,-2\alpha i) \\ - \log|\beta| - e^{-2\beta i}\Gamma(0,-2\beta i) - i\pi(\varepsilon(\alpha)-\varepsilon(\beta))/2\Big] \\ - \delta_{\alpha\beta}\frac{\pi}{2}\operatorname{Im} e^{-2\alpha i}\Gamma(0,-2\alpha i) \end{aligned} \tag{D.136}$$

Consequently, we find

$$\begin{aligned} K(b,0;m\pi,n\pi) = \frac{1-\delta_{nm}}{2\sin\pi b}\operatorname{Im}\frac{q(b,m\pi)-q(b,n\pi)}{m-n} \\ - \delta_{mn}e^{i\pi(\vartheta(n)(b+1)-1/2)}\frac{-1+\pi b\cot\pi b + b\log|n\pi| - i\pi b\varepsilon(n)/2}{2\pi^b|n|^{b+1}\sin\pi b} \\ - \frac{(1-\delta_{mn})\Gamma(1-b)}{\pi^b(m-n)}\operatorname{Re}\Big[e^{i\pi b\vartheta(n)}|n|^{-b}\tilde{\Gamma}(b,-2n\pi i) \\ -e^{i\pi b\vartheta(m)}|m|^{-b}\tilde{\Gamma}(b,-2m\pi i)\Big] \\ + \frac{\delta_{mn}\Gamma(1-b)}{4\pi^b|n|^{b+1}}\operatorname{Im} e^{i\pi(b+\varepsilon(n)(b+1))/2}\Big[e^{-i\pi b\varepsilon(n)}|2n\pi|^b - \Gamma(b+1) \\ +(b+2n\pi i)\Gamma(b,-2n\pi i)] \\ + (1-\delta_{nm})\operatorname{Im} e^{i\pi b/2}\frac{P(b;m\pi)-P(b;n\pi)}{2\pi(n-m)} \\ + \delta_{nm}\operatorname{Im} e^{i\pi b/2}P'(b;n\pi) \end{aligned} \tag{D.137}$$

for $b \neq 0$. In the case $b = 0$, we have

$$\begin{aligned} K(0,0;m\pi,n\pi) = \frac{1-\delta_{nm}}{4\pi^2}\frac{q(0,n\pi)-q(0,m\pi)}{m-n} - \frac{\delta_{nm}\varepsilon(n)}{4n} \\ + \frac{1-\delta_{nm}}{4(m-n)}\operatorname{Re}\left[\log|n\pi| + \Gamma(0,-2n\pi i)\right. \\ \left. - \log|m\pi| - \Gamma(0,-2m\pi i) - i\pi(\varepsilon(n)-\varepsilon(m))/2\right] \\ - \frac{\pi\delta_{nm}}{2}\operatorname{Im}\Gamma(0,-2n\pi i) \end{aligned} \tag{D.138}$$

for $m, n \in \mathbb{Z} \setminus \{0\}$.

The final breakdown we require is for the integral

$$J(b;\alpha) = \int_0^\infty \frac{dx}{x^{b+1}}\frac{H(0,0;x)}{x-\alpha} \tag{D.139}$$

required for the first row elements of $C^{\pm}$ and D as

$$C^{\pm}_{m0} = J(\mp 1/2; m\pi), \qquad D_{m0} = J(0; m\pi). \tag{D.140}$$

To do this, we return to the decomposition of H, first given in (D.81), which we recall as

$$H(0,0;x) = -\frac{\sin 2x(g(0,x) - g(0,0)) - 2\sin^2 x(f(0,x) - f(0,0))}{2x}. \tag{D.141}$$

Making use of the closed expressions for $f(0,0)$, $f(0,x)$, $g(0,0)$ and $g(0,x)$ summarised in (D.42), (D.40), (D.77) and (D.75) respectively, we can write

$$f(0,x) - f(0,0) = \operatorname{Re}\left[-ie^{2xi}\Gamma(0,2xi) - \frac{\pi}{2} + \pi e^{2xi}\right], \tag{D.142}$$

$$g(0,x) - g(0,0) = \operatorname{Im}\left[-i\left(e^{2xi}\Gamma(0,2xi) + \log 2x + \gamma\right) + \pi e^{2xi}\right]. \tag{D.143}$$

This inspires writing $H(0,0;x)$ as

$$H(0,0;x) = \frac{\operatorname{Im}\left(\tilde{W}(x) + \pi e^{2xi}\right)\sin 2x - 2\operatorname{Re}\left(\tilde{W}(x) + \pi\left(e^{2xi} - 1/2\right)\right)\sin^2 x}{2x}. \tag{D.144}$$

where for $x > 0$,

$$\tilde{W}(x) = -i\left(e^{2xi}\Gamma(0,2xi) + \gamma + \log 2x\right). \tag{D.145}$$

By a simple calculation, one can rewrite (D.144) in terms of complex exponentials as

$$H(0,0;x) = -\frac{1}{2}\frac{\operatorname{Re}\left(1 - e^{-2xi}\right)\tilde{W}(x)}{x} - \frac{2\pi\sin^2 x}{x} \tag{D.146}$$

where we have made use once again of the identity $\sin^2 2x - 2\cos 2x \sin^2 x = 2\sin^2 x$. Combining (D.139) with (D.144) and recalling the definition of the G integral, we find

$$J(b;\alpha) = -2\pi G(b,0;\alpha) + \tilde{J}(b;\alpha) \tag{D.147}$$

where for $|b| < 1$ and $\alpha \in \mathbb{R}$.

$$\tilde{J}(b;\alpha) = -\frac{1}{2}\operatorname{PV}\operatorname{Re}\int_0^\infty \frac{dx}{x^{b+1}}\frac{-i\left(e^{2xi}\Gamma(0,2xi) + \log 2x + \gamma\right)}{x - \alpha}. \tag{D.148}$$

Making use of lemma D.1.1, we find $\tilde{J}(b;\alpha)$ can be written as

$$\tilde{J}(b;\alpha) = -\frac{1}{2}\operatorname{Re} e^{i\pi b/2}\operatorname{PV}\int_0^\infty \frac{dx}{x^{b+1}}\frac{1 - e^{-2x}}{x - \alpha i}\left(e^{2x}\Gamma(0,2x) + \gamma + \log(2x)\right). \tag{D.149}$$

D.3 THE L AND L_2 INTEGRALS

The L and L_2 integrals are required for the calculation of the integrals

$$K(-1/2, 1/2; n\pi, m\pi)$$

with $n, m \in \mathbb{Z}$. Recall that the L integral is given by

$$L(\alpha) = \mathrm{Re} \int_0^\infty dx \frac{(1 - e^{-2x})e^{2x}\Gamma(1/2, 2x)}{x - \alpha i}. \tag{D.150}$$

We can write the L integral as

$$L(\alpha) = \sqrt{\pi}\,\mathrm{Re} \int_0^\infty dy \frac{(1 - e^{-2y})e^{2y}\mathrm{erfc}(\sqrt{2y})}{y - i\alpha} \tag{D.151}$$

$$= 2\sqrt{\pi}\,\mathrm{Re} \int_0^\infty dz \frac{z(1 - e^{z^2})\mathrm{erfc}(z)}{z^2 - 2\alpha i}, \tag{D.152}$$

after making the transformation $y = z^2$. For $\alpha \neq 0$, we split up the integral into $L(\alpha) = L_0(\alpha) + L_1(\alpha)$ where

$$L_0(\alpha) = 2\sqrt{\pi}\,\mathrm{Re} \int_0^\infty dz \frac{ze^{z^2}\mathrm{erfc}(z)}{z^2 - 2\alpha i}, \tag{D.153}$$

$$L_1(\alpha) = -2\sqrt{\pi}\,\mathrm{Re} \int_0^\infty dz \frac{z\mathrm{erfc}(z)}{z^2 - 2\alpha i}. \tag{D.154}$$

To calculate the L_0 integral, we first note that the integrand has poles at $z = \pm\sqrt{2\alpha}e^{i\pi/4}$. Then rotating the integral contour to the negative imaginary axis we find

$$L_0(\alpha) = 2\sqrt{\pi}\,\mathrm{Re} \int_0^\infty dz \frac{ze^{-z^2}\mathrm{erfc}(z)}{z^2 + 2\alpha i}. \tag{D.155}$$

Similarly, one can rotate the contour to the positive imaginary axis by picking up a contribution from a residue as

$$L_0(\alpha) = 2\sqrt{\pi}\,\mathrm{Re}\left(\int_0^\infty dz \frac{ze^{-z^2}\mathrm{erfc}(iz)}{z^2 + 2\alpha i} + 2\pi i\,\mathrm{Res}_{z=\sqrt{2\alpha}e^{i\pi/4}} \frac{ze^{z^2}\mathrm{erfc}(iz)}{z^2 - 2\alpha i}\right) \tag{D.156}$$

$$= 2\sqrt{\pi}\,\mathrm{Re} \int_0^\infty dz \frac{ze^{-z^2}\mathrm{erfc}(iz)}{z^2 + 2\alpha i} - 2\pi^{3/2}\,\mathrm{Im}\, e^{2\alpha i}\mathrm{erfc}(\sqrt{\alpha}(1 + i)). \tag{D.157}$$

Summing (D.155) and (D.157), and then making use of the identity $\mathrm{erfc}(w) + \mathrm{erfc}(-w) = 2$ we find

$$L_0(\alpha) = \sqrt{\pi}\,\mathrm{Re} \int_0^\infty dz \frac{2ze^{-z^2}}{z^2 + 2\alpha i} - \pi^{3/2}\,\mathrm{Im}\, e^{2\alpha i}\mathrm{erfc}(\sqrt{\alpha}(1 + i)). \tag{D.158}$$

Once again making the change of variables $y = z^2$ and using (D.1), we find

$$L_0(\alpha) = \sqrt{\pi}\,\mathrm{Re}\int_0^\infty dy \frac{e^{-y}}{y+2\alpha i} - \pi^{3/2}\,\mathrm{Im}\, e^{2\alpha i}\mathrm{erfc}(\sqrt{\alpha}(1+i)) \tag{D.159}$$

$$= \sqrt{\pi}\,\mathrm{Re}\, e^{2\alpha i}\Gamma(0,2\alpha i) - \pi^{3/2}\,\mathrm{Im}\, e^{2\alpha i}\mathrm{erfc}(\sqrt{\alpha}(1+i)). \tag{D.160}$$

Now moving onto the L_1 integral, we first note that the derivative of the erfc function is $\mathrm{erfc}'(z) = -2e^{-z^2}/\sqrt{\pi}$ and so using integration by parts we find

$$L_1(\alpha) = -2\sqrt{\pi}\int_0^\infty dz \frac{z\ \mathrm{erfc}(z)}{z^2-2\alpha i} \tag{D.161}$$

$$= -\sqrt{\pi}\,\mathrm{Re}\left[\mathrm{erfc}(z)\log\left(z^2-2\alpha i\right)\right]_0^\infty - 2\,\mathrm{Re}\int_0^\infty dz\, e^{-z^2}\log\left(z^2-2\alpha i\right) \tag{D.162}$$

$$= \sqrt{\pi}\,\mathrm{Re}\left(\log(-2\alpha i) + \gamma + 2\log 2 + i\pi\mathrm{erfc}(\sqrt{\alpha}(1+i))\right.$$
$$\left. -4\alpha i\ {}_2F_2(1,1;3/2,2;-2\alpha i)\right) \tag{D.163}$$

$$= \sqrt{\pi}\,(\log 2\alpha + \gamma + 2\log 2) - \pi^{3/2}\,\mathrm{Im}\,\mathrm{erfc}(\sqrt{\alpha}(1+i))$$
$$+ 4\sqrt{\pi}\alpha\,\mathrm{Im}\ {}_2F_2(1,1;3/2,2;-2\alpha i) \tag{D.164}$$

where to go from (D.162) to (D.163), we made use of Maple 2024. Now combining (D.160) and (D.164) we find

$$L(\alpha) = \sqrt{\pi}\,\mathrm{Re}\, e^{2\alpha i}\Gamma(0,2\alpha i) - \pi^{3/2}\,\mathrm{Im}(e^{2\alpha i}+1)\mathrm{erfc}(\sqrt{\alpha}(1+i))$$
$$+ \sqrt{\pi}\,(\log 2\alpha + \gamma + 2\log 2) + 4\sqrt{\pi}\alpha\,\mathrm{Im}\ {}_2F_2(1,1;3/2,2;-2\alpha i). \tag{D.165}$$

To find the value of $L(0)$, we take the limit of (D.165). Using Maple, we can calculate the series of $L(\alpha)$ about $\alpha = 0$ where we find

$$L(\alpha) = 2\sqrt{\pi}\log 2 + \mathcal{O}(\alpha) \tag{D.166}$$

and hence

$$L(0) = 2\sqrt{\pi}\log 2. \tag{D.167}$$

We now move onto the L_2 integral, which is given by

$$L_2(\alpha) = \int_0^\infty dy \frac{y e^{2y}\Gamma(1/2,2y)}{(y^2+\alpha^2)^2} \tag{D.168}$$

for $\alpha \in \mathbb{R}\setminus\{0\}$. Since L_2 is an even function of a real variable, without loss of generality we assume $\alpha > 0$. Making use of equation 8.4.6 of the DLMF [24], we find

$$L_2(\alpha) = \sqrt{\pi}\int_0^\infty dy \frac{y\ \mathrm{erfc}(\sqrt{2y})}{(y^2+\alpha^2)} \tag{D.169}$$

$$= -\frac{\sqrt{\pi}}{2\alpha}\,\mathrm{Im}\int_0^\infty dy \frac{y\ \mathrm{erfc}(\sqrt{2y})}{(y+i\alpha)^2}. \tag{D.170}$$

Making the change of variables $z = \sqrt{2y}$, we now find

$$L_2(\alpha) = -\frac{2\sqrt{\pi}}{\alpha} \operatorname{Im} \int_0^\infty dz \frac{z e^{z^2} \operatorname{erfc}(z)}{(z - 2\alpha i)^2}. \tag{D.171}$$

The integrand is meromorphic with poles at $z = \pm\sqrt{2\alpha} e^{-i\pi/4}$ with decay like $|z|^{-4}/\sqrt{\pi}$ as $z \to \infty$ for $|\arg z| < 3\pi/4$. As such, we can rotate the integral to both the positive and negative imginary axes independently as

$$L_2(\alpha) = \frac{2\sqrt{\pi}}{\alpha} \operatorname{Im} \int_0^\infty dz \frac{z e^{-z^2} \operatorname{erfc}(iz)}{(z^2 - 2\alpha i)^2} \tag{D.172}$$

$$= \frac{2\sqrt{\pi}}{\alpha} \operatorname{Im} \left[\int_0^\infty dz \frac{z e^{-z^2} \operatorname{erfc}(-iz)}{(z^2 - 2\alpha i)^2} + 2\pi i R(\alpha) \right] \tag{D.173}$$

where

$$R(\alpha) = \operatorname{Res}_{z=\sqrt{2\alpha}e^{-i\pi/4}} \frac{z e^{z^2} \operatorname{erfc}(z)}{(z^2 + 2\alpha i)^2} \tag{D.174}$$

$$= \frac{1}{2} \left(e^{-2\alpha i} \operatorname{erfc}(\sqrt{\alpha}(1 - i) - \frac{1 + i}{\sqrt{\pi\alpha}} \right) \tag{D.175}$$

where the residue has been computed using Cauchy's formula for higher order residues. Next, by noting that the complementary error function admits the identity

$$\operatorname{erfc}(z) + \operatorname{erfc}(-z) = 2 \tag{D.176}$$

for all $z \in \mathbb{C}$, we find

$$L_2(\alpha) = \frac{2\sqrt{\pi}}{\alpha} \operatorname{Im} \left[\int_0^\infty dz \frac{z e^{-z^2}}{(z^2 - 2\alpha i)^2} + \pi i R(\alpha) \right]. \tag{D.177}$$

The integral here can be calculated by making the change of variables $x = z^2$ and writing

$$\int_0^\infty dz \frac{z e^{-z}}{(z^2 - 2\alpha i)} = \int_0^\infty dx \frac{e^{-x}}{(x - 2\alpha i)^2} \tag{D.178}$$

$$= -\frac{1}{2\alpha i} \frac{d}{d\alpha} \int_0^\infty dx \frac{e^{-x}}{(x - 2\alpha i)} \tag{D.179}$$

$$= -e^{2\alpha i} \Gamma(0, -2\alpha i) + \frac{e^{4\alpha i}}{2\alpha i}. \tag{D.180}$$

Combining (D.175), (D.177) and (D.180) and simplifying, we find

$$L_2(\alpha) = -\frac{\sqrt{\pi}}{\alpha} \operatorname{Im} e^{2\alpha i} \Gamma(0, -2\alpha i) + \frac{\pi^{3/2}}{\alpha} \operatorname{Re} e^{-2\alpha i} \operatorname{erfc}(\sqrt{\alpha}(1 - i)) - \frac{\sqrt{\pi}}{2\alpha^2} \cos 4\alpha - \frac{\pi}{2\alpha^{3/2}}.$$

This concludes any work done prior to the start of my PhD.

D.4 THE $\tilde{J}$ INTEGRAL

The first row elements of $C^{\pm}$ and D are calculated using the $\tilde{J}$ integral given by

$$\tilde{J}(b;\alpha) = -\frac{1}{2}\operatorname{Re} e^{i\pi b/2}\operatorname{PV}\int_0^\infty \frac{dx}{x^{b+1}}\frac{1-e^{-2x}}{x-\alpha i}\left(e^{2x}\Gamma(0,2x)+\gamma+\log 2x\right) \tag{D.181}$$

for $|b|<1$ and $\alpha\in\mathbb{R}$. In particular, the closed forms we require are given in the below table.

b	α
$\{0,\pm 1/2\}$	0
$\{0,1/2\}$	$\pi\mathbb{N}$

To begin calculating, we will write

$$\tilde{J}(b;\alpha) = -\frac{1}{2}\operatorname{Re} e^{i\pi b/2}\left[I_\Gamma(b;\alpha)+\gamma I_1(b;\alpha)+I_{\log}(b;\alpha)\right] \tag{D.182}$$

where for $\beta>0$

$$I_\Gamma(b;\alpha) = \int_0^\infty \frac{dx}{x^{b+1}}\frac{1-e^{-2x}}{x-i\alpha}e^{2x}\Gamma(0,2x), \tag{D.183}$$

$$I_1(b;\alpha) = \int_0^\infty \frac{dx}{x^{b+1}}\frac{1-e^{-2x}}{x-i\alpha}, \tag{D.184}$$

$$I_{\log}(b;\alpha) = \int_0^\infty \frac{dx}{x^{b+1}}\frac{1-e^{-2x}}{x-i\alpha}\log 2x. \tag{D.185}$$

To begin calculating I_Γ, we make use of the following representation of the incomplete gamma function,

$$e^z\Gamma(a,z) = \int_0^\infty dt\,(z+t)^{a-1}e^{-t}, \tag{D.186}$$

which holds for $z\in\mathbb{C}\setminus\mathbb{R}^-$ and $\operatorname{Re} a>0$. The integral representation follows from the simple change of variable $t\mapsto z+t$ of equation 8.2.2 of the DLMF [24]. Substituting (D.186) into (D.183) and rearranging the order of integration, we obtain

$$I_\Gamma(b;\alpha) = \frac{1}{2}\int_0^\infty dt\,e^{-t}\int_0^\infty \frac{dx}{x^{b+1}}\frac{1-e^{-2x}}{(x+t/2)(x-\alpha i)} \tag{D.187}$$

$$= \Gamma(-b)\int_0^\infty dt\,\frac{e^{-t}}{t+2\alpha i}\left[(-\alpha i)^{-b-1}\tilde{\Gamma}(b+1,-2\alpha i)-2^{b+1}t^{-b-1}\tilde{\Gamma}(b+1,t)\right] \tag{D.188}$$

$$= \Gamma(-b)(-\alpha i)^{-b-1}e^{2\alpha i}\Gamma(0,2\alpha i)\tilde{\Gamma}(b+1,-2\alpha i) - 2^{b+1}\Gamma(-b)\int_0^\infty \frac{dt}{t^{b+1}}\frac{e^{-t}\tilde{\Gamma}(b+1,t)}{t+2\alpha i} \tag{D.189}$$

where the second line has been computed using (D.3) and (D.5), and the third line by a single application of (D.186). Note that the new integral in (D.189) converges for any $b \in (-1, \infty) \setminus \{0\}$. We will write

$$\tilde{I}_\Gamma(b;\alpha) = \int_0^\infty \frac{dt}{t^{b+1}} \frac{e^{-t}\left(\Gamma(b+1) - e^t \Gamma(b+1,t)\right)}{t+2\alpha i}, \tag{D.190}$$

whose closed form and limiting values will be of particular interest here-on in this subsection. Immediately, since $\tilde{\Gamma}(1;t) = \Gamma(1) - e^t\Gamma(1,t) = 0$ we have

$$\tilde{I}_\Gamma(0;\alpha) = 0 \tag{D.191}$$

for all $\alpha \in \mathbb{C} \setminus \mathbb{R}^-$.

For $b \neq 0$, it will be convenient to decompose $\tilde{I}_\Gamma$ according to

$$\tilde{I}_\Gamma(b;\alpha) = \lim_{c\to b} \tilde{I}_\Gamma^{(1)}(b,c;\alpha) - \tilde{I}_\Gamma^{(2)}(b,c;\alpha), \tag{D.192}$$

with

$$\tilde{I}_\Gamma^{(1)}(b,c;\alpha) := \Gamma(c+1)\int_0^\infty \frac{dt}{t^{b+1}} \frac{e^{-t}}{t+2\alpha i} \tag{D.193}$$

$$= \Gamma(c+1)\Gamma(-b)(2\alpha i)^{-b-1} e^{2\alpha i}\Gamma(b+1,2\alpha i) \tag{D.194}$$

and

$$\tilde{I}_\Gamma^{(2)}(b,c;\alpha) := \int_0^\infty \frac{dt}{t^{b+1}} \frac{\Gamma(c+1,t)}{t+2\alpha i} \tag{D.195}$$

$$= \frac{1}{c-b}\left[\frac{\pi(c-b)e^{i\pi(c+1)}(2\alpha i)^{-b-1}}{\sin\pi(c-b)}\left(\Gamma(c+1) - \Gamma(c+1,-2\alpha i)\right)\right.$$
$$\left. - \frac{\Gamma(c-b+1)}{b+1}{}_2F_2(1,b+1;2+b,1+b-c;2\alpha i)\right]$$
$$- \frac{\pi^2 c(2\alpha i)^{-b-1}}{\Gamma(1-c)\sin\pi b\sin\pi c} \tag{D.196}$$

can be computed in closed form by Maple 2024 and simplified using an identity of the incomplete gamma function. Before computing a closed form for $\lim_{c\to b}\tilde{I}^{(2)}(b,c;\alpha)$, we note that

$$\lim_{c\to b}\tilde{I}_\Gamma^{(1)}(b,c;\alpha) = -\frac{\pi(2\alpha i)^{-b-1}e^{2\alpha i}\Gamma(b+1,2\alpha i)}{\sin\pi b}. \tag{D.197}$$

We now turn to computing the limit of (D.196) as $b \to c$, we first note that

$$\lim_{c\to b}\frac{\Gamma(c-b+1){}_2F_2(1,1+b;2+b,1+b-c;2\alpha i)}{1+b}$$
$$= (-2\alpha i)^{-c-1}\left(\Gamma(c+1) - \Gamma(c+1,-2\alpha i)\right) \tag{D.198}$$
$$= \lim_{c\to b}\frac{\pi(c-b)(2\alpha i)^{-1-b}e^{i\pi(c+1)}}{\sin\pi(c-b)}\left(\Gamma(c+1,-2\alpha i) - \Gamma(c+1)\right). \tag{D.199}$$

As such, by L'Ĥopital's rule, we find that

$$\begin{aligned}\lim_{c\to b}\tilde{I}^{(2)}_{\Gamma}(b,c;\alpha) &= \lim_{c\to b}\frac{d}{dc}\left[\frac{\pi(c-b)(2\alpha i)^{-b-1}e^{i\pi(c+1)}(\Gamma(c+1)-\Gamma(c+1,-2\alpha i)}{\sin\pi(c-b)}\right.\\ &\quad\left.-\frac{\Gamma(c-b+1)_2F_2(1,b+1;b+2,1+b-c;2\alpha i)}{b+1}\right]\\ &\quad-\frac{\pi^2 b(2\alpha i)^{-b-1}}{\Gamma(1-b)\sin^2\pi b} \qquad \text{(D.200)}\\ &= \lim_{c\to b}\left[\frac{\pi z^{-b-1}e^{i\pi(c+1)}(\Gamma(c+1)-\Gamma(c+1,-z))}{\sin\pi(c-b)}\right.\\ &\quad\left.-\frac{\pi^2(c-b)}{\sin\pi(c-b)}\frac{z^{-b-1}e^{i\pi(c+1)}(\Gamma(c+1)-\Gamma(c+1,-z)\cos\pi(c-b)}{\sin\pi(c-b)}\right] \qquad \text{(D.201)}\\ &\quad+i\pi z^{-b-1}e^{i\pi(b+1)}(\Gamma(b+1)-\Gamma(b+1,-z))\\ &\quad+\frac{\gamma}{b+1}{}_2F_2(1,1+b;2+b,1;z)\\ &\quad+z^{-b-1}e^{i\pi(b+1)}\left(\psi(b+1)\Gamma(b+1)-\Gamma(b+1,-z)\log(-z)\right.\\ &\quad\left.-G^{3,0}_{2,3}\left(\begin{smallmatrix}1,1\\0,0,1+b\end{smallmatrix}\middle|-z\right)\right)+\frac{1}{b+1}\frac{d}{dc}\bigg|_{c=1}{}_2F_2(1,1+b;2+b;c;z)\\ &\quad-\frac{\pi^2 b z^{-b-1}}{\Gamma(1-b)\sin^2\pi b} \qquad \text{(D.202)}\end{aligned}$$

where $z=2\alpha i$ and $G^{3,0}_{2,3}$ is a Meijer G function. The limit in (D.201) vanishes and so we find

$$\begin{aligned}\lim_{c\to b}\tilde{I}^{(2)}_{\Gamma}(b,c;\alpha) &= i\pi(2\alpha i)^{-b-1}e^{i\pi(b+1)}(\Gamma(b+1)-\Gamma(b+1,-2\alpha i))\\ &\quad+\frac{\gamma}{b+1}{}_2F_2(1,1+b;2+b,1;2\alpha i)\\ &\quad+(2\alpha i)^{-b-1}e^{i\pi(b+1)}\left(\psi(b+1)\Gamma(b+1)\right.\\ &\quad\left.-\Gamma(b+1,-2\alpha i)\log(-2\alpha i)-G^{3,0}_{2,3}\left(\begin{smallmatrix}1,1\\0,0,1+b\end{smallmatrix}\middle|-2\alpha i\right)\right)\\ &\quad+\frac{1}{b+1}\frac{d}{dc}\bigg|_{c=1}{}_2F_2(1,1+b;2+b,c;2\alpha i)-\frac{\pi^2 b(2\alpha i)^{-b-1}}{\Gamma(1-b)\sin^2\pi b}.\end{aligned} \qquad \text{(D.203)}$$

Substituting the closed forms (D.197) and (D.203) into (D.192), we find

$$\begin{aligned}
\tilde{I}_\Gamma(b;\alpha) = &-\frac{\pi(2\alpha i)^{-b-1}e^{2\alpha i}\Gamma(b+1,2\alpha i)}{\sin\pi b} + \frac{\pi^2 b(2\alpha i)^{-b-1}}{\Gamma(1-b)\sin^2\pi b} \\
&- i\pi(2\alpha i)^{-b-1}e^{i\pi(b+1)}(\Gamma(b+1)-\Gamma(b+1,-2\alpha i)) \\
&- \frac{\gamma}{b+1}{}_2F_2(1,1+b;2+b;1;2\alpha i) \\
&- (2\alpha i)^{-b-1}e^{i\pi(b+1)}\left(\psi(b+1)\Gamma(b+1)\right. \\
&\left.-\Gamma(b+1,-2\alpha i)\log(-2\alpha i) - G^{3,0}_{2,3}\left(\begin{smallmatrix}1,1\\0,0,1+b\end{smallmatrix}\middle|-2\alpha i\right)\right) \\
&- \frac{1}{b+1}\frac{d}{dc}\bigg|_{c=1}{}_2F_2(1,1+b;2+b,c;2\alpha i) \qquad \text{(D.204)} \\
= &-\frac{\pi e^{-i\pi\varepsilon(\alpha)(b+1)/2}e^{2\alpha i}\Gamma(b+1,2\alpha i)}{|2\alpha|^{b+1}\sin\pi b} + \frac{\pi^2 b e^{-i\pi\varepsilon(\alpha)(b+1)/2}}{|2\alpha|^{b+1}\sin^2\pi b} \\
&- i\pi e^{i\pi(3/2-\vartheta(\alpha))(b+1)}|2\alpha|^{-b-1}\left(\Gamma(b+1)-\Gamma(b+1,-2\alpha i)\right) \\
&- \frac{\gamma}{b+1}{}_2F_2(1,1+b;2,2+b;2\alpha i) \\
&- e^{i\pi(3/2-\vartheta(\alpha))(b+1)}|2\alpha|^{-b-1}\left[\psi(b+1)\Gamma(b+1)\right. \\
&- \Gamma(b+1,-2\alpha i)(\log|2\alpha| - i\pi\varepsilon(\alpha)/2) \\
&\left.+\frac{\pi b(\log|2\alpha| - i\pi\varepsilon(\alpha)/2 + \pi\cot\pi b - \psi(-b))}{\Gamma(1-b)\sin\pi b}\right] \\
&+ \frac{e^{i\pi(b+1)}}{b+1}{}_2F_2(b+1,b+1;b+2,b+2;-2\alpha i) \\
&- \frac{1}{b+1}\frac{d}{dc}\bigg|_{c=1}{}_2F_2(1,1+b;c,2+b;2\alpha i) \qquad \text{(D.205)}
\end{aligned}$$

It is of note that the derivative of the hypergeometric function with respect to a parameter has not been simplified. In principle it is possible to write this as a Kampé de Férier function; a double sum generalisation of the hypergeometric function. However, for the purposes of numerical calculation we make use of a trick implemented in the python library Arb, [44].

Let f be some function for which we would like to compute the derivative. Suppose the computational implementation of f allows for its argument to be a formal power series in some variable λ, in which case $f(a_0+a_1\lambda+\cdots) = b_0+b_1\lambda+\cdots$ as a formal power series. It follows by simple Taylor expansion, that if $f \in \mathcal{C}^2(\mathbb{R})$, we have $f(a+\lambda) = f(a) + \lambda f'(a) + \mathcal{O}(\lambda^2)$, where $\mathcal{O}(\lambda^2)$ simply indicates the next

leading order coefficient. It hence follows that

$$\left.\frac{d}{dc}\right|_{c=1} {}_2F_2(1,1+b;2+b,c;2\alpha i) = {}_2F_2(1,1+b;2+b,1+\lambda;2\alpha i)[\lambda^1] \tag{D.206}$$

where for $k \in \mathbb{N} \cup \{0\}$ and $P \in \mathbb{C}[\![\lambda]\!]$, $P[\lambda^k]$ indicates the coefficient of λ^k in the formal power series.

With $\tilde{I}_\Gamma$ calculated for all b of interest, we return to (D.189) to find

$$\begin{aligned}
I_\Gamma(b;\alpha) &= -\Gamma(1-b)(-i\alpha)^{-b-1}e^{2\alpha i}\Gamma(0,2\alpha i)\frac{\tilde{\Gamma}(b+1,-2\alpha i)}{b} \\
&\quad + \frac{2^{b+1}\Gamma(1-b)}{b}\tilde{I}_\Gamma(b;\alpha) \qquad \text{(D.207)} \\
&= -\frac{e^{i\pi\varepsilon(\alpha)(b+1)/2}\Gamma(1-b)e^{2\alpha i}\Gamma(0,2\alpha i)\tilde{\Gamma}(b+1,-2\alpha i)}{b|\alpha|^{b+1}} \\
&\quad - e^{-i\pi\varepsilon(\alpha)(b+1)/2}\frac{\pi\Gamma(1-b)}{b|\alpha|^{b+1}\sin\pi b}\left(e^{2\alpha i}\Gamma(b+1,2\alpha i) - \frac{\pi b}{\sin\pi b}\right) \\
&\quad - e^{i\pi(3/2-\vartheta(\alpha))(b+1)}\frac{i\pi\Gamma(1-b)}{b|\alpha|^{b+1}}\left(\Gamma(b+1)-\Gamma(b+1,-2\alpha i)\right) \\
&\quad - \frac{\gamma 2^{b+1}\Gamma(1-b)}{b(b+1)}{}_2F_2(1,b+1;2,b+2;2\alpha i) \\
&\quad - \frac{e^{i\pi(3/2-\vartheta(\alpha))(b+1)}\Gamma(1-b)}{b|\alpha|^{b+1}}\left[\psi(b+1)\Gamma(b+1)-\Gamma(b+1,-2\alpha i)(\log|2\alpha|\right. \\
&\quad \left. -i\pi\varepsilon(\alpha)/2) + \frac{\pi b(\log|2\alpha| - i\pi\varepsilon(\alpha)/2 + \pi\cot\pi b - \psi(-b))}{\Gamma(1-b)\sin\pi b}\right] \qquad \text{(D.208)} \\
&\quad + \frac{2^{b+1}\Gamma(1-b)}{b(b+1)}\left(e^{i\pi(b+1)}{}_2F_2(b+1,b+1;b+2,b+2;-2\alpha i)\right. \\
&\quad \left. -\left.\frac{d}{dc}\right|_{c=1}{}_2F_2(1,b+1;c,b+2;2\alpha i)\right). \qquad \text{(D.209)}
\end{aligned}$$

In particular, we require this for $b \in \{0, \pm 1/2\}$. The values $b = \pm 1/2$ are a simple case of substitution and simplification and we find

For the case $b = 0$, by taking the limit and applying LĤopital's rule we find

$$I_\Gamma(0;\alpha) = \frac{1}{\alpha i}\left.\frac{d}{db}\right|_{b=1}\tilde{\Gamma}(b,-2\alpha i) + 2\left.\frac{d}{db}\right|_{b=0}\tilde{I}_\Gamma(b;\alpha). \tag{D.210}$$

The first term in (D.210) admits a closed form from the fact that

$$\left.\frac{d}{db}\right|_{b=1}\tilde{\Gamma}(b,-2\alpha i) = \left.\frac{d}{db}\right|_{b=1}\left(\Gamma(b)-e^{-2\alpha i}\Gamma(b,-2\alpha i)\right) \tag{D.211}$$

$$= \Gamma'(1)-e^{-2\alpha i}\Gamma'(1,-2\alpha i) \tag{D.212}$$

where we make use of the notation $\Gamma'(b,z)=\partial_b\Gamma(b,z)$. Using the standard integral representation of the incomplete Gamma function we find

$$\left.\frac{d}{db}\right|_{b=1}\tilde{\Gamma}(b,-2\alpha i) = -\gamma - e^{-2\alpha i}\int_{-2\alpha i}^{\infty} dt\, e^{-t}\log t \tag{D.213}$$

$$= -\gamma - \log(-2\alpha i) - e^{-2\alpha i}\Gamma(0,-2\alpha i) \tag{D.214}$$

after an application of integration by parts. It remains then to calculate

$$d/db|_{b=0}\tilde{I}_\Gamma(b;\alpha).$$

Using Maple 2024, the series expansion of $\tilde{I}_\Gamma(b,z)$ centered at $b=0$ can be computed and the b^1 coefficient coincides with the derivative required. Hence we find

$$\begin{aligned}\left.\frac{d}{db}\right|_{b=0}\tilde{I}_\Gamma(b;\alpha) = {}& \gamma\frac{e^{2\alpha i}-1}{2\alpha i} + e^{2\alpha i}{}_2F_2(1,1;2,2;-2\alpha i) + {}_2F_2(1,1;2,2;2\alpha i)\\ & + \gamma\,{}_2F_2(1,1;2,1;2\alpha i) - \gamma\left.\frac{d}{db}\right|_{b=0}{}_2F_2(1,1+b;2+b,1;2\alpha i)\\ & + \left.\frac{d}{dc}\right|_{c=1}{}_2F_2(1,1;2,c;2\alpha i)\\ & - \left.\frac{d}{dc}\right|_{c=1}\left.\frac{d}{db}\right|_{b=0}{}_2F_2(1,1+b;2+b,c;2\alpha i).\end{aligned} \tag{D.215}$$

At this stage, we will derive a simpler form of the derivative $d/db|_{b=0}{}_2F_2(1,1+b;2+b,1;2\alpha i)$. By equation 16.2.1 of the DLMF [24], we have

$${}_2F_2(1,1+b;c,2+b;z) = \sum_{n=0}^{\infty}\frac{(1)_n(1+b)_n}{(c)_n(2+b)_n}\frac{z^n}{n!} = \Gamma(c)(b+1)\sum_{n=0}^{\infty}\frac{\Gamma(n+1)}{\Gamma(n+c)(b+1)}\frac{z^n}{n!} \tag{D.216}$$

and hence

$$\frac{d}{db}{}_2F_2(1,b+1;c,b+2;z) = \Gamma(c)\sum_{n=0}^{\infty}\frac{\Gamma(n+1)\Gamma(n+b+1)}{\Gamma(n+c)\Gamma(n+b+2)}\frac{z^n}{n!} - \Gamma(c)(b+1)\sum_{n=0}^{\infty}\frac{\Gamma(n+1)\Gamma(n+b+1)^2}{(n+c)\Gamma(n+b+2)^2}\frac{z^n}{n!} \tag{D.217}$$

$$= \frac{\Gamma(b+1)}{\Gamma(b+2)}\sum_{n=0}^{\infty}\frac{(1)_n(b+1)_n}{(c)_n(b+2)_n}\frac{z^n}{n!} - \frac{\Gamma(b+1)}{\Gamma(b+2)}\sum_{n=0}^{\infty}\frac{(1)_n(b+1)_n^2}{(c)_n(b+2)_n^2}\frac{z^n}{n!} \tag{D.218}$$

$$= \frac{1}{b+1}\left[{}_2F_2(1,b+1;c,b+2;z) - {}_3F_3(1,b+1,b+1;c,b+2,b+2;z)\right]. \tag{D.219}$$

In particular for $c=1$ we have

$$\frac{d}{db}{}_2F_2(1,b+1;1,b+2;z) = \frac{1}{b+1}\left[{}_1F_1(b+1;b+2;z) - {}_2F_2(b+1,b+2;b+2,b+2;z)\right]. \tag{D.220}$$

Returning to (D.215), after simplification we find

$$\left.\frac{d}{db}\right|_{b=0}\tilde{I}_\Gamma(b;\alpha) = \gamma\frac{e^{2\alpha i}-1}{2\alpha i} - e^{2\alpha i}{}_2F_2(1,1;2,2;-2\alpha i) + {}_2F_2(1,1;2,2;2\alpha i) + \gamma\,{}_2F_2(1,1;2,2;2\alpha i) + \left.\frac{d}{dc}\right|_{c=1}{}_3F_3(1,1,1;c,2,2;2\alpha i). \tag{D.221}$$

Now we can calculate $I_\Gamma(0;\alpha)$ according to (D.210) and after simplification we find

$$I_\Gamma(0;\alpha) = -\frac{1}{\alpha i}\left[\gamma(2-e^{2\alpha i}) + \log(-2\alpha i) + e^{-2\alpha i}\Gamma(0,-2\alpha i)\right] - 2e^{2\alpha i}{}_2F_2(1,1;2,2;-2\alpha i) + 2(1+\gamma){}_2F_2(1,1;2,2;2\alpha i) + 2\left.\frac{d}{dc}\right|_{c=1}{}_3F_3(1,1,1;c,2,2;2\alpha i). \tag{D.222}$$

The integral I_1 can be calculated immediately using (D.3) and (D.5) and we find

$$I_1(b;\alpha) = \lim_{\beta\to 0}\frac{\Gamma(1-b)}{\beta+i\alpha}\left[(-i\alpha)^{-b}\tilde{\Gamma}(b,-2\alpha i) - \beta^{-b}\tilde{\Gamma}(b,2\beta)\right] \tag{D.223}$$

$$= \frac{2^b\Gamma(1-b)}{i\alpha}\left[(-2\alpha i)^{-b}\tilde{\Gamma}(b,-2\alpha i) - \frac{1}{b}\right]. \tag{D.224}$$

By the recurrence relations of the gamma and incomplete gamma functions we find

$$I_1(b;\alpha) = \frac{2^b\Gamma(1-b)}{i\alpha}(-2\alpha i)^{-b}\frac{\Gamma(b+1)-e^{-2\alpha i}\Gamma(b+1,-2\alpha i)}{b} \tag{D.225}$$

$$= \Gamma(1-b)e^{i\pi(b+1)\varepsilon(\alpha)/2}\frac{e^{-2\alpha i}\Gamma(b+1,-2\alpha i)-\Gamma(b+1)}{b|\alpha|^{b+1}} \tag{D.226}$$

from which it is straightforward to see that

$$I_1(0;\alpha) = -\frac{1}{i\alpha}\left(\gamma + e^{-2\alpha i}\Gamma'(1,-2\alpha i)\right). \tag{D.227}$$

By simple inspection, we obtain

$$I_{\log}(b;\alpha) = -2^b\frac{\partial}{\partial b}2^{-b}I_1(b;\alpha). \tag{D.228}$$

This derivative is simple enough to compute and we find

$$I_{\log}(b,\alpha) = \psi(1-b)I_1(b,\alpha) - \frac{\Gamma(1-b)}{i\alpha}\frac{\partial}{\partial b}\left[(-2\alpha i)^{-b}\frac{\Gamma(b+1)-e^{-2\alpha i}\Gamma(b+1,-2\alpha i))}{b}\right] \tag{D.229}$$

$$= \psi(1-b)I_1(b,\alpha) - \frac{\Gamma(1-b)}{i\alpha}\left[(-\alpha i)^{-b}\left(-\log(-2\alpha i)\tilde{\Gamma}(b,-2\alpha i) + \tilde{\Gamma}'(b,-2\alpha i)\right) + \frac{2^b}{b^2}\right] \tag{D.230}$$

$$= -\frac{e^{i\pi(b+1)\varepsilon(\alpha)/2}\Gamma'(1-b)\tilde{\Gamma}(b,-2\alpha i)}{b|\alpha|^{b+1}} + \frac{e^{i\pi(b+1)\varepsilon(\alpha)/2}\Gamma(1-b)}{|\alpha|^{b+1}}\left[\tilde{\Gamma}'(b,-2\alpha i) - \tilde{\Gamma}(b,-2\alpha i)\left(\log|2\alpha| - \frac{i\pi\varepsilon(\alpha)}{2}\right)\right] + \frac{i2^b\Gamma(1-b)}{\alpha b^2} \tag{D.231}$$

We now proceed with calculating $I_{\log}(0,\alpha)$ by taking the limit of (D.229) as $b \to 0$. It follows that

$$I_{\log}(0,\alpha) = -\gamma I_1(0,\alpha) - \frac{1}{2\alpha i}\left[2\gamma\log(-2\alpha i) + \gamma^2 + \frac{\pi^2}{6} + 2e^{-2\alpha i}\log(-2\alpha i)\Gamma'(1,-2\alpha i) - e^{-2\alpha i}\Gamma''(1,-2\alpha i)\right] \tag{D.232}$$

$$= \frac{1}{2\alpha i}\left[\gamma^2 - \frac{\pi^2}{6} + i\pi\gamma\varepsilon(\alpha) - 2\gamma\log|2\alpha| + 2\left(\gamma - \log|2\alpha| + \frac{i\pi\varepsilon(\alpha)}{2}\right)e^{-2\alpha i}\Gamma'(1,-2\alpha i) + e^{-2\alpha i}\Gamma''(1,-2\alpha i)\right]. \tag{D.233}$$

Hence, we find

$$\begin{aligned}\tilde{J}(b,\alpha) = \operatorname{Im}\frac{e^{i\pi\vartheta(\alpha)(b+1)}\Gamma(1-b)e^{2\alpha i}\Gamma(0,2\alpha i)\tilde{\Gamma}(b+1,-2\alpha i)}{2b|\alpha|^{b+1}}\\ -\operatorname{Im}e^{-i\pi(\vartheta(\alpha)(b+1)+b)}\frac{\pi\Gamma(1-b)}{2b|\alpha|^{b+1}\sin\pi b}\left(e^{2\alpha i}\Gamma(b+1,2\alpha i)-\frac{\pi b}{\sin\pi b}\right)\\ +\operatorname{Re}e^{i\pi(2b-\vartheta(\alpha)(b+1))}\frac{\pi\Gamma(1-b)}{2b|\alpha|^{b+1}}\left(\Gamma(b+1)-\Gamma(b+1,-2\alpha i)\right)\\ +\operatorname{Re}e^{i\pi b/2}\frac{\gamma 2^b\Gamma(1-b)}{b(b+1)}{}_2F_2(1,b+1;2,b+2;2\alpha i)\\ +\operatorname{Im}\frac{e^{i\pi(2b-\vartheta(\alpha)(b+1))}\Gamma(1-b)}{2b|\alpha|^{b+1}}\left[\psi(b+1)\Gamma(b+1)-\Gamma(b+1,-2\alpha i)(\log|2\alpha|\right.\\ \left.-i\pi\varepsilon(\alpha)/2)+\frac{\pi b(\log|2\alpha|-i\pi\varepsilon(\alpha)/2+\pi\cot\pi b-\psi(-b))}{\Gamma(1-b)\sin\pi b}\right]\end{aligned}\tag{D.234}$$

and similarly

$$\begin{aligned}\tilde{J}(0,\alpha) = \frac{\gamma}{2\alpha}(2-\cos 2\alpha)-\frac{\pi\varepsilon(\alpha)}{4\alpha}+\frac{1}{2\alpha}\operatorname{Im}e^{-2\alpha i}\Gamma(0,-2\alpha i)\\ +\operatorname{Re}e^{2\alpha i}{}_2F_2(1,1;2,2;-2\alpha i)-(1+\gamma)\operatorname{Re}{}_2F_2(1,1;2,2;2\alpha i)\\ -\operatorname{Re}\frac{d}{dc}\bigg|_{c=1}{}_3F_3(1,1,1;c,2,2;2\alpha i)+\frac{\gamma}{2\alpha}\operatorname{Im}e^{-2\alpha i}\Gamma'(1,-2\alpha i)\\ -\frac{\pi\gamma\varepsilon(\alpha)}{2\alpha}-\frac{1}{2\alpha}\operatorname{Im}\left(\gamma-\log|2\alpha|+\frac{i\pi\varepsilon(\alpha)}{2}\right)e^{-2\alpha i}\Gamma'(1,-2\alpha i)\\ -\frac{1}{4\alpha}\operatorname{Im}e^{-2\alpha i}\Gamma''(1,-2\alpha i)\end{aligned}\tag{D.235}$$

D.5 THE P INTEGRALS

The remaining integrals to calculate are the P integrals, given in (D.117), with closed forms

$$P(b,\alpha)=\int_0^\infty\frac{dx}{x^b}\frac{(1-e^{-2x})e^{2x}\Gamma(0,2x)-e^{-2x}\log x}{x-i\alpha},\tag{D.236}$$

$$P'(b,\alpha)=\int_0^\infty\frac{dx}{x^b}\frac{(1-e^{-2x})e^{2x}\Gamma(0,2x)-e^{-2x}\log x}{(x-i\alpha)^2}.\tag{D.237}$$

Immediately we notice that

$$P'(b,\alpha)=-i\frac{\partial}{\partial\alpha}P(b,\alpha)\tag{D.238}$$

and by inspection we note that

$$P(b,\alpha) = P_1(b,\alpha) + P_2(b,\alpha) \tag{D.239}$$

$$P_1(b,\alpha) = \int_0^\infty \frac{(1-e^{-2x})e^{2x}\Gamma(0,2x)}{x-i\alpha}, \tag{D.240}$$

$$P_2(b,\alpha) = \frac{\partial}{\partial b}\int_0^\infty \frac{dx}{x^b}\frac{e^{-2x}}{x-i\alpha} \tag{D.241}$$

for $b \in (-1,1)$ and $\alpha \in \mathbb{R}$. From (D.1), for $b \neq 0$, we obtain

$$P_2(b,\alpha) = \frac{\partial}{\partial b}(-i\alpha)^{-b}e^{-2\alpha i}\Gamma(1-b)\Gamma(b,-2\alpha i) \tag{D.242}$$

$$= (-i\alpha)^{-b}e^{-2\alpha i}\Gamma(1-b)\left[\Gamma'(b,-2\alpha i) - \Gamma(b,-2\alpha i)(\log(-i\alpha)+\psi(1-b))\right]. \tag{D.243}$$

We proceed with the calculation of P_1 with a similar method to the calculation of I_Γ. First, we use the integral representation of $\Gamma(0,2x)$ in (D.186) to find

$$P_1(b,\alpha) = \frac{1}{2}\int_0^\infty ds\, e^{-s}\int_0^\infty \frac{dx}{x^b}\frac{1-e^{-2x}}{(x+s/2)(x-i\alpha)}. \tag{D.244}$$

We define the inner integrand of (D.244) as $I(b,\alpha;s)$ which by (D.3) admits the closed form

$$I(b,\alpha;s) := \frac{1}{2}\int_0^\infty \frac{dx}{x^b}\frac{1-e^{-2x}}{(x+s/2)(x-i\alpha)} \tag{D.245}$$

$$= \frac{\Gamma(1-b)(-i\alpha)^{-b}}{s+2\alpha i}\tilde{\Gamma}(b,-2\alpha i) - \frac{\Gamma(1-b)\Gamma(b)}{s^b(s+2\alpha i)} + 2^b\Gamma(1-b)\frac{e^s\Gamma(b,s)}{s^b(s+2\alpha i)} \tag{D.246}$$

again for $b \in (-1,1)\setminus\{0\}, \alpha \in \mathbb{R}$ and $s \in \mathbb{R}^+$. It follows that

$$P_1(b,\alpha) = \int_0^\infty ds e^{-s} I(b,\alpha;s) \tag{D.247}$$

and

$$P_1(b,\alpha) = P_{11}(b,\alpha) + P_{12}(b,\alpha) + P_{13}(b,\alpha) \tag{D.248}$$

where for b and α in the same domains as P_1 we have

$$P_{11}(b,\alpha) = (-i\alpha)^{-b}\Gamma(1-b)\tilde{\Gamma}(b,-\alpha i)\int_0^\infty ds\,\frac{e^{-s}}{s+2\alpha i}, \tag{D.249}$$

$$P_{12}(b,\alpha) = -\Gamma(1-b)\Gamma(b)\int_0^\infty \frac{ds}{s^b}\frac{e^{-s}}{s+2\alpha i}, \tag{D.250}$$

$$P_{13}(b,\alpha) = 2^b\Gamma(1-b)\int_0^\infty \frac{ds}{s^b}\frac{\Gamma(b,s)}{s+2\alpha i}. \tag{D.251}$$

By appealing to (D.1), we immediately find

$$P_{11}(b,\alpha) = (-i\alpha)^{-b}\Gamma(1-b)e^{2\alpha i}\Gamma(0,2\alpha i)\tilde{\Gamma}(b,-2\alpha i), \tag{D.252}$$

$$P_{12}(b,\alpha) = -\frac{\pi(i\alpha)^{-b}e^{2\alpha i}\Gamma(0,2\alpha i)\Gamma(1-b)}{\sin\pi b}. \tag{D.253}$$

To calculate the integral of the incomplete gamma function in P_{13}, we first note that the incomplete gamma function can be written as the Meijer G function

$$\Gamma(0,s) = G^{2,0}_{1,2}\left(\begin{smallmatrix}1\\0,0\end{smallmatrix}\middle|\, s\right) \tag{D.254}$$

for $s \in \mathbb{R}^+$. To calculate the integral we make use of the identity

$$\int_0^\infty ds\, s^{c-1}(s+a)^{-\sigma}G^{m,n}_{p,q}\left(\begin{smallmatrix}a_1,\ldots,a_p\\b_1,\ldots,b_q\end{smallmatrix}\middle|\, s\right) = \frac{a^{c-\sigma}}{\Gamma(\sigma)}G^{m+1,n+1}_{p+1,q+1}\left(\begin{smallmatrix}1-c,a_1,\ldots,a_p\\\sigma-c,b_1,\ldots,b_q\end{smallmatrix}\middle|\, a\right) \tag{D.255}$$

taken from page 418 of volume II of [5]. Applying (D.255), we find

$$P_{13}(b,\alpha) = (i\alpha)^{-b}\Gamma(1-b)G^{3,1}_{2,3}\left(\begin{smallmatrix}b,1\\b,b,0\end{smallmatrix}\middle|\, 2\alpha i\right). \tag{D.256}$$

Combining (D.252), (D.253) and (D.256), we arrive at

$$\begin{aligned}P(b,\alpha) = {} & e^{-i\pi b\varepsilon(\alpha)}|\alpha|^{-b}\Gamma(1-b)e^{2\alpha i}\Gamma(0,2\alpha i)\tilde{\Gamma}(b,-2\alpha i)\\ & - \frac{\pi e^{-i\pi b\varepsilon(\alpha)/2}e^{2\alpha i}\Gamma(b,2\alpha i)\Gamma(1-b)}{|\alpha|^b\sin\pi b}\\ & + e^{-i\pi b\varepsilon(\alpha)/2}|\alpha|^{-b}\Gamma(1-b)G^{3,1}_{2,3}\left(\begin{smallmatrix}b,1\\b,b,0\end{smallmatrix}\middle|\, 2\alpha i\right)\\ & + e^{i\pi b\varepsilon(\alpha)/2}|\alpha|^{-b}e^{-2\alpha i}\Gamma(1-b)\left[\Gamma'(b,-2\alpha i)\right.\\ & \left.-\Gamma(b,-2\alpha i)(\log|\alpha| - i\pi\varepsilon(\alpha)/2 + \psi(1-b))\right]\end{aligned} \tag{D.257}$$

for $b \in (-1,1)\setminus\{0\}$ and $\alpha \in \mathbb{R}$.

We also require the limit of $P(b,\alpha)$ as $b \to 0$. Naively taking the limit, we find

$$\begin{aligned}P(0,\alpha) = \lim_{b\to 0}\left((-i\alpha)^{-b}\Gamma(1-b)e^{2\alpha i}\Gamma(0,2\alpha i)\Gamma(b) - \frac{\pi(i\alpha)^{-b}e^{2\alpha i}\Gamma(b,2\alpha i)\Gamma(1-b)}{\sin\pi b}\right)\\ - \Gamma(0,2\alpha i)\Gamma(0,-2\alpha i) + G^{3,1}_{2,3}\left(\begin{smallmatrix}0,1\\0,0,0\end{smallmatrix}\middle|\, 2\alpha i\right)\\ + e^{-2\alpha i}\left[\Gamma'(0,-2\alpha i) - \Gamma(0,-2\alpha i)(\log(-i\alpha)+\gamma)\right].\end{aligned} \tag{D.258}$$

We only require then the calculation of the non-trivial limit of (D.258) which we can simply calculate according to L'Hôpital's rule and hence

$$\begin{aligned}P(0,\alpha) = {} & e^{2\alpha i}\left(-\gamma + i\pi\varepsilon(\alpha)\right)\Gamma(0,2\alpha i) - e^{2\alpha i}\Gamma'(0,2\alpha i)\\ & - \Gamma(0,2\alpha i)\Gamma(0,-2\alpha i) + G^{3,1}_{2,3}\left(\begin{smallmatrix}0,1\\0,0,0\end{smallmatrix}\middle|\, 2\alpha i\right)\\ & + e^{-2\alpha i}\left[\Gamma'(0,-2\alpha i) - \Gamma(0,-2\alpha i)(\log|\alpha| - i\pi\varepsilon(\alpha)/2 + \gamma)\right].\end{aligned} \tag{D.259}$$

At this stage we can calculate $P'(b,\alpha)$ by applying $-i\partial/\partial\alpha$ to (D.257) and (D.259). Hence, we find

$$\begin{aligned}
P'(b,\alpha) = {} & (i\alpha - b)e^{2\alpha i}e^{i\pi(b+1)\varepsilon(\alpha)/2}|\alpha|^{-b-1}\Gamma(1-b)\tilde{\Gamma}(b,-2\alpha i)\Gamma(0,2\alpha i) \\
& + \frac{i2^b\Gamma(1-b)e^{2\alpha i}\Gamma(0,2\alpha i)}{\alpha} \\
& - 2\Gamma(1-b)e^{i\pi b\varepsilon(\alpha)/2}|\alpha|^{-b}\Gamma(b,-2\alpha i)\Gamma(0,2\alpha i) \\
& - e^{i\pi(b+1)\varepsilon(\alpha)/2}|\alpha|^{-b-1}\Gamma(1-b)\tilde{\Gamma}(b,-2\alpha i) \\
& + \frac{\pi\Gamma(1-b)}{\sin\pi b}\left[(b-2\alpha i)e^{2\alpha i}e^{i\pi(b+1)\varepsilon(\alpha)/2}|\alpha|^{-b-1}\Gamma(b,2\alpha i) - \frac{e^{i\pi b}2^b}{i\alpha}\right] \\
& + e^{-i\pi(b+1)\varepsilon(\alpha)/2}|\alpha|^{-b-1}\Gamma(1-b)G^{3,1}_{2,3}\left(\begin{smallmatrix} b,1 \\ b+1,b,0 \end{smallmatrix}\middle|\, 2\alpha i\right) \\
& + (b-2\alpha i)\Gamma(1-b)e^{2\alpha i}e^{i\pi(b+1)\varepsilon(\alpha)/2}|\alpha|^{-b-1}\left[\Gamma(b,-2\alpha i)(\log|\alpha|\right. \\
& \left. -i\pi\varepsilon(\alpha)/2 + \psi(1-b)) - \Gamma'(b,-2\alpha i)\right] \\
& + e^{i\pi(b+1)\varepsilon(\alpha)/2}|\alpha|^{-b-1}e^{2\alpha i}\Gamma(1-b)\left[\frac{\Gamma(b,-2\alpha i)}{i\alpha}\right. \\
& \left. + 2^b e^{-i\pi(b-1)\varepsilon(\alpha)/2}|\alpha|^{b-1}e^{2\alpha i}(\psi(1-b) - \log 2)\right]. \qquad \text{(D.260)}
\end{aligned}$$

for $b \in (-1,1)\setminus\{0\}$ and $\alpha \in \mathbb{R}$. For the case $b = 0$, we find

$$\begin{aligned}
P'(0,\alpha) = {} & 2e^{2\alpha i}\left[(-\gamma + i\pi\varepsilon(\alpha))\Gamma(0,2\alpha i) - \Gamma'(0,2\alpha i)\right] - e^{2\alpha i}\left[(-\gamma + i\pi\varepsilon(\alpha))\frac{e^{-2\alpha i}}{i\alpha}\right. \qquad \text{(D.261)} \\
& \left. - \frac{e^{2\alpha i}(\log|2\alpha| - i\pi\varepsilon(\alpha)/2)}{i\alpha}\right] + \frac{e^{-2\alpha i}\Gamma(0,-2\alpha i) + e^{2\alpha i}\Gamma(0,2\alpha i)}{\alpha i} \\
& + 2\partial G^{3,1}_{2,3}\left(\begin{smallmatrix} 0,1 \\ 1,0,0 \end{smallmatrix}\middle|\, 2\alpha i\right) - 2e^{-2\alpha i}\left[\Gamma'(0,-2\alpha i)\right. \\
& \left. + (\gamma - (\log|\alpha| - i\pi\varepsilon(\alpha)/2)\Gamma(0,-2\alpha i) + \frac{\log 2 + \gamma + \Gamma(0,-2\alpha i)}{i\alpha}\right]. \qquad \text{(D.262)}
\end{aligned}$$

This finally concludes all of the integrals required to calculate the matrix elements of the Bracken-Melloy operator with respect to the sinc-like vectors.

— E —

Simplification of Meijer G functions

Numerical experimentation showed that the main time bottleneck to the computation of the matrix elements of the Bracken–Melloy operator with respect to the dense sequence $(\varphi_n^{\pm})_{n\in\mathbb{N}}$, was the evaluation of Meijer G functions that appear in the evaluation of the C matrix, see equations (4.112) to (4.114). These functions were initially computed using the Python library mpmath [51]. The next section is dedicated to the evaluation of these Meijer G functions in terms of hypergeometric functions that are readily handled in Arb.

Let

$$G_0(b;z) = G_{2,3}^{3,1}\left(\begin{smallmatrix} b,1 \\ b,b,0 \end{smallmatrix}\middle|\, z\right), \qquad G_1(b;z) = G_{2,3}^{3,1}\left(\begin{smallmatrix} b,1 \\ b+1,b,0 \end{smallmatrix}\middle|\, z\right). \tag{E.1}$$

From equation 16.17.1 of the DLMF [24], we find

$$G_{p,q}^{m,n}\left(\begin{smallmatrix} a_1,\dots,a_p \\ b_1,\dots,b_q \end{smallmatrix}\middle|\, z\right) = \frac{1}{2\pi i}\int_L ds \frac{\prod_{l=1}^{m}\Gamma(b_l - s)\prod_{l=1}^{n}\Gamma(1-a_l+s)}{\prod_{l=m}^{q-1}\Gamma(1-b_{l+1}+s)\prod_{l=n}^{p-1}\Gamma(a_{l+1}-s)} z^s \tag{E.2}$$

where the integration path L separates the poles of the factors $\Gamma(b_l - s)$ from those of the factors $\Gamma(1 - a_l + s)$. After the change of variable $s = -w$, we obtain

$$G_0(b,z) = \frac{1}{2\pi i}\int_{L'} dw \frac{\Gamma(w+b)^2\Gamma(w)\Gamma(1-b-w)}{\Gamma(w+1)} z^{-w} \tag{E.3}$$

where the contour L' encloses all the poles of the integrand contained in the left-hand plane. We will define the integrand in (E.3) as $f_{\text{Meijer}}(b,z;w)$, given by

$$f_{\text{Meijer}}(b,z;w) = \frac{\Gamma(w+b)^2\Gamma(w)\Gamma(1-b-w)}{\Gamma(w+1)} z^{-w}. \tag{E.4}$$

The contour integral is equal to the sum of the residues at the poles of the integrand. These poles qualitatively depend on the value of b.

Value of b	Poles	Order of Poles
$b = 0$	$w = 0$ $w = -n$ for $n \in \mathbb{N}$	$\text{ord}(w = 0) = 3$ $\text{ord}(w = -n) = 2$
$b \in \mathbb{R} \setminus \mathbb{Z}$	$w = 0$ $w = -n-b$ for $n \in \mathbb{N}$	$\text{ord}(w = 0) = 1$ $\text{ord}(w = -b-n) = 2$

For each b of interest, we use the residue theorem to write

$$G_0(b, z) = R_0(b, z) + \sum_{n=1}^{\infty} R_0(b, z) \tag{E.5}$$

where

$$R_0(b, z) = \text{Res}_{w=0}\, f_{\text{Meijer}}(b, z; w), \qquad R_n(b, z) = \text{Res}_{w=-b-n}\, f_{\text{Meijer}}(b, z; w). \tag{E.6}$$

We begin with the case $b = 0$ where, after applying the addition and reflection formulae for the gamma function, we find

$$f_{\text{Meijer}}(0, z; w) = \frac{\pi\Gamma(w)}{w \sin \pi w} z^{-w} \tag{E.7}$$

has a pole of order 3 at $w = 0$ as well as poles of order 2 at $w = -n$ for $n \in \mathbb{N}$. The residue at $w = 0$ is easily computed in Maple 2024 since

$$R_0(0, z) = \frac{1}{(3-1)!} \left(w^3 f_{\text{Meijer}}(z; w) \right) [w^0] \tag{E.8}$$

$$= \frac{1}{2} \left(\gamma^2 + \frac{\pi^2}{2} + 2\gamma \log z + \log(z)^2 \right). \tag{E.9}$$

To calculate the residues of the poles of f_{Meijer} at $w = -n$ for $n \in \mathbb{N}$, we make use of

the Cauchy residue formula for higher order poles and hence find

$$R_n(0,z) = \frac{1}{(2-1)!}\lim_{w\to -n}\frac{d}{dw}\frac{\pi(w+n)^2\Gamma(w)z^{-w}}{w\sin\pi w} \tag{E.10}$$

$$\begin{aligned}
&= \lim_{w\to -n}\left(-\frac{\pi z^{-w}\log z\Gamma(w)(w+n)^2}{w\sin\pi w} - \frac{\pi z^{-w}\Gamma(w)(w+n)^2}{w^2\sin\pi w}\right.\\
&\quad + \frac{\pi z^{-w}\psi(w)\Gamma(w)(w+n)^2}{w\sin\pi w}\\
&\quad - \frac{\pi^2 z^{-w}\Gamma(w)\cos\pi w(w+n)^2}{w\sin^2\pi w}\\
&\quad \left. + \frac{2\pi z^{-w}\Gamma(w)(w+n)}{w\sin\pi w}\right)
\end{aligned} \tag{E.11}$$

$$\begin{aligned}
&= \log z\frac{z^n}{n\cdot n!} - \frac{z^n}{n^2\cdot n!}\\
&\quad + \lim_{z\to -n}\frac{\pi z^{-w}\Gamma(w)(w+n)}{w\sin\pi w}\left[\psi(w)(w+n)\right.\\
&\quad \left. - \frac{\pi\cos\pi w(w+n)}{\sin\pi w} + 2\right]
\end{aligned}$$

$$= \frac{z^n}{n\cdot n!}\left(\gamma + \log z - \frac{1}{n} - H_n\right) \tag{E.12}$$

where H_n is the nth harmonic number. Summing up all the residues, we find

$$\begin{aligned}
G_0(0,z) &= \frac{1}{2}\left(\gamma^2 + \frac{\pi^2}{2} + 2\gamma\log(z) + \log(z)^2\right) + (\gamma + \log(z))\sum_{n=1}^{\infty}\frac{z^n}{n\cdot n!}\\
&\quad - \sum_{n=1}^{\infty}\frac{z^n}{n^2\cdot n!} - \sum_{n=1}^{\infty}\frac{H_n z^n}{n\cdot n!}
\end{aligned} \tag{E.13}$$

$$\begin{aligned}
&= \frac{1}{2}\left(\gamma^2 + \frac{\pi^2}{2} + 2\gamma\log(z) + \log(z)^2\right) - (\gamma + \log(z))(\gamma + \log(-z)\\
&\quad + \Gamma(0,-z)) - z_3F_3(1,1,1;2,2,2;z) - H(0,z)
\end{aligned} \tag{E.14}$$

where suggestively, we write

$$H(b,z) = \sum_{n=1}^{\infty}\frac{H_n z^n}{(n+b)\cdot n!} \tag{E.15}$$

for $b \in \mathbb{R}\setminus\mathbb{Z}$. Note that we will only make use of $b = \pm 1/2$. The residue $R_0(b)$ is immediate and we find

$$R_0(b,z) = \frac{\pi\Gamma(b)}{\sin\pi b}. \tag{E.16}$$

By Cauchy's residue formula once again we find

$$\begin{aligned} R_n(b,z) = &- \lim_{w\to -b-n}\left[\frac{\pi(w+b+n)^2\Gamma(w+b)z^{-w}\log z}{w\sin\pi(w+b)}\right. \\ &\left.-\frac{\pi(w+b+n)^2\Gamma(w+b)z^{-w}}{w^2\sin\pi(w+b)}\right] \\ &+\lim_{w\to -b-n}\left[\frac{2\pi(w+b+n)\Gamma(w+b)z^{-w}}{w\sin\pi(w+b)}\right. \\ &+\frac{\pi(w+b+n)^2\psi(w+b)\Gamma(w+b)z^{-w}}{w\sin\pi(w+b)} \\ &\left.-\frac{\pi^2(w+b+b)^2\Gamma(w+b)\cos\pi(w+b)z^{-w}}{w\sin^2\pi(w+b)}\right]. \end{aligned} \tag{E.17}$$

The limits on the first line of (E.17) are found by the well known residues of the Γ and csc functions and hence we obtain

$$\begin{aligned} &-\lim_{w\to -b-n}\left[\frac{\pi(w+b+n)^2\Gamma(w+b)z^{-w}\log z}{w\sin\pi(w+b)}+\frac{\pi(w+b+n)^2\Gamma(w+b)z^{-w}}{w^2\sin\pi(w+b)}\right] \\ &\quad=\frac{z^{b+n}\log z}{(n+b)\cdot n!}-\frac{z^{b+n}}{(n+b)^2\cdot n!} \end{aligned} \tag{E.18}$$

for $n\in\mathbb{N}, b\in\mathbb{R}\setminus\mathbb{Z}$. In order to calculate the remaining limits of (E.17), which we define as

$$\begin{aligned} L_n(b,z) = &\lim_{w\to -b-n}\left(\frac{2\pi(w+b+n)\Gamma(w+b)z^{-w}}{w\sin\pi(w+b)}\right. \\ &+\frac{\pi(w+b+n)^2\psi(w+b)\Gamma(w+b)z^{-w}}{w\sin\pi(w+b)} \\ &\left.-\frac{\pi^2(w+b+n)^2\Gamma(w+b)\cos\pi(w+b)z^{-w}}{w\sin^2\pi(w+b)}\right), \end{aligned} \tag{E.19}$$

we factorise as

$$\begin{aligned} L_n(b,z) &= \lim_{w\to -b-n}\frac{(w+b+n)\Gamma(w+b)z^{-w}}{w}\lim_{w\to -b-n}\left[\frac{2\pi}{\sin\pi(w+b)}\right. \\ &\quad\left.+\frac{\pi\psi(w+b)(w+b+n)}{\sin\pi(w+b)}-\frac{\pi^2(w+b+n)\cos\pi(w+b)}{\sin^2\pi(w+b)}\right] \\ &=-\frac{\pi(-1)^n z^{n+b}}{(n+b)n!}\lim_{w\to -b-n}\left[\frac{2\pi}{\sin\pi(w+b)}+\frac{\pi\psi(w+b)(w+b+n)}{\sin\pi(w+b)}\right. \\ &\quad\left.-\frac{\pi^2(w+b+n)\cos\pi(w+b)}{\sin^2\pi(w+b)}\right] \\ &=-\frac{\pi(-1)^n z^{n+b}}{(n+b)n!}L_n^{(0)}(b,z) \end{aligned} \tag{E.20}$$

where

$$L_n^{(0)}(b,z) = \lim_{w\to -b-n}\left[\frac{2\pi}{\sin\pi(w+b)} + \frac{\pi\psi(w+b)(w+b+n)}{\sin\pi(w+b)} - \frac{\pi^2(w+b+n)\cos\pi(w+b)}{\sin^2\pi(w+b)}\right]. \tag{E.21}$$

To calculate $L_n^{(0)}$, we first, we first note that

$$\lim_{w\to -b-n}(w+b+n)\psi(w+b) = -1 \tag{E.22}$$

and consequently

$$L_n^{(0)}(b,z) = \lim_{w\to -b-n}\left[\frac{(w+b+n)\psi(w+b)}{\sin\pi(w+b)} + \frac{1}{\sin\pi(w+b)}\right] \tag{E.23}$$

$$+ \lim_{w\to -b-n}\left[\frac{1-\pi(w+b+n)\sin(w+b)\cot\pi(w+b)}{\sin\pi(w+b)}\right]. \tag{E.24}$$

By multiplying the limits through by $\mathrm{sinc}\pi(w+b)$ and making use once again of L'Hôpital's rule, we find the final result to be

$$L_n^{(0)}(b,z) = \frac{(-1)^n}{\pi}\left[\lim_{w\to -b-n}\frac{\psi(w+b)(w+b+n)+1}{w+b+n} + \lim_{w\to -b-n}\frac{1-(w+b+n)\cot\pi(w+b)}{w+b+n}\right] \tag{E.25}$$

$$= \lim_{w'\to -n}\frac{d}{dw'}(w'+n)\psi(w') \tag{E.26}$$

$$= H_n - \gamma. \tag{E.27}$$

Combining (E.20) and (E.27) and recalling the relation to R_b, we obtain

$$R_n(b,z) = (\log z+\gamma)\frac{z^{b+n}}{(n+b)\cdot n!} - \frac{z^{b+n}}{(n+b)^2\cdot n!} - \frac{H_n z^{n+b}}{n!\cdot(n+b)} \tag{E.28}$$

for $n\in\mathbb{N}$ and $b\in\mathbb{R}\setminus\mathbb{Z}$. Summing (E.16) and the closed forms of R_n given in (E.28), we find

$$G_0(b,z) = \frac{\pi\Gamma(b)}{\sin\pi b} + \frac{(\log z+\gamma)z^{b+1}}{1+b}{}_2F_2(1,1+b;2,2+b;z) - \frac{z^{1+b}}{(1+b)^2}{}_3F_3(1,1+b,1+b;2,2+b,2+b;z) - z^b H_0(b,z) \tag{E.29}$$

where H_0 is defined in (E.15).

It remains to calculate a closed form for the Harmonic number power series, which we label

$$H(b,z) = \sum_{n=1}^{\infty} \frac{H_n z^n}{(n+b)\cdot n!}. \tag{E.30}$$

To do this, we first note that the harmonic numbers can be written as

$$H_n = \frac{1}{(1)_n} \frac{d}{d\alpha}\bigg|_{\alpha=1} (\alpha)_n \tag{E.31}$$

where $(\alpha)_n$ is the Pochhammer symbol. Hence we find

$$H(0,z) = \frac{d}{d\alpha}\bigg|_{\alpha=1} \sum_{n=1}^{\infty} \frac{(\alpha)_n}{n(1)_n} \frac{z^n}{n!} = \frac{d}{d\alpha}\bigg|_{\alpha=1} \sum_{n=1}^{\infty} \frac{(\alpha)_n (1)_n}{(1)_n (2)_n} \frac{z^n}{n!} = \frac{d}{d\alpha}\bigg|_{\alpha=0} {}_1F_1(\alpha;2;z). \tag{E.32}$$

For $b \in \mathbb{R}\setminus\mathbb{Z}$, we similarly find

$$\begin{aligned} H(b,z) &= \frac{d}{d\alpha}\Big|_{\alpha=1} \sum_{n=1}^{\infty} \frac{(\alpha)_n z^n}{(1)_n (n+b) n!} && \text{(E.33)} \\ &= \frac{d}{d\alpha}\Big|_{\alpha=1} \sum_{n=1}^{\infty} \frac{(\alpha)_n (b)_n}{(1)_n (1+b)_n} \frac{z^n}{n!} && \text{(E.34)} \\ &= \frac{d}{d\alpha}\Big|_{\alpha=1} {}_2F_2\left(\alpha, b; 1, 1+b; z\right) && \text{(E.35)} \end{aligned}$$

and so the final closed form of the G_0 Meijer G functions are

$$\begin{aligned} G_0(0;z) &= \frac{1}{2}\left(\gamma^2 + \frac{\pi^2}{2} + 2\gamma\log(z) + \log(z)^2\right) + (\gamma + \log(z)) \sum_{n=1}^{\infty} \frac{z^n}{n\cdot n!} \\ &\quad - \sum_{n=1}^{\infty} \frac{z^n}{n^2\cdot n!} - \sum_{n=1}^{\infty} \frac{H_n z^n}{n\cdot n!} && \text{(E.36)} \\ &= \frac{1}{2}\left(\gamma^2 + \frac{\pi^2}{2} + 2\gamma\log(z) + \log(z)^2\right) - (\gamma + \log(z))(\gamma + \log(-z) \\ &\quad + \Gamma(0,-z)) - z\,{}_3F_3(1,1,1;2,2,2;z) - \frac{d}{d\alpha}\bigg|_{\alpha=1} {}_1F_1(\alpha;2;z), && \text{(E.37)} \\ G_0(b;z) &= \frac{\pi\Gamma(b)}{\sin\pi b} + \frac{(\log z + \gamma) z^{b+1}}{1+b} {}_2F_2(1, 1+b; 2, 2+b; z) \\ &\quad - \frac{z^{1+b}}{(1+b)^2} {}_3F_3(1, 1+b, 1+b; 2, 2+b, 2+b; z) \\ &\quad - z^b \frac{d}{d\alpha}\bigg|_{\alpha=1} {}_2F_2(\alpha, b; 1, 1+b; z) && \text{(E.38)} \end{aligned}$$

for $b \in \mathbb{R} \setminus \mathbb{Z}$ and $z \in \mathbb{C} \setminus \mathbb{R}^-$.

It remains to calculate a simpler form of G_1. To do this we make use of a neat indentity first derived by Meijer in [50, page 1064].

$$G_1(b,z) = -z^{b+1}\frac{\partial}{\partial z}(z^{-b}G_0(b,z)). \tag{E.39}$$

Simply applying this, we find

$$\begin{aligned} G_1(b,z) = &-\frac{z^b}{b} + \frac{\pi b\Gamma(b)}{\sin \pi b} - \frac{(1+\gamma+\log z)z^{b+1}}{b+1}{}_2F_2(1,1+b;2,2+b;z) \\ &- \frac{(\gamma+\log z)z^{b+2}}{2(b+2)}{}_2F_2(2,2+b;3,3+b;z) \\ &+ \frac{z^{b+1}}{(1+b)^2}{}_3F_3(1,1+b,1+b;2,2+b,2+b;z) \\ &+ \frac{z^{b+2}}{2(b+2)^2}{}_3F_3(2,2+b,2+b;3,3+b,3+b;z) + z^{b+1}H_1(b,z) \end{aligned} \tag{E.40}$$

where $H_1(b,z)$ is a power series containing the harmonic numbers for which, with similar techniques to that we used for H_0, we find

$$H_1(b,z) = \frac{1}{b^2}\frac{d}{d\alpha}\bigg|_{\alpha=1} {}_3F_3(\alpha,b,b;1,1+b,1+b;z) \tag{E.41}$$

for $b \neq 0$.

References

[1] L. V. Ahlfors. *Complex analysis*. Third. International Series in Pure and Applied Mathematics. An introduction to the theory of analytic functions of one complex variable. McGraw-Hill Book Co., New York, 1978, pp. xi+331. ISBN: 0-07-000657-1.

[2] G. Allcock. "The time of arrival in quantum mechanics III. The measurement ensemble". In: *Annals of physics* 53.2 (1969), pp. 311–348.

[3] J. Ashfaque, J. Lynch, and P. Strange. "Relativistic quantum backflow". In: *Physica Scripta* 94.12 (2019), p. 125107.

[4] M. Barbier, A. Goussev, and S. C. L. Srivastava. "Unbounded quantum backflow in two dimensions". In: *Phys. Rev. A* 107.3 (2023), Paper No. 032204, 10. ISSN: 2469-9926,2469-9934.

[5] H. Bateman. *Higher transcendental functions [volumes i-iii]*. Vol. 1. McGraw-Hill Book Company, 1953.

[6] G. Beer. *Topologies on closed and closed convex sets*. Vol. 268. Mathematics and its Applications. Kluwer Academic Publishers Group, Dordrecht, 1993, pp. xii+340. ISBN: 0-7923-2531-1.

[7] M. V. Berry. "Quantum backflow, negative kinetic energy, and optical retro-propagation". In: *J. Phys. A* 43.41 (2010), pp. 415302, 15.

[8] M. S. Birman and M. Z. Solomjak. *Spectral theory of selfadjoint operators in Hilbert space*. Mathematics and its Applications (Soviet Series). Translated from the 1980 Russian original by S. Khrushchëv and V. Peller. D. Reidel Publishing Co., Dordrecht, 1987, pp. xv+301. ISBN: 90-277-2179-3.

[9] D. Biswas and S. Ghosh. "Quantum backflow across a black hole horizon in a toy model approach". In: *Phys. Rev. D* 104.10 (2021), Paper No. 104061, 11. ISSN: 2470-0010,2470-0029.

[10] H. Bostelmann, D. Cadamuro, and G. Lechner. "Quantum backflow and scattering". In: *Phys. Rev. A* 96.1 (2017), pp. 012112, 11. ISSN: 2469-9926,2469-9934.

[11] A. J. Bracken. "Probability flow for a free particle: new quantum effects". In: *Physica Scripta* 96.4 (Jan. 2021), p. 045201.

[12] A. J. Bracken and G. F. Melloy. "Probability backflow and a new dimensionless quantum number". In: *J. Phys. A* 27.6 (1994), pp. 2197–2211. ISSN: 0305-4470,1751-8121.

[13] A. J. Bracken and G. F. Melloy. "Probability backflow and a new dimensionless quantum number". In: *J. Phys. A* 27.6 (1994), pp. 2197–2211. ISSN: 0305-4470,1751-8121.

[14] C. Brezinski and M. Redivo-Zaglia. "A survey of Shanks' extrapolation methods and their applications". In: *Comput. Math. Math. Phys.* 61.5 (2021), pp. 699–718. ISSN: 0965-5425,1555-6662.

[15] A. Bultheel and R. Cools, eds. *The birth of numerical analysis*. World Scientific Publishing Co. Pte. Ltd., Hackensack, NJ, 2010, pp. xviii+221. ISBN: 978-981-283-625-0; 981-283-625-X.

[16] P. L. Butzer, G. Schmeisser, and R. L. Stens. "An introduction to sampling analysis". In: *Nonuniform sampling*. Inf. Technol. Transm. Process. Storage. Kluwer/Plenum, New York, 2001, pp. 17–121. ISBN: 0-306-46445-4.

[17] P. L. Butzer, W. Splettstösser, and R. L. Stens. "The sampling theorem and linear prediction in signal analysis". In: *Jahresber. Deutsch. Math.-Verein.* 90.1 (1988), p. 70. ISSN: 0012-0456.

[18] J. Chen, J. Tiong, L. H. Zaw, and V. Scarani. "Even-parity precession protocol for detecting nonclassicality and entanglement". In: *Phys. Rev. A* 110.6 (2024), Paper No. 062408, 11. ISSN: 2469-9926,2469-9934.

[19] E. B. Davies and M. Plum. "Spectral pollution". In: *IMA J. Numer. Anal.* 24.3 (2004), pp. 417–438. ISSN: 0272-4979,1464-3642.

[20] E. B. Davies. *Linear operators and their spectra*. Vol. 106. Cambridge Studies in Advanced Mathematics. Cambridge University Press, Cambridge, 2007, pp. xii+451. ISBN: 978-0-521-86629-3; 0-521-86629-4.

[21] S. P. Dawson. "A quantum weak energy inequality for the Dirac field in two-dimensional flat spacetime". In: *Classical Quantum Gravity* 23.1 (2006), pp. 287–293. ISSN: 0264-9381,1361-6382.

[22] S. P. Dawson and C. J. Fewster. "An explicit quantum weak energy inequality for Dirac fields in curved spacetimes". In: *Classical Quantum Gravity* 23.23 (2006), pp. 6659–6681. ISSN: 0264-9381,1361-6382.

[23] L. Di Bari, V. D. Paccoia, O. Panella, and P. Roy. "Quantum backflow for a massless Dirac fermion on a ring". In: *Phys. Lett. A* 474 (2023), Paper No. 128831, 7. ISSN: 0375-9601,1873-2429.

[24] NIST Digital Library of Mathematical Functions. https://dlmf.nist.gov/, Release 1.2.4 of 2025-03-15. F. W. J. Olver, A. B. Olde Daalhuis, D. W. Lozier, B. I. Schneider, R. F. Boisvert, C. W. Clark, B. R. Miller, B. V. Saunders, H. S. Cohl, and M. A. McClain, eds.

[25] J. D. Dollard. "Scattering into cones I: Potential scattering". In: *Communications in Mathematical Physics* 12.3 (1969), pp. 193–203.

[26] J. Duoandikoetxea. *Fourier analysis*. Vol. 29. Graduate Studies in Mathematics. Translated and revised from the 1995 Spanish original by David Cruz-Uribe. American Mathematical Society, Providence, RI, 2001, pp. xviii+222. ISBN: 0-8218-2172-5.

[27] Y. Eliezer, T. Zacharias, and A. Bahabad. "Observation of optical backflow". In: *Optica* 7.1 (Jan. 2020), pp. 72–76.

[28] H. Epstein, V. Glaser, and A. Jaffe. "Nonpositivity of the energy density in quantized field theories". In: *Nuovo Cimento (10)* 36 (1965), pp. 1016–1022. ISSN: 0029-6341,1827-6121.

[29] S. P. Eveson, C. J. Fewster, and R. Verch. "Quantum inequalities in quantum mechanics". In: *Ann. Henri Poincaré* 6.1 (2005), pp. 1–30. ISSN: 1424-0637,1424-0661.

[30] G. Fang. "Whittaker-Kotelnikov-Shannon sampling theorem and aliasing error". In: *J. Approx. Theory* 85.2 (1996), pp. 115–131. ISSN: 0021-9045,1096-0430.

[31] C. J. Fewster. "A general worldline quantum inequality". In: *Classical Quantum Gravity* 17.9 (2000), pp. 1897–1911. ISSN: 0264-9381,1361-6382.

[32] C. J. Fewster. "Quantum energy inequalities". In: *Wormholes, warp drives and energy conditions*. Vol. 189. Fundam. Theor. Phys. Springer, Cham, 2017, pp. 215–254. ISBN: 978-3-319-55181-4; 978-3-319-55182-1.

[33] C. J. Fewster and H. J. Kirk-Karakaya. *Repeated quantum backflow and overflow*. 2025. arXiv: 2505.13184 [quant-ph].

[34] C. J. Fewster and M. J. Pfenning. "A quantum weak energy inequality for spin-one fields in curved space-time". In: *J. Math. Phys.* 44.10 (2003), pp. 4480–4513. ISSN: 0022-2488,1089-7658.

[35] C. J. Fewster and J. Thompson. "Quantum energy inequalities along stationary worldlines". In: *Classical Quantum Gravity* 40.17 (2023), Paper No. 175008, 32. ISSN: 0264-9381,1361-6382.

[36] The FLINT team. *FLINT: Fast Library for Number Theory*. Version 2.9.0, https://flintlib.org. 2022.

[37] L. H. Ford. "Inequalities which constrain negative energy in quantum field theory". In: *Quantum gravity (Moscow, 1990)*. World Sci. Publ., River Edge, NJ, 1991, pp. 330–341. ISBN: 981-02-0440-X.

[38] G. H. Golub and C. F. Van Loan. *Matrix computations*. Fourth. Johns Hopkins Studies in the Mathematical Sciences. Johns Hopkins University Press, Baltimore, MD, 2013, pp. xiv+756. ISBN: 978-1-4214-0794-4; 1-4214-0794-9; 978-1-4214-0859-0.

[39] A. Goussev. "Quantum backflow in a ring". In: *Phys. Rev. A* 103.2 (2021), Paper No. 022217, 6. ISSN: 2469-9926,2469-9934.

[40] G. Grübl, S. Kreidl, M. Penz, and M. Ruggenthaler. "Arrival time and backflow effect". In: *Quantum mechanics*. Vol. 844. AIP Conf. Proc. Amer. Inst. Phys., Melville, NY, 2006, pp. 177–191. ISBN: 0-7354-0337-6.

[41] J. J. Halliwell, E. Gillman, O. Lennon, M. Patel, and I. Ramirez. "Quantum backflow states from eigenstates of the regularized current operator". In: *J. Phys. A* 46.47 (2013), pp. 475303, 12. ISSN: 1751-8113,1751-8121.

[42] L. Hörmander. *The analysis of linear partial differential operators. I.* Classics in Mathematics. Distribution theory and Fourier analysis, Reprint of the second (1990) edition [Springer, Berlin; MR1065993 (91m:35001a)]. Springer-Verlag, Berlin, 2003, pp. x+440. ISBN: 3-540-00662-1.

[43] R. A. Horn and C. R. Johnson. *Matrix analysis*. Corrected reprint of the 1985 original. Cambridge University Press, Cambridge, 1990, pp. xiv+561. ISBN: 0-521-38632-2.

[44] F. Johansson. "Arb: efficient arbitrary-precision midpoint-radius interval arithmetic". In: *IEEE Transactions on Computers* 66 (8 2017), pp. 1281–1292.

[45] F. Johansson. "Computing hypergeometric functions rigorously". In: *ACM Trans. Math. Software* 45.3 (2019), Art. 30, 26. ISSN: 0098-3500,1557-7295.

[46] T. Kato. *Perturbation theory for linear operators*. Classics in Mathematics. Reprint of the 1980 edition. Springer-Verlag, Berlin, 1995, pp. xxii+619. ISBN: 3-540-58661-X.

[47] K. Kuratowski. *Topology. Vol. I.* New. Translated from the French by J. Jaworowski. Academic Press, New York-London; Państwowe Wydawnictwo Naukowe [Polish Scientific Publishers], Warsaw, 1966, pp. xx+560.

[48] R.-C. Li. "Rayleigh quotient based optimization methods for eigenvalue problems". In: *Matrix functions and matrix equations*. Vol. 19. Ser. Contemp. Appl. Math. CAM. Higher Ed. Press, Beijing, 2015, pp. 76–108. ISBN: 978-981-4675-76-5.

[49] A. C. Matos. "Acceleration methods based on convergence tests". In: *Numer. Math.* 58.3 (1990), pp. 329–340. ISSN: 0029-599X,0945-3245.

[50] C. S. Meijer. "Multiplikationstheoreme für die Funktion $G^{m,n}_{p,q}(z)$". In: *Nederl. Akad. Wetensch., Proc.* 44 (1941), pp. 1062–1070. ISSN: 0370-0348.

[51] T. mpmath development team. *mpmath: a Python library for arbitrary-precision floating-point arithmetic (version 1.3.0)*. http://mpmath.org/. 2023.

[52] M. Palmero, E. Torrontegui, J. G. Muga, and M. Modugno. "Detecting quantum backflow by the density of a Bose-Einstein condensate". In: *Physical Review A* 87.5 (2013), p. 053618.

[53] M. Penz, G. Grübl, S. Kreidl, and P. Wagner. "A new approach to quantum backflow". In: *J. Phys. A* 39.2 (2006), pp. 423–433. ISSN: 0305-4470,1751-8121.

[54] M. Razavy. *Quantum theory of tunneling*. World Scientific, 2013.

[55] M. Reed and B. Simon. *Methods of modern mathematical physics. I.* Second. Functional analysis. Academic Press, Inc. [Harcourt Brace Jovanovich, Publishers], New York, 1980, pp. xv+400. ISBN: 0-12-585050-6.

[56] M. Reed and B. Simon. *Methods of modern mathematical physics. IV. Analysis of operators*. Academic Press [Harcourt Brace Jovanovich, Publishers], New York-London, 1978, pp. xv+396. ISBN: 0-12-585004-2.

[57] J. W. Robbin and D. A. Salamon. "The exponential Vandermonde matrix". In: *Linear Algebra Appl.* 317.1-3 (2000), pp. 225–226. ISSN: 0024-3795,1873-1856.

[58] W. Rudin. *Real and complex analysis*. Third. McGraw-Hill Book Co., New York, 1987, pp. xiv+416. ISBN: 0-07-054234-1.

[59] C. Shannon. "A mathematical theory of communication (1948)". In: *Ideas that created the future—classic papers of computer science*. Reprinted from [0026286]. MIT Press, Cambridge, MA, [2021] ©2021, pp. 121–134. ISBN: [9780262045308].

[60] A. Sidi. *Practical extrapolation methods*. Vol. 10. Cambridge Monographs on Applied and Computational Mathematics. Theory and applications. Cambridge University Press, Cambridge, 2003, pp. xxii+519. ISBN: 0-521-66159-5.

[61] A. Sidi. *Practical extrapolation methods*. Vol. 10. Cambridge Monographs on Applied and Computational Mathematics. Theory and applications. Cambridge University Press, Cambridge, 2003, pp. xxii+519. ISBN: 0-521-66159-5.

[62] G. W. Stewart and J. G. Sun. *Matrix perturbation theory*. Computer Science and Scientific Computing. Academic Press, Inc., Boston, MA, 1990, pp. xvi+365. ISBN: 0-12-670230-6.

[63] G. Szegő. *Orthogonal polynomials*. Fourth. Vol. XXIII. American Mathematical Society Colloquium Publications. American Mathematical Society, Providence, RI, 1975, pp. xiii+432.

[64] D. Trillo, T. P. Le, and M. Navascués. "Quantum advantages for transportation tasks - projectiles, rockets and quantum backflow". In: *npj Quantum Information* 9.1 (2023), p. 69.

[65] B. Tsirelson. *How often is the coordinate of a harmonic oscillator positive?* 2006. arXiv: quant-ph/0611147 [quant-ph].

[66] V. S. Vladimirov, V. V. Zharinov, and A. G. Sergeev. "Bogolyubov's edge-of-the-wedge theorem, its development and applications". In: *Uspekhi Mat. Nauk* 49.5(299) (1994), pp. 47–60. ISSN: 0042-1316,2305-2872.

[67] W. Yang and I. Zurbenko. "Kolmogorov–Zurbenko filters". In: *WIREs Computational Statistics* 2.3 (2010), pp. 340–351. eprint: https://wires.onlinelibrary.wiley.com/doi/pdf/10.1002/wics.71.

[68] J. M. Yearsley and J. J. Halliwell. "An introduction to the quantum backflow effect". In: *Journal of Physics: Conference Series* 442.1 (2013), p. 012055.

[69] J. M. Yearsley, J. J. Halliwell, R. Hartshorn, and A. Whitby. "Analytical examples, measurement models, and classical limit of quantum backflow". In: *Phys. Rev. A* 86 (4 Oct. 2012), p. 042116.

[70] L. H. Zaw, C. C. Aw, Z. Lasmar, and V. Scarani. "Detecting quantumness in uniform precessions". In: *Phys. Rev. A* 106.3 (2022), Paper No. 032222, 16. ISSN: 2469-9926,2469-9934.

[71] L. H. Zaw and V. Scarani. "All three-angle variants of Tsirelson's precession protocol, and improved bounds for wedge integrals of Wigner functions". Preprint arXiv:2411.03132. 2024.

[72] L. H. Zaw, M. Weilenmann, and V. Scarani. "Tsirelson's inequality for the precession protocol is maximally violated by quantum theory". In: *Phys. Rev. Lett.* 134.19 (2025), Paper No. 190201, 8. ISSN: 0031-9007,1079-7114.

[73] Z.-F. Zhang, P.-F. Huang, S.-C. Dong, Y.-X. Rong, J.-S. Xu, Y.-J. Gu, and Y. Xiao. "Observation of single-photon azimuthal backflow with weak measurement". In: *Opt. Lett.* 50.2 (Jan. 2025), pp. 333–336.

[74] I. G. Žurbenko. *The spectral analysis of time series*. Vol. 2. North-Holland Series in Statistics and Probability. With a foreword by A. N. Kolmogorov. North-Holland Publishing Co., Amsterdam, 1986, pp. x+247. ISBN: 0-444-87607-3.